CONVENTION ON LONG-RANGE TRANSBOUNDARY AIR POLLUTION
of the United Nations Economic Commission for Europe

# CALCULATION AND MAPPING OF CRITICAL THRESHOLDS IN EUROPE

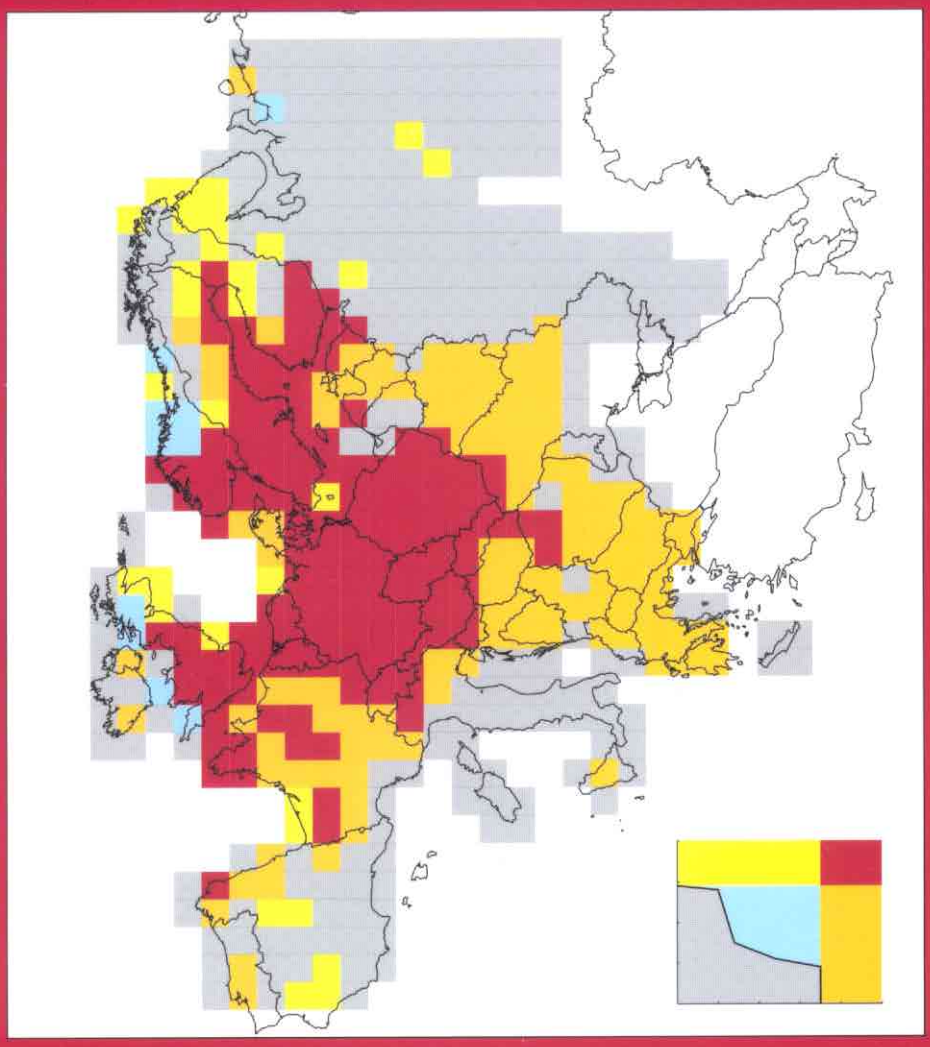

## STATUS REPORT 1995
## COORDINATION CENTER FOR EFFECTS

M. Posch, P.A.M. de Smet, J.-P. Hettelingh, R.J. Downing (eds.)

rivm
research for
man and environment

RIJKSINSTITUUT VOOR VOLKSGEZONDHEID EN MILIEU
NATIONAL INSTITUTE OF PUBLIC HEALTH AND THE ENVIRONMENT

# *Calculation and Mapping of Critical Thresholds in Europe:*

# *Status Report 1995*

Edited by:

Maximilian Posch
Peter A.M. de Smet
Jean-Paul Hettelingh
Robert J. Downing

**Coordination Center for Effects**
**National Institute of Public Health and the Environment**
**Bilthoven, the Netherlands**

RIVM Report No. 259101004

ISBN No. 90-6960-060-9

# Acknowledgements

The calculation methods and resulting maps contained in this report are the product of collaboration within the Effects Program of the UN/ECE Convention on Long-Range Transboundary Air Pollution, involving many individuals and institutions throughout Europe. The various National Focal Centers whose reports on their respective mapping activities appear in Part III, are gratefully acknowledged for their contributions to this work.

In addition, the Coordination Center for Effects thanks the following for their efforts:

- Anton Eliassen, Erik Berge and Helge Styve from EMEP for providing the European deposition data.

- the UN/ECE Task Force on Mapping, for their collaboration and assistance.

- the UN/ECE Task Force on Integrated Assessment Modelling for its collaboration in implementing the critical loads results into integrated models.

- Elmy Heuvelmans and Evert Meijer of GEODAN, for their expert assistance in the maintenance of the CCE's geographic information systems.

- The staff of the RIVM graphics department, for their assistance in producing this report.

- The Directorate of Air and Energy of the Dutch Ministry of Public Health, Physical Planning and Environment, in particular Volkert Keizer and Johan Sliggers, for funding and support of the CCE.

# Table of Contents

# Introduction

*J.-P. Hettelingh, M. Posch, and P.A.M. de Smet*

The aim of the Coordination Center for Effects (CCE) is to give scientific and technical support, in collaboration with the Program Centers under the Convention on Long-Range Transboundary Air Pollution, to the Working Group on Effects and, as required, to the Working Group on Strategies, and their relevant Task Forces in their work related to the environmental effects of air pollution, including the practical development of critical loads/levels maps and their exceedances.

The work of the CCE is conducted in close collaboration with a broad network of national scientific institutions (National Focal Centers). Progress on data and methodologies are reviewed annually at CCE Mapping Workshops. Six workshops have been organized since CCE started to operate in 1990: at the RIVM (1990, 1991), the Institute for the Ecology of Industrial Areas (Poland, 1992), the Research Center for Energy, Environment and Technology (Spain, 1993), the National Institute for Agricultural Research (France, 1994) and the Finnish Environment Agency (Finland, 1995). The consensus-based approach to the technical support of UN/ECE policy negotiations resulted in a European map of critical loads synthesizing the contributions of National Focal Centers. This map was used to assist the policy analysis of environmental effects of sulfur emission reduction alternatives, which finally led to the "Protocol to the 1979 Convention on Long-Range Transboundary Air Pollution on Further Reduction of Sulfur Emissions" (the 'Second Sulfur Protocol') signed in Oslo in June 1994.

The work of the CCE has been described in reports (Hettelingh *et al.* 1991, Downing *et al.* 1993) and in the open literature. The first CCE report described the critical load of acidity methodology which had been adopted by National Focal Centers, and the alterations made to accommodate for the policy requirement of identifying critical loads for sulfur. The second report presented the final results of this approach and introduced the development towards the application of both the critical loads for acidity and the critical load for eutrophication. The critical load approach is further broadened to different *kinds* of impacts. In addition to the indirect effects of geochemical changes in soils and lakes, consideration of the direct effects of air concentrations on vegetation and human health may become important for the scientific support of protocol negotiations which aim to reduce different pollutants.

This is the third report of the Coordination Center for Effects. It reflects the spirit of the current impact research for the support of UN/ECE protocols on long-range transboundary air pollution, away from *single* critical loads towards the future application of *multiple critical thresholds.* This has led to the creation of so-called *protection isolines,* which depict combinations of sulfur and nitrogen deposition at which protection against acidification and/or eutrophication is ensured.

This report consists of four parts. Part I gives an overview of the maps of critical loads, exceedances, and ecosystem protection (Chapter 1). Chapter 2 describes the national data contributions used to produce European critical loads maps. The aim of Chapter 3 is to synthesize notation, methodology and parameter values of the Simple Mass Balance used to compute critical loads for sulphur- and nitrogen-based acidity and eutrophication, and discusses methods of characterizing the exceedance of critical loads. Part I ends with a chapter defining percentiles in general and ecosystem protection isolines in particular.

Part II contains five papers on research developments which are relevant to the Effects Programme under the Convention. The paper on land use describes the background of the maps which were distributed by the CCE to National Focal Centers earlier this year to prepare for the assessments of stock at risk due to exceedances of both critical loads and levels.

Two papers deal with the issue of downscaling broad-scale information on base cation deposition and ozone to a higher resolution. The fourth paper proposes a methodology for computing critical loads for heavy metals and persistent organic pollutants, and was presented at the 1995 CCE workshop in Helsinki and detailed in a report to National Focal Centers, in view of possible future

work within the Effects Programme of the Convention. The last paper treats critical thresholds for biodiversity.

Part III consists of National Focal Center reports. It is very satisfying to note that, in comparison to the CCE Status Report 1993, three additional National Focal Centers: Estonia, France and the Czech Republic, have joined the collaborative work on critical loads, bringing the total number of contributions to fourteen. Also, a development of national mapping work from critical loads towards the inclusion of critical levels, with emphasis on AOT40 values for ozone, is evident from many NFC reports. Part III demonstrates the convergence of the scientific methods for developing critical thresholds, enabling the consistent mapping of critical loads and levels on a pan-European scale.

Lastly, four appendices provide details on geographical issues involved in critical loads mapping, on routines to calculate percentiles, on the CCE's anonymous FTP server, and a list of mathematical notation and acronyms.

This report shows that progress has been made with the implementation of impact-related methodologies which can be enhanced, provided a mechanism is furthered to achieve a more structural support of the work under the Effects Programme of the Convention.

# PART I. Status of Maps and Methods

Part I gives an overview of the maps of critical loads for acidity (sulfur- and nitrogen-based), eutrophication, exceedances and exploratory other maps, e.g., on *deposition reduction requirements* and *binding critical thresholds* (Chapter 1), describes the national and European data, with emphasis on the kinds of ecosystems behind the critical load computations (Chapter 2), summarizes the critical load computation methodology, providing consensus on the mathematics and the notation (Chapter 3) and finally describes the concept of *percentile critical loads*, with respect to single pollutant critical loads, applied in the past, and protection isolines, which is currently applied.

Protection isolines describe combinations of sulfur and nitrogen deposition at which protection against acidification and/or eutrophication is obtained. For example, the 5-percentile protection isoline reflects the combinations of sulfur and nitrogen deposition at which 95 percent of the ecosystems in a grid cell are protected against acidification, and when the critical load for nutrient nitrogen is included, also against eutrophication. Protection isolines are computed for all ecosystems in each grid cell from (1) the maximum critical load for sulfur $Cl_{max}(S)$, which corresponds to the well-known critical load of acidity, (2) the maximum critical load for nitrogen, $Cl_{max}(N)$, which includes nitrogen uptake, immobilization and denitrification, (3) the minimum critical load for nitrogen, $Cl_{min}(N)$, which is the sum of nitrogen uptake and immobilization, and (4) the critical load for eutrophication $Cl_{nut}(N)$. Chapter 1 includes maps of the 5 and 50-percentile of each of these thresholds.

# 1. Analysis of European Maps

*J.-P. Hettelingh, M. Posch, and P.A.M. de Smet*

## 2.1 Introduction

This chapter gives an overview of maps reflecting critical loads, protection percentages, required deposition reductions and binding effects. In preparing the scientific support to the negotiation of a revised UN/ECE LRTAP protocol on the reduction of nitrogen, a new methodology has been designed within the Effects Program to take multiple effects (i.e. acidification and eutrophication) of multiple pollutants (sulfur and nitrogen) into account. This methodology replaces the approach used to support the Second Sulphur Protocol negotiations for which only acidification was considered caused by a single pollutant, i.e. sulphur (see e.g. Hettelingh *et al.* 1995). Critical loads have been computed for acidification and eutrophication for a large range of ecosystems in every EMEP grid square. So-called *protection isolines* have been derived which reflect the combinations of sulphur and nitrogen deposition at which the protection of ecosystems against acidification and eutrophication does not change. Different isolines correspond to different protection levels, and the 5-percentile protection isoline is used to identify grid cells where more than 5 percent of the ecosystems is at risk. The use of these protection isolines means that the exceedance is no longer expressed as the difference between a single critical load and the deposition of a single pollutant, as was done in the research supporting the negotiations of the Second Sulphur Protocol. By considering two pollutants, many combinations of sulphur and nitrogen deposition can be formulated which provide the same protection against acidification and eutrophication. Therefore, exceedance is expressed in terms of the proportion of the ecosystems in each EMEP grid cell which is protected, given a certain combination of sulfur and nitrogen deposition onto each grid cell. The combinations which have been analyzed are (1) 1990 sulfur and nitrogen deposition, (2) 2010 sulfur protocol and nitrogen deposition, and (3) the combination of the critical sulfur deposition, used for the support of the Second Sulphur Protocol, and the 1990 nitrogen deposition.

This chapter also includes a tentative analysis in view of the possible requirement to provide scientific support to a multi-pollutant, multi-effect protocol. A preliminary effort is made to map the limiting critical thresholds, i.e. reflecting whether critical levels or critical loads for sulfur and nitrogen compounds are more binding from the point of view of emission reduction requirements.

Finally, it should be mentioned that the results of the collaborative work of CCE within the effect related program of the UN/ECE-LRTAP has recently been used for the scientific support of a wider policy audience, including the European Environmental Agency, and other bodies of the European Union.

## 1.1. Second sulfur protocol exceedances of the critical sulfur deposition

Until 1994 the work of the CCE focused on the development of methodologies and synthesis of national data to produce a map of critical sulfur deposition (i.e., critical loads corrected for base cations). These results were used in the preparation of the protocol to the 1979 Convention on Long-Range Transboundary Air Pollution on Further Reduction of Sulfur Emissions. The protocol results in terms of exceedances are reflected in Figure 1.1. Exceedances are shown of the base year sulfur deposition in 1990 (Figure 1.1a) and the deposition in 2010 (Figure 1.1b) due to the sulfur emissions as projected in the agreement. In 1990 areas of high exceedance (> 1500 eq $ha^{-1}$ $yr^{-1}$) are found in a belt ranging from the south eastern part of United Kingdom to the eastern part of central European countries including Poland and the Czech and Slovak Republics. Areas with moderate exceedance are found in large areas in Scandinavian countries. Areas where the critical sulfur deposition is not exceeded are in southern European countries and in the east of Europe.

In 2010 exceedances become smaller and areas of high exceedances are reduced. However, in spite of reductions achieved, ecosystems in central west, middle and northern Europe continue to be subject to risk of damage.

Note that the concept of the critical sulfur deposition, which reflects the share of the critical load of acidity assigned to sulfur (using a *sulfur fraction*), is no longer used. In the following maps exceedances are shown which are based on the simultaneous treatment of sulfur and nitrogen.

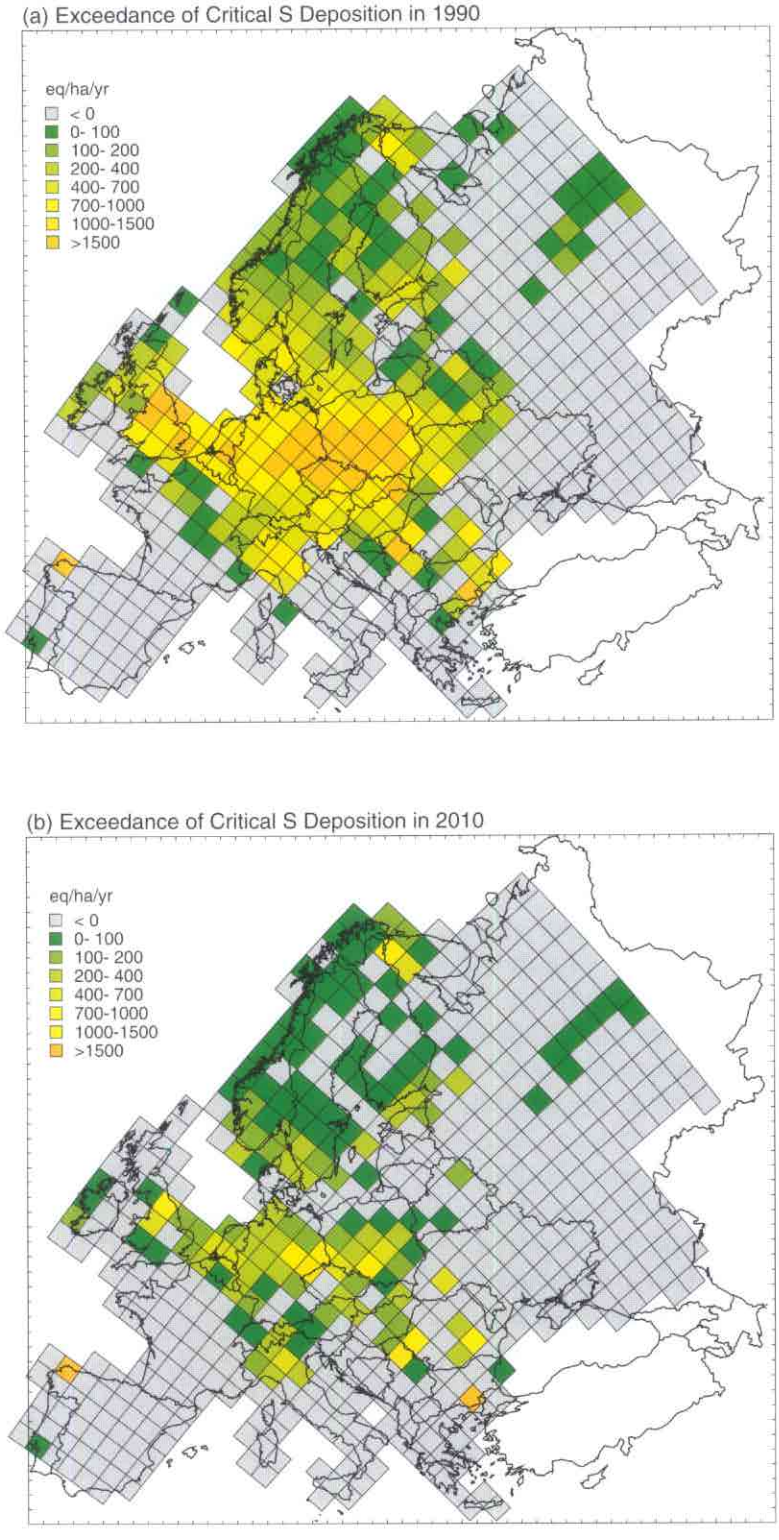


**Figure 1.1**. Exceedance of the critical load for sulfur, which was developed for support of the Second Sulfur Protocol negotiations, (a) due to the sulfur deposition in 1990, and (b) in 2010 according to agreed sulfur emissions in this target year of the protocol.

## 1.2. Maximum critical loads of sulfur and nitrogen

Data on the basis of which critical loads were computed in the past have been improved both at a national level and in the European data base which is used to compute critical loads in areas for which national contributions are not available (see Chapter 2). Data on base cation uptake, base cation deposition and nitrogen uptake were established on a site specific basis rather than using a single value for a grid cell as a whole as had been done in the past. Knowledge on denitrification has increased, leading to its inclusion in the present exercise.

Figure 1.2 shows the fifth percentile (*pentile*) and the median of the maximum critical load of sulfur, $Cl_{max}(S)$, and the maximum critical load of nitrogen, $Cl_{max}(N)$. The maximum critical load of sulfur is similar to the critical load of acidity from which, after inclusion of nitrogen uptake, immobilization and denitrification, the maximum critical load of nitrogen is derived. When the maximum critical load of sulfur is exceeded by sulfur deposition, than a mandatory reduction of sulfur deposition is required. If, in addition nitrogen deposition also exceeds the maximum critical load of nitrogen, then also a mandatory deposition reduction of nitrogen is required. More details on the mathematical formulation can be found in Chapter 3.

The median critical loads, which protects only 50% of the ecosystems obviously yields higher values than the pentile critical loads, which protect 95% of the ecosystems. This is shown in Figure 1.2. The pentile maximum critical load for sulfur (upper left) results in very low critical loads (< 200 eq $ha^{-1}$ $yr^{-1}$, i.e. lower than 320 mg S $m^2$ $yr^{-1}$) in Scandinavia, central and western Europe and in Spain. The median of the maximum critical load of sulfur (upper right) leaves a few areas with very low critical loads in northern Europe, but results in markedly higher critical loads over the whole of Europe. The *values* of the pentile and median maximum critical load for sulfur are given in Figure 1.3.

The pentile maximum critical load of nitrogen (Figure 1.2, lower left) shows low critical loads (< 400 eq $ha^{-1}$ $yr^{-1}$, i.e., lower than 560 mg N $m^2$ $yr^{-1}$) mostly in areas of northern Europe. These areas are significantly reduced when the median maximum critical load of nitrogen is considered.

It has turned out that the improvements made to the data, as mentioned above, occasionally lead to lower pentile critical loads for acidity in comparison to the critical acid deposition used for the derivation of the basis for the second sulfur protocol, i.e., the critical sulfur deposition. These discrepancies rapidly vanish as higher percentile critical loads are considered.

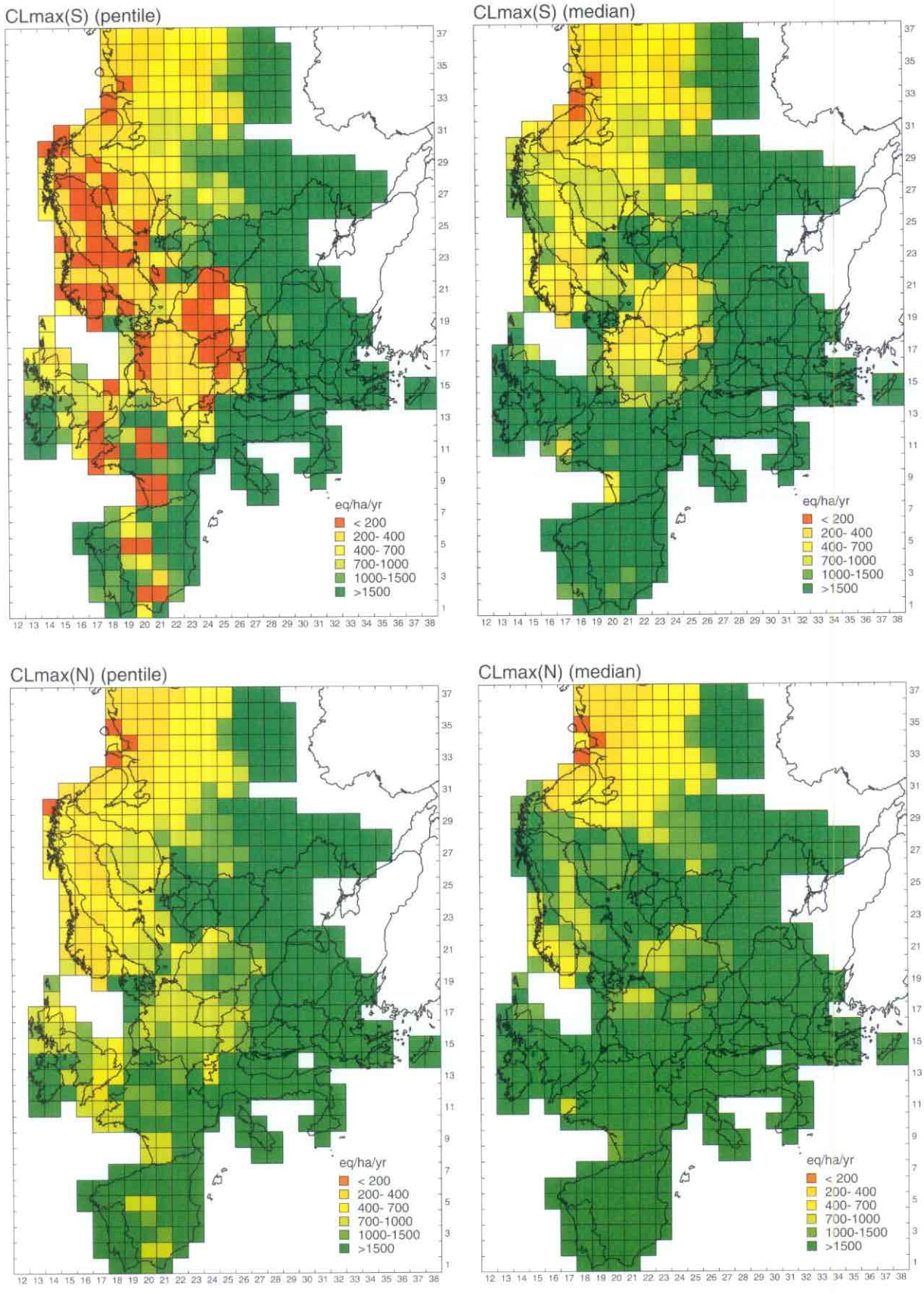


**Figure 1.2.** The pentile and median value ranges of the maximum critical load of sulfur (upper left and right, respectively) and of the maximum critical load of nitrogen (lower two maps).

## 1.3. Maximum critical loads for sulfur (pentile and median) expressed as numbers

Figure 1.3 shows the numbers behind the shadings used for the display of the maximum critical load of sulfur (pentile and median) in Figure 1.2. This map is included to illustrate the material which is provided to the integrated modellers of the UN/ECE LRTAP Task Force on Integrated Assessment Modelling. Also, Figure 1.3 enables close comparisons between the pentile (5th percentile) and median (50th percentile) of the maximum critical load of sulfur which would protect respectively 95% and 50% of the ecosystems from damage due to sulfur based acidity, i.e., in the case where nitrogen deposition is fully taken up or immobilized.

Please refer to Chapter 2 for other mapping details for the maximum critical load for sulfur and to Chapter 3 for methodological aspects.

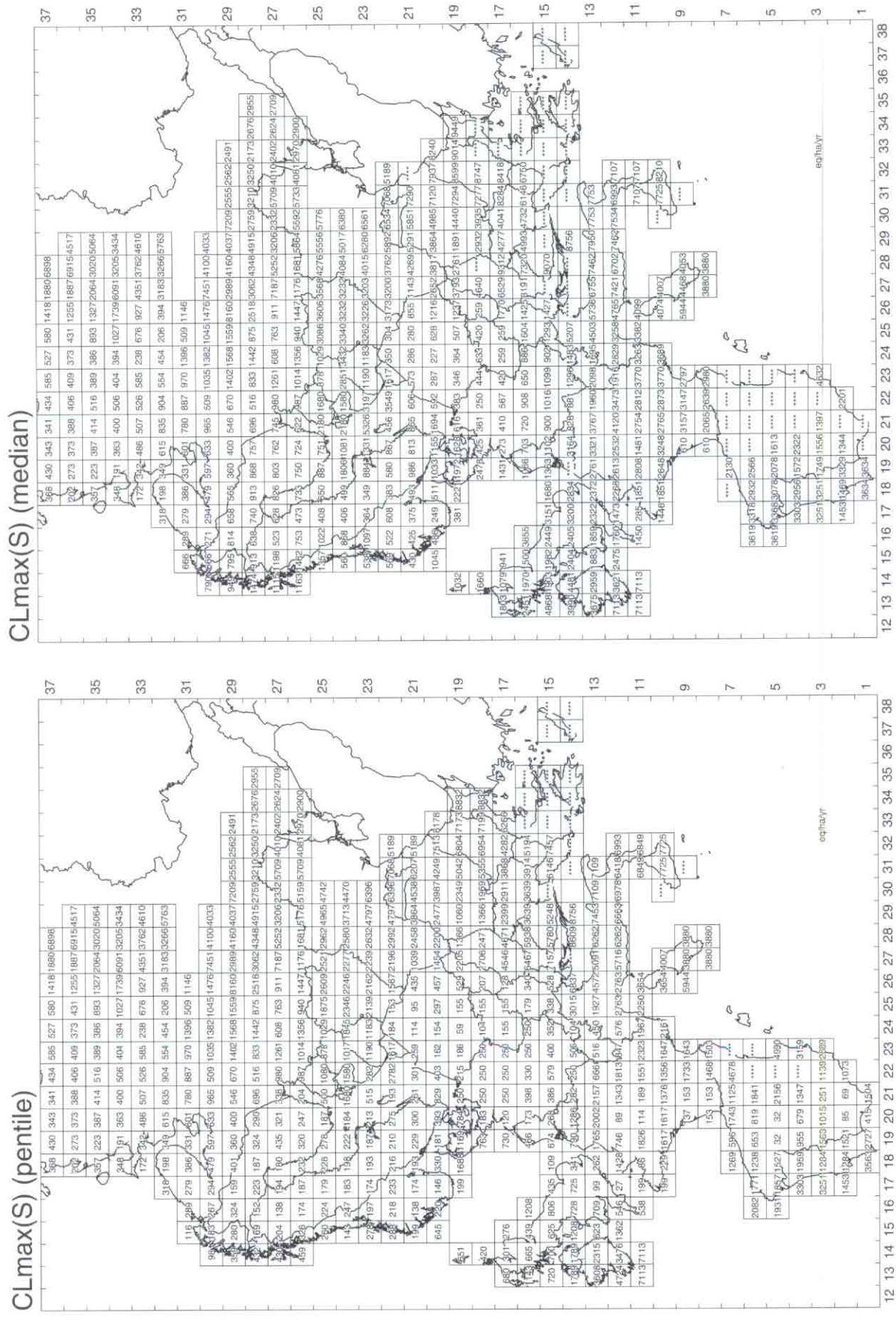


**Figure 1.3.** The pentile and median values of the maximum critical load of sulfur, $CL_{max}(S)$. ("****" denotes critical load values larger than 9999 eq $ha^{-1}$ $yr^{-1}$.)

## 1.4. The minimum critical load of nitrogen and the critical load for eutrophication

The minimum critical load for nitrogen, $CL_{min}(N)$, is the sum of nitrogen uptake and nitrogen immobilization. If nitrogen deposition is lower than $Cl_{min}(N)$, than nitrogen nutrient deficiency would occur. If nitrogen deposition exceeds $Cl_{min}(N)$, than acidification occurs when denitrification is too low and/or the sulfur deposition too high. If nitrogen deposition becomes even higher, i.e., exceeding the critical load for eutrophication, $Cl_{nut}(N)$, than too much nitrogen is leached, leading to vegetation changes favoring nitrogen-tolerant species.

Figure 1.4 shows the pentile and median value ranges of $Cl_{min}(N)$, (upper left and right graph respectively) and of $Cl_{nut}(N)$. The pentile minimum critical loads for nitrogen are lowest in the United Kingdom, Scandinavia and the northern part of Russia. Higher values occur especially in the United Kingdom and in the southern parts of Finland and Sweden as the median of the minimum critical loads of nitrogen is considered.

With regards to $Cl_{nut}(N)$, low value ranges (< 400 $eq^{-1}$ $yr^{-1}$) occur in northern Europe in particular. The median value ranges show higher values (as compared to the pentile) in Norway, west and central Europe and large parts in southern Europe.

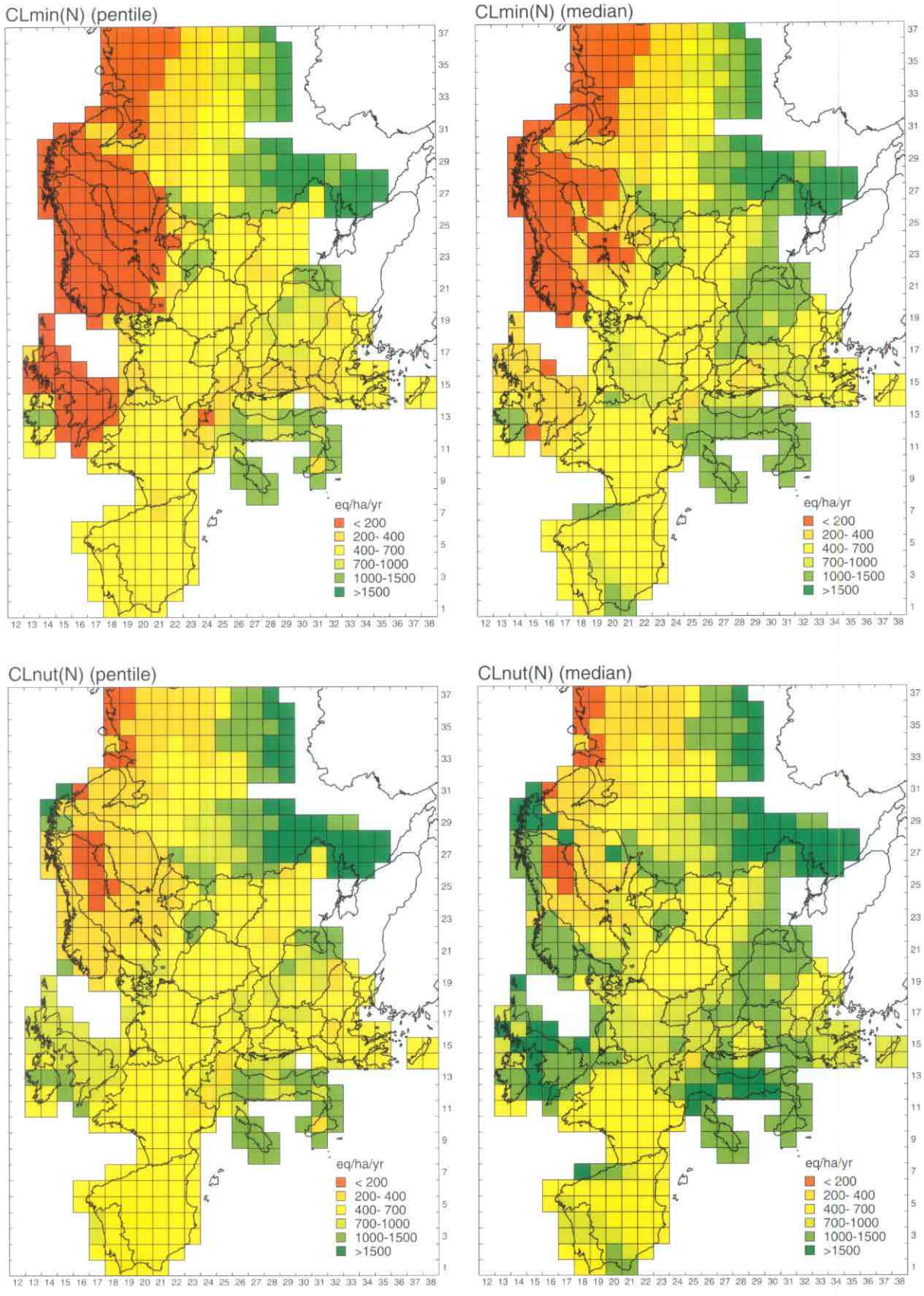


**Figure 1.4.** The pentile and median value ranges of the minimum critical load of nitrogen (upper left and right graph, respectively) and of the critical load for eutrophication (lower left and right maps respectively).

## 1.5. Required sulfur and nitrogen deposition reductions in 1990

Figure 1.5 shows:

(a) **Acidifying and eutrophying deposition reduction requirements in 1990 (upper left graph):** To achieve protection of 95% of the ecosystems in each grid cell against *both acidification and eutrophication*, 5 cases of reduction requirements of sulfur and/or nitrogen deposition can be distinguished: (1) no deposition reduction required (**grey** shading) in cases where the combination of sulfur and nitrogen deposition lies below the pentile protection isoline, (2) either sulfur or nitrogen deposition reduction are required (**blue** shading) in cases where the combination of sulfur and nitrogen deposition in 1990 lies outside the pentile protection isoline, but within the area delimited by the maximum critical load of sulfur, $Cl_{max}(S)$, on one hand, and the minimum of both the critical load for eutrophication, $Cl_{nut}(N)$, and the maximum critical load of nitrogen, $Cl_{max}(N)$, on the other hand, (3) only sulfur deposition reduction is required (**yellow** shading) in cases where sulfur deposition lies outside the pentile protection isoline, i.e., exceeds $Cl_{max}(S)$, and nitrogen deposition does not exceed the minimum of both $Cl_{nut}(N)$, and $Cl_{max}(N)$, (4) only nitrogen deposition reduction is required (**orange** shading) in cases where nitrogen deposition lies outside the pentile protection isoline, i.e., exceeds the minimum of both $Cl_{nut}(N)$ and $Cl_{max}(N)$, and sulfur deposition does not exceed $Cl_{max}(S)$, and (5) both sulfur and nitrogen deposition are required (**red** shading) in cases where the deposition combination lies outside the area delimited by $Cl_{max}(S)$ and the minimum of both $Cl_{nut}(N)$ and $Cl_{max}(N)$.

In 1990, the result shows that in large areas in central, western and northern Europe both sulfur and nitrogen deposition need to be reduced, and that mandatory nitrogen deposition reductions are required in south eastern Europe.

(b) **Ecosystem protection against acidification and eutrophication in 1990 (upper right graph):** This graph shows the actual percentage of the ecosystem area protected against both acidification and eutrophication due to the sulfur and nitrogen deposition in 1990. The graph shows that the combination of sulfur and nitrogen depositions in 1990, though not protecting 95% of the ecosystems everywhere in Europe, does achieve lower protection levels. This means that the combination of sulfur and nitrogen deposition lies on higher percentile protection isolines than the pentile protection isoline in (a). Note that in Germany and Poland a large majority of ecosystems is unprotected due to relatively high 1990 depositions of both sulfur and nitrogen and the relatively stringent critical loads for eutrophication in these areas.

(c) **Acidifying deposition reduction requirements in 1990 (lower left graph):** This graph is similar to (a) with the difference that *only acidification* is considered for the identification of deposition reduction requirements of sulfur and/or nitrogen. A much smaller area, in comparison to the area described in (a), is subject to required reductions of both sulfur and nitrogen deposition to achieve 95% protection against acidification. However, the area where mandatory reductions of sulfur deposition is required (yellow shading) increases as compared to (a). Note that hardly any area can be identified where only nitrogen deposition reduction is required.

(d) **Ecosystem protection against acidification in 1990 (lower right graph):** When protection against acidification due to 1990 sulfur and nitrogen deposition is considered a comparison to the graph described in (b) shows that in general higher protection percentages are achieved. The shift towards higher percentage protection is less significant in central European countries where depositions of both sulfur and nitrogen are relatively high. The shift to high protection in southern east Europe is due to relatively high maximum critical loads of nitrogen. For these regions it is clear from comparison to (b) that the critical load for eutrophication is limiting.

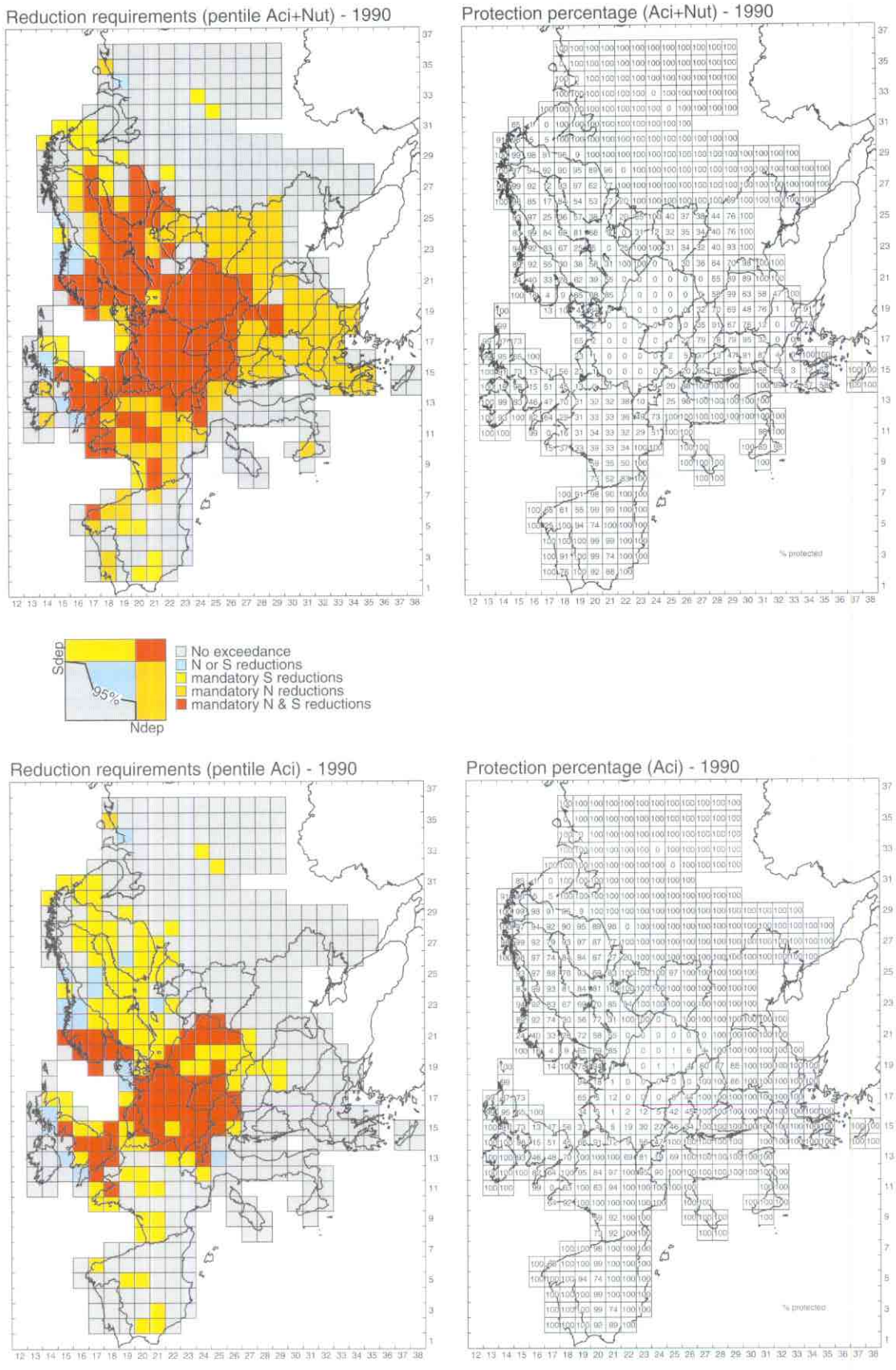


**Figure 1.5.** Using the deposition of sulfur and nitrogen based on 1990 emissions, the following graphs are shown: (a) Acidifying *and* eutrophying (sulfur and nitrogen based) deposition reduction requirements (upper left graph); (b)Ecosystem protection against acidification *and* eutrophication (upper right graph); (c) Acidifying deposition reduction requirements (lower left graph); (d) Ecosystem protection against acidification (lower right graph).

## 1.6. Required sulfur and nitrogen deposition reductions in 2010

Figure 1.6 is similar to Figure 1.5 with the exception of the target year 2010. The results shown in Figure 1.6 are based on an analysis of the sulfur deposition in 2010, computed from the $SO_2$ emissions as agreed in the Second Sulfur Protocol, and the nitrogen deposition computed from UN/ECE data on Current Reduction Plans for emissions of reduced and oxidized nitrogen (EB.AIR/WG.5/R52, pp. 10-11). Results from Figure 1.6 can be summarized as follows (see Figure 1.5 for background information on the kinds of maps):

(a) **Acidifying and eutrophying deposition reduction requirements in 2010 (upper left graph):** In 2010, still a large area (red shading) in central and western Europe is subject to the requirement to reduce *both sulfur and nitrogen deposition* to protect 95% of the ecosystems against both acidification and eutrophication. In comparison to Figure 1.5, a shift to the requirement of only reducing nitrogen deposition (orange shading) is seen in southern parts of Scandinavia. Note that nitrogen deposition reductions, as in Fig. 1.5a, are required in large parts of south eastern Europe, including Greece, Bulgaria, Rumania and the Western part of the Ukraine.

(b) **Ecosystem protection against acidification and eutrophication in 2010 (upper right graph):** This graph shows the percentage of the ecosystem area protected against both acidification and eutrophication due to the sulfur and nitrogen deposition in 2010. The graph shows that the combination of sulfur and nitrogen depositions in 2010, though not protecting 95% of the ecosystems everywhere in Europe, does achieve lower protection levels. This means that the combination of sulfur and nitrogen deposition lies on higher percentile protection isolines than the pentile protection isoline used for the analysis described in (a). In comparison to Figure 1.5, an increase of the protection level is occurring in many areas in Europe, in particular in the United Kingdom and in Scandinavia. Also the area where 95% of the ecosystems is protected increases in comparison to Figure 1.5b. Hardly any change in protection against both acidification and eutrophication occurs in Germany and Poland.

(c) **Acidifying deposition reduction requirements in 2010 (lower left graph):** This graph is similar to (a) with the difference that *only acidification* is considered for the identification of deposition reduction requirements of sulfur and or nitrogen. A much smaller area, in comparison to the area described in (a), is subject to required reductions of both sulfur and nitrogen deposition to achieve 95% protection against acidification. Note the area of mandatory nitrogen-only deposition reduction is reduced in comparison to (a) and that also the area of mandatory sulfur-only deposition reductions is reduced in comparison to Figure 1.5c.

(d) **Ecosystem protection against acidification in 2010 (lower right graph):** The percentage of areas protected against acidification, due to 2010 sulfur and nitrogen deposition, increases markedly also in other areas in Europe in comparison to the graph described in (b). The increased protection levels due to exclusion of nitrogen nutrient impacts, demonstrates the limiting characteristics of the critical load for eutrophication.

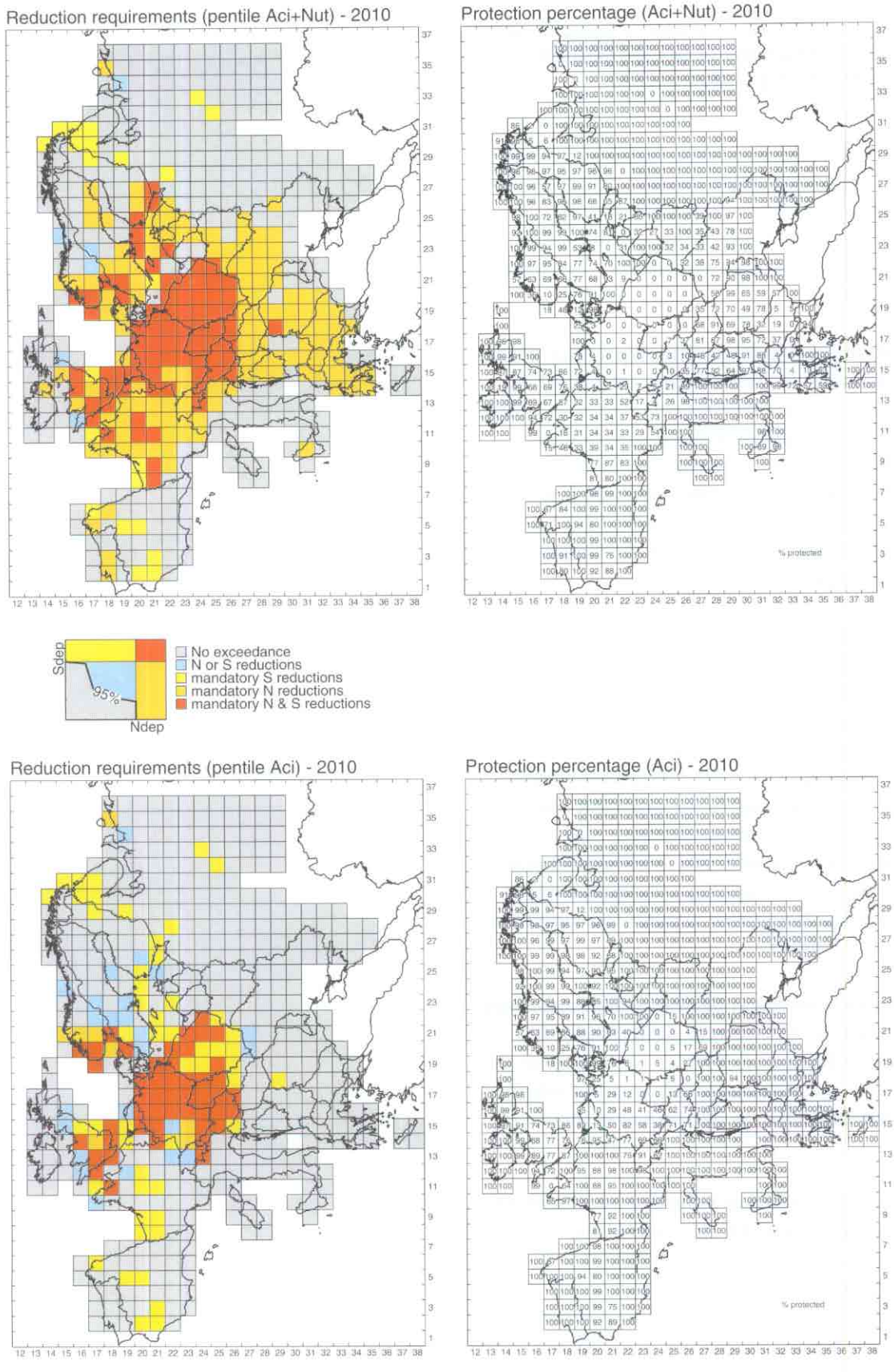


**Figure 1.6.** Using the sulfur deposition in 2010 based on the Second Sulfur Protocol $SO_2$ emissions, and nitrogen deposition in 2010 based on Current Reduction Plans (CRP) for emissions of oxidized and reduced nitrogen, the following graphs are shown: (a) Acidifying *and* eutrophying (sulfur and nitrogen based) deposition reduction requirements (upper left graph); (b) Ecosystem protection against acidification *and* eutrophication (upper right graph); (c) Acidifying deposition reduction requirements (lower left graph); (d) Ecosystem protection against acidification in 2010 (lower right graph).

## 1.7. Required reductions of the combined CD(S) and nitrogen deposition in 1990

Figure 1.7 shows the deposition reduction requirements and protection levels resulting from investigating the critical sulfur deposition which was developed for the support of the Second Sulfur Protocol and 1990 nitrogen deposition. The results are as follows:

(a) **Acidifying and eutrophying deposition reduction requirements in 1990 (upper left graph):** In comparison to Figure 1.6a the area increases where reductions of nitrogen deposition is required to achieve 95% protection of ecosystem areas. Areas where reductions of both sulfur and nitrogen deposition are required are predominantly found in central Europe, the eastern part of the United Kingdom and the western part of France.

In comparison to Figure 1.5a a much larger area, including south eastern parts of Europe, becomes subject to deposition reduction requirements of nitrogen only, rather than both sulfur and nitrogen. However, some grid cells of Figure 1.7 exhibit an increased requirement for the reduction of sulfur deposition in comparison to the same grid cells in Figure 1.6., which is counter-intuitive. The reason are the data improvements which have been summarized in Section 1.2 leading to instances where the critical sulfur deposition exceeds the maximum critical load for sulfur.

(b) **Ecosystem protection against acidification and eutrophication in 1990 (upper right graph):** In comparison to Figure 1.6, a lower percentage of the ecosystems is protected especially in areas where the nitrogen deposition in 2010 is lower than in 1990.

(c) **Acidifying deposition reduction requirements in 2010 (lower left graph):** In comparison to Figures 1.5 and 1.6, a smaller area in Europe is subject to reduction requirements of both sulfur and nitrogen deposition to achieve 95% protection against acidification. Mandatory reductions of nitrogen deposition remain in western Europe, and in southern Norway.

(d) **Ecosystem protection against acidification in 1990 (lower right graph):** The same conclusion as expressed under (b) holds.

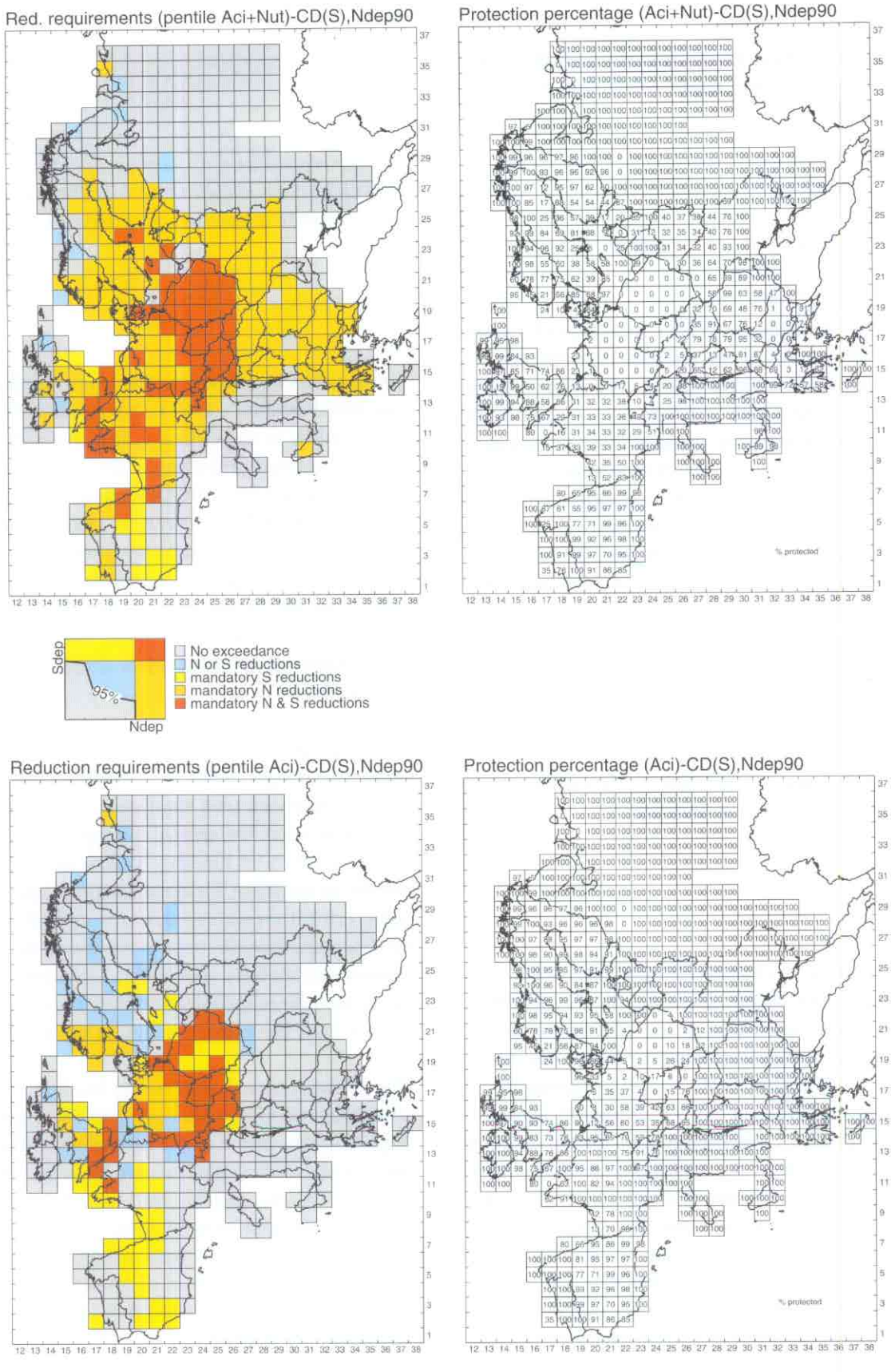


**Figure 1.7.** Using the critical sulfur deposition developed for the support of the Second Sulfur Protocol and CRP emission based depositions of oxidized and reduced nitrogen in 1990, the following graphs are shown: (a) Acidifying *and* eutrophying (sulfur and nitrogen based) deposition reduction requirements (upper left graph); (b) Ecosystem protection against acidification *and* eutrophication (upper right graph); (c) Acidifying deposition reduction requirements (lower left graph); (d) Ecosystem protection against acidification (lower right graph).

## 1.8. Binding critical thresholds through the comparison of critical loads, levels and health guidelines

This section describes a tentative analysis of the relative importance of critical loads, critical levels, and WHO health guidelines. The analysis attempts to derive atmospheric concentrations from critical loads in order to allow comparisons with atmospheric threshold indicators, both from an environmental sustainability as well as from a health point of view. The result of the analysis is to identify which of the three critical thresholds, (critical loads, critical levels and health guidelines) are most limiting, i.e. binding from the point of view of emission reduction requirements. The 9-year average sulfur deposition velocity, $v_{d,S}$, of the atmospheric concentrations of all sulfur compounds was derived using EMEP data on sulfur concentrations and sulfur deposition in each grid cell between 1985 and 1993. Similarly, a 9-year average nitrogen-deposition velocity, $v_{d,N}$, was computed using concentrations of NO and $NO_2$ and deposition of oxidized nitrogen. The following derived critical thresholds were then computed:

(a) The critical level of $SO_x$ due to the critical sulfur deposition, $[SO_x]_{CD(S)}$ was derived:

$$[SO_x]_{CD(S)} = \frac{CD(S)}{v_{d,S}}$$

The comparison in each EMEP grid cell, of the computed values of this derived critical level for $SO_x$ with the annual mean of the environmental (agricultural crop) critical level for sulfur dioxide (30 µg $m^{-3}$ $yr^{-1}$) and with the health guideline for sulfur dioxide (50 µg $m^{-3}$ $yr^{-1}$) is shown in Figure 1.8 (upper graph). The preliminary results indicate that health guidelines are binding in southern Europe in general and Greece in particular (red shadings). Therefore, in these areas the critical sulfur deposition might not be binding, i.e., too high in comparison to other critical thresholds, and its use in integrated modelling assessments might not lead to appropriate emission reduction recommendations for these areas.

Some other areas (yellow shadings) indicate that the critical level of $SO_2$ for agricultural crop is binding. However, the critical sulfur deposition used for the scientific support of the Second Sulfur Protocol remains binding in most parts of Europe.

(b) The critical level of nitrogen oxides due to the critical load of nitrogen based acidity given the critical sulfur deposition was derived as follows:

$$[NO_x]_{CL(N|CD(S))} = \frac{CL(N|CD(S))}{v_{d,N}}$$

Using protection isolines, the critical load of nitrogen-based acidity, $CL(N|CD(S))$, is derived by fixing sulfur to the critical sulfur deposition, $CD(S)$, and the derived critical level for nitrogen oxides is easily obtained from this equation. The comparison, in each EMEP grid cell, of the computed values of this derived critical level for $NO_x$ with the annual mean of the environmental critical level for sulfur dioxide (30 µg $m^{-3}$ $yr^{-1}$) and, for illustrative purposes, with the 4-hour mean (95 µg $m^{-3}$ $yr^{-1}$) environmental critical level, is shown in Figure 1.8 (lower graph).

In a large part of Greece the 4-hour mean critical level for nitrogen oxide is lower than the critical load for nitrogen (red shadings). In other southern European areas the annual averaged critical level shows to be more binding (yellow shading). Again, results in southern European regions indicate that other critical thresholds than the critical load may be more appropriate targets for use in integrated assessment models. However, extending the analysis to include eutrophication, it turns out that the critical load for eutrophication is most binding.

The analysis aimed at deriving binding critical thresholds should be extended to other pollutants. Especially the effect of the reduction of the exceedance of the critical load for nitrogen (i.e. the minimum of $Cl_{max}(N)$ and $Cl_{nut}(N)$) and the relationship between nitrogen dioxide concentrations, critical levels for nitrogen and tropospheric ozone formation in EMEP grid cells is of interest. For example, Figures 1.5 and 1.6 indicate that nitrogen deposition reduction are required in areas (western Europe) where the formation of tropospheric ozone is VOC-limited (cf. also Hettelingh and de Leeuw 1994). This means that reductions of nitrogen deposition, and related nitrogen oxide concentrations, may lead to an increase of tropospheric ozone concentrations.

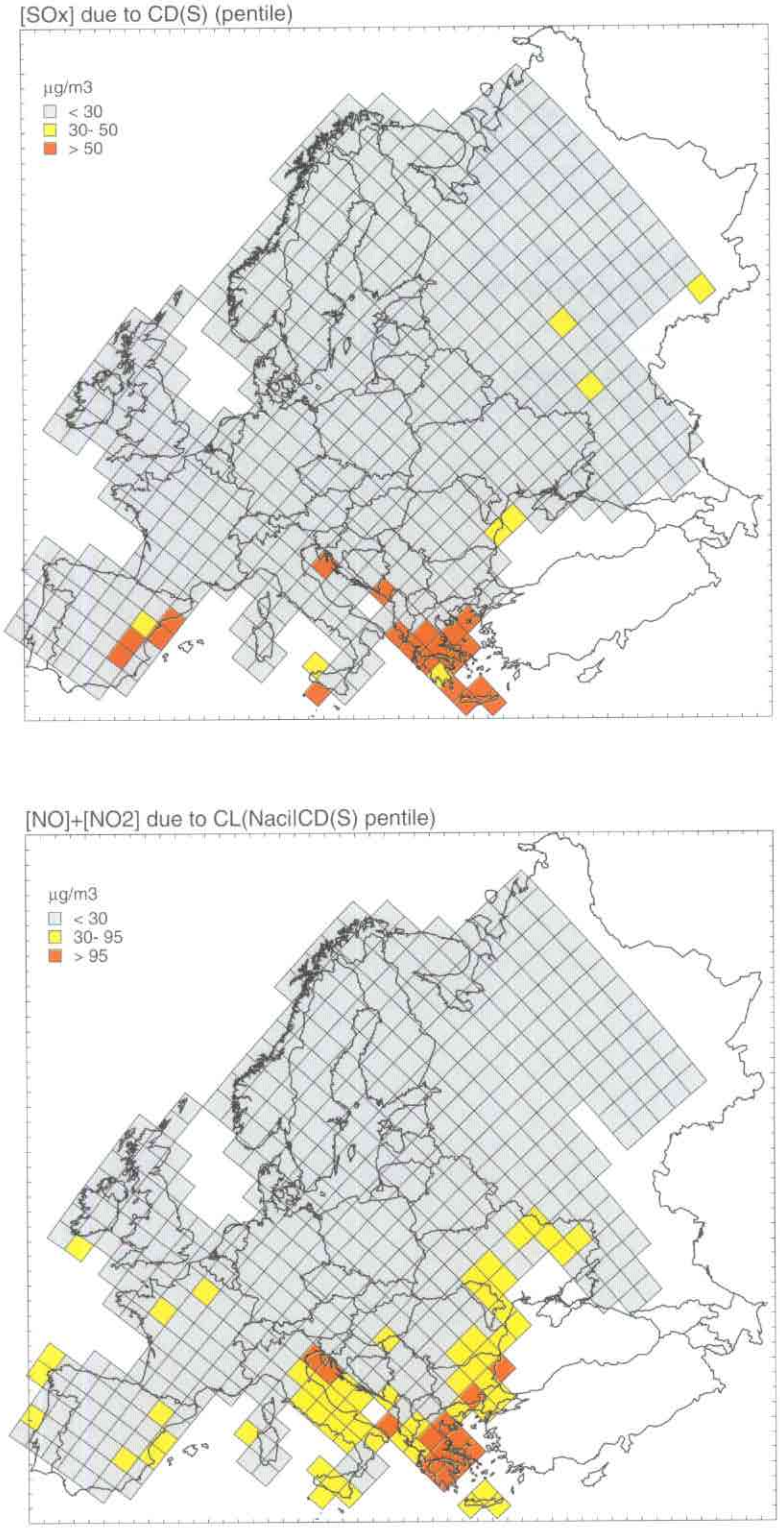


**Figure 1.8.** The upper graph shows where in Europe health guidelines for sulfur dioxide (red shadings) or environmental critical levels (yellow shading) are lower (i.e., binding from an integrated assessment point of view) than the critical sulfur deposition which was used for the scientific support of the Second Sulfur Protocol. The lower graph shows where in Europe 4-hour mean environmental critical levels for NOx (red shadings) and annual average critical levels (yellow shadings) are lower than the critical load for nitrogen given the critical sulfur deposition.

## References


Downing, R.J., J.P. Hettelingh, and P.A.M. de Smet (eds.), 1993. Calculation and Mapping of Critical Loads in Europe: Status Report 1993. CCE, RIVM Rep. 259101003. Bilthoven, The Netherlands.

Hettelingh, J.-P. and F.A.A.M. de Leeuw, 1994. Mapping Critical Loads and Levels in Europe. In: Fuhrer, J. and B. Achermann (eds.), Critical levels for ozone. Proceedings, Federal Office of Environment, Forests and landscape, Bern, Switzerland.

Hettelingh, J.-P., R.J. Downing, and P.A.M. de Smet (eds.), 1991. Mapping Critical Loads for Europe. Technical Report No. 1, RIVM Rep. 259101001, Bilthoven, the Netherlands.

Hettelingh, J.-P., M. Posch, P.A.M. de Smet, and R.J. Downing, 1995. The Use of Critical Loads in Emission Reduction Agreements in Europe. *Water Air Soil Pollut.*, in press.

# 2. Summary of National Data Contributions

*P.A.M. de Smet*

## 2.1 Introduction

Since the April 1995 CCE workshop in Helsinki, critical load data bases for Europe have been updated. The products are maps and data bases with critical load percentiles and ecosystem protection percentages (See Chapter 1). At the workshop, the National Focal Centers (NFCs) were requested to submit an update on their national data by 31 May 1995. Many NFCs submitted improved or revised critical load data. However, some submissions arrived after the deadline. The resulting European maps were adopted by the Working Group for Effects (WGE, July 1995) and presented to the Working Group on Strategies (WGS, August 1995). After eliminating inconsistencies in the calculation of European background critical loads, the Task Force on Integrated Assessment Modelling (TFIAM) was provided data bases with protection isolines.

This chapter gives an overview of which countries contributed national data, and summarizes the contents of the data bases. It concludes with some experiences the CCE has had with collating European maps and data bases based on a variety of national contributions.

## 2.2 National contributions

The countries for which the European maps consist of national data are listed in Table 2.1. Countries which sent updated data were the Denmark, Finland, Germany, Norway, Poland, Switzerland, Sweden and the United Kingdom. For Russia and the Netherlands no updated data were received, and thus previous submissions were used. For the Czech Republic the update was received after the deadline, and could not be incorporated.

From Austria data including nitrogen critical loads were received for the first time. Estonia submitted national contributions for the first time.

First national submissions by Spain and Italy were unfortunately too late to be incorporated, and the data require some adaption before being incorporated in the European maps. France expects to have a national data base available for the CCE shortly. In total, 13 national contributions were received.

The critical loads maps presented in this report are based on recently updated European background data (September 1995). For those EMEP cells which are not covered by any national data submissions, critical loads have been computed from the European background data base.

Figure 2.1 shows the countries that (a) contributed with national data or from which a contribution is expected soon, and (b) the EMEP cells in which the critical load calculations are based on either national data or on European background data. When a country contributes data for an EMEP cell, the critical loads based on the European background data base for that cell are not used, independent of the area of that country in that cell.

## 2.3 Selected receptors and ecosystems

Every country has selected one or more specific ecosystem types as receptors for mapping critical loads of sulfur and nitrogen. Some NFCs selected an ecosystem/receptor to quantify the critical loads concerning the eutrophying effects only (i.e. critical load for nutrient nitrogen). Others included for the same receptor type critical loads concerning acidification effects (i.e. maximum and minimum critical loads for sulfur and nitrogen). For the receptor type 'fresh water (catchments)', only the critical loads for acidification were calculated, assuming that eutrophication does not occur in fresh water ecosystems. Table 2.2 and Figure 2.2 describe which receptor types have been selected in each country.

**Table 2.1.** National data contributions used in the European maps.

| Country | Submission date | Remarks |
|---|---|---|
| Austria | July 1995 | WGE map amended, new data submission incorporated before WGS. |
| Czech Republic | March 1994 | Update (23 June 1995) not used: too late and not required information. |
| Denmark | June 1995 | |
| Estonia | June 1995 | First contribution. |
| Finland | June 1995 | |
| Germany | May 1995 | |
| Netherlands | June 1994 | No update. |
| Norway | May 1995 | |
| Poland | June 1995 | |
| Russia | May, Nov. 1993 | No update. |
| Sweden | June 1995 | |
| Switzerland | May 1995 | WGE map amended: for EMEP cell (24,12) Swiss data excluded. |
| United Kingdom | May 1995 | |
| **Not included:** | | |
| Spain | July 1995 | First contribution not used: too late and not required information. |
| Italy | August 1995 | First contribution not used: too late and not required information. |
| France | October 1995 | NFC report in this report; data to be delivered in the near future. |

**Table 2.2.** Receptor ecosystems selected by the NFCs for calculating critical loads.

| Country | Forest | | Freshwater (catchments) | | Peatland | | Heathland | | Grassland | |
|---|---|---|---|---|---|---|---|---|---|---|
| | acid | eutro | acid | eutro | acid | eutro | acid | eutro | acid | eutro |
| Austria | + | + | | | | | | | | |
| Czech Republic | + | + | | | | | | | | |
| Denmark | + | + | | | | | | | | |
| Estonia | + | + | | | + | + | | | | |
| Finland | + | + | + | | | | | | | |
| Germany | + | + | | | | | | | | |
| Netherlands | + | + | | | | | | | | |
| Norway | + | + | + | | | | | | | |
| Poland | + | + | | | | | | | | |
| Russia | + | + | + | | | | | | | |
| Sweden | + | + | + | | | | | | | |
| Switzerland | + | + | + | | | + | | | | + |
| United Kingdom | + | + | + | | | | + | + | + | + |

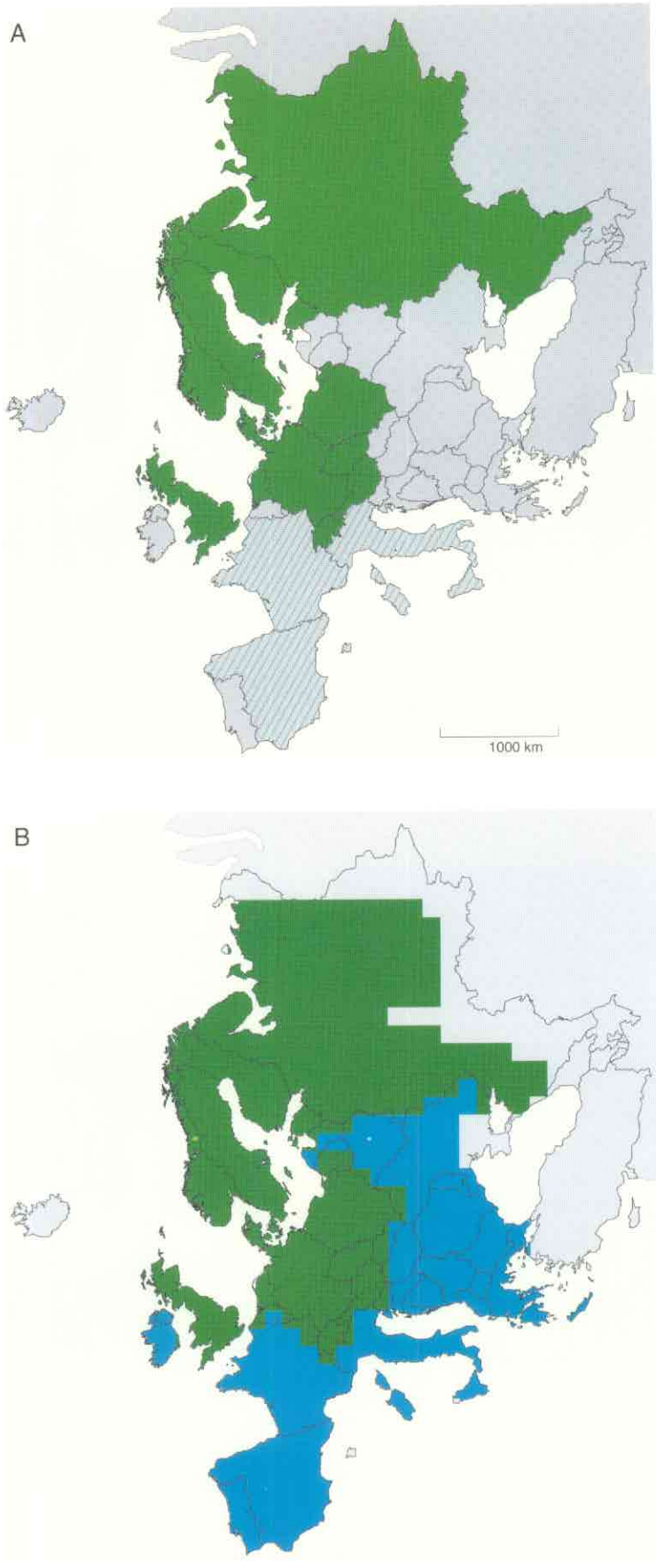


**Figure 2.1.** National contributions on critical loads for nitrogen and sulfur: (a) Contributions by country. Thirteen countries contributed national data (dark green). From three countries (Spain, France and Italy) a contribution is expected soon (striped green). (b) Data sources per EMEP cell. Dark green denotes national contributions; light green, the European background data base.

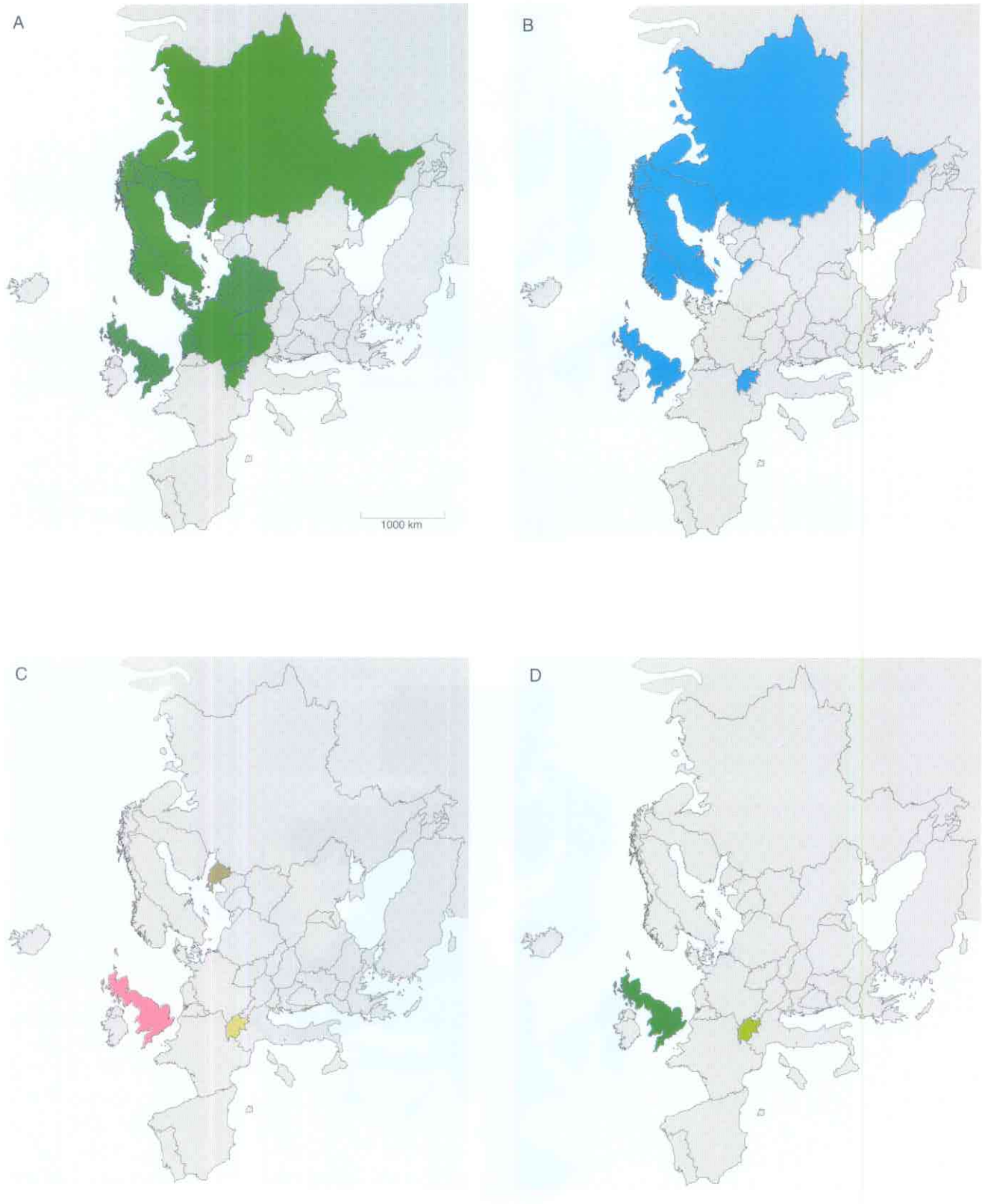


**Figure 2.2.** The ecosystems selected as receptors for calculation of the loads. (a) countries with forests as receptors (green). All calculated acidification and eutrophication critical loads. Some countries subdivide their forests into its specific forest type (striped); (b) countries with fresh water (catchments) as receptor. All calculated eutrophication critical loads only; (c) countries with peatland (green) or heathland (pink) as receptor. Calculated critical loads: Estonia: both acidification and eutrophication (dark green); Switzerland: eutrophication only (light green); U.K.: both acidification and eutrophication (pink); (d) countries with grassland receptors. Calculated critical loads: U.K.: both acidification and eutrophication (dark green); Switzerland: eutrophication only (light green).

The following is an overview of the receptor types selected by each country. (See also individual NFC reports in Part III).

*Austria* selected forests, natural grasslands and bogs. Due to some complications, only the forest critical loads have been used for the European maps. *Czech Republic* and *Germany* submitted data for forest soils only. *Denmark* submitted data for four forest types: beech, oak, spruce and pine. *Estonia* selected pine-podzol, pine-bog, spruce-podzol, spruce-alvar, deciduous-podzol and deciduous-wet as forest soils and bogs as peatland. *Finland* contributed with three forest types (spruce, pine and deciduous) and lake catchments. The *United Kingdom* submitted ecosystem critical loads for Great Britain for the following receptors: deciduous and coniferous woods, grassland, heathland and aquatic catchments (refer to the NFC report for special details on applied methods). *The Netherlands* selected 12 forest types as receptor. Six types are deciduous: black alder, birch, ash, beech, poplar and oak. The other six are coniferous types: Japanese larch, Norway spruce, Douglas fir, black pine, Scots pine and willow. *Norway* collected critical load data points for forest and lake catchments, and submitted the receptor type with the lowest critical load per national grid cell. *Poland* submitted national data for deciduous and coniferous forests, and submitted the lowest critical loads. The data bases for *Russia* and *Sweden* consist of critical loads for forests and fresh water catchments. *Switzerland* has selected a wide range of receptors: for critical loads of acidity, it submitted data for managed forests and alpine lake catchments. For eutrophying critical loads it used only managed forests data. In addition, it submitted data bases with empirical eutrophying critical loads concerning (semi-)natural ecosystems: ground flora in acidic (managed) coniferous, acidic (managed) deciduous and calcareous forests, calcareous and neutral-acid species-rich grassland, montane (sub)alpine grassland, shallow soft-water bodies, mesotrophic fens, and ombrotrophic bogs.

The different resolutions of the national data collections are not discussed in this chapter, but are described in the individual NFC reports in Part III. Figure 2.3 presents the number of records per EMEP grid cell for acidifying critical loads. Countries with high-resolution data (i.e. small national grid cells or points), or which have selected more then one receptor type show larger numbers of data points (blue classes). The EMEP grid cells containing data from the European background data base are all represented by the class 11-100 records (cf. to Figure 2.1b). The cells with Russian national data show that the critical loads percentiles are actually based on one data point for an entire EMEP grid cell. Thus, all percentiles and protection isolines are identical for these cells. Where multiple receptors in each grid cell were used, and the lowest critical loads submitted, the CCE has computed percentiles and protection isolines out of this reduced set of critical load values. This may increase uncertainties compared to using the complete set of critical loads.

## 2.4 Experiences with national contributions

This chapter concludes with some experiences the CCE has with collating European maps and data bases based on a variety of national contributions.

Most NFCs followed the requested setup and format in which the data should be submitted very well. However, a few NFCs need to invest more effort in preparing their data in the requested format. Unfortunately, some countries do not meet agreed submission deadlines, or submit data inadequate to calculate the percentiles.
Both situations cause significant time delays and jeopardize the timely delivery of European maps and data bases to Task Forces and Working Groups. The most time-consuming task in collating European maps is checking the national data bases for inconsistencies, working with NFCs to resolve problems, and receiving corrections. This lengthy process could be avoided if the NFCs would thoroughly check their data before submission.

Due to tight deadlines for delivering the products needed in the TFM, TFIAM, WGE and WGS, the CCE has to become stricter in accepting data bases that are not in the requested format. Furthermore, the growing size of national data bases, continuing updating activities and the increasing number of pollutants to be mapped require the CCE to adhere more rigorously to agreed-upon deadlines. To improve the consistency of the national data submitted, the CCE will include in its next request for data instructions which the NFCs can use for checking their data bases before submission.

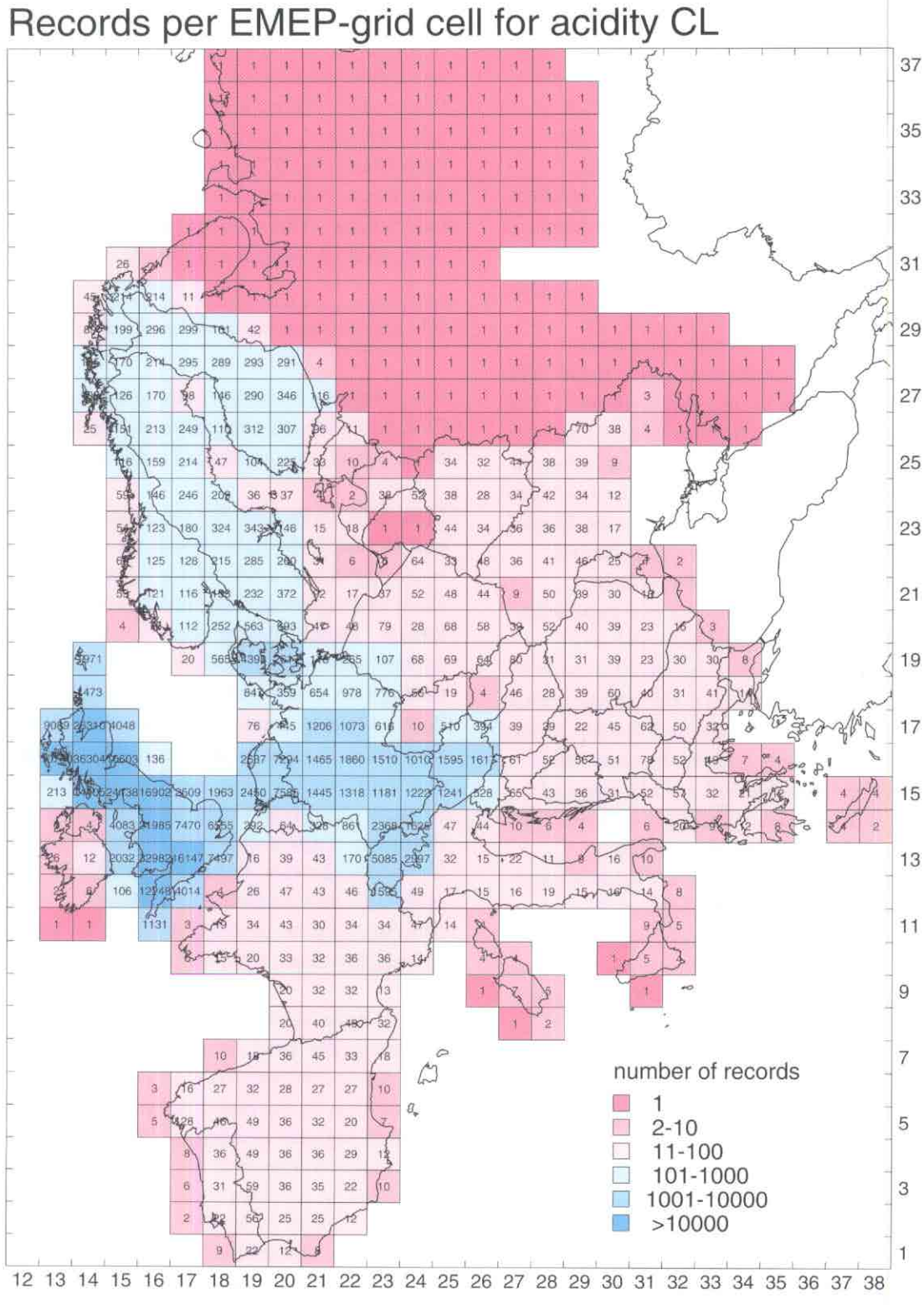


**Figure 2.3.** The number of ecosystems per EMEP cell for the acidifying critical loads. (The legend represents a logarithmic scale.) Data for eutrophying critical loads show a very similar picture.

As is clear from Figure 2.3, some countries should consider increasing their data resolution. The percentile and protection isoline computations will then become more meaningful. Furthermore, the pre-selection of only the lowest critical load data in a national grid cell should also be avoided.

As a general conclusion, the quality of national data contributions has improved significantly since the CCE Status Report 1993. The data bases prove that the NFCs have made important progress in national mapping activities and critical load calculation methods.

# 3. Critical Loads of Sulfur and Nitrogen

*M. Posch, W. de Vries* and J.-P. Hettelingh*
*DLO Winand Staring Centre, P.O.Box 125, NL-6700 AC Wageningen

## Introduction

Critical loads of sulfur (S) and nitrogen (N) are derived with the Simple Mass Balance (SMB) equation/model, also called Steady-State Mass Balance (SSMB) equation/model. The first name indicates that we are simplifying the description of the biogeochemical processes involved, a necessity when considering the large-scale application (Europe) and the lack of adequate input data. The second name indicates that we are dealing with steady-state conditions only, leading to considerable simplifications. These models and methods have been elaborated in several Task Force Meetings and workshops (see Nilsson and Grennfelt 1988, Sverdrup *et al.* 1990, Grennfelt and Thörnelöf 1992, Downing *et al.* 1993, Hornung *et al.* 1995) and are also subject of various publications in the open literature (for an in-depth treatment in a wider context see also de Vries 1994).

In the following we derive critical loads for forest soils. In the SMB model the soil is treated as a single homogeneous compartment and its depth is equal to the root zone. Further simplifying assumptions include:

- weathering and uptake are evenly distributed over the soil profile
- the weathering rate is independent of soil chemical conditions (such as pH)
- all evapotranspiration occurs at the top of the soil profile
- percolation is constant through the soil profile and occurs only vertically
- physico-chemical constants (such as $K_{gibb}$) are assumed uniform in the whole soil profile
- critical chemical values determined in laboratory experiments apply to field conditions

Critical loads for surface waters are not treated here. A recent summary of a method to calculate such critical loads, based on the SMB model, can be found in Henriksen and Posch (1995).

## 3.1 Critical loads of acidifying sulfur and nitrogen

In this section we derive a simplified acidity balance for a homogeneous soil compartment considering the main sources and sinks of sulfur and nitrogen and then use this balance to derive critical loads for S and N, both for constant and deposition-dependent sink terms.

### 3.1.1 Deriving a simplified acidity balance:

We start from the charge balance of the ions in the soil leachate flux (see de Vries 1991):

$$H_{le} + Al_{le} + BC_{le} + NH_{4,le} = \\ = SO_{4,le} + NO_{3,le} + Cl_{le} + HCO_{3,le} + RCOO_{le} \quad (3.1)$$

where the subscript *le* stands for leaching, *BC* is the sum of base cations ($BC=Ca+Mg+K+Na$), *RCOO* is the sum of organic anions, and *Al* stands for all aluminum species. The concentrations of *OH* and $CO_3$ are assumed zero, which is a reasonable assumption even for calcareous soils. The units used are eq/ha/yr (identical to $mol_c\ ha^{-1}a^{-1}$ in proper SI nomenclature). We define (the leaching of) alkalinity as:

$$Alk_{le} = HCO_{3,le} + RCOO_{le} - H_{le} - Al_{le} \quad (3.2)$$

Combination with Eq.3.1 yields:

$$BC_{le} + NH_{4,le} - SO_{4,le} - NO_{3,le} - Cl_{le} = Alk_{le} \quad (3.3)$$

which also displays an alternative definition of alkalinity as "sum of (base) cations minus strong acid anions". While the pH of the soil leachate is dependent on the partial pressure of $CO_2$, alkalinity is not (since the left-hand side of Eq.3.3 is not). It is therefore a preferred measure for the acidification status of a soil.

Chloride is assumed to be a tracer, i.e. there are no sources or sinks of chloride within the soil compartment, and therefore it is equal to the chloride deposition (subscript *dep*):

$$Cl_{le} = Cl_{dep} \tag{3.4}$$

In a steady-state situation the leaching of base cations has to be balanced by the net input of base cations. Consequently the following equation holds:

$$BC_{le} = BC_{dep} + BC_{w} - BC_{u} \tag{3.5}$$

where the subscripts *w* and *u* stand for weathering and net growth uptake, i.e. the net uptake by vegetation that is needed for long-term average growth. Base cation input by litterfall and base cation removal by maintenance uptake (needed to re-supply base cations in leaves) is not considered here, assuming that both fluxes are equal (in a steady-state situation). Also the finite pool of base cations at the exchange sites (cation exchange capacity, CEC) is not considered here. Although it might buffer incoming acidity for decades, its influence is only a temporary phenomenon, which cannot be taken into account when considering long-term steady-state conditions.

The leaching of sulfate and nitrate can be linked to the deposition of these compounds by means of mass balances for S and N. For sulfur this reads (de Vries 1991):

$$S_{le} = S_{dep} - S_{ad} - S_{u} - S_{i} - S_{re} - S_{pr} \tag{3.6}$$

where the subscripts *ad*, *i*, *re* and *pr* refer to adsorption, immobilization, reduction and precipitation, respectively. An overview of sulfur cycling in forests by Johnson (1984) suggests that uptake, immobilization and reduction of S is generally insignificant. Adsorption (and in some cases precipitation with Al complexes) can temporarily lead to a strong accumulation of sulfate (Johnson *et al.* 1979, 1982). However, sulfate is only stored or released at the adsorption complex when the input (deposition) *changes*, since the adsorbed S is in equilibrium with the soil solution S. Only dynamic models can describe the time pattern of ad- and desorption of sulfate (and of base actions at the exchange sites), but under long-term steady-state conditions S ad- and desorption and precipitation/mobilization should not be considered. Since sulfur is completely oxidized in the soil profile, $SO_{4,le}$ equals $S_{le}$, and consequently:

$$SO_{4,le} = S_{dep} \tag{3.7}$$

For nitrogen the mass balance reads:

$$N_{le} = N_{dep} + N_{fix} - N_{i} - N_{u} - N_{de} - N_{ad} - N_{fire} - N_{eros} - N_{vol} \tag{3.8}$$

where the subscripts *fix* refers to fixation of N, *de* to denitrification, and *fire*, *eros* and *vol* to the loss of N due to forest fires, erosion and volatilization. $N_i$ is the long-term immobilization of N in the root zone, and $N_u$ the net growth uptake (see $BC_u$ above). Nitrogen adsorption is neglected for the same reasons as sulfur adsorption. Nitrogen fixation is considered negligible in most forest ecosystems, except for nitrogen-fixing species such as red alder (Van Miegroet and Cole 1984). The loss of N due to forest fires, erosion and volatilization is small for most forest ecosystems, and therefore neglected in the following discussion (see, however, Hornung *et al.* 1995 and UN/ECE 1995). Alternatively, one can consider these terms included in the $N_i$-term, i.e. replace $N_i$ by $N_i+N_{fire}+N_{eros}+N_{vol}-N_{fix}$ in all following equations. Furthermore, the leaching of ammonium can be neglected in almost all forest ecosystems due to (preferential) uptake and complete nitrification within the root zone, i.e. $NH_{4,le}=0$. Under these various assumptions Eq.3.8 simplifies to:

$$N_{le} = NO_{3,le} = N_{dep} - N_{i} - N_{u} - N_{de} \tag{3.9}$$

Inserting Eqs.3.4,3.5,3.7 and 3.9 into Eq.3.3 leads to the following simplified acidity balance between sources and sinks of S and N in the soil compartment:

$$S_{dep} + N_{dep} = BC_{dep} - Cl_{dep} + BC_{w} - BC_{u} + N_{i} + N_{u} + N_{de} - Alk_{le} \tag{3.10}$$

Strictly speaking, we should replace $NO_{3,le}$ in the charge balance not by the right-hand side of Eq.3.9, but by $\max\{N_{dep}-N_i-N_u-N_{de},0\}$, since leaching cannot become negative. However, this would lead to unwieldy critical load expressions. Therefore we

go ahead with Eq.3.10, keeping this constraint in mind. (See Eq. 3.15 below.)

### 3.1.2 Critical loads of S and N for constant sinks:

The simplified balance equation (3.10) holds for every deposition of S and N. Specifying a critical alkalinity leaching, i.e. a criterion linking chemical changes to a "harmful effect", yields the maximum sum of S and N deposition allowed, i.e. the critical load for S and N:

$$CL(S+N) = CL(S) + CL(N) = \\ = BC_{dep} - Cl_{dep} + BC_w - BC_u + N_i + N_u + N_{de} - Alk_{le(crit)} \quad (3.11)$$

A so-called critical load for potential acidity has been defined by subtracting the deposition of base cations, corrected for chloride deposition, from the critical load of S and N:

$$CL(Ac_{pot}) = BC_w - BC_u + N_i + N_u + N_{de} - Alk_{le(crit)} \quad (3.12)$$

where $Ac_{pot}=S_{dep}+N_{dep}-BC_{dep}+Cl_{dep}$. The term "potential" is used because $NH_3$ is counted as potential acid due to complete nitrification (see above). A critical load of (potential) acidity has been defined to have no deposition terms on the right-hand side of the equation since base cation and chloride deposition may change in time. In addition, a distinction has even been made between "land use acidity", $N_i+N_u+N_{de}-BC_u$, and "soil acidity", $BC_w-Alk_{le}$, the latter leading to the definition of the so-called critical load of (actual) acidity (see Sverdrup and de Vries 1994):

$$CL(Ac_{act}) = BC_w - Alk_{le(crit)} \quad (3.13)$$

The reason for making this distinction (see Hettelingh and de Vries 1992) was to derive a critical load which is an intrinsic ecosystem property that will not change over time. The idea was to exclude all input terms that may change in the long term such as (i) base cation deposition, which might be reduced by paving dust roads, (ii) uptake of BC and N which are influenced by forest management and harvest regime, and (iii) N immobilization and denitrification which may change due to changes in the hydrological regime.

The problem, however, is that the remaining terms in Eq.3.13 are also liable to change. First of all, $BC_{dep}$ and the precipitation surplus are used to calculate the critical alkalinity leaching (see below), which are both changing. And in the long run even the weathering rate is not a fixed value, as it is influenced by temperature and moisture conditions, which may change, e.g. due to climate change and desiccation (lowering of the groundwater table). In practice, the values used should be long-term average values during one rotation period of a tree, and the uncertainty in these data is likely to be much larger than possible future changes. From a practical point of view it is therefore much better to derive critical loads of S and N, since the critical load of actual acidity is not directly comparable to any deposition, and therefore of little practical use for deposition reduction negotiations. For these reasons we are not going to use the critical loads defined by Eq.3.12 and Eq.3.13 in the sequel.

When comparing S and N deposition to $CL(S+N)$ (see Eq.3.11) one should bear in mind that the nitrogen sinks cannot compensate incoming sulfur acidity, i.e. the maximum critical load for sulfur is given by:

$$CL_{max}(S) = BC_{dep} - Cl_{dep} + BC_w - BC_u - Alk_{le,crit)} \quad (3.14)$$

This expression has also been termed critical load/deposition of acidity; and it had been used to derive the critical deposition of S – used in the negotiations of the Second Sulphur Protocol – by multiplying it with the so-called sulfur fraction (see, e.g., Posch *et al.* 1993). Furthermore, if

$$N_{dep} \le N_i + N_u + N_{de} =: CL_{min}(N) \quad (3.15)$$

all deposited N is consumed by the N sinks in the soil, and sulfur can be considered alone (see also footnote to Eq.3.10). The maximum amount of allowable N deposition (in case of zero S deposition) is indeed given by $CL(S+N)$:

$$CL_{max}(N) = CL(S+N) = CL_{min}(N) + CL_{max}(S). \quad (3.16)$$

Figure 3.1 shows the relationship between S and N deposition and the critical loads defined by Eqs.3.14-3.16.

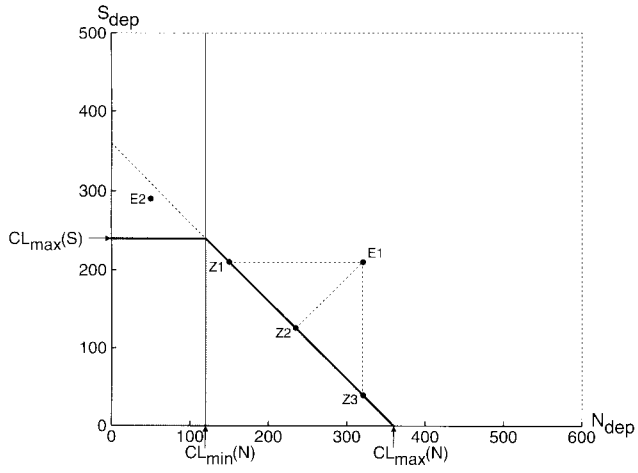


**Figure 3.1.** Relationship between N and S deposition and the critical load of sulfur and nitrogen. For every pair of deposition $(N_{dep},S_{dep})$ lying on the function shown as thick line or below in the grey shaded area (see Eqs.3.14-3.16), we have non-exceedance of the critical load *CL(S+N)* (Eq.3.11). The points E1, E2 and Z1-Z3 are explained in Section 4 below.

### 3.1.3 Critical loads for deposition-dependent sinks of nitrogen:

When defining a critical load via Eq.3.11 it is implicitly assumed that all the terms on the right-hand side do not depend on the deposition of S and/or N. However, this is unlikely to be the case. Therefore, it is often recommended that all quantities be taken *at critical load*, and a subscript *(crit)* is affixed to (some of) them in various publications (see, e.g., UN/ECE 1995). However, to compute the "N immobilization at critical load" one needs to know the critical load, the very quantity one tries to compute. The only way to avoid this circular reasoning is to establish a relationship between the deposition and the sink of S or N, insert this function into Eq.3.10 and solve for the deposition. Actually, this has been done for denitrification (see Posch *et al.* 1993). In the simplest case denitrification is linearly related to the net input of N by (de Vries *et al.* 1993):

$$N_{de} = \begin{cases} f_{de}(N_{dep}-N_i-N_u) & \text{if } N_{dep}>N_i+N_u \\ 0 & \text{otherwise} \end{cases} \qquad (3.17)$$

where $f_{de}$ is the so-called denitrification fraction. This formulation implicitly assumes that immobilization and growth uptake are faster processes than denitrification. Note that, e.g., $f_{de}$=0.8 does *not* mean that 80% of $N_{dep}$ is denitrified, but rather 80% of $N_{dep}-N_i-N_u$.

Inserting Eq.3.17 into Eq.3.10, replacing $Alk_{le}$ with $Alk_{le(crit)}$ and solving for the depositions leads to the following critical load equation:

$$CL(S) + (1-f_{de})CL(N) = \\ = BC_{dep} - Cl_{dep} + BC_w - BC_u + (1-f_{de})(N_i + N_u) - Alk_{le(crit)} \qquad (3.18)$$

The minimum critical load for N is now given by (cf. Eq.3.15):

$$CL_{min}(N) = N_i + N_u \qquad (3.19)$$

and the maximum allowable deposition of N is obtained from Eq.3.18 by setting *CL(S)*=0 and solving for *CL(N)*:

$$CL_{max}(N) = CL_{min}(N) + \frac{CL_{max}(S)}{1-f_{de}} \qquad (3.20)$$

In Figure 3.2 all pairs of deposition $(N_{dep},S_{dep})$ are shown which fulfil Eq.3.18, and they are said to define the *critical load function* (for acidity). In contrast to Figure 3.1, where the slope of the critical load function is always one, it is now dependent on the ecosystem and equal to $1-f_{de}$; furthermore, $CL_{min}(N)$ depends on $N_i$ and $N_u$ only.

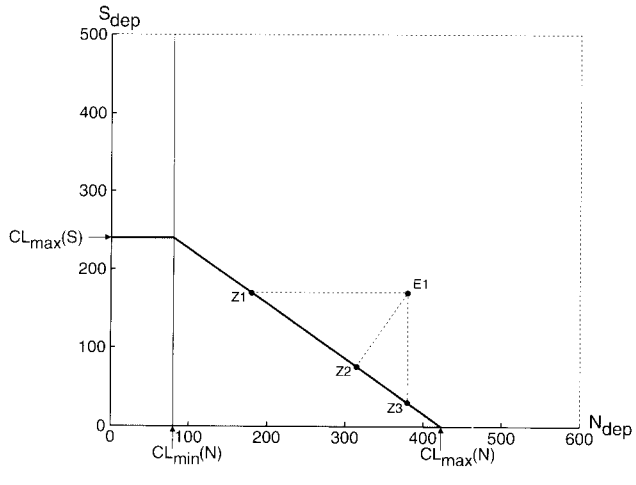


**Figure 3.2.** Relationship between $N_{dep}$ and $S_{dep}$ and the critical loads for acidifying S and N for a hypothetical ecosystem (cf. Figure 3.1). The points E1 and Z1-Z3 are explained in Section 4 below.

Another – non-linear – equation for the deposition dependence of denitrification has been given by Sverdrup and Ineson (1993) based on a Michaelis-Menten reaction mechanism (see also Posch *et al.* 1993):

$$N_{de} = \begin{cases} \dfrac{k(N_{dep}-N_i-N_u)}{K+(N_{dep}-N_i-N_u)} & \text{if } N_{dep}>N_i+N_u \\ 0 & \text{otherwise} \end{cases} \qquad (3.21)$$

where $K$ is a saturation coefficient (=2900 eq/ha/yr) and the rate coefficient $k$ is a function of temperature, $T$ (°C), soil wetness and pH:

$$k = k_0 \cdot f(T) \cdot g(w) \cdot h(pH) \qquad (3.22)$$

where $k_0$ is a kinetic rate constant (=1710 eq/ha/yr) and $w$ is the relative soil moisture (=$\Theta/\Theta_s$); and the modifying functions $f$, $g$ and $h$ are given by:

$$\begin{aligned} f(T) &= 10^{5660\left(\frac{1}{281}-\frac{1}{273+T}\right)} \\ g(w) &= \frac{5.96w}{0.96+w} \\ h(pH) &= 0.408pH^2-2.7808pH+5.15 \end{aligned} \qquad (3.23)$$

When including the pH dependence, different acidity deposition levels will lead to different soil pH, causing the critical load to change with soil acidity, and thus iterative models would have to be used. Therefore it is suggested to use $pH$=5.0, leading to $h(pH)$=1.

Although more involved, this formulation still allows to compute an explicit expression for $CL_{max}(N)$. Inserting Eq.3.21 into Eq.3.10 yields after some calculations:

$$CL_{max}(N) = N_i+N_u+\sqrt{\bar{a}^2+\bar{b}}-\bar{a} \qquad (3.24)$$

where

$$\bar{a} = \frac{1}{2}\left(K-k-CL_{max}(S)\right) \quad \text{and} \quad \bar{b} = K \cdot CL_{max}(S) \qquad (3.25)$$

and $CL_{max}(S)$ is given by Eq.3.14. Using this formulation the tilted line in the critical load function in Figure 3.2 is no longer a straight line but a curve, the curvature depending on the parameters (temperature and soil wetness) of the denitrification function.

Ideally, the other sink terms in the critical load formula should also be expressed as functions of deposition, but at present there are no accepted formulations available. See, however, Sverdrup (1993), which proposes a deposition-dependent formula for N immobilization.

## 3.2 The critical load of nutrient nitrogen

In addition to the acidifying aspect of nitrogen, the effects of N deposition on the nutrient status (eutrophication) of an ecosystem should be considered when determining critical loads. A critical load for nutrient nitrogen, $CL_{nut}(N)$, is derived from the mass balance for N (see Eq.3.8) by neglecting N adsorption and inserting a critical N leaching:

$$CL_{nut}(N) = N_i+N_{fire}+N_{eros}+N_{vol}-N_{fix} + N_u+N_{de}+N_{le(crit)} \qquad (3.26)$$

Again, we simplify notation by subsuming the fire, erosion, volatilization and fixation terms into $N_i$ (see Eq.3.9):

$$CL_{nut}(N) = N_i+N_u+N_{de}+N_{le(crit)} \qquad (3.27)$$

Expressing denitrification as a linear function of net deposition (Eq.3.17) one obtains:

$$CL_{nut}(N) = N_i+N_u+\frac{N_{le(crit)}}{1-f_{de}} \qquad (3.28)$$

Alternatively, using the non-linear expression for denitrification (Eq.3.21) results in:

$$CL_{nut}(N) = N_i+N_u+\sqrt{a^2+b}-a \qquad (3.29)$$

where

$$a = \frac{1}{2}\left(K-k-N_{le(crit)}\right) \quad \text{and} \quad b = K \cdot N_{le(crit)} \qquad (3.30)$$

When considering the critical load of acidifying and nutrient nitrogen simultaneously, two possibilities arise (see Figure 3.3):

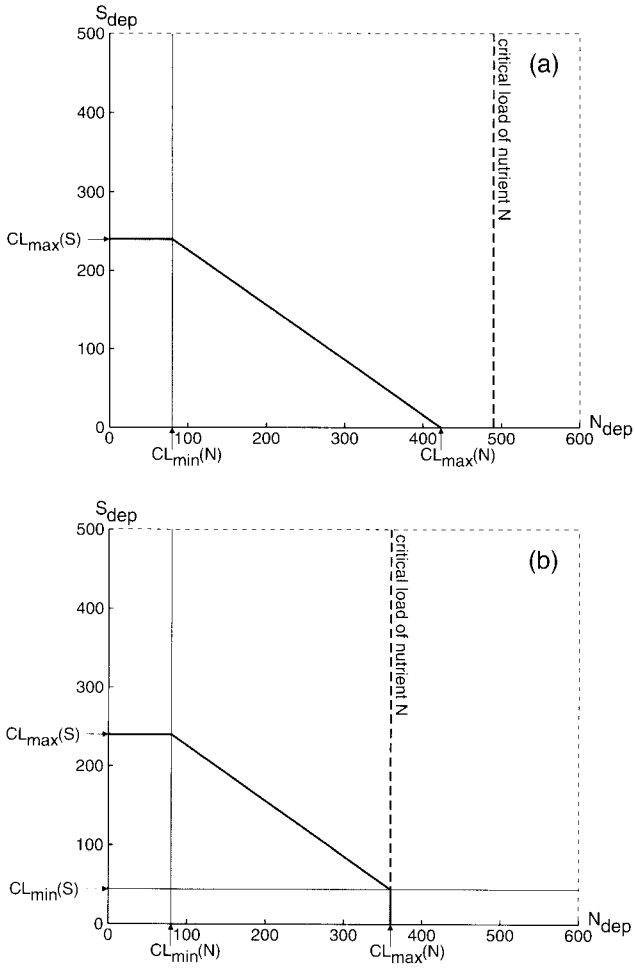


**Figure 3.3.** Relationship between sulfur and nitrogen deposition and the critical loads of acidifying N and S and the critical load of nutrient N: (a) $CL_{nut}(N)>CL_{max}(N)$, (b) $CL_{nut}(N)<CL_{max}(N)$. The grey area indicates deposition combinations causing no exceedance.

(a) $CL_{nut}(N)\geq CL_{max}(N)$:
In this case $CL_{nut}(N)$ is of no consequence and can be ignored; the maximum permissible N deposition is given by $CL_{max}(N)$.

(b) $CL_{nut}(N)<CL_{max}(N)$:
In this case $CL_{nut}(N)$ limits the maximum permissible N deposition, and the sulfur deposition permitted at this N deposition is given by $CL_{min}(S)$:

$$CL_{min}(S) = CL_{max}(S) - N_{le(crit)} \qquad (3.31)$$

## 3.3 The computation of alkalinity leaching and N quantities

In the previous sections we derived expressions for critical loads of acidifying S and N as well as for nutrient N. In this section we will summarize how to arrive at concrete values for critical loads, i.e. we show to compute the alkalinity leaching and the N transformation terms, and provide some default values.

### 3.3.1 Critical alkalinity leaching:

Alkalinity leaching is defined in Eq.3.2. For acid forest soils $HCO_{3,le}$ and $RCOO_{le}$ can be neglected, and the critical alkalinity leaching is calculated as:

$$Alk_{le(crit)} = -Al_{le(crit)} - H_{le(crit)} = -Q\cdot\left([Al]_{crit} + [H]_{crit}\right) \qquad (3.32)$$

where $Q$ is the precipitation surplus (in $m^3/ha/yr$), i.e. the water leaving the root zone, and the square brackets denote concentrations (in $eq/m^3$). The precipitation surplus is calculated as the precipitation minus the sum of the interception evaporation by the forest canopy, the actual soil evaporation and the actual transpiration (water uptake) in the root zone (see, e.g., De Vries *et al.* 1993). Operationally, the relationship between $[H]$ and $[Al]$ is described by a gibbsite equilibrium:

$$[Al] = K_{gibb}\cdot[H]^3 \quad \text{or} \quad [H] = \left([Al]/K_{gibb}\right)^{1/3} \qquad (3.33)$$

where $K_{gibb}$ is the gibbsite equilibrium constant. Its value depends on the soil, and a few commonly used values are given in the following table:

| $\log_{10}(K_{gibb}$ [(l/mol)$^2$]): | 8.0 | 8.2 | 8.5 | 8.7 | 9.0 |
|---|---|---|---|---|---|
| $K_{gibb}$ [$m^6/eq^2$]: | 300 | 475 | 950 | 1500 | 3000 |

A widely used default value is $K_{gibb}$=300 $m^6/eq^2$.

To obtain a critical alkalinity leaching one could specify either a critical Al concentration (such as $[Al]_{crit}$=0.2eq/$m^3$; see, e.g., Hettelingh and de Vries, 1992) or a critical pH (e.g., $[H]_{crit}$=0.1eq/$m^3$, corresponding to pH=4.0) and then compute the other concentration via Eq.3.33. In the following we describe 3 methods for calculating the critical alkalinity leaching: 2 for mineral soils and one for organic soils (peatlands).

(1) *$Alk_{le(crit)}$ determined by a critical base cation to Al ratio:*

Most widely used is the connection between soil chemical status and plant response via a critical molar base cation to aluminum ratio, $(Bc/Al)_{crit}$. Here *Bc* stands for the sum of Ca, Mg and K, i.e. $Bc=Ca+Mg+K$; Na is excluded, since it provides no protection against Al for plants. The critical Al leaching is then calculated from the leaching of base cations and the critical Bc/Al ratio:

$$Al_{le(crit)} = 1.5 \cdot \frac{Bc_{le}}{(Bc/Al)_{crit}} \qquad (3.34)$$

The factor 1.5 arises from the conversion of mols to equivalents. In doing so we implicitly assume that K has charge +2, i.e. it gets only half the weight of Ca+Mg when computing the Bc/Al ratio. The default value for the critical Bc/Al ratio is 1 mol/mol (for coniferous forests), and values for a large variety of plant species can be found in Sverdrup and Warfvinge (1993). The base cation leaching, $Bc_{le}$, is calculated from the mass balance for base cations given by (see also Eq.3.5):

$$Bc_{le} = Bc_{dep} + Bc_{w} - Bc_{u} \qquad (3.35)$$

The weathering of base cations is either known for each base cation separately, or computed as

$$Bc_{w} = x_{CaMgK} \cdot BC_{w} \qquad (3.36)$$

where $x_{CaMgK}$ is the fraction of weathering as Ca+Mg+K; default values are 0.7 for poor sandy soils and 0.85 for rich (sandy) soils. Crude values for weathering dependent on soil type and parent material and soil texture are provided in de Vries *et al.* (1993). If the necessary information is available (such as soil mineralogy), weathering rates can be calculated with a weathering rate model such as PROFILE (Warfvinge and Sverdrup, 1992).

Due to physiological limitations, base cations will not be taken up by plants below a certain concentration $[X]_{min}$, implying for the net growth uptake of base cations:

$$X_{u} = \max\left\{X_{dep} + X_{w} - Q \cdot [X]_{min}, 0\right\} \quad \text{for} \quad X = Ca, Mg, K \qquad (3.37)$$

The deposition and weathering of base cations will not always be available individually and therefore Eq.3.37 will have to be used for $Bc=Ca+Mg+K$.

A general range for $[Bc]_{min}$ is 0.002-0.005 eq/m$^3$ (Ingestad, 19xx). Some base cations also escape from plant uptake due to root inactivity at temperatures below 5°C. This can be considered by raising $[Bc]_{min}$ (up to 0.015 eq/m$^3$). Another possibility is to make a fraction of the weathering rate unavailable, corresponding to the fraction of weathering occurring when plant uptake is not active (5-25%). Since tree growth may not only be limited by nutrients but also by other stress factors (e.g. water availability and light), it is recommended to calculate the uptake as the minimum of Eq.3.37 and the present uptake, $Bc_u^0$:

$$Bc_{u} = \min\left\{\max\{Bc_{dep} + Bc_{w} - Q[Bc]_{min}, 0\}, Bc_{u}^{0}\right\} \qquad (3.38)$$

$Bc_u^0$ depends on forest practice and can be estimated by the amount of base cations removed in tree biomass during harvesting, divided by the rotation time (see also de Vries *et al.* 1993 for methods for estimating base cation and nitrogen uptake from growth data).

Inserting Eqs.3.32-3.36 into Eq.3.14 we obtain for $CL_{max}(S)$ as determined by a Bc/Al ratio:

$$CL_{max}^{(1)}(S) = BC_{dep} - Cl_{dep} + BC_{w} - BC_{u} + 1.5 \cdot \frac{Bc_{dep} + Bc_{w} - Bc_{u}}{(Bc/Al)_{crit}} + Q^{2/3} \cdot \left(1.5 \cdot \frac{Bc_{dep} + Bc_{w} - Bc_{u}}{(Bc/Al)_{crit} \cdot K_{gibb}}\right)^{1/3} \qquad (3.39)$$

Recall that $BC_y=Bc_y+Na_y$ for every subscript *y*; Na is not taken up by plants, $Na_u=0$, i.e. $Bc_u=BC_u$; furthermore $Bc_w=x_{CaMgK}BC_w$ (see Eq.3.36). As is the case for N, we should write $\max\{X_{dep}+X_w-X_u,0\}$ in the critical load formula for each base cation *X*; Eq.3.38 guarantees this for $X=Ca,Mg,K$, and for Na it is always true since $Na_u=0$. If one assumes $Na_{dep}+Na_w=Cl_{dep}$, which is a good approximation in most cases, Eq. 3.39 can be expressed in *Bc*-terms alone.

(2) *$Alk_{le(crit)}$ determined by a critical Al mobilization rate:*

Another criterium that can be used to calculate a critical Al leaching rate is that depletion of secondary aluminum phases and complexes is not allowed as it may cause structural changes in soils.

Secondary Al compounds are important structure elements, and the stability of these soils depends on the stability of the reservoir of these substances. Furthermore, Al depletion may cause a further pH decline. Al depletion occurs when acid deposition leads to aluminum leaching in excess of the Al produced by weathering of primary minerals. The equation for the critical Al leaching is thus derived from the requirement that it must not exceed net Al weathering from primary minerals, $Al_w$:

$$Al_{le(crit)} = Al_w \tag{3.40}$$

The production of Al from weathering is related to the weathering of base cations via the stoichiometry of the minerals involved according to:

$$Al_w = r \cdot BC_w \tag{3.41}$$

where $r$ is the stoichiometric ratio of Al to base cation weathering in primary minerals (eq/eq). A default value, using typical mineralogy of North European soils, is $r$=2 (range 1.5-3.0). The maximum critical load of S, based on soil stability, is then given by:

$$CL^{(2)}_{max}(S) = BC_{dep} - Cl_{dep} - BC_u + (1+r) \cdot BC_w + Q^{2/3} \cdot \left( \frac{r \cdot BC_w}{K_{gibb}} \right)^{1/3} \tag{3.42}$$

The critical load to be used is the minimum of the critical load calculated from plant tolerance of Al (Bc/Al-ratio) and the critical load calculated via the soil stability criterium:

$$CL_{max}(S) = \min\left\{ CL^{(1)}_{max}(S), CL^{(2)}_{max}(S) \right\} \tag{3.43}$$

(3) *$Alk_{le(crit)}$ determined by a critical base cation to H ratio:*

For organic soils and peat bogs not containing Al-(hydr)oxides the critical alkalinity leaching can be determined by an critical (molar) base cation to proton ratio, $(Bc/H)_{crit}$. The critical proton leaching is then given by:

$$H_{le(crit)} = 0.5 \cdot \frac{Bc_{le}}{(Bc/H)_{crit}} \tag{3.44}$$

where the factor 0.5 arises from the conversion from mols to equivalents (see above). And since Al leaching is zero ($Al_{le(crit)}$=0), we get for the critical load for organic and peat soils:

$$CL^{(3)}_{max}(S) = BC_{dep} - Cl_{dep} + BC_w - BC_u + 0.5 \cdot \frac{Bc_{dep} + Bc_w - Bc_u}{(Bc/H)_{crit}} \tag{3.45}$$

As mentioned, this formula is applicable for soils with no aluminum or where the content of Al is completely masked by a high content of DOC (more than 100 mg/l). Default numerical values for the critical base cation to proton ratio are: $(Bc/H)_{crit} \approx (Bc/Al)_{crit}$ for spruce and ground vegetation and $(Bc/H)_{crit} \approx \frac{1}{3}(Bc/Al)_{crit}$ for pine and deciduous trees (H. Sverdrup, *pers. comm.*).

### 3.3.2 Nitrogen transformation processes:

In addition to the critical alkalinity leaching, the different terms involving nitrogen compounds have to be specified; and this is done in the sequel:

**Nitrogen immobilization** is the long-term immobilization rate, which is in the order of 2 to 5 kg N/ha/yr (142 to 357 eq/ha/yr). Note that under present conditions with acidified soils and high growth due to elevated N deposition, immobilization may be substantially higher.

**Nitrogen uptake** is estimated from base cation uptake (see above). Ideally, one computes N uptake from

$$N_u = \min\left\{ \frac{Ca_u}{x_{Ca:N}}, \frac{Mg_u}{x_{Mg:N}}, \frac{K_u}{x_{K:N}}, \frac{P_u}{x_{P:N}} \right\} \tag{3.46}$$

where $Ca_u$,...,$P_u$ are computed via Eq.3.37. If individual quantities are not available, N uptake is computed as

$$N_u = \frac{Bc_u}{x_{Bc:N}} \tag{3.47}$$

Approximate nutrient ratios (eq/eq) for three major tree species are given in the following table:

| Tree species | $x_{Ca:N}$ | $x_{Mg:N}$ | $x_{K:N}$ | $x_{P:N}$ | $x_{BC:N}$ |
|---|---|---|---|---|---|
| Norway spruce | 0.60 | 0.20 | 0.20 | 0.20 | 0.90 |
| Scots pine | 0.50 | 0.15 | 0.12 | 0.20 | 0.70 |
| European beech | 0.40 | 0.20 | 0.20 | 0.20 | 0.70 |

For the same reasons as given for base cation uptake, N uptake has to be taken as the minimum of the uptake given by Eq.3.47 and the present N uptake.

Formulations for **denitrification** as a function of net N input have been given above (see Eqs.3.17 and 21). In a European application (De Vries *et al.* 1993) $f_{de}$ has been related to soil type on the basis of data in Steenvoorden (1984) and Breeuwsma *et al.* (1991): $f_{de}$=0.1 for loess soils and sandy soils without gleyic features; $f_{de}$=0.5 for sandy soils (FAO texture classes 1, 2 and 1/2) with gleyic features; $f_{de}$=0.7 for clay soils (FAO texture classes 2, 3 and 2/3); and $f_{de}$=0.8 for peat soils.

For computing the critical load of nutrient N a **critical nitrogen leaching** has to be specified. Relatively small concentrations of N in the soil solution may induce nutrient imbalances in coniferous stands. When nitrogen appears in significant amounts in the soil solution, plant species composition on the forest or ground vegetation may change, and N-tolerant species may gain ground over less tolerant species. The critical N leaching can be computed as

$$N_{le(crit)} = Q \cdot [N]_{crit} \qquad (3.48)$$

where $[N]_{crit}$ is a critical N soil solution concentration. Values for $[N]_{crit}$ for some vegetation changes can e.g., be found in Table 4.2 in Posch *et al.* (1993).

However, a critical $NO_3$ concentration related to vegetation changes can be very unreliable. A nitrogen mass balance for e calcareous grassland in the Netherlands indicates that vegetation changes may occur in a situation in which N leaching hardly increased above natural background (Van Dam 1990). Similarly, N leaching is nearly negligible in Dutch heathlands changing into grasslands. It is the increase in N availability through enhanced N cycling that triggers this vegetation changes (Berendse *et al.* 1987). Empirical data are likely to be more reliable for these effects.

A critical N leaching could be also derived with the objective to avoid nitrogen pollution of groundwaters. Internationally agreed values, like 25 and 50 mg N/l (EC target and limit value, resp.) could be used for this purpose.

## 3.4 The exceedance of critical loads

Critical loads are calculated to express the sensitivity of ecosystems to the deposition of sulfur and nitrogen in quantitative terms. Therefore, the emphasis in this chapter has been on critical loads of S and N, which can be directly compared to the deposition of S and N and thus be used in negotiations on emission reductions of these compounds. The comparison between deposition and critical loads has (traditionally) been done by computing the so-called exceedance, i.e. the difference between deposition and critical loads:

$$Ex(S+N) = S_{dep} + N_{dep} - CL(S+N) \qquad (3.49)$$

This makes sense (within limits), if the critical loads are given by Eq.3.11 (i.e. the sink terms are all independent of the amount deposited), as is illustrated by an example in Figure 3.1: Let the point E1 denote the (current) deposition of N and S, then the amount of the S+N deposition to be reduced to reach non-exceedance (the thick line in Figure 3.1) is independent of the path, i.e. it is the same for reaching the points Z1, Z2 or Z3 (since the slope of the line is one). But there are limits as given by Eqs.3.14-3.16: If $S_{dep}$ is greater than $CL_{max}(S)$, the critical load is exceeded, although $S_{dep}$ might be smaller than $CL(S+N)$ and $Ex(S+N)$ might be negative (e.g., the deposition situation represented by point E2).

It is impossible to define a unique critical load and thus exceedance if one of the sink terms is a function of N deposition (like denitrification as detailed above). This is obvious from Eq.3.18, and is also illustrated in Figure 3.2: Reducing $N_{dep}$ substantially, one reaches the point Z1 and therefore non-exceedance without reducing S; on the other hand one can reach non-exceedance by only reducing $S_{dep}$ (by a smaller amount) until reaching Z3; finally, with a smaller reduction of both $S_{dep}$ and $N_{dep}$ one can reach non-exceedance as well (e.g. point Z2). In practice external factors such as the costs of emission reductions, will determine which path will be followed to reach zero exceedance.

If one wants to calculate unique critical loads of N and S, and consequently be able to compute unique exceedances $Ex(N)$ and $Ex(S)$, there are several reasonable possibilities to do so:

(1) If $CL_{nut}(N)<CL_{max}(N)$ (see Figure 3.3b), as will probably be the case for most ecosystems, one can *define* the critical load of nitrogen, $CL(N)$, as $CL_{nut}(N)$ (see Eq.3.28 or Eq.3.29), and the critical load of sulfur, $CL(S)$, as $CL_{min}(S)$ (see Eq.3.31) and work with these two quantities. This approach has been taken for the Netherlands in De Vries (1991).

(2) If future negotiations are not to involve S deposition reductions – and this is likely considering that a sulfur protocol has recently been signed – the critical load functions can serve as a valuable tool for determining critical loads of N for a *fixed* S deposition (conditional critical load): intersecting the critical load function for each ecosystem with the (present or any future) $S_{dep}$ yields critical loads for N for the given S deposition, $CL(N \mid S_{dep})$. (See Figure 3.4, where the computation of conditional critical loads of N is illustrated for $S_{dep}=S_1$, $S_2$ and $S_3$). These critical N loads can then be used in the 'traditional way', with the additional benefit that they are compatible with the present or any anticipated S deposition. This conditional critical load is given by:

$$CL(N \mid S_{dep}) = \qquad (3.50)$$

$$\begin{cases} CL_{min}(N) & \text{if } S_{dep} \geq CL_{max}(S) \\ CL_{min}(N) + \dfrac{CL_{max}(S) - S_{dep}}{1 - f_{de}} & \text{if } CL_{min}(S) < S_{dep} \leq CL_{max}(S) \\ CL_{nut}(N) & \text{if } S_{dep} < CL_{min}(S) \end{cases}$$

Note, that if $CL_{nut}(N)>CL_{max}(N)$, the third line in Eq.3.50 becomes superfluous. In an analogous manner a conditional critical load for sulfur, $CL(S \mid N_{dep})$, can be defined.

Both approaches reduce the problem of critical loads and exceedances to mere numbers and facilitate communication with non-technical users (policy makers), but they sacrifice the inherent flexibility of the full critical load function, allowing to determine (cost-)optimal reductions considering both N and S emissions.

For use in European emission reduction negotiations, the large number of critical loads have to be aggregated. Cumulative distribution functions and percentiles have been used to present critical loads of sulfur and acidity in map format. As outlined above, the simultaneous treatment of sulfur and nitrogen does not allow the calculation

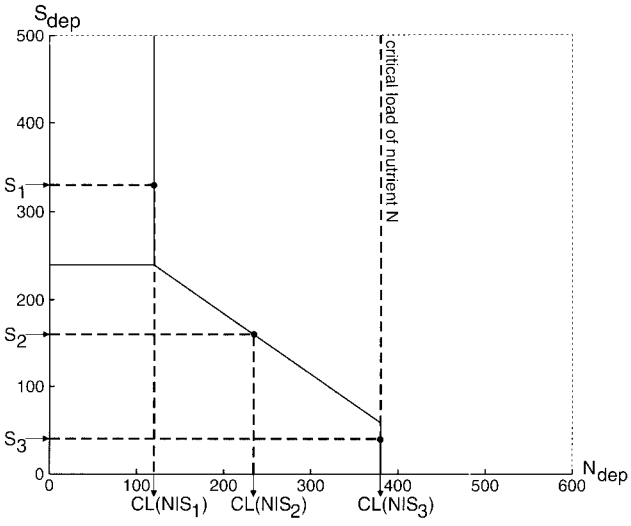


**Figure 3.4.** Examples of computing conditional critical loads of N – $CL(N \mid S_1)$, $CL(N \mid S_2)$ and $CL(N \mid S_3)$ – for a hypothetical ecosystem for different S deposition values $S_1$, $S_2$ and $S_3$, respectively.

of a single critical load value, and thus the concept of a percentile has to be generalized. This is outlined in detail in Chapter 4, where the concept of a *percentile function* or *protection isoline* is introduced. An example of a protection isoline is shown in Figure 3.5. All combinations of $N_{dep}$ and $S_{dep}$ lying below the $p$-th percentile function protect $100-p$ percent of the ecosystems in a given grid cell. Although no unique exceedance can be defined, one can distinguish five cases: (0) the point $(N_{dep},S_{dep})$ lies below the percentile function, i.e. no exceedance; (1) reductions in $N_{dep}$ or $S_{dep}$ are interchangeable, i.e. non-exceedance can be reached by either N reductions or S reductions alone; (2) some reductions in S deposition are mandatory; (3) some reductions in $N_{dep}$ are mandatory; and (4) both reductions in N and S are required to achieve non-exceedance.

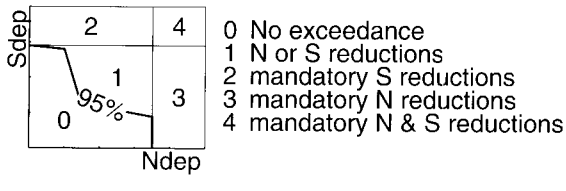


**Figure 3.5.** Example of a protection isoline (percentile function; see Chapter 4 for its definition and computation). Also indicated are the five cases of exceedance which can arise irrespective of the exact shape of the function (see text for a classification).

## 3.5 Concluding remarks and acknowledgements

This chapter is the result of an effort to arrive at formulations for critical loads which satisfy both scientists and decision makers. The number of people who, directly or indirectly, have stimulated this development are too numerous to be thanked individually. It should be noted that this is not an official document, but presents a synthesis of developments to date. All errors and mistakes are the sole responsibility of the authors.

## References

Berendse, F., B. Beltman, R. Bobbink, R. Kwant and M.B. Schmitz, 1987. Primary production and nutrient availability in wet heathland ecosystems. *Acta Oec./Oecol. Plant.*: 265-276.

Breeuwsma, A., J.P. Chardon, J.F. Kragt and W. de Vries, 1991. Pedotransfer functions for denitrification. In: Nitrate in Soils. Commission of the European Communities, pp.207-215.

De Vries, W., 1991. Methodologies for the assessment and mapping of critical loads and of the impact of abatement strategies on forest soils. The Winand Staring Centre for Integrated Land, Soil and Water Research, Report 46, Wageningen, The Netherlands, 109 pp.

De Vries, W., M. Posch, G.J. Reinds and J. Kämäri, 1993. Critical loads and their exceedance on forest soils in Europe. The Winand Staring Centre for Integrated Land, Soil and Water Research, Report 58 (revised version), Wageningen, The Netherlands, 116 pp.

De Vries, W., 1994. Soil response to acid deposition at different regional scales – Field and laboratory data, critical loads and model predictions. PhD thesis, University of Agriculture, Wageningen, The Netherlands, 487 pp.

Downing, R.J., J.-P. Hettelingh and P.A.M. de Smet (Eds.), 1993. Calculation and Mapping of Critical Loads in Europe. CCE Status Report, RIVM, Bilthoven, The Netherlands, 163 pp.

Grennfelt, P. and E. Thörnelöf (Eds.), 1992. Critical Loads for Nitrogen. NORD 1992:41, Nordic Council of Ministers, Copenhagen, Denmark, 428 pp.

Henriksen, A. and M. Posch, 1995. Critical loads for nitrogen: surface waters. In: M. Hornung, M.A. Sutton and R.B. Wilson (Eds.) Mapping and Modelling of Critical Loads for Nitrogen: a Workshop Report. Proceedings of the Grange-over-Sands Workshop, 24-26 October 1994. Institute of Terrestrial Ecology, United Kingdom, pp. 55-62.

Hettelingh, J.-P. and W. de Vries, 1992. Mapping Vademecum. Report No. 259101002, RIVM, Bilthoven, The Netherlands, 39 pp.

Hornung, M., M.A. Sutton and R.B. Wilson (Eds.), 1995. Mapping and Modelling of Critical Loads for Nitrogen: a Workshop Report. Proceedings of the Grange-over-Sands Workshop, 24-26 October 1994. Institute of Terrestrial Ecology, United Kingdom, 207 pp.

Ingestad, 19xx. Unknown reference.

Johnson, D.W., 1984. Sulfur cycling in forests. *Biogeochemistry* **1**:29-43.

Johnson, D.W., D.W. Cole and S.P. Gessel, 1979. Acid precipitation and soil sulphate adsorption properties in a tropical and in a temperate forest soil. *Biotropica* **11**:38-42.

Johnson, D.W., G.S. Henderson, D.D. Huff, S.E. Lindberg, D.D. Richter, D.S. Shriner, P.E. Todd and J. Turner, 1982. Cycling of organic and inorganic sulfur in a chestnut oak forest. *Oecologia* **54**:141-148.

Nilsson, J. and P. Grennfelt (Eds.), 1988. Critical Loads for Sulphur and Nitrogen. NORD 1988:97, Nordic Council of Ministers, Copenhagen, Denmark, 418 pp.

Posch, M., J.-P. Hettelingh, H.U. Sverdrup, K. Bull and W. de Vries, 1993. Guidelines for the computation and mapping of critical loads and exceedances of sulphur and nitrogen in Europe. In: R.J. Downing, J.-P. Hettelingh and P.A.M. de Smet (Eds.), Calculation and Mapping of Critical Loads in Europe, Status Report 1993, Coordination Center for Effects (RIVM) Bilthoven, The Netherlands, pp. 25-38.

Steenvoorden, J., 1984. Invloed van wijzigingen in de waterhuishouding op de waterkwaliteit (in Dutch). Rep. 1554, Inst. for Land and Water Management Research, Wageningen, The Netherlands.

Sverdrup, H., W. de Vries and A. Henriksen, 1990. Mapping Critical Loads. NORD 1990:98, Nordic Council of Ministers, Copenhagen, Denmark, 124 pp.

Sverdrup, H., 1993. Immobilization of N in soils. Unpublished manuscript.

Sverdrup, H. and P. Ineson, 1993. Kinetics of denitrification in forest soils. Unpublished manuscript.

Sverdrup, H. and P. Warfvinge, 1993. The effect of soil acidification on the growth of trees, grass and herbs as expressed by the (Ca+Mg+K)/Al ratio. Report 2:1993, Dept. of Chemical Engineering II, Lund University, Lund, Sweden. 177 pp.

Sverdrup, H. and W. de Vries, 1994. Calculating critical loads for acidity with the simple mass balance method. *Water Air Soil Pollut.* **72**:143-162.

UN/ECE, 1995. Calculation of Critical Loads of Nitrogen as a Nutrient. Summary report on the development of a library of default values. Document EB.AIR/WG.1/R 108, Geneva.

Van Dam, D., 1990. Atmospheric deposition and nutrient cycling in chalk grasslands. PhD thesis, University of Utrecht, The Netherlands, 119 pp.

Van Miegroet, H. and D.W. Cole, 1984. The impact of nitrification on soil acidification and cation leaching in a red alder ecosystem. *J. Environ. Qual.* **13**:586-590.

Warfvinge, P. and H. Sverdrup, 1992. Calculating critical loads of acid deposition with PROFILE - a steady-state soil chemistry model. *Water Air Soil Pollut.* **63**:119-143.

# 4. Percentiles and Protection Isolines

*Maximilian Posch*

## Introduction

In this chapter we first define and investigate different methods for calculating percentiles of a cumulative distribution function (CDF) given by a finite number of values. Then we generalize the concept of a percentile to the case in which the CDF is defined by a set of functions (critical load functions), resulting in the so-called percentile function (protection isoline).

## 4.1 Cumulative distribution function

Let us assume we have $n$ critical load values (for a single grid cell). We sort these values in ascending order, resulting in a sequence $x_1 \le x_2 \le ... \le x_n$. Each value is accompanied by a weight $A_i$ ($i$=1,...,$n$), characterizing the size (importance) of the respective ecosystem. From these we compute normalized weights $w_i$ according to

$$w_i = \frac{A_i}{\sum_{j=1}^{n} A_j}, \quad i = 1,...,n \quad \text{resulting in} \quad \sum_{i=1}^{n} w_i = 1 \tag{4.1}$$

The cumulative distribution function (CDF) of these $n$ critical load values is then defined by

$$F(x) = \begin{cases} 0 & \text{for } x < x_1 \\ W_k & \text{for } x_k \le x < x_{k+1}, \quad k = 1,...,n-1 \\ 1 & \text{for } x \ge x_n \end{cases} \tag{4.2}$$

where

$$W_k = \sum_{i=1}^{k} w_i, \quad k = 1,...,n \tag{4.3}$$

and $F(x)$ is the probability of a critical load being smaller than (or equal to) $x$, i.e. $1-F(x)$ is the fraction of ecosystems protected. With this definition $F(x)$ has the properties required for a CDF: $F$ is a monotonously increasing right-continuous function with $F(-\infty)=0$ and $F(\infty)=1$. In Figure 4.1 an example of a CDF is shown; note that the function assumes only a finite number of values.

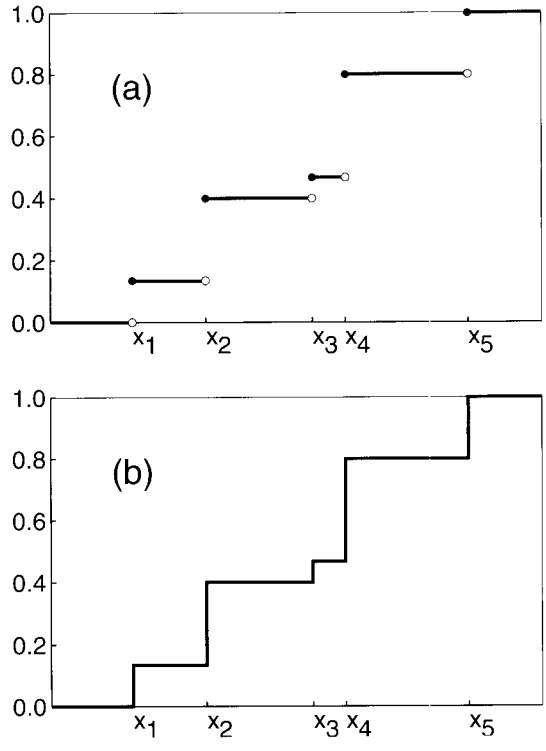


**Figure 4.1.** Example of a cumulative distribution function for five data points ($n$=5; $x_1<x_2<x_3<x_4<x_5$, with weights $w_1$=2/15, $w_2$=4/15, $w_3$=5/15, $w_4$=1/15, $w_5$=3/15). The filled (empty) circles in (a) indicate whether a point is part (not part) of the function. In (b) the same CDF is drawn by connecting all points, the way a CDF is usually displayed.

## 4.2 Percentiles

All ecosystems in a grid cell are protected, if deposition stays below the minimum of the critical load values. However, to discard outliers and to account for uncertainties in the critical load calculations, but also to ensure that a sufficient percentage of ecosystems are protected, it has been agreed to use a (low) percentile of the CDF.
The $q$-th quantile ($0 \le q \le 1$) of a CDF $F$, denoted by $x_q$, is the value satisfying

$$F(x_q) = q \tag{4.4}$$

which means that $x_q$, viewed as a function of $q$, is the inverse of the CDF, i.e. $x_q=F^{-1}(q)$.

Percentiles are obtained by scaling quantiles to 100, i.e. the $p$-th percentile corresponds to the $(p/100)$-th quantile. Other terms used are median for the 50th percentile, lower and upper quartile for the 25th an 75th percentile, resp., and here we introduce the term **pentile** (from the Greek word *penta* for *five*) for the 5th percentile. Note that the $p$-th percentile critical load protects $100-p$ percent of the ecosystems.

Computing quantiles, i.e. the inverse of CDF given by a finite number of points (critical loads) poses a problem: due to the discrete nature of the CDF, a unique inverse simply does not exist. For many values of $q$ no value $x_q$ exists at all so that Eq. 4.4 holds; and for the $n$ values $x_i$ such a value exists (i.e. $q=F(x_i)$), but the resulting quantile is not unique, every value between $x_i$ and $x_{i+1}$ could be taken (see Figure 4.1). Therefore, the CDF is approximated (interpolated) by a function which allows to solve Eq. 4.4 for every $q$. There is neither a unique approximation, nor is there a single accepted way for calculating percentiles. For example, in Posch *et al.* (1993) six methods for calculating percentiles are discussed. Note that commonly definitions are given for data with identical weights (i.e. $w_i=1/n$), but the generalization to arbitrary weights is mostly straightforward. It should be also born in mind that the differences between different approximation methods vanish when the number of points (critical loads) becomes very large.

In the following we have a closer look at two types of quantile functions: (a) derived from linearly interpolating the CDF, and (b) using the empirical CDF. After defining their equations for arbitrary weights we discuss their advantages and disadvantages.

(a) *Linear interpolation of the CDF:*

In this case the quantile function is the inverse of the linearly interpolated CDF:

$$x_q = \begin{cases} x_1 & \text{for } q \le w_1 = W_1 \\ x_k + (x_{k+1} - x_k)\dfrac{q - W_k}{w_{k+1}} & \text{for } W_k < q \le W_{k+1} \\ & k=1,\ldots,n-1 \end{cases} \qquad (4.5)$$

where $W_k$ is given by Eq. 4.3. An example is shown in Figure 4.2a.

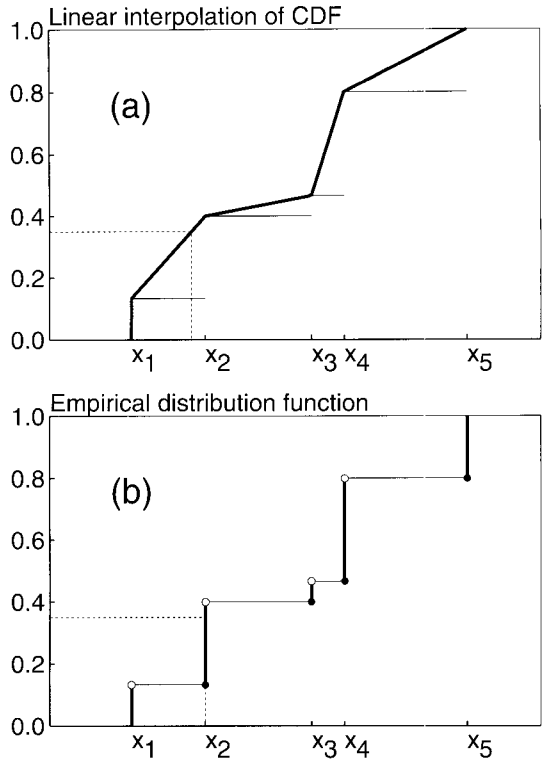


**Figure 4.2.** Examples of the two quantile functions discussed in the text. Values and weights are the same as in Figure 4.1. The filled (empty) circles indicate whether a point is part (not part) of the function. The thin horizontal lines indicate the cumulative distribution function. Note that for certain values of $q$ (e.g. $q$=0.35) the resulting quantile in (a) is smaller than the value obtained in (b).

The advantage of this quantile function is that it is continuous, i.e. a small change in $q$ leads to only a small change in the resulting quantile $x_q$. However, it has the following 3 disadvantages:
(i) In case of two (or more) identical data points the definition of the quantile function is not unique: for identical critical load values the shape of the interpolation function depends on the order of the weights (see Figures 4.3a,a'). Earlier this had been resolved by sorting the weights of identical data points according to size (smallest first, as in Figures 4.3a.b). This minimizes the difference to the empirical distribution function (see below), but requires fairly complicated (and time-consuming) routines for the actual computations.

(ii) As mentioned above, a critical load $x_q$ is selected to protect the $(1-q)$-th fraction of the ecosystems within a grid. However, for the linear interpolated quantile function certain choices of $q$ result in $x_q$-values which are *below* the actual value needed to

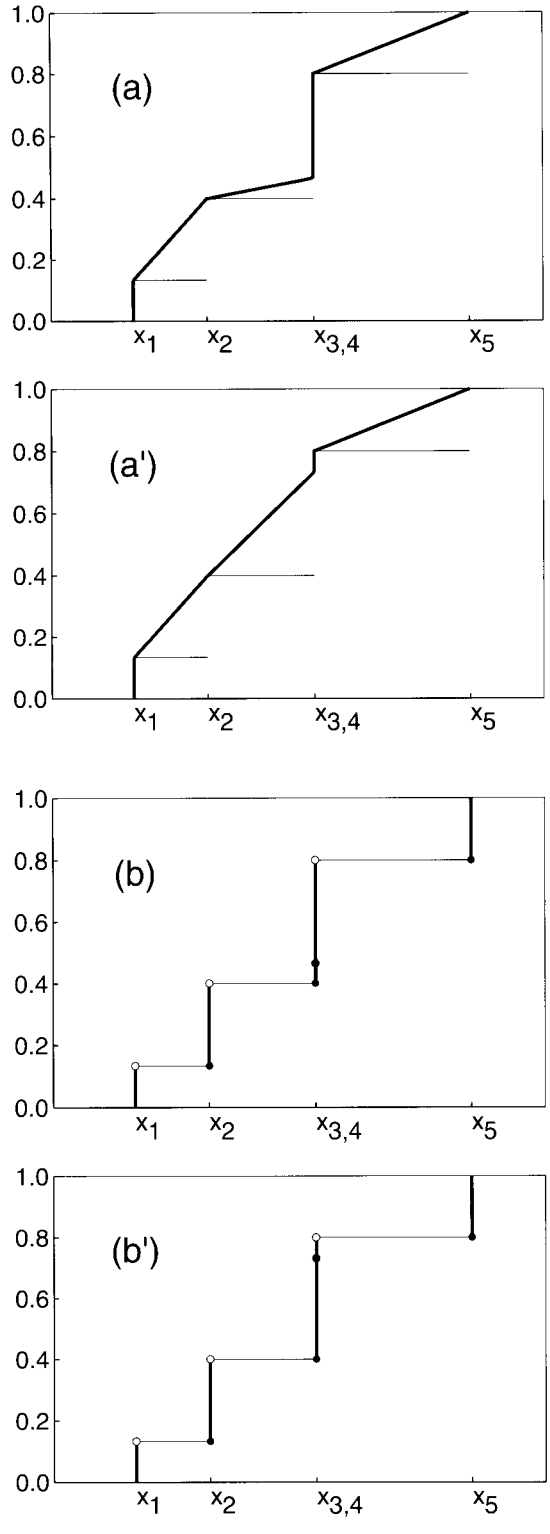


**Figure 4.3.** Examples of the two quantile functions discussed in the text. Values and weights are the same as in Figure 4.1, except that $x_3$=$x_4$ (cf. Figure 4.2). For the linear interpolated quantile function (a,a') its shape depends on the order of the weights for the identical values.

protect a fraction 1–$q$ of the ecosystems (see example in Figure 4.2). This is fine for the ecosystems, but may lead to higher costs for abatement.

(iii) The computation of quantiles is not order-preserving when using linear interpolation. We say the order is preserved by a quantile function, if the following holds for two CDFs

$$F_1(x) \le F_2(x) \text{ for all } x \Rightarrow x_q^{(1)} \le x_q^{(2)} \text{ for all } q \qquad (4.6)$$

i.e. the smaller CDF leads to smaller quantiles. In Figure 4.4a an example is shown with two data sets for the same $n$ ecosystems, $x_1,...,x_n$ and $y_1,...,y_n$ with common weights $w_1,...,w_n$ and the property $x_i < y_i$ for $i$=1,...,$n$ (e.g. $CL_{min}$'s and $CL_{max}$'s), and for certain values of $q$ it turns out that $x_q > y_q$ when computed by linear interpolation.

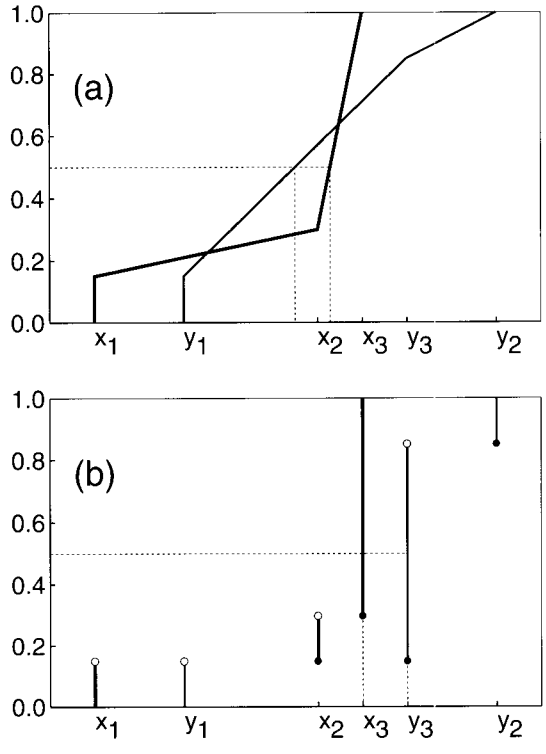


**Figure 4.4.** Example of two quantile functions for 3 values each ($x_1$, $x_2$, $x_3$ and $y_1$, $y_2$, $y_3$) and common weights $w_1$, $w_2$, $w_3$ and the property $x_i$<$y_i$ for $i$=1,2,3. However, in case (a) the median $x_{0.5}$ is greater than the median $y_{0.5}$.

(b) *Empirical distribution function:*

In this case the quantile function assumes only values defining the CDF:

$$x_q = \begin{cases} x_1 & \text{for } q < w_1 = W_1 \\ x_k & \text{for } W_{k-1} \le q < W_k,\ k=2,...,n-1 \\ x_n & \text{for } q \ge W_{n-1} \end{cases} \quad (4.7)$$

An examples of this quantile function is shown in Figure 4.2b. The disadvantage of this quantile function is that it is not continuous, i.e. a very small change in $q$ may lead to a significant change in the quantile $x_q$ (jump from $x_i$ to $x_{i+1}$).

However, none of the disadvantages of the linear interpolation holds for this function, but:
(i) identical values don't lead to ambiguities (see Figures 4.3b,b'),
(ii) the quantile $x_q$ protects (at least) a fraction $q$ of the ecosystems (see Figure 4.2b), and
(iii) the computation of quantiles is order-preserving (see Eq. 4.6 and Figure 4.4b).

Earlier, linear interpolation has been used by the CCE for producing critical load maps for Europe. But in view of the current guidelines for computing critical loads, it is especially the property (iii) which makes the empirical distribution function the only viable choice for computing percentiles.

## 4.3 Percentile functions and protection isolines

Above we have treated the case in which only one value (critical load) is given for an ecosystem. Now we shall discuss the generalization of percentiles to the case when critical loads are given as a function (rather than as single values), which is the case when considering two pollutants (sulfur and nitrogen) which interact with each other, leading to the so-called percentile function or (ecosystem) protection isoline (see Chapter 3).

In the following we assume that a critical load function is defined by a set of pairs of values $(x_j,y_j)$, $(j=1,...,m)$, and the function is given by connecting $(x_1,y_1)$ with $(x_2,y_2)$, and so on, in this way generating a polygon in the x-y plane. We denote this polygon (critical load function) by

$$f = [(x_1,y_1),...,(x_m,y_m)] \quad (4.8)$$

For the values $x_j$ and $y_j$ we assume that

$$0 = x_1 \le x_2 \le ... \le x_m \quad \text{and} \quad y_1 \ge y_2 ... \ge y_m = 0 \quad (4.9)$$

i.e. the points on the polygon are numbered from left to right, starting on the y-axis and ending on the x-axis. Eq. 4.9 also ensures that the polygon is monotonically decreasing, when considered as a function of $x$ or $y$. With the notation $(x,y)<f$ we mean that the point $(x,y)$ lies below the polygon (i.e. critical loads are not exceeded).

Considering the critical load for S and N acidity the critical load function for an ecosystem is defined by 3 values, namely $CL_{min}(N)$, $CL_{max}(N)$ and $CL_{max}(S)$, which define a polygon with $m$=3 points (see Chapter 3):

$$f = [(0,CL_{max}(S)),(CL_{min}(N),CL_{max}(S)),(CL_{max}(N),0)] \quad (4.10)$$

where we assumed that the N-deposition is measured along the x-axis and the S-deposition along the y-axis.

Now we assume that we have $n$ critical load functions $f_1,...,f_n$ in a grid cell, with respective weights $w_1,...,w_n$ ($\sum w_i=1$). However, it is not possible to sort these critical load functions, i.e. in general it is not possible to say that $f_i$ is larger or smaller than $f_j$, because $CL_{max}(S)$ for $f_i$ could be larger and $CL_{max}(N)$ smaller than the corresponding values for $f_j$ (see Figure 4.5 for examples). Nevertheless, we can define a cumulative distribution function $F$ in the following way:

$$F(x,y) = \sum_{(x,y)<f_i} w_i \quad (4.11)$$

meaning that for a given point $(x,y)$ we sum all weights $w_i$ for which $(x,y)<f_i$, i.e. for which there is no exceedance. Obviously $0 \le F(x,y) \le 1$, and $F$ has also otherwise all properties of a (two-dimensional) CDF. And a percentile $p$ is now easily defined as the intersection of such a function with a horizontal plane at height $q=p/100$. The result (projected onto the x-y plane) is a curve, more precisely a polygon which has the property defined in Eq. 4.9. Let $f_q$ be the quantile function (percentile function) for a given $q$, then every point $(x,y)$, i.e. every pair of N and S deposition, with $(x,y)<f_q$ protects (at least) a fraction of $1-q$ of the ecosystems; and $f_q$ is also called a *(ecosystem) protection isoline*. Note that protection isolines for the same set of polygons (critical load functions) do not intersect (although

they might coincide in parts), and for $r<s$ $f_r$ lies below $f_s$.

Since an exact computation of a percentile function is hardly feasible (especially in case of a large number of critical load functions), we have to use an approximate method (see Figure 4.5): We draw rays through the origin of the x-y plane (i.e. lines with a constant S:N deposition ratio) and compute the intersections of these rays with all critical load functions (small circles in Figure 4.5b). For each ray the intersection points are sorted according to their distance from the origin and a chosen quantile $q$ of these distances is calculated according to Eq. 4.7 (small diamonds in Figure 4.5c). Finally, the resulting quantile values are connected to obtain the percentile function (protection isoline) $f_q$. Obviously, the more rays are used in this procedure, the more accurate is the protection isoline. As the example in Figure 4.5c shows, a protection isoline need not be convex.

In Appendix B Fortran subroutines are provided which allow the computation of percentiles and can assist in the computation of protection isolines and protection percentages.

## Reference


Posch, M., J. Kämäri, M. Johansson and M. Forsius, 1993. Displaying inter- and intra-regional variability of large-scale survey results. *Environmetrics* **4**:341-352.


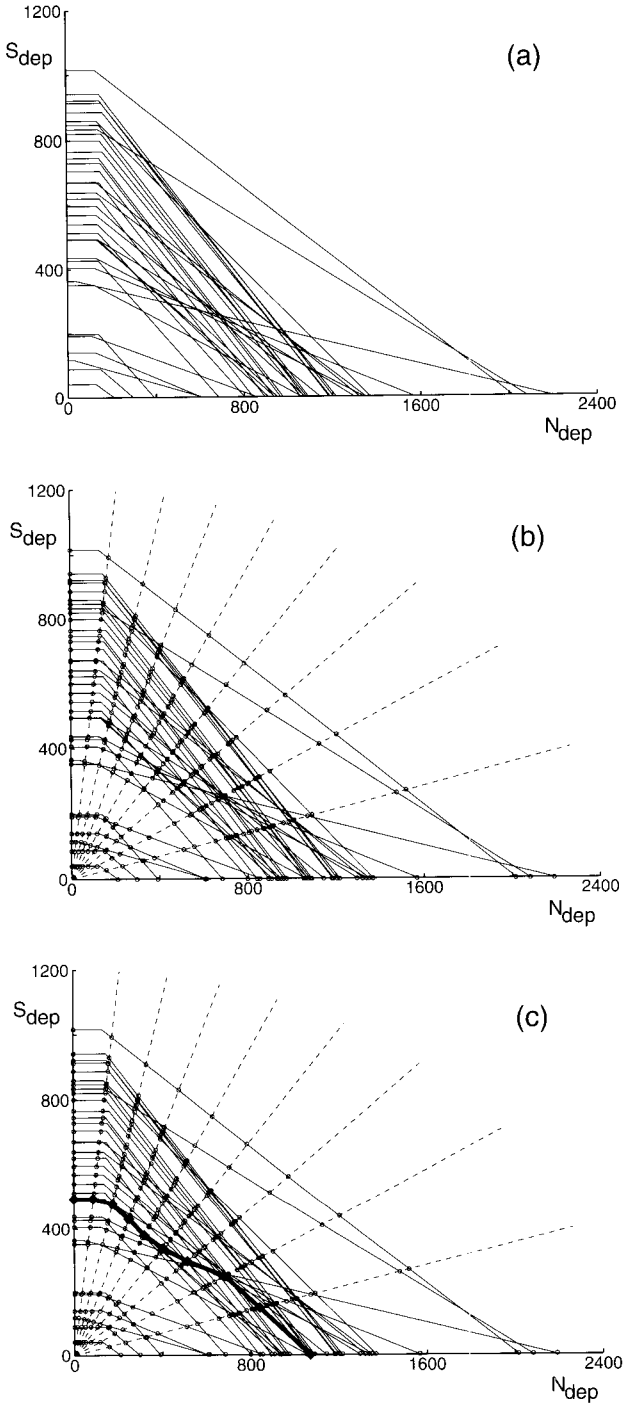


**Figure 4.5.** Critical load functions and the computation of a protection isoline: (a) set of critical load functions ($n$=36). (b) Intersection of this CL-functions with rays from the origin (small circles); (c) computing the percentile ($q$=0.5 in this case) along each ray (small diamonds) and connecting them to obtain the protection isoline (thick line).

# PART II. Related Research and Development

This part contains five papers on research developments which are relevant to the Effects Programme under the Convention:

1. *Mapping Land Use and Land Cover for Environmental Monitoring on a European Scale* describes the background of the maps which were also distributed by the CCE to the National Focal Centers earlier this year. After incorporating NFC revisions, they will be used for assessments of stock at risk due to exceedances of critical loads and levels.

2. *A Generalized Description of the Deposition of Acidifying Pollutants and Base Cation on a Small Scale in Europe* is relevant with respect to the issue of downscaling broad-scale information on base cation deposition to a higher resolution.

3. *EDEOS: European Deposition and Exposure of Ozone on a Small Scale* introduces the work which will contribute to an increased compatibility between small-scale national assessments of ozone exposure and the broad scale of the European modelling domain.

4. *Methods to Calculate Critical Loads for Heavy Metals and Persistent Organic Pollutants* proposes a methodology for the computation of critical loads for heavy metals and persistent organic pollutants (POPs), which was detailed in a report to National Focal Centers, in view of a possible future elaboration within the Effects Programme under the Convention.

5. *Critical Thresholds for Dutch Target Ecosystems Based on Risk Assessment* using the Netherlands as an example, introduces an alternative to the biogeochemical approach of computing critical loads by formulating critical thresholds for biodiversity.

# Mapping Land Use and Land Cover for Environmental Monitoring on a European Scale

Hans Veldkamp and Rob van de Velde
*National Institute of Public Health and the Environment (RIVM)*
*P.O. Box 1, 3720 BA Bilthoven, the Netherlands*

## Abstract

Integrated environmental monitoring and forecasting studies on a European scale are influenced significantly by the availability and accuracy of land use and land cover data. Due to an urgent need for a geo-referenced European Land Use (ELU) data base, the National Institute of Public Health and the Environment (RIVM, the Netherlands) created together with the Stockholm Environment Institute (SEI, United Kingdom), Geodan (the Netherlands) and INENCO (Russia) a digital pan-European land use data base. The spatial resolution is 10×10 minutes (geographical projection). This first version, released in 1994, distinguished 7 land use classes including arable land, grassland for agricultural use, permanent crops, forest and urban areas. More data from statistical sources as well as more spatial (map) data became available in the course of 1994 and 1995. Recently the second version has been released, which includes a number of enhancements.

## 1. Introduction

The monitoring of the environment and the development of environmental policies rely to a great extent on the outcome of environmental forecasting and process models. These models are significantly influenced by the accuracy of geo-referenced land use and land cover data. On a pan-European level this kind of data is very scarce.

Many initiatives exist which try to harmonize land use versus land cover data collection and integration. UNEP/FAO (1994) provides an excellent overview of such harmonization. According to Turner *et al.* (1993), *land cover* refers to the attributes of the land surface and immediate substrate including biotypes, soil, surface and groundwater, whereas *land use* refers to the purposes for which humans exploit land cover. Widespread land uses include agriculture (crop production and grazing), forestry, mineral extraction and recreation. Changes in the characteristics of land use and land cover affect sustainability of the environment and biodiversity. In Europe, most land cover change is driven by changes in land use.

In this study, the focus is on 'land use', and more importantly, the distinction between 'agricultural' land use and 'non-agricultural' land use. The way in which land is utilized determines the inherent threats to soil and groundwater.

The objectives of the study were to:
- make an inventory of existing and available land cover and land use data in Europe, and
- develop a European land Use Data Base the can be used for environmental monitoring.

To meet the first objective, a data inventory questionnaire was distributed to a large number of institutes and agencies in Europe and the United States. Multiple spatial and non-spatial data sources have been used as input for ELU.

It is a major requirement that the estimated land use areas are to be compared with external sources, such as the statistical land use data collected by Eurostat and the FAO. The methodology for creating ELU requires the derivation of the following three distinct data bases:
- a Pan-European Land Use Vector Data Base (LuVec)
- a Pan-European Land Use Statistical Data Base (LuStat)
- a 10×10 Minute Pan-European Land Use Data Base (LuGrid).

The 10×10 Minute Pan-European Land Use Data Base is the result of the integration of the vector and statistical data bases. The basic assumption is that this approach provides an optimal combination of spatial data (in the vector data base), and relatively sound areal estimates (extracted from the statistical data base).

The 10×10 Minute Pan-European Land Use Data Base includes the following land use types:

- arable land
- grassland for agricultural use
- permanent crops
- deciduous forest
- coniferous forest
- urban areas
- inland water
- other (natural areas and extensive agricultural land).

In the data base, the area of each land use type is stored per unit cell (10×10 minutes).

Feedback from the users of the first version of the Land Use Data Base showed that the most urgently needed improvements were the introduction of two classes: coniferous and deciduous forest, replacing the class 'forest', and an improvement of the spatial resolution for large regions in Eastern Europe. This apparent low resolution was caused by the low resolution of the statistics for these regions (country level). The most important enhancements of the second version of the data base are the following:

- new regional statistics for the Czech and Slovak Republics, Hungary, Poland and Romania
- incorporation of ESA's European Forest Map
- the land use class 'forest' was split into 'coniferous' and 'deciduous' forest
- an improved calibration algorithm for matching statistical and map data and assigning land use to the 10×10 minute cells.

This chapter describes the main sources, the methodology and results of ELU. The first version of ELU is documented in Van de Velde *et al.* (1994). The second version will be described in Veldkamp *et al.* (in prep.).

## 2. Sources of the European land use data base

LuVec is the Land Use VECtor data base. In short, it is a combination of all spatial (map) sources that were collected. It is available in digital vector format.

LuStat is the Land Use STATistical data base. It holds, for all regions in Europe at the most detailed level available, the area estimates for all land use classes.

### 2.1 The LuVec data base

The land use vector data base is the result of the integration of five different data sets. The most important source is the data set of the Stockholm Environment Institute (Kuylenstierna and Chadwick 1990). Classes not available in the SEI data set were adopted from other sources: the Digital Chart of the World (DCW), the World Data Bank II (WDBII), the FAO-Cartographia land use map of Europe, a Russian land use map, and the Remote Sensing Forest Map of Europe (ESA 1993).

*a. Stockholm Environment Institute*

Due to the similarity in land use classes between the SEI data set and the proposed nomenclature of the 10×10 Minutes Pan-European Land Use Data Base, the SEI data were used as a basic land use map. The SEI data set was constructed by digitizing the 1:2,500,000 scale Land Use Map of Europe (FAO Cartographia 1980) and the Types of Agriculture Map of Europe (Kostrowicki 1984). The FAO map is based on pre-1980 data. It covers most of Europe, including Iceland and the western part of Turkey. The land use of the former USSR was digitized from the Types of Agriculture Map of Europe (Kostrowicki 1984) with reference to the Weltforstatlas (1975). The SEI data set was created as a basis for studies on the environmental impacts of acid deposition (Chadwick and Kuylenstierna 1990). The SEI data set discriminates the following classes:

- coniferous forest and mixed forest
- broad-leaved forest
- intensive agriculture, including all arable land and improved grassland
- extensive agriculture and natural areas
- glaciers.

The digitizing of the Land Use Map of Europe by SEI entailed a degree of generalization and simplification commensurate with the use of the map to study acidic deposition on a Europe-wide scale.

*b. Digital Chart of the World*

The Digital Chart of the World (1991) is a geographical, vector-based data set published by the US Defense Mapping Agency to support the display and analysis of geographic data (MIL-STD-89009). The DCW, available on CD-ROM, was first published in 1992. The primary (analog) sources for the DCW include a series of 1:1,000,000 scale

maps from the Operational Navigational Chart, and the 1:2,000,000 scale Jet Navigation Charts. DCW contains many data layers, from which only the 'urban areas' were extracted for LuVec.

*c. World Data Bank II*

The World Data Bank II (WDBII) 1989-1993 is a global data set produced by the Environmental Systems Research Institute (ESRI 1993) with a scale of 1:3,000,000. The data set contains of six types of digital cartographic boundaries: coastlines, islands and lakes, international boundaries, internal administrative boundaries, rivers, roads and railroads. For LuVec only lakes were extracted.

*d. Land Use Map of Europe (FAO-Cartographia 1980)*

The land use class 'permanent crops' was digitized from this analog map.

*e. Digital Land Use of the USSR (1993)*

A data set, extending eastward to the Ural Mountains, has been digitized from the 'Land Use Map of the USSR', on a scale of 1:22,000,000. The country border, on the other hand, is extracted from a 1:8,000,000 scale map. This map replaces the SEI data in the eastern part of Russia.

*f. ESA Remote Sensing Forest Map of Europe*

The Remote Sensing Forest Map of Europe (ESA 1992) was derived from NOAA-AVHRR satellite data dating from 1989 to 1992 by digital classification. Accuracy checks performed by comparing the NOAA classification results with classified Landsat MSS imagery show an overall accuracy of 82.5% and a surface accuracy of 93.8% on the average. The digital data set contains the classes 'forest' and 'water'. The water bodies represented are lakes and the wider rivers like Volga and Dnieper. The fact that water was detected digitally assures a constant accuracy throughout the entire map. The WDBII, which was used for the extraction of water bodies in the first version of ELU, is not very consequent when it comes to lakes: some small lakes are represented whereas some larger ones are not. The resolution is very high: 1 square kilometer. Further advantages are the recent age, and the fact that it covers the entire study area of the 10×10 Minute Pan-European Land Use Data Base. This data base was not in itself included in LuVec, but instead was used in the calibration routine that matches area estimates from statistical sources with those of LuVec (described later in this document), for allocating water and forest to 10×10 minute cells.

**Integration of the various map sources**

LuVec was created by merging the various source data using different priorities. In order of decreasing priority these are:

- 'lakes' from WDBII
- 'urban areas' from DCW
- 'permanent crops' from FAO Cartographia
- 'forest' from ESA
- SEI data

In other words, if a certain location is identified as a lake by WDBII, but an urban area by DCW, it will be a lake in LuVec. The administrative (regional) codes originate from an RIVM data set with European administrative regional boundaries.

The seven classes of LuVec and their contents are the following:

1. Arable land and intensively used grassland such as:
   - Temporary crops: arable land of constant use, and/or temporary fallow on at least 50% of the territory, and grain crops.
   - Improved grassland: dry as well as wet grassland

2. Permanent crops such as:
   - Vineyards; intermixed with arable land, in orchards, on grassland
   - Olives; intermixed with arable land, in orchards, on grassland
   - Soft fruits, citrus fruits, stone fruits, nuts, mixed orchards and berries

3. Broad-leaved forest:
   - Includes all forests and woodlands with mainly deciduous forest types; productive as well as non-productive forest and woodland.

4. Coniferous and mixed forest:
   - Includes all forests and woodlands with mainly coniferous and mixed forest types; productive as well as non-productive forest and woodland.

5. Inland water:
   - For inland waters (lakes) the WDBII is used, where only large inland waters in Europe are represented. The data on rivers in WDBII are not used due to the very global character. This 'water' class takes precedence over any of the original water classes from LuVec, urban areas

from the DCW and permanent crops. Water bodies originating from the SEI data set, are also present in the FAO-Cartographia Land Use Map (natural lakes and reservoirs). Additional information about inland water was taken from the ESA Remote Sensing Forest Map during the calibration phase.

6. Urban areas:
   - This class is taken from DCW. It only represents the larger cities in Europe. Airports, large road networks, industrial areas outside cities and other built-up areas not directly located within city borders are excluded. Urban areas may also come directly from the SEI data set. Whenever this is the case, they represent the built-up areas of the larger cities in Europe introduced on the map for orientation purposes.

7. Extensive agriculture and natural areas include:
   - Unimproved grassland; dry as well as wet grassland
   - Waste lands: rocks, glaciers, sand dunes, swamps and marshlands
- Zones of very low productivity: scattered grass, (reindeer) moss, rocks, low shrubs, permanent snow-cover (for over 6 months), areas dominated by peat and/or bog.

## 2.2 The LuStat data base

LuStat is the ELU Land Use STATistical data base. It contains land use statistics at the most detailed level (national or sub-national) at which collection was possible, given the amount of time available. It was constructed from a wide variety of different sources.

The creation of a pan-European Land Use Statistical data base (LuStat) out of recent data requires the use of a variety of sources. Data at the lowest regional level are preferred. The following section summarizes sources of data that are incorporated in LuStat.

- Eurostat (1991): Agri2landuse; scale NUTS regions 0,1,2,3, Eurostat 1991.
- FAO-Agrostat (1991): FAO-Agrostat computerized information series; scale countries, FAO 1991.
- EC-Brussels/Eurostat (1993): Pan-European Questionnaire Eurostat; scale countries.
- Statistics delivered by national statistics bureaus. For western European countries, regional statistics were gathered from the national agencies of Austria (1992), Norway (1989), Switzerland (1985) and Finland (1992).

To overcome the lack of official regional level statistical data for Eastern European countries, special inventories were assembled by Geodan Polska and an INENCO contact. The results of these two inventories were partially used as input for LuStat.

The majority of statistical sources collected are generated for agricultural purposes. Therefore the classes 'water' and 'urban' are often not available. Instead, a class 'land use not agricultural' has been given as a kind of an 'other' class. In order to be comparable with LuVec a relationship with the LuVec classes 'intensive agriculture' and 'extensive agriculture/natural areas' must be established. The statistical classes 'grass' and 'arable' were therefore summarized into 'intensive agriculture'. The sum of the LuVec classes 'extensive agriculture/rough areas', 'water' and 'urban' can be compared with the statistical class 'no agricultural land use'.

**Integration of the various statistical sources:**
The first part of the integration consists of the conversion of all different sources to a common platform (Arc/Info), and the translation of the classes to the FAO land use classes. Next, the complex process of integrating the data into one European data set was performed. It is important to note that the scale of the statistical data ranges from national level (small scale) to NUTS 3 level (large scale, for example in the INENCO data set for Russia).
A complex link exists between the spatial reference data and the statistical data. This is done by means of a unique region code. This code, defined by the RIVM, consists of two letters followed by 4 numbers, depending on the level of differentiation of the statistical data. This code is introduced in the statistical data base using the matching regional or country level code. The spatial reference map contains, for example, the borders of all Russian regions. For Sweden, of which only national statistics were available, only a country border is provided. LuStat version 1 contains statistical data for 289 regions/countries. LuStat version 2 contains data for 401 regions/countries.

**Integration of the vector and statistical data bases:** The areal estimates of statistical data bases are usually superior to those of maps. On the other hand the areas for which the statistics are calculated usually measure hundreds of square kilometers, thus the spatial resolution is poor. Land use maps generally have a higher spatial resolution. Due to neglecting smaller polygons the areal estimates, however, are poor. An ideal land use data base combines a high spatial resolution (ie. where is which land use) and areal estimates (ie. how much of the various land use classes there is).

LuGrid is the result of the combination of the vector data base and statistical data base. The basic assumption is that this approach provides an optimal combination of the spatial data in the vector data base and the relatively sound areal estimates in the statistical data base.

Due to the resolution of the vector data, the land use in a polygon is by definition the dominant land use and not the exclusive land use. It will typically be mixed with a significant percentage of another class. As a result, some of the land use types will be regionally overestimated (e.g. the total area of permanent crops), while others may be underestimated. In the 'permanent crops' example, the LuVec vector data indicates the **areas** in which permanent crops are located, while the actual **coverage** within these areas is limited and will usually not be over fifty percent. This will be true, to some extent, for all classes.

## 3. Calibration

The calibration operates on the lowest regional level for which statistics are available. It tries to match the areal estimates per region (present in LuStat) with the regional sums derived from LuVec. This is achieved by increasing underestimated land use types and decreasing overestimated ones. In order to allow for land use types to be introduced in an area with another dominant land use, some initial adjustments were made. In a class with a zero percent land use, no increase is possible. After careful examination of the statistical data and the LuVec vector data, the following assumptions were made in the preparation process in order to introduce alternative land uses:

- a polygon with permanent crops may contain arable land and grass land
- a polygon with forest may contain grass land
- the land use classes arable and grass are added to replace the class corresponding to the class intensive agriculture in LuVec that combines these two classes. This operation is based upon the ratio between grass and arable from the statistical data set.

If a 10×10 minute cell partly or fully coincides with water according to the ESA map, a percentage of water is assigned to this cell proportionally. In this way the inconsistencies of LuVec for the class water (resulting from the global character of WDBII) are removed.

A special set of rules was adopted for the allocation of forest to cells. It uses the high spatial resolution of the ESA Forest Map, in combination with LuVec. The most important rule is that forest is allocated preferentially to those 10×10 minute cells where both LuVec and the ESA data base claim forest. This rule also works the other way around: if, compared to LuStat, too much 'LuVec forest' is present in a region, it will be removed from those cells for which the ESA data base indicates no forest.

The calibration works iteratively. Each consecutive step brings the regional totals calculated from LuGrid closer to the LuStat totals. It turns out that after approximately 25 runs no more significant improvements are achieved. By then only a small minority of the summed statistics for the individual regions exhibits deviations from the LuStat that exceed 5%.

### 3.1 LuGrid

LuGrid is the result of the calibration. It consists of two parts. The first part is the spatial reference map. It consists of a fishnet grid of square cells which measure 10×10 minutes. It covers the entire land surface of Europe. The entire map contains slightly over 60,000 cells. Each cell has a unique numerical identification value (grid-id) by which the cell is related to the second part, the attribute data base. In this data base the percentile distribution of the various land use classes is stored, i.e. the percentage of the cell covered by each of the classes. The area each class occupies per cell can also be calculated using the total area of the cell.

### 3.2 Nomenclature

The eight land use classes that are distinguished are:
- arable land
- coniferous forest
- deciduous forest
- grassland for agricultural use
- permanent crops
- urban areas
- inland water
- predominantly extensive agricultural and natural areas ('other' land use)

The structure of LuGrid allows the easy creation of 'percentage land use' and 'dominant class' maps. Figure 1 shows the dominant class per unit cell. Figures 2 and 3 show the percentages coniferous and deciduous forest, respectively.

## 4. Results

For evaluation purposes, country totals derived from LuGrid were compared with European-wide statistics: FAO-AgroStat and the pan-European questionnaire by EuroStat. In general the totals are very similar. The most important differences occur for the classes 'other' and 'grassland'. This is probably due to a difference in class definition. The ELU class 'other' includes grassland which is not used for cattle grazing.

LuGrid was also compared with high resolution national land use and land cover data bases from various (climatic, geographical) regions in Europe. Data came from the Iberian peninsula (CORINE 1992), the Netherlands (LGN-1, Thunissen *et al.* 1992) and Sweden (Swedish Space Corporation data). The results will be published in Veldkamp *et al.* (in prep.). In general LuGrid compares very well to the national data bases.

## 5. Conclusions

The attempt to develop a digital European land use data base has been completed successfully. However, it is only a first step to meet the demand for land use data for integrated environmental monitoring on a European scale. In this approach analytical geographical information systems play a important role.

The project attempted to define a reasonable land use nomenclature with a spatial resolution of 10×10 minutes, given limited resources and time. The concept of the integration of spatial data and statistical data was developed. Many sources of spatial and statistical land use and land cover were encountered. The meta-data were stored in a information system.

It is clear that some of the land use classes are heterogeneous in themselves. This is illustrated by the land use class 'other', which represents 21% of the total area in Europe. Geo-referenced statistical data on land use are becoming more and more available, but many internal inconsistencies remain. The availability of detailed regional land use statistics affect the accuracy of the derived land use data bases significantly.

A number of steps were taken to evaluate the areal accuracy of ELU. For evaluation of the areal accuracy the Pan-European Questionnaire Eurostat (1993) on national land use statistics was used. Significant differences occur for the land use classes 'grassland' and 'other'. The land use class 'other' includes extensive grasslands and wetlands (SEI data base), indicating the grassland which does not play an important role in cattle grazing. Eurostat (and national statistical offices) may include these grasslands in their land use category 'grassland/-pasture'. In general the Land Use Data Base shows a reasonable fit with the Eurostat questionnaire.

Since early 1994, ELU has been used in various projects. Within the framework of Europe's State of the Environment 1993 report (Meinardi *et al.* 1994) it was used to predict the nitrogen load and pesticides compounds in European soils. In a model which calculates deposition maps of acidifying components the land use data were used to calculate roughness length maps (Van Pul *et al.* 1995).

Future improvements of the European Land Use data base will include the construction of a NOAA--AVHRR derived land cover data base at a resolution of 1 kilometer in cooperation with the Winand Staring Center and Geodan. A pilot study investigating the potential value of NOAA-AVHRR was finished in 1994 (Mücher *et al.* 1994), and the results are promising. Clear advantages of a satellite imagery derived data base over ELU are the high spatial accuracy, and the homogeneity over the entire continent due to the use of a single methodology.

## References


Chadwick, M.J. and J.C.I. Kuylenstierna, 1990. The relative sensitivity of ecosystems in Europe to Acidic Depositions. A preliminary assessment of the sensitivity of aquatic and terrestrial ecosystems. Perspectives in Energy, Volume 1, p71-93.

CORINE, 1992. Corine land cover: A European Community project. Presented in the framework of the International Space Year. Brochure based on the draft final report of the Corine land cover project.

European Space Agency (ESA), 1993. ISY Forest Map of Europe based on NOAA-AVHRR. Rep. 9730/91/NL/FG.ESA/ ESTEC. Noordwijk, The Netherlands.

ESRI, 1993. World Data Bank II, 1989-1993. Vector-based data set, Scale 1:3,000,000. ESRI, Redlands, Calif., USA.

Eurostat, 1991. Land use data on NUTS 0, 1 and 2 level, Agri2landuse land use data base, Luxembourg.

Eurostat, 1993. Pan-European Questionnaire on Land Use Statistics. October 1993, M. Pau, Dir F. Eurostat (unpublished).

FAO-Cartographia, 1980. Land use map of Europe. Scale 1:2.500.000. Budapest.

FAO-Agrostat, 1991. Computerized information series. Rome.

Kostrowicki, J. (ed.), 1984. Types of Agriculture Map of Europe. Scale 1:2,500,000. Polish Academy of Science, Warsaw.

Kuylenstierna, J.C.I. and M.J. Chadwick (eds.), 1990. SEI data set. Data set created from several sources. The main sources are the Land Use Map of Europe (FAO-Cartographia, 1980), and the Types of Agriculture Map of Europe (Kostrowicki, 1984). Stockholm Environment Institute, York.

Meinardi C.R., A.H.W. Beusen, O. Klepper and W.J. Willems, 1994. Average nitrate contamination of European groundwater. RIVM Rep. 461501003. Bilthoven, the Netherlands.

Mücher, C.A., R.J. van de Velde and G.J. Nieuwenhuis, 1994. Mapping land cover for environmental monitoring on a European scale: pilot project for the applicability of NOAA/-AVHRR HRPT data. RIVM report number 402001004. SC-DLO/RIVM, Wageningen/Bilthoven.

Thunissen, H., R. Olthof, P. Getz and L. Vels, 1992. Grondgebruiksdatabank van Nederland vervaardigd met behulp van Landsat Thematic Mapper opnamen. DLO Staring Centrum rapport 168, Wageningen. (in Dutch)

Turner, B.L., R.H. Moss and D.L. Skole, 1993. Relating Land Use and Global Change: A Proposal for an IGBP-HDP Core Project No. 24 and HDP Report No. 5, International Geosphere-Biosphere Program and the Human Dimension of Global Environmental Change Program, Stockholm, 65p.

UNEP/FAO, 1994. Report of the UNEP/FAO Expert Meeting on Harmonizing Land Cover and Land Use Classifications. GEMS Report series no. 25, Nairobi.

United States Defense Mapping Agency, 1992. Digital Chart of the World. Scale 1:1.000.000. Washington DC.

Van de Velde, R.J., W.S. Faber, V.F. van Katwijk, J.C.I. Kuylenstierna, H.J. Scholten, T.J.M. Thewessen, M. Verspuij and M. Zevenbergen, 1994. The preparation of a European Land Use data base. RIVM report number 712401001. RIVM, Bilthoven, The Netherlands, 63 p.

Van Pul, W.A.J., C.J.M. Potma, E.P. van Leeuwen, G.P.J. Draaijers, J.W. Erisman, 1995. EDACS: European Deposition of Acidifying Components on a Small Scale. Model description and preliminary results. RIVM Rep. 722401005. RIVM, Bilthoven, The Netherlands.

Veldkamp, J.G., W.S. Faber, V.F. van Katwijk and R.J. van de Velde (in prep.). Enhancements of the 10×10 minutes Pan-European Land Use Data Base. RIVM, Bilthoven, The Netherlands.

Weltforstatlas, 1975. The World Forestry Atlas. Verlag Paul Parey, Stuttgart.

**Figure 1.** The dominant land use class per grid cell (10 x 10 minutes).

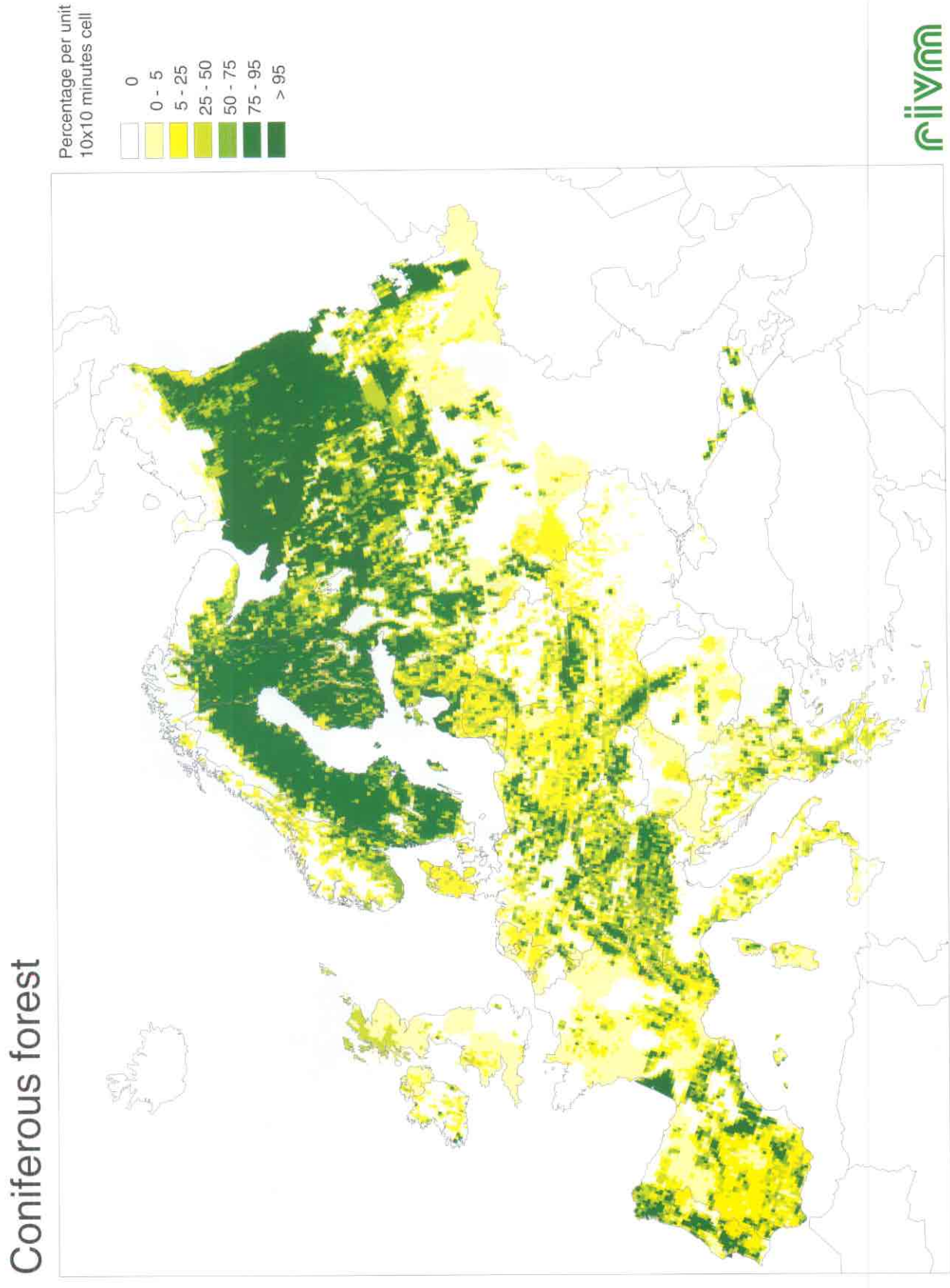


**Figure 2.** Percentage coniferous forest per grid cell (10 x 10 minutes).

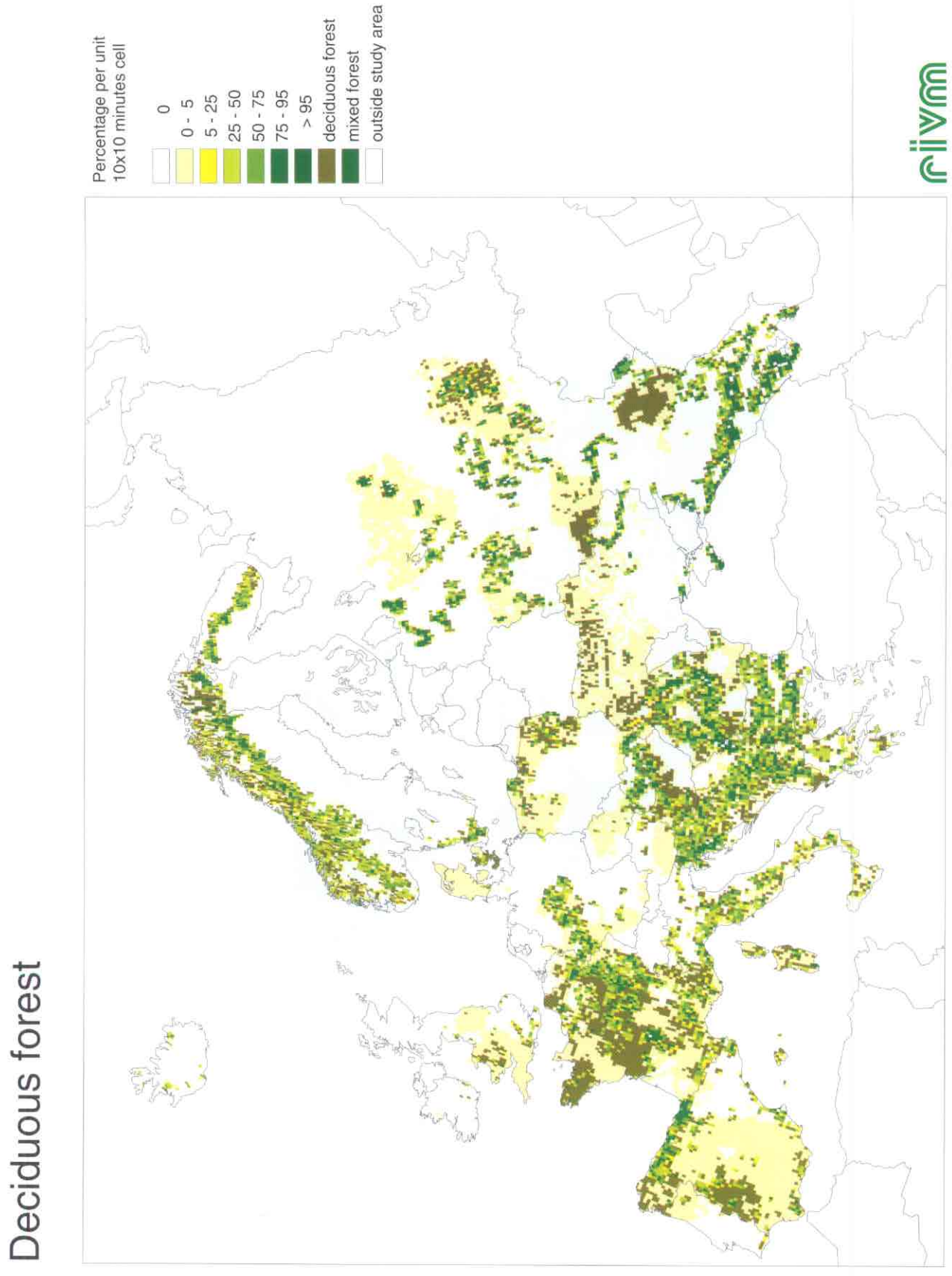


**Figure 3.** Percentage deciduous forest per grid cell (10 x 10 minutes).

# A Generalized Description of the Deposition of Acidifying Pollutants and Base Cations on a Small Scale in Europe

J. W. Erisman, C. Potma, W.A.J. van Pul, E.P. van Leeuwen and G.P.J. Draaijers
*National Institute of Public Health and the Environment (RIVM),*
*P.O. Box 1, 3720 BA Bilthoven, the Netherlands*

## Abstract

In describing the effects of acidification on the level of ecosystems, net acid loads should be available at least on the size of ecosystems. No deposition maps on this resolution are available, hampering accurate estimation of exceedances of critical loads in Europe. Here, the first maps of small scale fluxes in Europe are presented. The maps have been produced in close cooperation with EMEP. The acidifying components taken into account are oxidized sulfur and nitrogen and reduced nitrogen compounds. The method for estimating dry deposition is based on the combination of long-range transport model concentrations provided by EMEP and a detailed description of dry deposition processes. Dry deposition velocities are calculated on a small scale using the inferential technique. Resistances are modeled using observations of meteorological parameters in Europe and parametrization of surface exchange processes from deposition measurements. Wet deposition maps are derived using measured concentrations in precipitation at 750 sites in Europe together with precipitation amounts. Atmospheric deposition of base cations in Europe is also mapped on a 10 x 20 km grid using the inferential modeling technique. Deposition fields are found to resemble the geographic variability of sources, climate and land use. In large parts of southern Europe, more than 50% of the potential acid deposition is counteracted by deposition of base cations. In central and northwestern Europe, however, base cation deposition usually amounts less than 25% of the acid input. An uncertainty analysis to assess the quality of the base cation deposition maps revealed that for an average grid cell the deviation from the estimated value can be as large as 140%.

## 1. Introduction

In Europe, sulfur compounds and both reduced and oxidized nitrogen compounds have been shown to acidify soils and surface waters. Furthermore, nitrogen deposition causes eutrophication (e.g. Heij and Schneider 1991). The components considered in the acidification and eutrophication processes are $SO_2$ and aerosols of $SO_4^{2-}$ ($SO_x$); NO, $NO_2$, $HNO_2$, $HNO_3$ and aerosols of $NO_3^-$ ($NO_y$); and $NH_3$ and aerosols of $NH_4^+$ ($NH_x$). These pollutants are transferred to soil, vegetation and water surfaces by wet deposition, cloud and fog deposition and dry deposition. The amount of pollutants received by ecosystems through atmospheric deposition processes is considerable and for several reasons it is of interest to quantify it. Deposition can be studied from the atmospheric point of view, in order to determine how much is left in the atmosphere to be dispersed further, or from the receptor point of view, to determine the input of pollutants to ecosystems. For both purposes, reliable deposition monitoring or estimates are necessary, which may be characterized by different accuracy and spatial resolutions (Erisman and Draaijers 1995).

With regard to acidification, usually little emphasis is placed on the role of base cations such as $Na^+$, $Mg^{2+}$, $Ca^{2+}$ and $K^+$ in relation to acid deposition. Base cations play an integral role in the chemical processes of acid deposition since the acidity of any material is a function of both its acidic and basic compounds. Besides their ability to neutralize acid input, base cations are important nutrient elements for ecosystems. The depletion of exchangeable base cations in sensitive soils is currently thought to represent a major detrimental effect of acid deposition on terrestrial ecosystems (De Vries 1994). Atmospheric input may be a quantitatively important source of base cations to vegetation in nutrient-poor conditions.

Base cations in the atmosphere originate from both semi-natural and anthropogenic sources (Gorham 1994). Semi-natural sources of base cations are associated with wind erosion of arid soils, forest fires and biological mobilization (pollen). Especially soils on calcareous bedrock may emit large amounts of alkaline particles to the atmosphere. In maritime areas, sea spray may be an important source of $Na^+$ and $Mg^{2+}$-containing particles. Anthropogenic sources of alkaline particles include agricultural tillage practices (plowing, liming), traffic on unpaved roads, and oil/coal burning generating fly ash. Non-fossil fuel combustion (wood and peat) is found an important source for alkaline particles in, e.g. Scandinavia (Anttila 1990). Limestone quarries and cement factories are local sources of $Ca^{2+}$. Due to the large mass median diameters of alkaline particles and consequently high dry deposition velocities, most soil-derived particles are likely to deposit near the area of origin (Milford and Davidson 1985), although long-range transport of, for example, desert dust has also been reported (e.g. Swap *et al.* 1992).

Investigations on abatement strategies based on the critical load concept require relevant deposition data of acidifying substances and base cations on both local and regional scales (Nilsson and Grennfelt 1988, Hettelingh *et al.* 1991, Lövblad *et al.* 1993). On the local scale, large variations in deposition over landscape features and their variations in sensitivity make it essential to compare the critical load value for a specific ecosystem with the actual deposition so as to determine the exceedance value. On the larger regional scale, the essential parameters are dispersion and deposition, which must be estimated in order to assess the relevant abatement strategies. For pollution deposition over Europe and budget estimates the regional-scale approach is required (e.g. Tuovinen *et al.* 1994). The local-scale approach covers the calculation of the more site-specific critical load exceedances. The two approaches should be linked in order to evaluate the complete chain from emission to deposition and to develop relevant abatement strategies. This requires parametrization of the deposition processes on ecosystem level (Erisman and Draaijers 1995). On the national level there have been some studies showing the local variation in deposition: in the UK (URGAR 1990), in Sweden (Lövblad *et al.* 1993) and in the Netherlands (Erisman 1993). The dry deposition flux is inferred as the product of ambient concentration of the components of interest and its dry deposition velocity, whereas the wet deposition flux is obtained by interpolating wet deposition measurements.

Up to now, no reliable information is available on the spatial pattern of base cation deposition over Europe. There is lack of knowledge on the spatial and temporal variation of emissions and concentrations, hampering accurate deposition mapping. Here, a method is proposed to estimate local-scale deposition fluxes of acidifying substances in Europe by applying a combination of long-range transport (LRT) modeling and local scale inferential deposition modeling (Erisman 1993, Erisman and Baldocchi 1994, van Pul *et al.* 1992, 1994) as applied in the model Estimation of Deposition of Acidifying Components on a small scale in Europe (EDACS). Furthermore, first base cation deposition maps of Europe are presented which are also based on the inferential modeling technique. In this paper the method is explained and results of local scale deposition fluxes are presented. Base cation deposition is compared to the deposition of potential acid ($SO_x$+$NO_y$+$NH_x$). Furthermore, the uncertainty in results is assessed.

## 2. Description of Method

*Acidifying substances*

The deposition model developed at RIVM is the EDACS model (Estimation of Deposition of Acidifying Components on a Small scale in Europe, Van Pul *et al.* 1995). The outline of the EDACS model to estimate local and regional scale deposition fluxes is presented in Figure 1. The basis for the two estimates is formed by results of the EMEP long-range transport model. With this model dry, wet and total deposition is estimated on a 150 x 150 km grid over Europe using emissions of $SO_2$, $NO_x$ and $NH_3$ (e.g. Tuovinen *et al.* 1994). The model results are used for estimating country-to-country budgets, as a basis of sulfur and nitrogen protocols, and for assessments. The local-scale approach used by RIVM depends strongly on the long-range transport model results. Calculated ambient concentrations of the acidifying components (daily averages) are used along with a detailed land use map and meteorological observations to estimate small-scale dry deposition fluxes (Figure 1). By using calculated concentration maps, the relationship between emissions and deposition is maintained and scenario

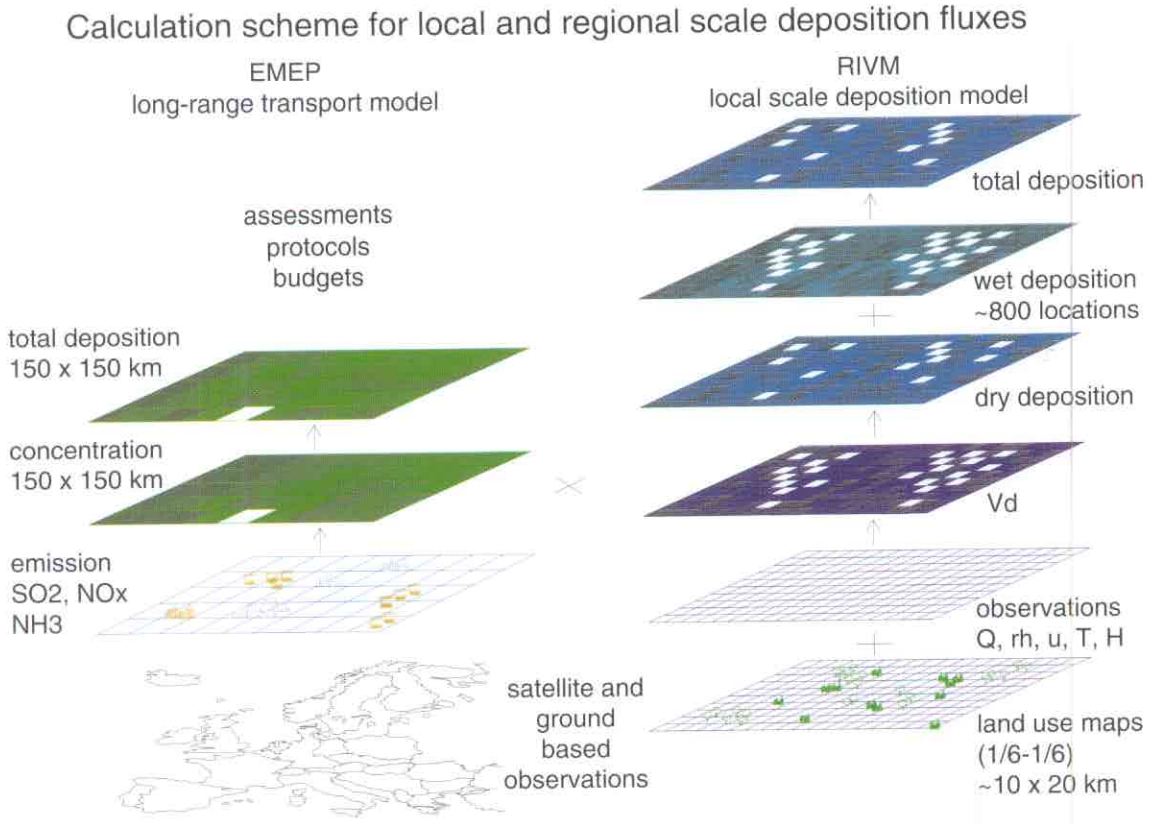


**Figure 1.** Outline of the method to estimate local-scale deposition fluxes.

studies, budget studies and assessments can be carried out on different scales. Wet deposition is added to the dry deposition to estimate total local scale deposition in Europe. Wet deposition can either be obtained directly from the EMEP model, or from measurements. The latter method is used here and will be described in the next section.

*Base cations*

The dry deposition flux of base cations is calculated as the product of the dry deposition velocity and air concentration at a reference height above the surface. In the inferential technique, the choice for a reference height (50 m) is a compromise between the height where the concentration is not severely affected by local deposition or emissions and is still within the constant flux layer (Erisman 1992). For this height, dry deposition velocity fields over Europe are constructed with EDACS. The parametrization of the dry deposition velocity for particles was based on the model of Slinn (1982) and tested with micrometeorological measurements recently performed at the Speulder forest in the Netherlands (Ruijgrok *et al.* 1994, Erisman *et al.* 1994). It includes both turbulent exchange and sedimentation of coarse particles. Six-hourly based dry deposition velocity fields were aggregated to annual means before being combined with annual mean air concentration fields, yielding dry deposition estimates on a small scale over Europe. This is in contrast to the acidifying components, where 6-hour average concentrations and deposition velocities are used.

Surface-level air concentrations were estimated from precipitation concentrations using scavenging ratios. These were derived from simultaneous measurements of base cation concentrations in precipitation and surface-level air performed by Eder and Dennis (1990) in Canada and Römer and Te Winkel (1994) in The Netherlands. This approach to estimate air concentrations is based on the premise that cloud droplets and precipitation efficiently scavenge aerosols, resulting in a strong correlation between concentrations within precipitation and the surface-level air (Eder and Dennis 1990). This assumption is only valid for well-mixed conditions at a sufficient distance from sources. Factors that will influence the magnitude and variability of scavenging ratios include particle size distribution and solubility, precipitation amount and rate, droplet accretion process and storm type (Galloway *et al.* 1993). Event scavenging ratios can differ by several orders of magnitude even for single species at a single location, but scavenging ratios have been found to be reasonably consistent when averaged over one year or longer (Galloway

*et al.* 1993). Therefore, annual mean precipitation concentrations were used to infer annual mean air concentrations of $Na^+$, $Mg^{2+}$, $Ca^{2+}$ and $K^+$. Precipitation concentration data were taken from Van Leeuwen *et al.* (1995) as described in the next section.

Deposition of $Na^+$ and part of the deposition of $Mg^{2+}$, $Ca^{2+}$ and $K^+$ will be the result of sea spray. In sea spray these ions are mainly associated with $Cl^-$, and thus do not contribute to neutralization of atmospheric acid. To estimate what fraction of $Mg^{2+}$, $Ca^{2+}$ and $K^+$ is of non-sea salt origin, correction factors have been derived based on the composition of sea water (Asman *et al.* 1981). It is assumed that $Na^+$ originates exclusively from sea spray and that the ratio between the concentration in sea spray for the component to be corrected and $Na^+$ is the same as in bulk sea water. Using such a correction will only yield reliable estimates on non-sea salt $Mg^{2+}$, $Ca^{2+}$ and $K^+$ in areas where sea salt is the only source of $Na^+$ in ambient air.

## 2.1 Wet deposition

Up to now, wet deposition maps on a European scale are based on long-range transport model results, whereas for most components wet deposition maps based on measurements are only available on national scales. Van Leeuwen *et al.* (1995) used measurements to estimate wet deposition in Europe. Acidifying components and basic cations were mapped on a 50 x 50 km scale over Europe for 1989, based on results of field measurements made at approximately 750 locations (the number of locations differs per component). Information on concentrations of ions in precipitation in 1989 was obtained from the EMEP data base and from organizations responsible for wet deposition monitoring in their countries. Concentrations measured with bulk samplers were corrected for the contribution of dry deposition onto the funnels of these samplers. Sulfate concentrations were corrected for the contribution of sea salt. Point observations were interpolated to a field covering the whole of Europe using the kriging interpolation technique.

As an example, the wet deposition flux maps of total potential acid (Figure 2) and total base cations (Figure 3) are presented. Total deposition is calculated as $NH_x+NO_y+2SO_x$ and $K^+ + 2Ca^{2+} + 2Mg^{2+}$, respectively, i.e. expressed in eq $ha^{-1}$ $yr^{-1}$. Potential acid can be used to determine the maximum acid input to ecosystems. Figure 2 clearly resembles European emissions of the three components and climate patterns. The highest input is found in areas with high rainfall (mountainous regions, coastal areas) and in areas with high sulfur emissions. Sulfur input yields the highest contribution to the potential acid input. The actual acid load depends on the input of alkaline components and the extend that $NH_3$ is nitrified in the soil (e.g. Heij and Schneider 1991, Erisman 1993). Total deposition of base cations is calculated as $K^+ + Ca^{2+} + Mg^{2+}$ (Draaijers *et al.* 1995). Deposition fields are found to resemble the geographic variability of sources, climate and land use.

## 2.2 Dry deposition

The method for dry deposition has been developed by Van Pul *et al.* (1992, 1995) for acidifying substances and by Draaijers *et al.* (1995) for base cations. Both methods are based on the methods used for the Netherlands (Erisman 1993). Dry deposition in EDACS is inferred from the combination of long-range transport model concentrations provided by EMEP, or base cation concentrations derived from wet deposition measurements, and parametrized dry deposition velocities (Van Pul *et al.* 1995). Concentrations at 50 m above the surface (blending height) are used. At this height it is assumed that concentrations and meteorological parameters are not influenced by surface properties to a large extent (Erisman 1993). Dry deposition velocities of gases and particles at this height are calculated on a small scale using a land use map, routinely available meteorological data and the inferential technique (Erisman *et al.* 1994). In the inferential technique the deposition at the surface is inferred from the concentration and the deposition velocity at the same height (Hicks *et al.* 1987). The deposition velocity is calculated using a resistance model in which the transport to and absorption or uptake of a component by the surface is described. Resistances are modeled using observations of meteorological parameters and parametrization of surface exchange processes for different receptor surfaces and pollution climates, as described in Erisman *et al.* (1994). Meteorological parameters (wind speed, friction velocity, radiation, temperature, humidity and precipitation) are obtained from the ODS (Observational Data Set) for every 6 hours and interpolated over Europe on a 1/6° x 1/6° grid.

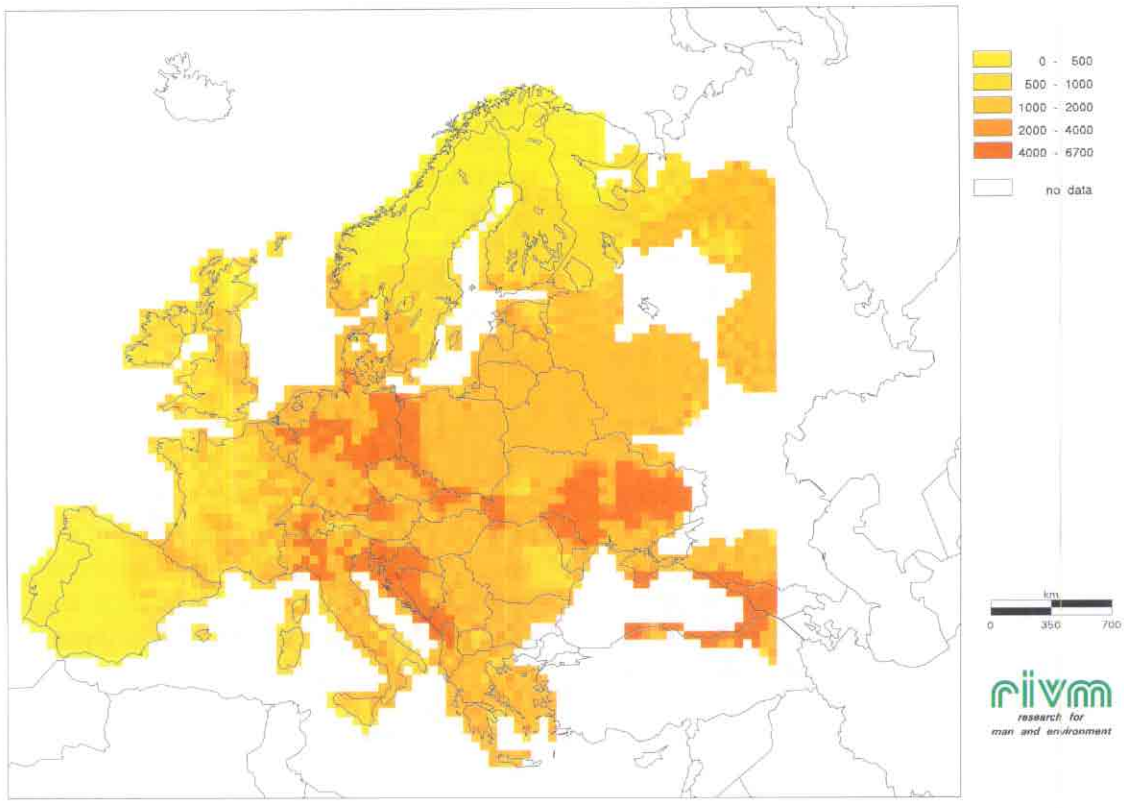


**Figure 2.** Wet deposition of potential acid in Europe on a 50 x 50 km basis in 1989 in eq $ha^{-1}$ $yr^{-1}$ (Van Leeuwen *et al.* 1995).

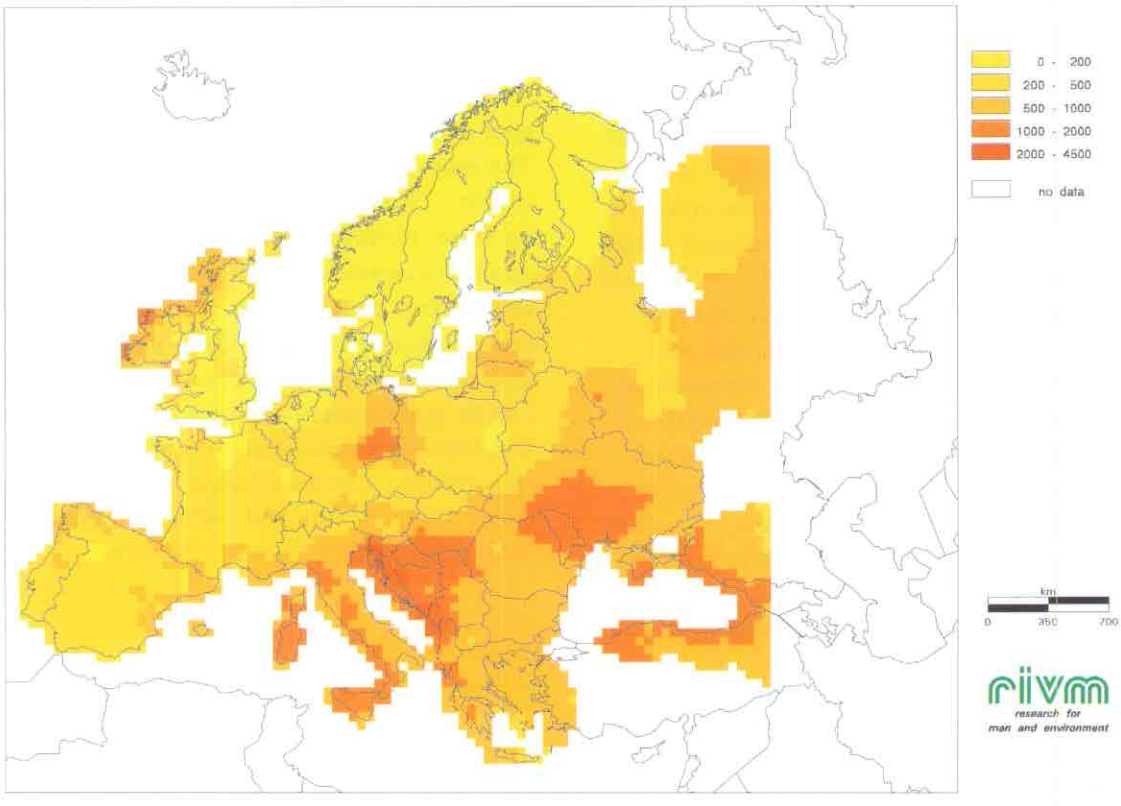


**Figure 3.** Wet deposition of base cations in Europe on a 50 x 50 km basis in 1989 in eq $ha^{-1}$ $yr^{-1}$ (Van Leeuwen *et al.* 1995).

The land use map of Europe, with a resolution of 1/6° x 1/6° (ca. 10 x 20 km), has been constructed by RIVM from ground-based and satellite observations (Van de Velde *et al.* 1995). Roughness length maps for the summer and winter season were derived from the land use map and $z_0$ classifications according to Erisman (1992). The roughness length is used to estimate atmospheric transport to the surface. The deposition velocity is calculated for the land use class coverage within a grid cell. The average deposition velocity $V_d$ for a grid cell is then calculated by weighting the land use-specific deposition velocities with the surface area within that specific grid cell.

Figure 4 shows a map of the annual average dry deposition of potential acid in Europe (the resolution of this map is 10 x 10 km, estimated from 1/6° x 1/6°). The dry deposition of sulfur contributes most to the total potential input. The effect of land use (roughness) and the difference in $V_d$ is clearly shown. In areas with forested terrain, the dry deposition is higher than at low vegetation areas, and, for example, in dry areas, the dry deposition is decreased as a result of a difference in $V_d$ estimates. Figure 5 shows a map of the annual average dry deposition of base cations in Europe. A clear pattern of increasing fluxes with decreasing distance to seas, in particular the Atlantic Ocean, can be observed. Large fluxes are also found (e.g.) northwest of the Black Sea, where they probably originate from wind erosion of salt-containing soils. Large deposition of non-sea salt $Mg^{2+}+Ca^{2+}+K^{+}$ in south and southeast Europe is mainly the result of wind erosion of calcareous soils, agricultural tillage practices and traffic on unpaved roads. In this part of Europe, the prevalence of warm and dry conditions in the summer period will enhance the suspension of alkaline particles in the atmosphere. Sahara dust might be an important additional source of alkaline particles. Anttila (1990) found 80% of the annual total deposition of particulate matter in Corsica caused by Sahara dust. The relatively high fluxes in the border area between Germany, Poland and the Czech Republic, as well as in (e.g.) Estonia, can be attributed to intensive industrial activity.

### 2.3 Contribution of base cation input to the total potential acid input

The total deposition of acidifying substances and base cations is determined by the sum of the dry and wet deposition. The spatial variability in total deposition is determined by the variation in dry and wet deposition and their contribution to the total. The total deposition fields reflect different source areas, climatic conditions and land use. The contribution of base cation deposition to total potential acid deposition is determined by taking the ratio of $2Mg^{2+}+2Ca^{2+}+K^{+}$ to $NH_x+NO_y+2SO_x$. It is assumed that deposition of sea salt does not contribute to potential acid or to potential base deposition.

Figure 6 shows the ratio of base cations to the total potential acid deposition. In large parts of southern Europe, more than 50% of the potential acid deposition is counteracted by deposition of non-sea salt $Mg^{2+}+Ca^{2+}+K^{+}$. In central and northwestern Europe, however, base cation deposition usually amounts less than 25% of the acid input.

## 3. Uncertainty in the EDACS results

The wet deposition maps are subject to several sources of uncertainty. These are divided into three main categories: *(1)* uncertainty associated with the measurements, *(2)* uncertainty associated with assumptions and simplifications in the methods used, and *(3)* uncertainty caused by the interpolation procedure. Van Leeuwen *et al.* (1995) give an extensive description of these uncertainties. The main source of uncertainty is found to vary by region. Three type of regions were distinguished: *(a)* West, northwest and Central Europe where data quality is assumed to be good and sufficient (representative) data are available, *(b)* East, southeast and southwest Europe, where less data are available of which the representativeness and quality can be questionable and *(c)* mountainous areas (e.g. the Alps) and upland areas, and areas with complex terrain. On the average, the overall uncertainty for a 50 x 50 km grid cell is estimated to be 50% in area *(a)*, 60% in *(b)* and 70% in *(c)*.

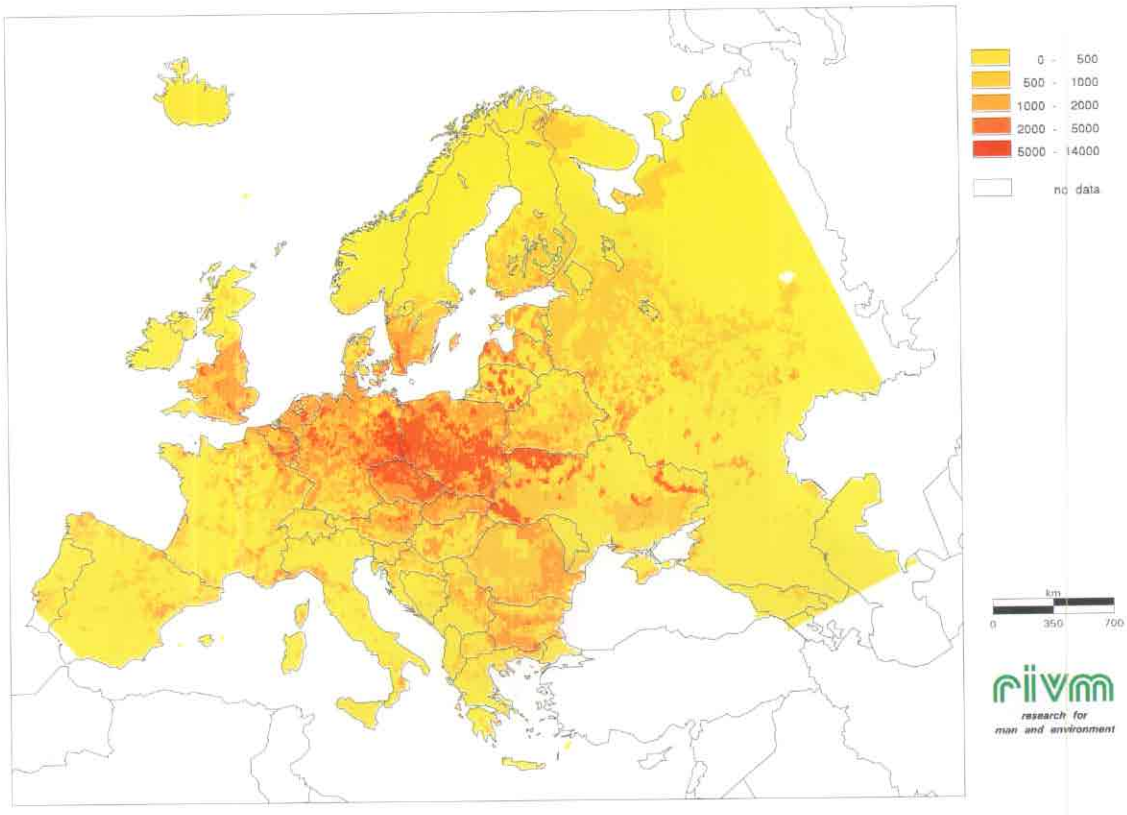


**Figure 4.** Dry deposition of total potential acid in Europe on a 1/6° x 1/6° scale in eq $ha^{-1}$ $yr^{-1}$ (Van Pul *et al.* 1995).

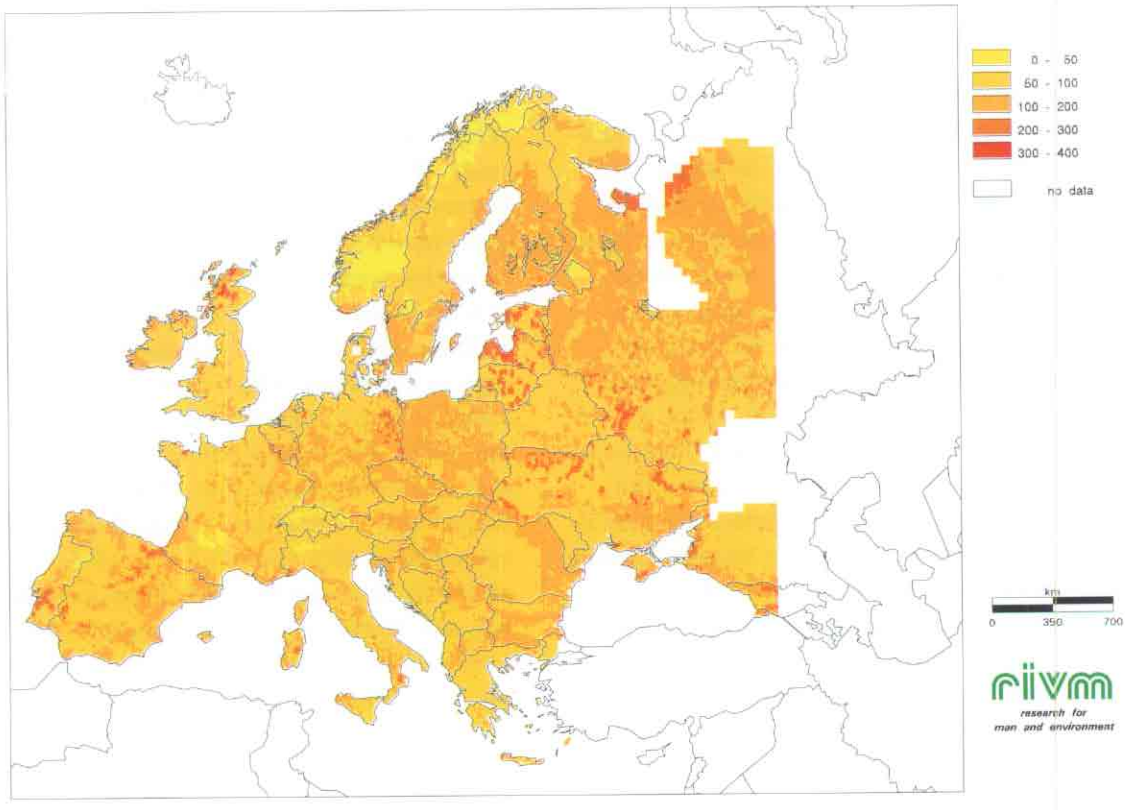


**Figure 5.** Dry deposition of base cations in Europe on a 1/6° x 1/6° scale in eq $ha^{-1}$ $yr^{-1}$ (Draaijers *et al.* 1995).

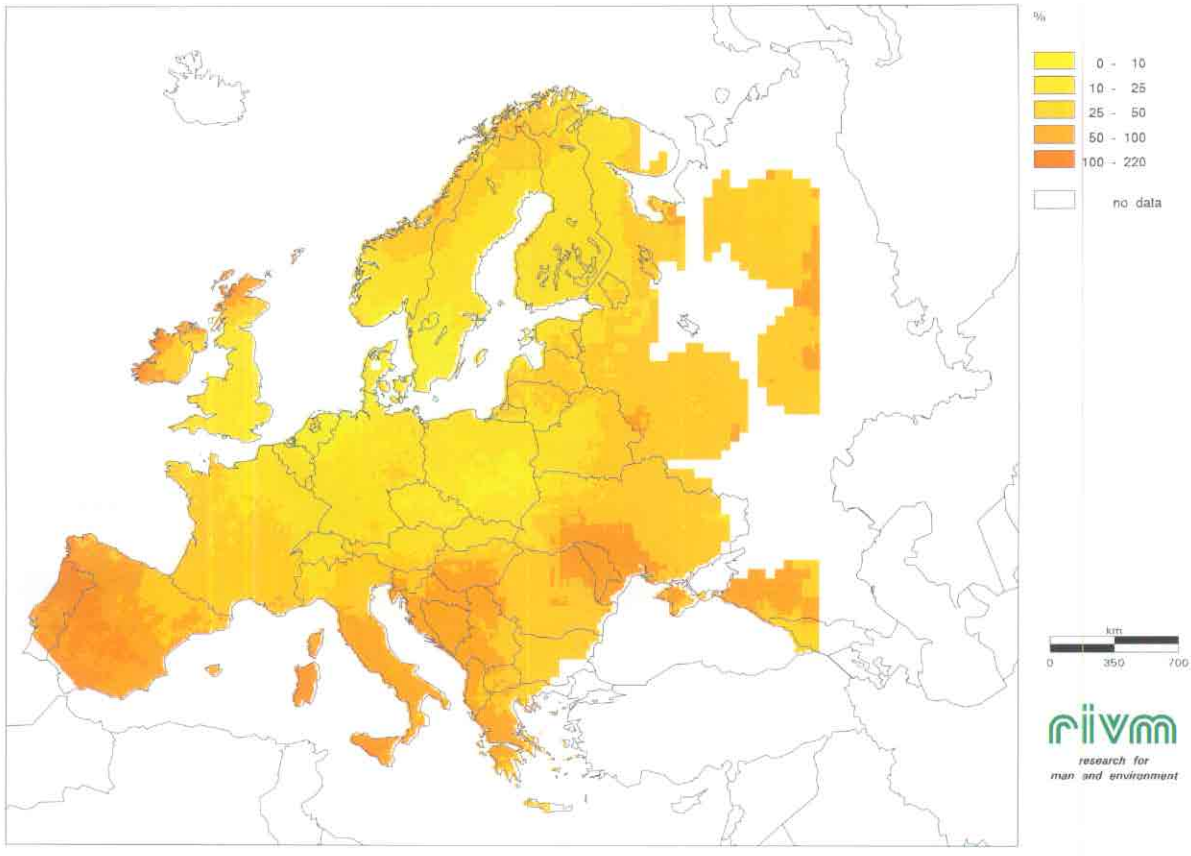


**Figure 6.** Deposition of non-sea salt $Mg^{2+}+Ca^{2+}+K^{+}$ as percentage of the potential acid deposition (Draaijers et al. 1995).

In most areas of Europe, the highest contribution of uncertainty in dry deposition of acidifying substances is the result of using the simple resistance formulation for a highly variable process, and, more specifically, the surface resistance parametrizations. It assumes a constant flux layer, i.e. there are no surface inhomogeneities, edge effects or chemical reactions. More and more accurate *Rc* parametrizations are needed for various vegetation species and surface types. Moreover, there is a lack of measurements which can be used to test these parametrizations, especially for southern and eastern European climates and surfaces. Surface wetness is found to be one of the major factors influencing the deposition process of soluble gases. In the present version of EDACS only rain and indication of dew are used. Processes leading to surface wetness should be taken into account in greater detail. The overall uncertainty in the surface resistance due to these factors is different for each component and surface type. This uncertainty varies on an annual basis and is assumed to range between 20% to more than 100%.

In the current version of EDACS, the EMEP-LRT modeled concentrations on a 150 x 150 km grid are used. The uncertainty in the concentrations are estimated to amount to 40-70% using a statistical analysis with EMEP measurements (Krüger 1993). In source areas the uncertainty can be even higher. It is assumed that the concentration distribution within a grid cell is homogeneous. This is not the case in a grid cell which contains industrialized areas or many scattered sources such as with $NH_3$ and $NO_x$. For such conditions, sub-grid concentration variations are present. The uncertainty in the deposition in a grid cell due to these gradients is estimated at 25% (Van Pul *et al.* 1995). Erisman *et al.* (1994) demonstrated that mass inconsistency between EMEP-calculated deposition and the small-scale maps of EDACS, which might be introduced by a difference in land use data and $V_d$ parametrizations in the two models, does not lead to large differences in country average depositions. In the future this problem will be completely resolved, because EMEP will use the same $V_d$ parametriza-

tions and land use data in the their model as those used in EDACS.

For dry deposition of base cations uncertainty is introduced by *i)* the parametrization of the deposition velocity, and *ii)* the scavenging ratios and precipitation concentration maps used to estimate air concentrations. Ruijgrok *et al.* (1994) assessed the uncertainty of the model on which the parametrization of the deposition velocity was based. The overall uncertainty in modeled deposition velocities integrated over the size distribution representative for alkaline particles at the Speulder forest was found to equal 60%. For other sites additional uncertainty will arise due to limited availability and accuracy of relevant land use information and meteorological parameters. The uncertainty in deposition velocity caused by variation in size distribution of alkaline particles amounts to 30-50%, assuming an average mass median diameter (MMD) of 5 μm and taking a geometric standard deviation ($\sigma_g$) of 2-3 to represent the variation (Ruijgrok *et al.* 1994). The MMD of particles at a particular site will depend on the distance to sources and on (e.g.) ambient relative humidity (Fitzgerald 1975). Theoretical models (Slinn 1983) and field measurements (Kane *et al.* 1994) suggest that the scavenging efficiency increases with particle diameter. Using the relationship between particle mass median diameter and scavenging efficiency presented by Kane *et al.* (1994), the uncertainty in estimated ambient air concentrations caused by variation in size distribution can be calculated to amount to 50-100%, assuming a mean MMD of 5 μm and taking a $\sigma_g$ of 2-3. Large errors in air concentrations will arise in areas very close to, or far from, major sources and in areas with an exceptional precipitation climatology.

Using error propagation methods and assuming that presented uncertainties in deposition velocities and air concentrations represent random errors, the total uncertainty in dry deposition of base cations for an average grid can be calculated to amount to 80-120% (Draaijers *et al.* 1995). Systematic errors in dry deposition may arise from e.g. *i)* using scavenging ratios which are based on only a limited set of simultaneous ambient air and precipitation concentration measurements, *ii)* neglecting complex terrain effects in the parametrization of the deposition velocity, and *iii)* using annual mean air concentrations and deposition velocities for flux calculation, thereby neglecting temporal correlations.

Van Leeuwen *et al.* (1995) estimated the uncertainty in wet deposition for an average grid at 50-70%. The uncertainty in total deposition of base cations can be calculated to amount to 90-140% (Draaijers *et al.* 1995).

The uncertainty in regional scale total deposition estimates strongly depends on the pollution climate and on landscape complexity of the area under study. The uncertainty is determined by the uncertainty in wet, dry or cloud and fog deposition. Fog and cloud water deposition is not taken into account. Furthermore, deposition estimates yield higher uncertainty in areas built up by complex terrain and with strong horizontal concentration gradients. Table 1 shows the uncertainties associated with major key factors in deposition for seven (pollution) regions in Europe. The seven regions are shown on a European map in Figure 7. These regions are chosen because *i)* there is a marked difference in dominating deposition process: e.g. in region 1 the main input is wet deposition, in region 6 the main input is fog or cloud deposition; or *ii)* there is a marked difference in climate, e.g. region 2 exhibits a sea climate, whereas region 7 exhibits a Mediterranean sea climate and region 4 mainly an inland climate; or *iii)* there is a marked difference in industrial activity, e.g. region 1 is remote, region 3 is mainly dominated by large old industrial complexes and region 2 exhibits high reduced nitrogen emission densities. This is only a crude classification. Because of the strong local variations in dry deposition and the associated uncertainty, local scales should be considered.

**Acknowledgements**

Anton Eliassen, Erik Berge and Helge Styve of EMEP MSC-W are thanked for providing the EMEP model concentration data.

**Table 1.** Uncertainty of key factors influencing deposition estimates of S and oxidized and reduced N in different pollution regions in Europe.

| Key Factors | $NO_y$ | | | | | | | $NH_x$ | | | | | | | $SO_x$ | | | | | | |
|---|---|---|---|---|---|---|---|---|---|---|---|---|---|---|---|---|---|---|---|---|---|
| Regions[a]: | 1 | 2 | 3 | 4 | 5 | 6 | 7 | 1 | 2 | 3 | 4 | 5 | 6 | 7 | 1 | 2 | 3 | 4 | 5 | 6 | 7 |
| emission/ | – | ++ | ++ | + | ++ | + | + | – | ++ | + | + | + | + | – | – | + | ++ | + | + | + | – |
| type of source | 2 | 2 | 2 | 2 | 2 | 2 | 2 | 2 | 3 | 3 | 3 | 3 | 3 | 2 | 1 | 1 | 3 | 1 | 3 | 1 | 1 |
| concentration | ++ | ++ | ++ | ++ | ++ | ++ | ++ | ++ | ++ | ++ | ++ | ++ | ++ | ++ | ++ | ++ | ++ | ++ | ++ | ++ | ++ |
| | 2 | 2 | 3 | 3 | 3 | 3 | 2 | 1 | 3 | 3 | 3 | 3 | 3 | 2 | 1 | 2 | 3 | 3 | 3 | 2 | 2 |
| wind speed | – | + | + | – | – | + | – | + | ++ | ++ | + | ++ | ++ | – | + | ++ | ++ | + | ++ | ++ | – |
| | 1 | 1 | 1 | 1 | 1 | 1 | 1 | 1 | 1 | 1 | 1 | 1 | 1 | 1 | 1 | 1 | 1 | 1 | 1 | 1 | 1 |
| roughness | – | + | + | + | + | + | – | + | + | + | + | + | + | + | + | + | + | + | + | + | + |
| length | 1 | 1 | 2 | 2 | 2 | 2 | 2 | 1 | 1 | 2 | 2 | 2 | 2 | 2 | 1 | 1 | 2 | 2 | 2 | 2 | 2 |
| surface | – | – | – | – | – | – | – | + | ++ | ++ | + | ++ | + | + | + | ++ | ++ | + | ++ | ++ | + |
| wetness | 1 | 1 | 1 | 1 | 1 | 1 | 1 | 3 | 2 | 3 | 2 | 3 | 3 | 3 | 3 | 2 | 3 | 2 | 3 | 3 | 3 |
| orography | – | – | – | – | – | ++ | – | ++ | – | – | + | + | ++ | – | + | – | + | + | + | ++ | – |
| | 1 | 1 | 1 | 1 | 1 | 1 | 1 | 2 | 1 | 1 | 2 | 2 | 2 | 1 | 2 | 2 | 2 | 2 | 2 | 2 | 1 |
| co- | – | – | – | – | – | – | – | – | ++ | ++ | + | + | + | – | – | ++ | ++ | + | + | + | + |
| deposition | 1 | 1 | 1 | 1 | 1 | 1 | 1 | 3 | 2 | 3 | 3 | 3 | 3 | 3 | 3 | 2 | 3 | 3 | 3 | 3 | 3 |
| surface | ++ | ++ | ++ | ++ | ++ | ++ | ++ | ++ | ++ | ++ | + | ++ | + | + | ++ | ++ | ++ | + | ++ | + | – |
| resistance | 2 | 2 | 2 | 2 | 2 | 2 | 2 | 3 | 3 | 3 | 3 | 3 | 3 | 3 | 3 | 3 | 3 | 3 | 3 | 3 | 3 |
| dry | – | + | + | + | + | + | – | – | ++ | ++ | + | ++ | + | – | – | ++ | ++ | + | ++ | + | – |
| deposition | 3 | 3 | 3 | 3 | 3 | 3 | 3 | 3 | 3 | 3 | 3 | 3 | 3 | 3 | 3 | 3 | 3 | 3 | 3 | 3 | 3 |
| wet | ++ | + | + | + | + | ++ | + | ++ | + | + | + | + | ++ | + | ++ | + | + | + | + | ++ | + |
| deposition | 1 | 1 | 1 | 1 | 2 | 2 | 2 | 1 | 1 | 1 | 1 | 2 | 2 | 2 | 1 | 1 | 1 | 1 | 2 | 2 | 2 |
| cloud and | + | ++ | – | – | + | ++ | – | + | ++ | – | – | + | ++ | – | + | ++ | – | – | + | ++ | – |
| fog | 3 | 3 | 3 | 3 | 3 | 3 | 3 | 3 | 3 | 3 | 3 | 3 | 3 | 3 | 3 | 3 | 3 | 3 | 3 | 3 | 3 |

legend:

importance of key factors:
++ dominating
\+ important
– neutral
-- unimportant

uncertainty:
1 low <30%
2 median 30-70%
3 high > 70%

[a]the distribution of these regions is given in Fig. 7.

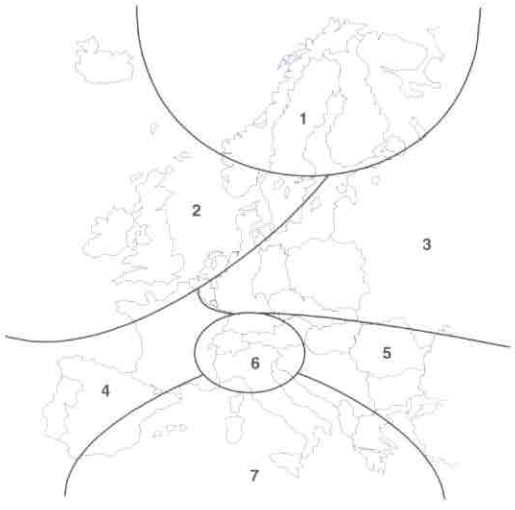


**Figure 7.** Distribution of the pollution regions in Table 1.

## References


Anttila, P., 1990. Characteristics of alkaline emissions, atmospheric aerosols and deposition. In: P. Kauppi, P. Anttila and K. Kenttämies (eds.), Acidification in Finland. Springer, Berlin, Germany.

Asman, W.A.H., J. Slanina and J.H. Baard, 1981. Meteorological interpretation of the chemical composition of rain water at one measuring site. *Water Air Soil Pollut.* **16**:159-175.

De Vries, W., 1994. Soil response to acid deposition at different regional scales; Field and laboratory data, critical loads and model predictions. Ph.D. thesis, University of Wageningen, The Netherlands.

Draaijers, G.P.J., E.P. Van Leeuwen, C. Potma, W.A.J. Van Pul, and J.W. Erisman, 1995. Base cation deposition in Europe. RIVM Rep. (in prep.)

Draaijers, G.P.J., E.P. van Leeuwen, C. Potma, W.A.J. van Pul, and J.W. Erisman, 1995. Mapping base cation deposition in Europe on a 10 x 20 km grid. *Water Air Soil Pollut.*, in press.

Eder, B.K. and R.L. Dennis, 1990. On the use of scavenging ratios for the inference of surface-level concentrations and subsequent dry deposition of $Ca^{2+}$, $Mg^{2+}$, $Na^{+}$ and $K^{+}$. *Water Air Soil Pollut.*, 52:197-215.

Erisman, J.W., 1992. Atmospheric deposition of acidifying compounds in the Netherlands. Ph.D. Thesis, Utrecht University, The Netherlands.

Erisman, J.W., 1993. Acid deposition onto nature areas in the Netherlands: Part I. Methods and results. *Water Soil Air Pollut.* 71:51-80.

Erisman, J.W. and D.D. Baldocchi, 1994. Modelling dry deposition of $SO_2$. *Tellus* 46B:159-171.

Erisman, J.W., A. van Pul, and P. Wyers, 1994. Parametrization of dry deposition mechanisms for the quantification of atmospheric input to ecosystems. *Atmos. Environ.* 28:2595-2607.

Erisman, J.W., G.J.P. Draaijers, J.H. Duyzer, P. Hofschreuder, N. van Leeuwen, F.G. Römer, W. Ruijgrok and G.P. Wyers, 1994. Contribution of aerosol deposition to atmospheric deposition and soil loads onto forests. National Institute of Public Health and Environmental Protection, Rep. No. 722108005, Bilthoven, The Netherlands.

Erisman, J.W. and G.P.J. Draaijers, 1995. Atmospheric deposition in relation to acidification and eutrophication. Studies in Environmental Research 63, Elsevier, the Netherlands.

Fitzgerald, J.W., 1975. Approximation formulas for the equilibrium size of an aerosol particle as a function of its size and composition and the ambient relative humidity. *J. Appl. Meteor.* 14:1044-1049.

Galloway, J.N., D.L. Savoie, W.C. Keene, and J.M. Prospero, 1993. The temporal and spatial variability of scavenging ratios for nns sulphate, nitrate, methane sulphanate and sodium in the atmosphere over the North Atlantic ocean. *Atmos. Environ.* **27A**:235-250.

Gorham, E., 1994. Neutralizing acid rain. *Nature* **367**:321.

Heij, G.J. and T. Schneider, 1991. Final report, Dutch Priority Programme on Acidification, Second Phase. Rep. 200-09, National Institute of Public Health and Environmental Protection, Bilthoven, The Netherlands.

Hettelingh, J.P., R.J. Downing, and P.A.M. de Smet, 1991. Mapping critical loads for Europe, Rep. 259101001. Coordination Center for Effects, National Institute of Public Health and Environmental Protection, Bilthoven, The Netherlands.

Hicks, B.B., D.D. Baldocchi, T.P. Meyers, R.P. Hosker Jr., and D.R. Matt, 1987. A preliminary multiple resistance routine for deriving dry deposition velocities from measured quantities. *Water Air Soil Pollut.* 36:311-330.

Hicks, B.B., R.P. Hosker, T.P. Meyers, and J.D. Womack, 1991. Dry deposition inferential measurement techniques - I. Design and tests of a prototype meteorological and chemical system for determining dry deposition. *Atmos. Environ.* 25A:2345-2359.

Iversen, T., N. Halvorsen, S. Mylona, and H. Sandnes, 1991. Calculated budgets for airborne acidifying components in Europe, 1985, 1987, 1988 and 1990. MSC-West, Norwegian Meteorological Institute, Oslo.

van Jaarsveld, H.J.A., 1990. A quantitative model analysis of year to year changes in concentration and deposition. Presented at the NATO CCMS meeting, Vancouver, Canada.

van Jaarsveld, H.J.A., 1995. Modelling the long-term atmospheric behavior of pollutants on various spatial scales. Ph.D. thesis, University of Utrecht, the Netherlands.

Kane, M.M., A.R. Rendell and T.D. Jickells, 1994. Atmospheric scavenging processes over the North sea. *Atmos. Environ.* **28**:2523-2530.

Krüger, O., 1993. The applicability of the EMEP-code to estimate budgets for airborne acidifying components in Europe. In: Proc. CEC/BIATEX Workshop 4-7 May 1993, Aveiro, Portugal.

van Leeuwen, E.P., C. Potma, G.P.J. Draaijers, J.W. Erisman, and W.A.J. van Pul, 1995. European wet deposition maps based on measurements. RIVM Rep. 722108006, National Institute for Public Health and Environmental Protection, Bilthoven, The Netherlands.

van Leeuwen, E.P., C. Potma, G.P.J. Draaijers, J.W. Erisman, and W.A.J. van Pul, 1995. European wet deposition maps based on measurements. *Water Air Soil Pollut.* in prep.

Legates, D.R. and C.J. Willmott, 1990. Mean seasonal and spatial variability in gauge-corrected, global precipitation. *Intern. J. Climatology* **10**:111-123.

Lövblad, G., J.W. Erisman, and D. Fowler, 1993. Models and methods for the quantification of atmospheric input to ecosystems. Report Nord 1993:573 Göteborg, Sweden, 3-7 November 1992. Nordic Council of Ministers, Copenhagen, Denmark.

Milford, J.B. and C.I. Davidson, 1985. The sizes of particulate trace elements in the atmosphere - A review. *J. Air Pollut. Contr. Assoc.* 35:1249-1260.

Potma, C.J.M., 1993. Description of the ECMWF/WMO Global Observational data set and associated data extraction and interpolation procedures. RIVM Rep. 722401001.

van Pul, W.A.J., J.W. Erisman, J.A. van Jaarsveld, and F.A.A.M. de Leeuw, 1992. High resolution assessment of acid deposition fluxes. In: T. Schneider (ed.), Acidification research: evaluation and policy application. Studies in Environmental Science 50. Elsevier, Amsterdam.

van Pul, W.A.J., C. Potma, Leeuwen, E.P. van, Draaijers, G.P.J. and Erisman, J.W. (1994. EDACS: European Deposition maps of Acidifying Compounds on a Small scale. Model description and results. RIVM Rep. 722401005.

Römer, F.G. and B.W. te Winkel, 1994. Droge depositie van aerosolen op vegetatie: verzurende componenten en basische kationen. Rep. 63591-KES/MLU 93-3243, KEMA, Arnhem, The Netherlands.

Ruijgrok, W., H. Tieben, and P. Eisinga, 1994. The dry deposition of acidifying and alkaline particles on Douglas fir. Rep. 20159-KES/MLU 94-3216, KEMA, Arnhem, The Netherlands.

Slinn, W.G.N., 1982. Predictions for particle deposition to vegetative surfaces. *Atmos. Environ.* 16:1785-1794.

Slinn, W.G.N., 1983. In: P.S. Liss and W.G.N. Slinn (eds.), Air sea exchange of gases and particles, Reidel, Dordrecht, The Netherlands.

Swap, R.M., M. Garstang, and Greco, 1992. Saharan dust in the Amazon Basin. *Tellus* 44B:133-149.

Tuovinen, J.P., K. Barrett, and H. Styve, 1994. Transboundary acidifying pollution in Europe: Calculated fields and budgets 1985-1993. EMEP/MSC-W, Report 1/94, Norwegian Meteorological Institute, Oslo.

UK Review Group on Acid Rain (URGAR), 1990. Acid deposition in the United Kingdom 1986-1988. Warren Spring Laboratory, UK.

van de Velde, R.J., W.S. Faber, V.F. van Katwijk, J.C.I. Kuylenstierna, H.J. Scholten, T.J.M. Thewessen, M. Verspuij, and M. Zevenbergen, 1995. The preparation of a European land use database. Rep. 712401001, National Institute of Public Health and the Environment, Bilthoven, the Netherlands.

Wesely, M.L., 1989. Parametrization of surface resistances to gaseous dry deposition in regional-scale numerical models. *Atmos. Environ.* 23:1293-1304.

# EDEOS: European Deposition and Exposure of Ozone on a Small Scale

Eric Kirchner, Jeannette Beck, Frank de Leeuw and Addo van Pul
*Air Research Laboratory, National Institute of Public Health and the Environment (RIVM)*
*P.O. Box 1, 3720 BA Bilthoven, the Netherlands*

Since pre-industrial times the amount of ozone in the troposphere has at least doubled, and strong evidence exists that this increase has an anthropogenic origin (Bojkov 1986, Volz and Kley 1988, Feister and Warmbt 1987, Isaksen and Hov 1987). Tropospheric ozone has a direct impact on man and environment, and it indirectly influences our climate (IPCC, 1995). In this respect workshops within the UN/ECE Convention on Long-Range Transport of Air Pollution at Egham (UK) and Bern (Switzerland) have resulted in a definition of critical levels of ozone for agricultural crops, being an accumulated ozone exposure above a threshold of 40 ppb (AOT40) of 5,300 ppbh, within the months May, June and July, during daylight hours only. For forest trees, the critical level was defined as an AOT40 of 10,000 ppbh in the months from April to September, integrated 24 hours a day.

The concentrations of ozone show a large spatial variability. In order to evaluate the critical levels defined for crops and forests in relation to the spatial distribution of these receptors, as well as for the evaluation of abatement strategies, it is of paramount importance to map the exceedances of these critical levels with high resolution. We are developing a procedure named EDEOS for small-scale mapping of ozone exposure in Europe, on a dense grid of 1/6 x 1/6 degrees (circa 12 x 20 $km^2$). The design of the calculation procedure enables evaluation of abatement strategies, since emission data for nitrogen oxides ($NO_x$) and volatile organic compounds (VOC) are used as input parameters.

The various sources of data that are used as input for the EDEOS model are shown schematically in Figure 1. First, from the UN EMEP Lagrangian long-range transport model we use concentrations fields of ozone, NO and $NO_2$ at 50 m height, on a coarse grid of circa 150 x 150 $km^2$ (Simpson *et al.* 1993). These ozone concentrations are transformed to values at 1 m height, indicative of human and environmental exposure, by correcting for deposition and titration of ozone with NO.

Deposition fluxes and deposition velocities are calculated using small-scale maps of the spatial distribution in Europe of various classes of vegetation, serving as the second source of input data. These land use maps have been developed at RIVM (Van de Velde *et al.* 1994). The actual deposition velocities are calculated by including data from the European Centre for Medium-range Weather Forecasting (ECMWF) and synoptic meteorological data, a third data source. The ECMWF data is provided for 6-hour periods throughout the year. The procedures to calculate deposition velocities were taken from the EDACS model (Van Pul *et al.* 1995).

For calculating the effect of titration of ozone by NO, it is sufficient to have the ozone, NO and $NO_2$ concentration data at 50 m height from EMEP, as well as emission data. These emission data are the fourth data source, and originate from CORINAIR (EEA, 1995). They combine contributions from combustion and industries, process emitting industries, refineries, transport and domestic emissions. Moreover, point sources are accounted for separately. For its use in EDEOS, the emission data are transformed into effective concentration by using a box model. This model also demands meteorological data to be included in EDEOS. The boundary layer height was computed by a parameterization from the Royal Dutch Meteorological Institute using the same meteorological data. In the current, preliminary version of EDEOS, we assume photostationary equilibrium to hold, and $NO_2$ emissions to be a factor 20 smaller than NO emissions. Another approximation is the separate treatment of deposition and titration.

At this stage in the process, the model gives ground based concentrations of ozone on a dense grid for four times a day: at 0000, 0600, 1200 and 1800 hours. These values are used for an hourly parameterization of the ozone concentrations. In subsequent versions of EDEOS, we will improve this by accounting for the various terms in the ozone budget.

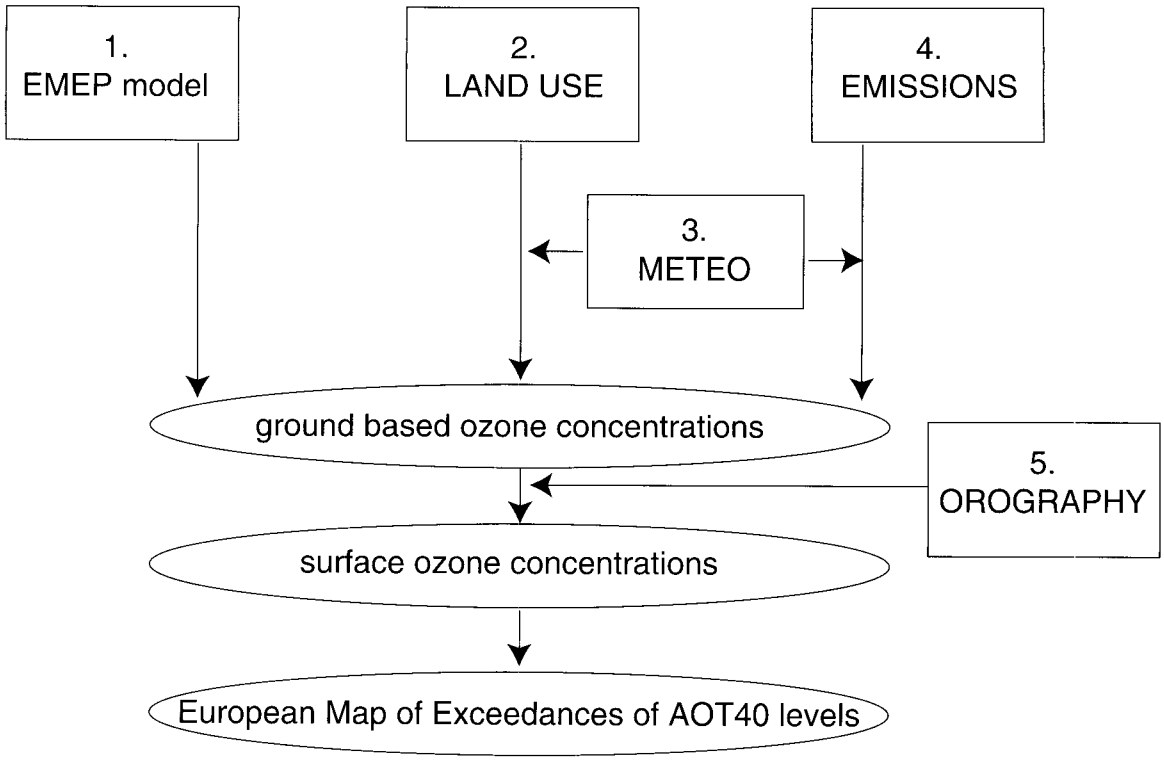


**Figure 1.** Schematic setup for the EDEOS model.

Another complication we account for is the dependence of ozone concentrations on local orography. The elevation of a particular location determines the extent to which it experiences the influence of air from the free troposphere and from the boundary layer. Based on data from the EUROTRAC-TOR and EMEP programs as well as on results in literature, we model this dependence and combine it with small scale orographic data that are provided by EPA. This is the fifth and last data source we use as input for EDEOS. Thus we obtain the concentration of ozone at the earth surface. These modeled data will be compared to concentration data from ground stations of the TOR/EMEP network in Europe and the Dutch national air pollution network, thus serving as a validation of the EDEOS model. From the modeled surface concentrations we will be able to produce the desired small scale map of AOT40 levels in Europe.

The EDEOS program, which is actually a set of programs, is still in development. Its design closely follows the EDACS program (European Deposition of Acidifying Components on Small scale).

Work similar to EDEOS but based on measured data only and on a smaller, national scale is carried out for the UK, Austria and Switzerland (Smith *et al.* 1994, Loibl 1995, Künzle 1995). The difference with EDEOS is not only the European scale of the EDEOS model, but also the fact that in EDEOS physical variables like deposition velocity and the dependence of ozone concentration on altitude are directly parameterized, rather than the highly aggregated AOT40 critical level. This will enable systematical improvement of the model in the future.

## References

Bojkov, R.D., 1986. Surface ozone during the second half of the nineteenth century. *J. Clim. Appl. Meteorol.* **25**:343.

European Environmental Agency (EEA), 1995. Review of CORINAIR 90 - Proposals for air emissions 94. Report to the European Environment Agency from the European Topic Centre on Air Emissions, Copenhagen, Denmark.

Feister, U. and W. Warmbt, 1987. Long-term measurements of surface ozone in the German Democratic Republic. *J. Atmos. Chem.* **5**:1.

Intergovernmental Panel on Climate Change (IPCC), 1995. Second Scientific Assessment of Climate Change, Intergovernmental Panel on Climate Change, Bracknell, United Kingdom (in press).

Isaksen, I. and Hov, Ø., 1987. Calculation of trends in the tropospheric concentration of $O_3$, OH, CO, $CH_4$ and $NO_x$. *Tellus* **39B**:271.

Künzle, Th., 1995. Pers. commun.

Loibl, W., 1995. Modelling the Spatial Distribution of Critical Levels of Ozone Considering the Influences of Complex Terrain. Working paper for the ECE Technical Meeting in Helsinki, April 1995. Seibersdorf, Austria.

Pul van, W.A.J., C.J.M. Potma, E.P. van Leeuwen, G.P.J. Draaijers and J.W. Erisman, 1995. EDACS: European Deposition maps of Acidifying Components on a Small Scale. Model description and preliminary results. RIVM Rep. 722401005, Bilthoven, the Netherlands.

Simpson, D., Y. Andersson-Sköld and M.E. Jenkin, 1993. Updating the chemical scheme for the EMEP MSC-W oxidant model: Current status. Norwegian Meteorological Inst. EMEP MSC-W Note 2/93.

Smith, R.I., C.W. Anderson and D. Fowler, 1994. Critical Levels of Ozone Over the United Kingdom: Mapping Aggregate Exceedances Over Moderate to High Thresholds. *J. Res. Natl. Inst. Stand. Technol.* **99**:353.

Van de Velde, R.J., W. Faber, V. Katwijk, H.J. Scholten, T.J.M. Thewessen, M. Verspuy and M. Zevenbergen, 1994. The preparation of a European Land-use Data base. RIVM Rep. 712401001. Bilthoven, The Netherlands.

Volz, A. and D. Kley, 1988. Evaluation of the Montsouris series of ozone measurements made in the nineteenth century. *Nature* **332**:240.

# Methods to Calculate Critical Loads for Heavy Metals and Persistent Organic Pollutants

W. de Vries[1] and D. J. Bakker[2]
[1]*DLO Winand Staring Centre, P.O. Box 125, 6700 AC Wageningen, The Netherlands*
[2]*TNO Insitute of Environmental Sciences, 2600 JA Delft, The Netherlands*

## 1. Introduction and aim

In the past years many studies have been carried out to assess critical loads of acidifying substances for forest soils and surface waters on a European scale (e.g. Hettelingh *et al.* 1991, Downing *et al.* 1993, De Vries *et al.* 1993). Critical loads of other air pollutants, such as heavy metals and persistent organic pollutants (POPs), however, are largely unknown, even though concern on the dispersion and impacts of these substances is large.

More than twenty working groups and task forces in Europe are presently working on policies for air pollution by heavy metals and persistent organic pollutants (Sliggers and de Jager, 1993). Most of these working groups have been established under international organizations, such as ministerial conferences (North Sea, Rhine, Arctic), the Paris and Helsinki Commissions, the United Nations Economic Commission for Europe and the European Union. Most groups are working on emission reduction programs. Others are concerned with monitoring, inventories of emissions and other data, state-of-the-environment surveys, etc. Although eventually all emission reduction strategies will have to be based on sustainable environmental loads, very few of the task forces and working groups have mandates which include the environmental effects and the relationship between pollution load and environmental capacity.

A first systematic assessment of critical loads for three heavy metals and two persistent organic pollutants was carried out by five research institutes in the Netherlands. This project, ESQUAD (European Soil and sea QUality due to Atmospheric Deposition of selected substances), was commissioned by the Dutch Ministry of Housing, Physical Planning and the Environment. In this project, critical loads of cadmium, copper, lead, lindane and benzo(a)pyrene were calculated for European forest soils and compared with the calculated present atmospheric deposition. Calculations for forest soils were carried out with essentially the same methods and data bases used for the assessment of critical loads for sulphur and nitrogen (De Vries *et al.* 1993). The results from this study are described by Van den Hout (1994).

Here we present the basic principles of calculation methods that can be used to quantify critical loads of heavy metals and POPs, ie, lead (Pb), cadmium (Cd), copper (Cu), zinc (Zn), nickel (Ni), chromium (Cr) and mercury (Hg), for soil and surface waters on the basis of environmental quality objectives for these compartments. The general approach is based on methods developed earlier within the framework of the ESQUAD study (cf. Bakker *et al.* 1994, Reinds *et al.* 1994). More information on the various methods for heavy metals and POPs in given in De Vries and Bakker (1995) and Bakker and De Vries (1995), respectively.

## 2. Differences between critical loads for acidity and those for heavy metals and POPs

As with acidity, the critical load concept for heavy metals is based on the assumption that every ecosystem, whether terrestrial or aquatic, has only a limited capacity to cope with pollution without experiencing unacceptable damage to flora and/or fauna. Critical loads for heavy metals, however, differ in some aspects from those derived for acidity as summarized in Table 1.

First of all, acidity only refers to sulphur (S) and nitrogen (N), whereas heavy metals include about 10 elements. For POPs, there are several thousands of compounds. Secondly, unlike acidity, calculation of critical loads is not limited to unlimed non-agricultural soils only. This implies that heavy metals not only enter ecosystems via the route of atmospheric deposition but also as a result of more direct emissions, such as application of animal manure on agricultural soils or via sewage water on surface waters. Therefore, the critical load of heavy metals

should not only be related to their deposition but to the total load, that will not cause significant harmful effects on the ecosystem. The phrase "significant harmful effects" in the definition of the critical load is of course susceptible to interpretation, depending on the kind of effects considered (cf. Table 1) and the amount of harm accepted. As with acidity, the time scale for which the critical load is intended to be valid is chosen to be infinitely long since the concept of an acceptable steady-state situation is used (cf. De Vries, 1991).

**Table 1.** Differences in various aspects related to critical loads for acidity and for heavy metals/POPs.

| Aspect | Acidity | Heavy metals/POPs |
|---|---|---|
| compounds | two | several/many[1)] |
| system | natural | natural and man-influenced |
| input loads | deposition | deposition and other |
| Effects: | | |
| soil | - root system<br>- soil stability | - soil organisms<br>- production loss<br>- acceptable daily intake fauna and humans |
| water | fish | aquatic organisms including fish |
| time to steady state | intermediate to long | long/short[1] |

[1)]The first item refers to heavy metals and the second item to POPs.

## 3. Calculation methods

The soil and surface water models developed all consist of a mass balance equation which describes the input-output fluxes of heavy metals or POPs, combined with rate-limited and equilibrium equations, describing the processes in either the soil or aquatic system.

The calculation methods are based on the following assumptions:

(i) The concentration of the heavy metal or POP in the soil system or the aquatic system (including the sediment compartment) has reached a steady state, ie, the concentration does not change in time because the amount of heavy metal or POP entering the system is equal to the amount that leaves the system.

(ii) The heavy metal or POP present in the system follows the concept of equilibrium partitioning. In the water compartment, the heavy metal or POP is thus assumed to partition between the dissolved phase, dissolved organic carbon (DOC), and suspended particles. In the soil and sediment compartments, the heavy metal or POP is assumed to partition between the pore water phase, DOC and the adsorbed phase of soil or the sediment. In all cases it is assumed that the concentration in each of these phases is in a state of equilibrium at any moment.

(iii) The soil, water, and sediment compartments are homogeneously mixed. Thus, system properties and concentrations of the pollutant do not show horizontal or vertical variation within the compartments.

(iv) In the aquatic system, sedimentation at least equals resuspension of sediment particles.

Figure 1 gives a schematic representation of the mass balance for heavy metals in the soil. Figure 2 gives a schematic representation of the mass balance for heavy metals in an aquatic system, including both a water and sediment compartment.

The mass balance of a certain heavy metal, M, in a soil layer (in mg $m^{-2}$ $yr^{-1}$) equals (cf. Fig. 1):

$$M_{tl} = -M_{br} + M_{bu} + M_{sr} + M_{bp} + M_{ru} - M_{we} + M_{le} \qquad (1)$$

For POPs, biomass return, biomass uptake and weathering are neglected or irrelevant, whereas degradation is included.

The steady-state mass balances of heavy metals in the water and the sediment compartment (in mg $yr^{-1}$) equal (cf. Fig. 2):

$$M_{tl} = M_{lo} + M_{inf} + M_{dif} + M_{sed} - M_{res} \qquad (2)$$

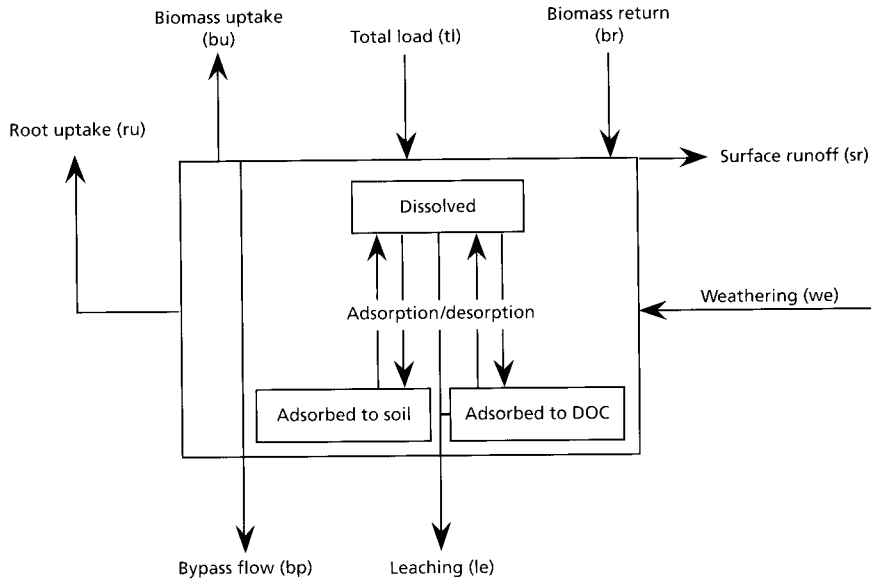


**Figure 1.** Schematic representation of the mass balance for heavy metals in the soil.

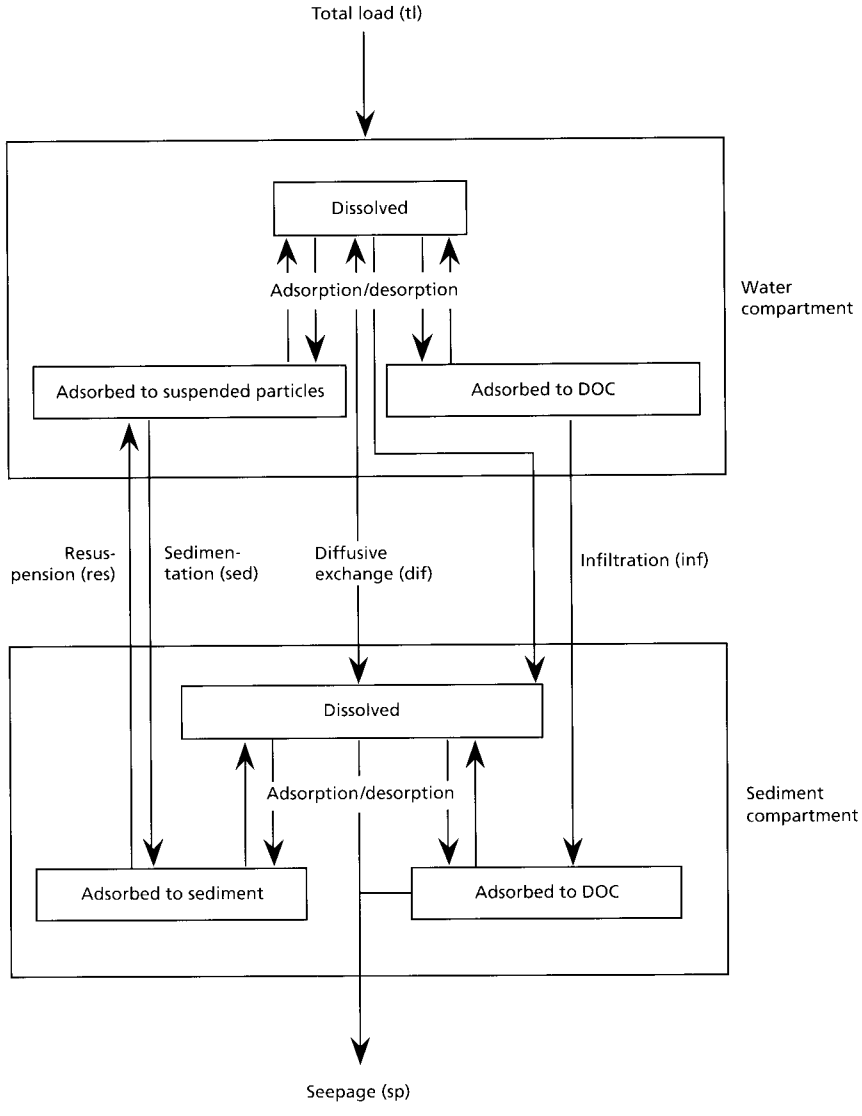


**Figure 2.** Schematic representation of the mass balance for heavy metals in an aquatic system.

$$M_{inf} + M_{dif} + M_{sed} = M_{res} + M_{bur} + M_{sp} \quad (3)$$

For POPs, the effect of degradation in the water and sediment compartment, respectively, is also included. Critical loads are derived by describing the various fluxes while assigning critical values for the contents/concentrations of heavy metals or POPs in either the solid phase (total contents in soil, sediments or suspended particles) or the dissolved phase (total concentrations in soil solution ar surface water). In all cases, the concept of equilibrium partitioning is used to derive the various fluxes at critical loads.

## 4. Uncertainties

The proposed method for the calculation of critical loads in soil or aquatic systems is based on a number of assumptions, which are discussed below.

*Steady state*
The assumption of steady state implies that the concentration in the soil or aquatic system does not change in time because the amount of heavy metal or POPs entering the system is equal to the amount that leaves the system. The validity of this assumption depends on the magnitude of the time scales of the various input, output and exchange processes. If the time scale of reaching steady state is much longer than the time scale of changes in the input or output processes, it is difficult to compare an actual load on the system with a critical load based on the assumption of a steady state.

Associated with the question of the time-scale of reaching steady-state is the averaging period assumed in the calculation of the critical load. In the method that is described, the default averaging period is one year. This means that the *yearly averaged* load on the considered soil system is maximally allowed to have the size of the calculated critical load. If, however, this yearly load mainly consists of a two months' peak, as may be the case for various POPs, the environmental quality objective will still be exceeded during these two months. In this case the critical load calculation should better be performed using a two months' averaging period for the input data.

*Equilibrium partitioning*
The concept of equilibrium partitioning is often employed to describe the distribution of heavy metals and POPs in both soil and aquatic systems, but different sorption and desorption rates may cause a different behavior of the heavy metal or POP in both systems. However, as hardly any quantitative or even qualitative information is available on the significance of these phenomena, it is difficult to incorporate them in the critical load calculation method.

*Homogenous mixing*
It is assumed that system properties and concentrations of the pollutant do not show horizontal or vertical variation within the compartments. This means that the mixing depth of a certain soil system must be chosen on the basis of the characteristics of the soil profile. The critical load can thus only be calculated for a distinctive layer and not for a soil profile as a whole. Since the value of the mixing depth directly influences the calculated critical load of degradable compounds, this depth must be chosen with care. With respect to waters it can be remarked that homogenous mixing applies less to very large surface waters, such as seas, than to smaller surface waters such as small lakes. In all cases, critical loads calculated on the assumption of homogenous mixing are more suitable to be compared to diffuse sources, such as atmospheric deposition, than to point sources.

*Sedimentation/resuspension*
The critical load calculation method is restricted to aquatic systems in which the sedimentation flux at least equals the resuspension flux. This is a consequence of the fact that when the resuspension flux would be greater that the sedimentation flux, the sediment layer would eventually disappear. Furthermore, critical loads can become negative in such a situation.

## References


Bakker, D.J. and W. de Vries, 1995. Calculating critical loads of persist organic pollutants for soils and surface waters. IMW-TNO, Delft, the Netherlands, Report.

Bakker, D.J., K.D. van der Hout, G.J. Reinds and W. de Vries, 1994. Critical loads and present loads of lindane and benzo(a)pyrene for european forest soils. IMW-TNO, Delft, the Netherlands, Report 94.

De Vries, W., 1991. Methodologies for the assessment and mapping of critical loads and of the impact of abatement strat-

egies on forest soils. DLO Winand Staring Centre, Wageningen, the Netherlands, Rep. 46, 109 pp.

De Vries, W. and D.J. Bakker, 1995. Manual for calculating critical loads of heavy metals for soils and surface waters. DLO Winand Staring Centre for Integrated Land Soil and Water Research Rep.

De Vries, W., M. Posch, G.J. Reinds and J. Kämäri, 1993. Critical loads and their exceedance on forest soils in Europe. DLO Winand Staring Centre, Wageningen the Netherlands, Rep. 58 (revised), 122 pp.

Downing, R.J., J.P. Hettelingh and P.A.M. de Smet, 1993. Calculation and mapping of critical loads in Europe: Status Report 1993. Coordination Center for Effects, National Institute of Public Health and Environmental Protection, Bilthoven, the Netherlands, Rep. 259101003.

Hettelingh, J.P., R.J. Downing and P.A.M. de Smet, 1991. Mapping critical loads for Europe. Coordination Center for Effects, National Institute of Public Health and Environmental Protection, Bilthoven, the Netherlands, Rep. 259101001.

Reinds, G.J., J. Bril, W. de Vries, J.E. Groenenberg and A. Breeuwsma, 1994. Critical and present loads for cadmium, copper and lead for European forest soils. DLO Winand Staring Centre, Rep. 96. Wageningen, the Netherlands.

Sliggers, C.J. and H.H. de Jager, 1993. Matrix International Working Groups/Task Forces on Heavy Metals and Persistent Organic Pollutants. Ministry of VROM, Directorate General for Environmental Protection, The Hague, the Netherlands.

Van den Hout, K.D. (ed), 1994. The impact of atmospheric deposition of non-acidifying pollutants on the quality of European forest soils and the North Sea. IMW-TNO, Delft, the Netherlands; Rep. R93/329, 143 pp.

# Critical Thresholds for Dutch Target Ecosystems Based on Risk Assessment

J.B. Latour and I.G. Staritsky
*National Institute of Public Health and the Environment (RIVM)*
*P.O. Box 1, 3720 BA Bilthoven, the Netherlands*

## Abstract

In this paper we review how critical thresholds of nature conservation target ecosystems in the Netherlands have been calculated for acidification, eutrophication and desiccation using risk assessment. We illustrate the method by means of an example (nature conservation target type: deciduous forest on nutrient-poor sandy soils) and we discuss how this approach can be applied in other European countries.

## Introduction

In the Netherlands, many ecosystems and (populations of) species have declined in the last couple of decades (Weinrich and Musters 1989, Latour and Reiling 1992, Bink *et al.* 1994). The decline is caused by various environmental problems such as acidification, eutrophication, desiccation, pollution, disturbance and habitat destruction. Most of these problems are still threatening Dutch ecosystems.

In response to this decline an 'Ecological Network' (LNV 1990, Lammers 1994) has been assigned that indicates how much area is needed to protect biodiversity, where these areas are (to be) located, and what ecosystems and species are to be protected. Species and ecosystems are specified using a system of 130 nature conservation target types (Jansen *et al.* 1993). Each target type is described in terms of target species, critical thresholds and critical loads, management strategies and minimum area. Critical thresholds have been assessed using a risk assessment approach (U.S. EPA 1990, VROM 1989) because risk assessment can be used for various environmental problems to quantify critical thresholds that correspond to similar protection levels for ecosystems. Risk assessment is based on probabilistic rather than deterministic analysis, and has been elaborated for various environmental problems.

With respect to ecotoxicology, concentrations of various compounds protecting 95% of the species of an ecosystem (VROM 1991) - the maximum tolerable concentrations (MTC) - have been calculated by extrapolation of single-species toxicity data (eg, No Observed Effect Concentrations, NOECs) to an ecosystem. Similarly, van der Eerden *et al.* (1992) calculated critical levels for $NH_3$ and $SO_2$ based on NOECs determined in laboratory. Latour *et al.* (1994) adopted the risk assessment for eutrophication, acidification and desiccation, using species--response functions for soil acidity, nutrient availability and soil moisture. This method uses percentiles of the species-response curves as measures for risk at the species level, analogous to NOECs, to quantify the critical thresholds that protects 95% of the species of an ecosystem. This method has been used to calculate critical thresholds for all 130 nature conservation target types (Jansen *et al.* 1993) in relation to acidification, eutrophication and desiccation.

In this paper we illustrate how critical thresholds of one nature conservation target types – deciduous forest on nutrient-poor sandy soils – have been assessed, and discuss how this approach can be applied in other European countries.

## Method

We used the **M**ultiple stress m**O**del for **VE**getation (MOVE) (Latour and Reiling 1991, 1993) to calculate critical thresholds. MOVE predicts probability of occurrence of individual plant species as a function of acidification, desiccation and eutrophication scenarios on a national scale. The model is linked to the soil model SMART (Simulation Model for Acidification Regional Trends, De Vries *et al.* 1989). SMART predicts changes in abiotic soil factors (soil moisture, soil acidity, and nutrient availability) relevant to the occurrence of plant species. The input consists of acid and nitrogen deposition, and changes in groundwater level. The following processes are included: net uptake and net immobiliza-

tion of nitrogen; weathering of carbonates, silicates and Al oxides and hydroxides; cation exchange and $CO_2$ equilibria; and nutrient dynamics.

The vegetation model MOVE predicts the probability of species occurrence as a function of three output variables of SMART: soil acidity, nutrient availability and soil moisture. With regression statistics the occurrence probability of a species can be calculated for each combination of soil factors or for each environmental variable separately (species--response curve). Species-response curves of 700 plant species have been described for soil moisture, nutrient availability and soil acidity (Wiertz *et al.* 1992) using Gaussian logistic regression models. Regression was based on an extensive data base developed for a revision of the Dutch classification of plant communities (Schaminee *et al.* 1989). This database consists of 17,000 vegetation relevées. No information on abiotic site factors of the vegetation relevées was available. These were assessed in retrospect with Ellenberg indication values (Ellenberg 1979), which indicate the relationship between the occurrence of plant species and nutrient availability, acidity, soil moisture, salt dependency, and temperature. These values have been assigned to most plant species of western and central Europe, and adjusted for the Netherlands (Wiertz 1992). The abiotic site factors of each vegetation relevée are assessed by averaging the indication values of all the species recorded. Calculated averages, in Ellenberg indication values, are used as a semi-quantitative assessment of the abiotic soil factors.

Next, the occurrence frequency of each species is established as a function of the averages of vegetation relevées. The occurrence frequency is described with Gaussian logistic regression models (Jongman *et al.* 1987). Since this analysis used floristic information to assess the abiotic site factors, any (historical) vegetation sample can be included in the analysis, extending the database. Moreover, such an analysis excludes potential bias caused by high temporal and spatial variation in the actual measurements of abiotic site factors. Deduction of values for the abiotic soil factors from the vegetation sample guarantees ecological relevance.

Species occurrence has been described as being significant for 95% of the species using unimodal and linear regression models. Most of the significant models were unimodal. Linear models were found for nutrients (4%) and salt (20%).

Ellenberg indication values have been calibrated with quantitative values for the abiotic soil factors using combined samples of vegetation and environmental variables. This calibration connects the soil module with the vegetation module. On the basis of 2000 combined samples with vegetation and soil pH, nitrogen availability and spring ground water level, the Ellenberg indication values have been calibrated (Alkemade et al. in prep).

We calculated critical threshold values according to Latour *et al.* (1994) using percentiles of the species--response curves as measures for risk at the species level, analogue to NOECs. For instance, the 10 and 90 percentiles of the species-response curves are used as NOEC-like measures for the risk at the species level (Figure 1). The 10 percentile corresponds with a reduced occurrence probability due to "limitation", the 90 percentile due to "intoxication". Next, the percentage of species protected is plotted for each value of the environmental variable and critical thresholds that protects 95% (or any other percentage) of the species can be calculated. Species are considered protected if the 10 percentile of the species is lower and the 90 percentile higher than the environmental variable. This approach has been applied for the nature conservation target type plant species of nutrient-poor deciduous forests. Characteristic species for nutrient-poor deciduous forest (*Quercion Robori-Petraeae* and *Fago-Quercetum)* are inferred from Jansen *et al.* (1993) and Loopstra and van der Maarel (1984). Ecological response curves of 13 plant species were inferred from Wiertz *et al.* (1992). These species are: *Convallaria majalis, Corydalis claviculata, Deschampsia flexuosa, Hieracium laevigatum, Hieracium umbellatum, Holcus mollis, Luzula piloas, Luzula sylvatica, Melampyrum pratense, Polypodium vulgare, Pteridium aquilinum, Solidago virgauria,* and *Teucrium scorodonia.*

## Results

Figure 2 gives the percentage of protected species of the nature conservation target type "nutrient--poor deciduous forest" according to the 10 and 90 percentiles of the species response functions as a function of nitrogen availability in the soil, soil moisture and soil acidity expressed in Ellenberg indication values.
Figures 3 and 4 give the predicted probability of plant species of deciduous forests as a function of

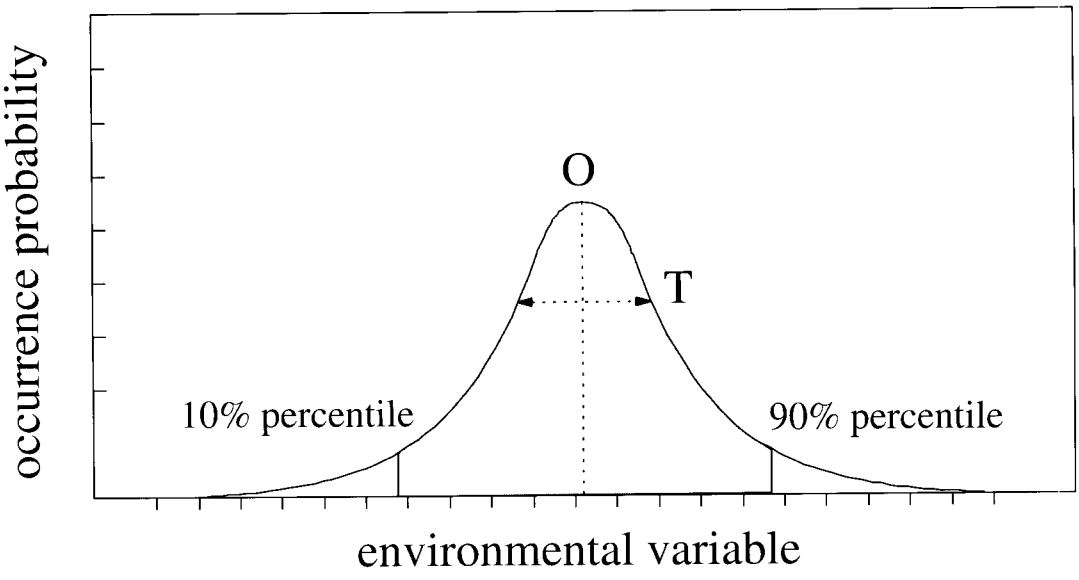


**Figure 1.** A species response function showing the occurrence probability of a species as a function of an environmental variable, characterized by its optimum (O) and the tolerance (T). The species protection levels that indicate the environmental load below which 10 and 90% of the species observations are found. Levels are plotted in a species response function.

eutrophication (nitrogen availability) and acidification (soil pH). Species are particularly threatened as to both soil pH and nitrogen availability in the central, southern and eastern sandy areas of the Netherlands. In most areas of the Netherlands, eutrophication (nitrogen availability) represents a more serious threat to the occurrence of plant species than soil pH. This type of analysis can be used to optimize abatement strategies.

## Discussion

At this moment, we see three advantages in our methodology, when comparing our approach in assessing risks related to eutrophication, acidification and desiccation with the assessment of critical loads:

1. Currently, assessment of critical loads is based on two different types of analysis: abiotic (exceedance of critical values for ion concentrations and ion ratios of soil and groundwater) and biotic (changes in species composition). In the approach as presented in this paper, abiotic and biotic response can be combined in a consistent framework. The SMART model can be used to predict exceedance of critical values for ion concentrations and ion ratios in soil and groundwater and to predict the input for the vegetation model MOVE: soil nutrient availability and soil acidity. With MOVE critical thresholds can be assessed referring to changes in species composition.

2. Empirical critical loads related to changes in species composition are based on an extensive yet inhomogeneous summary of field and laboratory experiments. It is unlikely that these empirical critical nitrogen loads protect various ecosystems equally. In our approach risk assessment is used to set ecological standards/thresholds for each ecosystem type and each environmental problem that corresponds to a similar protection, given by the percentiles and the species protection level.

3. Critical thresholds are directly linked by means of species response functions to nature conservation target types for which a clear conservation policy has been defined.

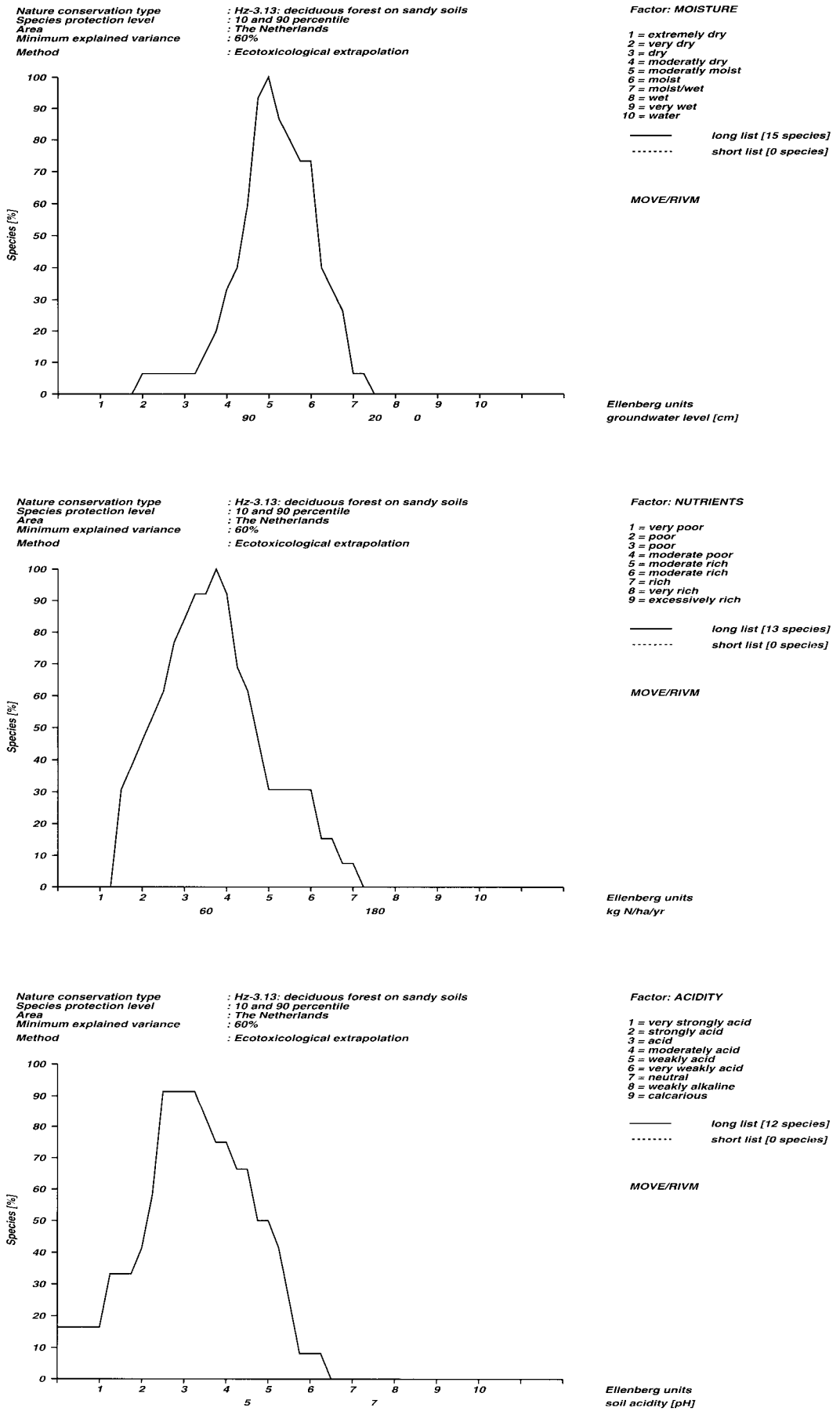


**Figure 2.** Percentage of the protected species of the nature conservation target type "nutrient-poor deciduous forest" as a function of nitrogen availability in the soil, soil moisture and soil acidity.

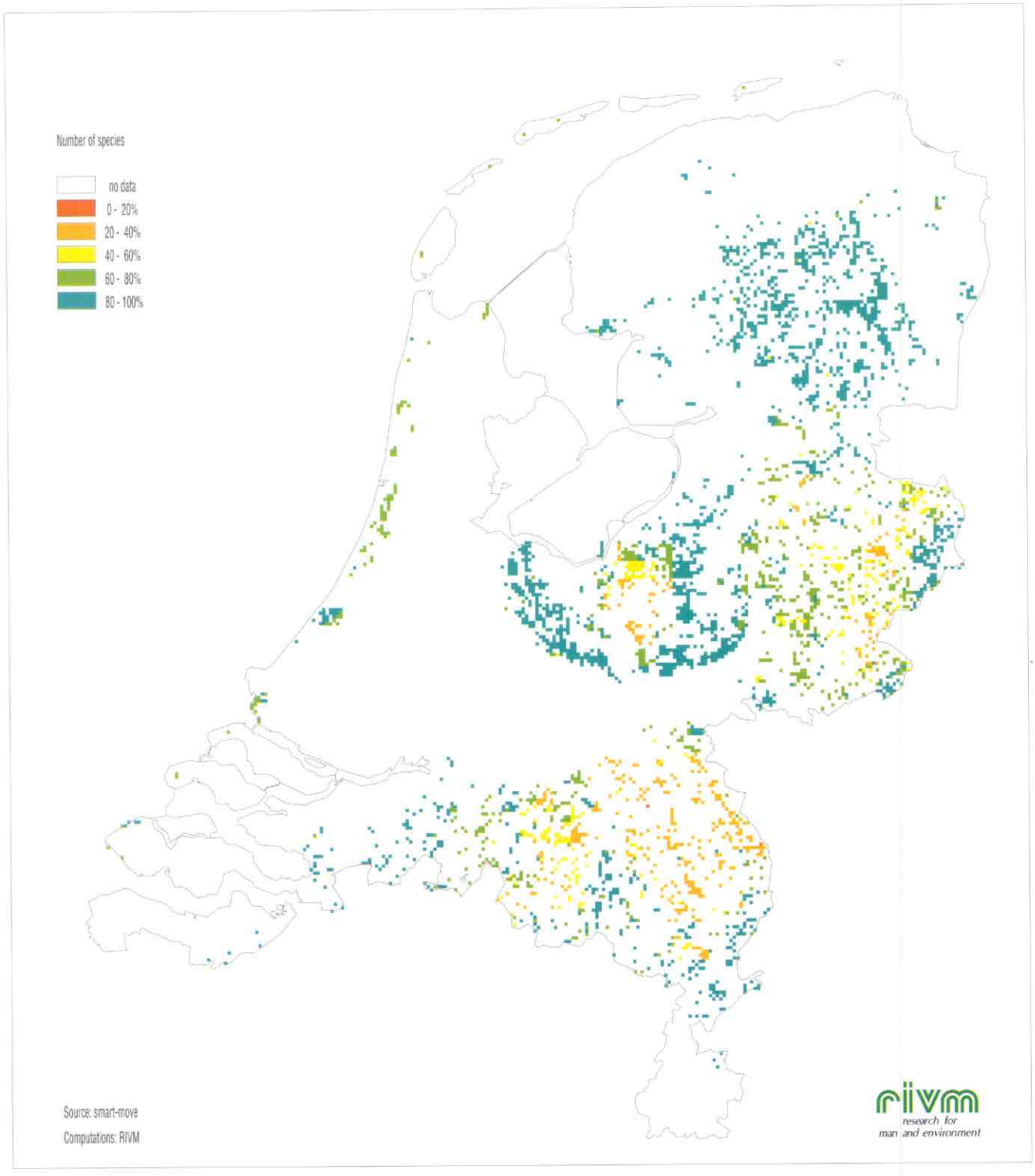


**Figure 3.** Predicted occurrence of plant species of deciduous forests as a function of modelled nitrogen availability.

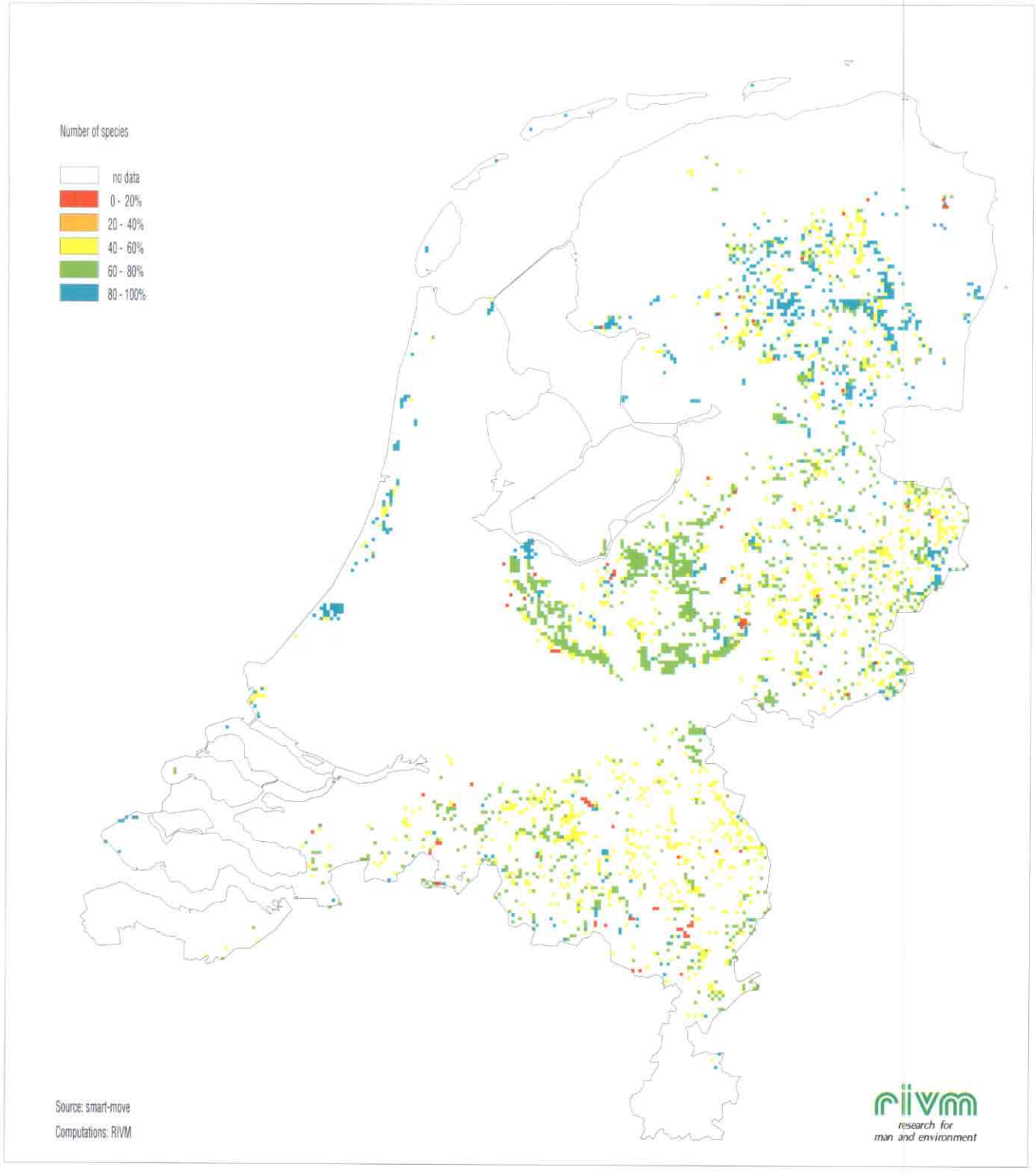


**Figure 4.** Predicted occurrence of plant species of deciduous forests as a function of modelled soil pH.

There are two methodological "disadvantages" of the method:

1. The species response curve is considered to be static without regarding temporal or spatial adaptations of species to environmental change. Species may, for instance, adapt to environmental loads in time. Temporal or regional differences have not been considered yet.

2. The use of empirical ecological response curves for assessing critical loads is constrained to be within values already experienced in the study area. This problem can be overcome to a large extent in two ways: by using vegetation relevées from regions with different environmental loads and from different periods in this century with low environmental loads.

The choice of percentiles and the species protection level is currently being studied for a limited number of well-researched ecosystems and plant communities by comparing results with field assessment. In this paper we used the 10 and 90 percentiles of the species-response curves to illustrate the method.

We believe that the approach as presented in this paper can also be applied in other countries. The soil model SMART was developed on a European scale in the context of critical load studies. The ecological response curves of plant species were based on a national Dutch analysis. The Ellenberg indication values required in the vegetation model, however, have been assigned to most European species. Therefore this analysis can also be elaborated in other countries provided that the necessary data are available. Elementary to an analysis of MOVE in other countries is a digital database of vegetation relevees with which ecological response curves can be calculated for each country. We estimate that this data-base should consist of about 10,000 to 20,000 vegetation relevees for each country and that the relevees should represent a mixture from pristine areas with low environmental loads and areas with high environmental loads. Obviously this number depends on the size of the country and the heterogeneity of biotopes in the country. Also needed in each country is a set of relevees with abiotic measurements for the calibration of the Ellenberg values. This data base should consist of approximately 1000-2000 vegetation relevees. Auxiliary data should include soil maps, deposition data and flora atlases.

## References


Bink, R.J., D. Bal, V.M. van den Berk, and L.J. Draaijer, 1994. Toestand van de Natuur 2. IKC-NBLF, Wageningen, Rep. 4.

De Vries, W., M. Posch, and J. Kämäri, 1989. *Water Air Soil Pollut.* **148**:349-390.

Ellenberg, H., 1979. *Scripta Geobotanica* 9:1-122.

Jansen, S.R.J., D. Bal, H.M. Beije, R. During, Y.R. Hoogeveen, and R.W. Uyterlinde, 1993. Ontwerp Nota Ecosysteemvisies EHS. IKC-NBLF, Wageningen, Rep.

Jongman, R.H.G., C.J.F. ter Braak, and O.F.R. van Tongeren, 1987. Data analysis in community and landscape ecology, Pudoc, Wageningen, The Netherlands, 299 pp.

Lammers, G.W., 1994. A new strategy in nature policy: towards a national ecological network in the Netherlands. In: Cook and Lier, V. (eds.), Landscape Planning and Ecological Networks, Elsevier Publishers, London, Amsterdam.

Latour, J.B. and R. Reiling, 1991. On the Move: concept voor een nationaal effecten model voor de vegetatie (MOVE). RIVM, Bilthoven, The Netherlands, Rep. 711901003. 23 pp.

Latour, J.B. and R. Reiling, 1992. Threats to nature. In: R. Maas (ed.), National Environmental Outlooks 1990-2010, RIVM, Bilthoven, The Netherlands, pp. 484-490.

Latour, J.B. and R. Reiling, 1993. *Sci. Tot. Environ.* **Supplement**, 1513-1526.

Latour, J.B., R. Reiling, and W. Slooff, 1994. *Water Air Soil Pollut.*

LNV, 1990. Natuurbeleidsplan: regeringsbeslissingen. Ministerie voor Landbouw, Natuur en Visserij, Den Haag, Rep. Tweede kamer vergaderjaar 1989-1990, 21149, nrs. 2-3. 272 pp.

Loopstra, I.L. and E. van der Maarel, 1984. Toetsing van de ecologische soortengroepen in de Nederlandse flora aan het systeem van indicatiewaarden volgens Ellenberg. De Dorschkamp, Wageningen, Rep. 381. 143 pp.

Schaminee, J.H.J., V. Westhoff, V. and G. van Wirdum, 1989. *De Levende Natuur* **90**:204-209.

U.S. EPA, 1990. Reducing risk: setting priorities and strategies for environmental protection. Report of the Science Advisory Board: Relative Risk Reduction Strategies Committee. US EPA, Washington DC.

Van der Eerden, L.J., T.A. Dueck, A.C. Posthumus, and A.E.G. Tonneijck, 1992. Assessment of critical levels for air pollutant effects on vegetation: some considerations and a case study on $NH_3$. UN/ECE Workshop on Critical Levels, Egham, U.K., 23-26 March 1992.

VROM, 1989. National Environmental Policy Plan: to choose or to lose. Ministry of Housing, Physical Planning and Environment, The Hague. Lower chamber parliamentary session 1988-1989, 21137, nos. 1-2. 257 pp.

VROM, 1991. Notitie Milieukwaliteitsdoelstellingen bodem en water. Tweede Kamer, vergaderjaar 1990-1991, nr. 21990, The Hague, report no. 38 pp.

Weinrich, J.A. and C.J.M. Musters, 1989. Toestand van de natuur: Veranderingen in de Nederlandse natuur. Ministerie van Landbouw, Natuurbeheer en Visserij, The Hague, Achtergrondreeks Natuurbeleidsplan nr. 4. 241 pp.

Wiertz, J., 1992. Schatting van ontbrekende vocht- en stikstofgetallen van Ellenberg (1979). IBN, Wageningen, report no. 92/7. 32 pp.

Wiertz, J., J. van Dijk, and J.B. Latour, 1992. De MOVE-vegetatie module: De kans op voorkomen van 700 plantesoorten als functie van vocht, pH, nutrienten en zout. IBN/RIVM, Wageningen/ Bilthoven, Rep. IBN 92/24; RIVM 711901006. 138 pp.

# PART III. National Focal Center Reports

This part consists of reports submitted by National Focal Centers summarizing progress made in mapping critical loads and levels over the past two years. A total of fourteen countries have contributed maps and data to the critical loads mapping program.

Some of the reports demonstrate an extension of the national critical load mapping work by including results on critical levels, with emphasis on the AOT40 values for ozone. Part III illustrates the consensus on the scientific methods for developing critical thresholds enabling the consistent mapping by CCE of critical loads and levels on a pan-European scale. The intensive involvement of the National Focal Centers ensures national characteristics of sensitive ecosystems to be reflected in the large scale assessments which are input to the Working Group on Strategies via the Task Force on Integrated Assessment Modelling.

# AUSTRIA


## National Focal Center/Contact:

Dr. Jürgen Schneider
Federal Environmental Agency
Spittelauer Lände 5
A-1090 Vienna
tel: + 1 313 04 5863
fax: + 1 313 04 5400
email: schneider_j@dev01.ubavie.gv.at

## Collaborating Institutions/Contacts:

Dr. Markus Knoflacher
Dr. Wolfgang Loibl
Austrian Research Center Seibersdorf
Dept. of Environmental Planning
A-2444 Seibersdorf
tel: + 2254 780 3874 (MK)
tel: + 2254 780 3875 (WL)
fax: + 2254 780 2051
email: loibl@zdfzs.arsc.ac.at


## A. Critical Loads of Nutrient Nitrogen

### Receptors mapped:

Forest soils, Alpine heaths and ombrotrophic bogs.

### Grid size: 2.75 x 2.75 km.

### Data sources:

**Geographical:** A number of different data bases were used to determine parameters necessary for calculating critical loads:

- The inventory of soil types in Austria based upon Fink (1978).
- Geological data taken from the "Hydrological Map of Austria" from the Austrian Atlas of the Academy of Science.
- Soil types classified according to FAO have been derived by overlaying the above mentioned maps.

Land use from the Austrian Atlas of the Academy of science, revised by NOAA/AVHRR satellite data.

- Catalogue of Austrian bogs from the Federal Environmental Agency.
- Forest data of the Austrian Forest Inventory, 2.75 x 2.75 km resolution.
- Forest ecological areas, published by "Österreichischen Forstverein".
- Digital elevation model of Austria

### Calculation Method:

#### 1. For forest soils:

The critical loads for forest soils were determined by using the steady state mass balance method, according to Eq. 4.18 of the CCE 1993 Status Report (Downing *et al.* 1993).

$$CL_{nut}(N) = N_u + N_i + N_l \,/\, (1 - f_{de})$$

The single terms are quite uncertain; therefore the following assumptions were made:

$N_u$: The concept of nutrient limitation was not supplied due to a lack of input data (e.g. no data on weathering rates for single basic cations). Therefore, present uptakes were calculated from known management regimes and nitrogen content of stems. These data were used to estimate long-term harvesting rates (which were assumed to be 20% higher than present rates).

The values for growth uptake vary from approx. 2 kg N $ha^{-1}$ $yr^{-1}$ to 7 kg N $ha^{-1}$ $yr^{-1}$, with a mean value of 5.6 kg N $ha^{-1}$ $yr^{-1}$.

$N_i$: The nitrogen immobilization at the critical load was approximated according to the 1993 Status Report. The following values were used:

$N_i$ = 3 kg N $ha^{-1}$ $yr^{-1}$ in histosols and podzols and
$N_i$ = 2 kg N $ha^{-1}$ $yr^{-1}$ for all other soils

A value of 2 kg N $ha^{-1}$ $yr^{-1}$ was assigned to approximately 83% of all grids, and the value of 3 kg N $ha^{-1}$ $yr^{-1}$ to the remaining 17%, resulting in an mean value of 2.17 kg N $ha^{-1}$ $yr^{-1}$ for all forest ecosystems.

$N_l$: The leaching was determined according to the CCE Status Report 1993, Eq. 4.9:

$$N_{l(crit)} = Q \cdot [N]$$

The critical [N] values were chosen according to the Mapping Manual, Table 4.2:
Coniferous forests: 0.0143 eq $m^{-3}$ and for
Deciduous forests: 0.0215 eq $m^{-3}$

The resulting values vary from approximately 2 to approximately 5 kg N $ha^{-1}$ $yr^{-1}$ with a mean value of 2.7 N $ha^{-1}$ $yr^{-1}$.

The values of $N_{de}$ were determined using $f_{de}$ values. These values were assigned to the grids according to drainage conditions. The values range from 0.1 for dry soils to 0.7 for wet soils.

### Results:

The values of $CL_{nut}(N)$ in forest ecosystems vary from approx. 7 kg N $ha^{-1}$ $yr^{-1}$ to approx. 32 kg N $ha^{-1}$ $yr^{-1}$. The mean value is 12.8 kg N $ha^{-1}$ $yr^{-1}$.

The 5th percentile of all grids with forest ecosystems is 8.3 kg N $ha^{-1}$ $yr^{-1}$, the mean 12.7 kg N $ha^{-1}$ $yr^{-1}$.

#### 2. For Alpine heaths and ombrotrophic bogs

**Empirical approach:**

The application of the empirical method is based on ecosystem inventories. The following data bases were used:

- The catalogue of Austrian bogs (Federal Environmental Agency, Vienna)
- Austrian Atlas, land use map (Austrian Academy of Science), revised by NOAA data.

According to the CCE 1993 Status Report, the following empirical values were assigned:

- for ombrotrophic bogs: 7 kg N $ha^{-1}$ $yr^{-1}$ (critical load range according to report: 5 - 10 kg)
- for alpine heaths: 10 kg N $ha^{-1}$ $yr^{-1}$ (range according to report: 5 - 15 kg).

205 grids were assigned to "ombrotrophic bogs", 1091 to Alpine heaths.

## B. Mapping of AOT40 values and exceedances of critical levels of ozone

The spatial ozone concentration over all of Austria (for grid cells with 5 x 5 km) was calculated starting from the ozone measurements conducted at approximately 120 monitoring sites located throughout the federal territory of Austria. For that purpose, a special daytime- and elevation-dependence function created according to the Austrian peculiarities was used (Loibl *et al.* 1993). Based on this function the AOT40 was calculated in two steps. First the measured ozone concentrations were interpolated over the whole investigation area. These calculations were carried out for every hour (i.e. every one-hour mean). In the second step the AOT40 was determined for each grid point by summing up the calculated ozone concentration depending on the receptor type (forest and agricultural areas) corresponding to the recommendations of the Bern Workshop (Fuhrer and Achermann 1994).

For forests a six-month observation period (from April to September, 24 hours a day) was taken, for agricultural areas a period from May to July (only daylight hours). An example AOT40 map for forest ecosystems is shown in Figure AT-3. The year chosen, 1993, had *atypically low* ozone concentrations during the summer.

The critical level was determined by assigning the value of 10,000 ppb-h to forest ecosystems using a digital land use map.

#### Calculation of exceedances of critical levels:

To determine the exceedances, the critical level (10 ppm-h) was subtracted from the mapped AOT40.

### References:


Downing, R.J., J.P. Hettelingh, and P.A.M. de Smet, 1993. Calculation and Mapping of Critical Loads in Europe: Status Report 1993. CCE, RIVM Report 259101003. Bilthoven, The Netherlands.

Fuhrer, J., and B. Achermann, 1994. Critical Levels for Ozone, Eidgenössische Foschnungsanstalt für Agrikulturchemie und Umwelthygiene, Liebefeld-Bern.

Loibl, W, 1995. Modelling the Spatial Distribution of Critical Levels for Ozone Considering the Influences of Complex Terrain. ARSC, Seibersdorf, Austria.

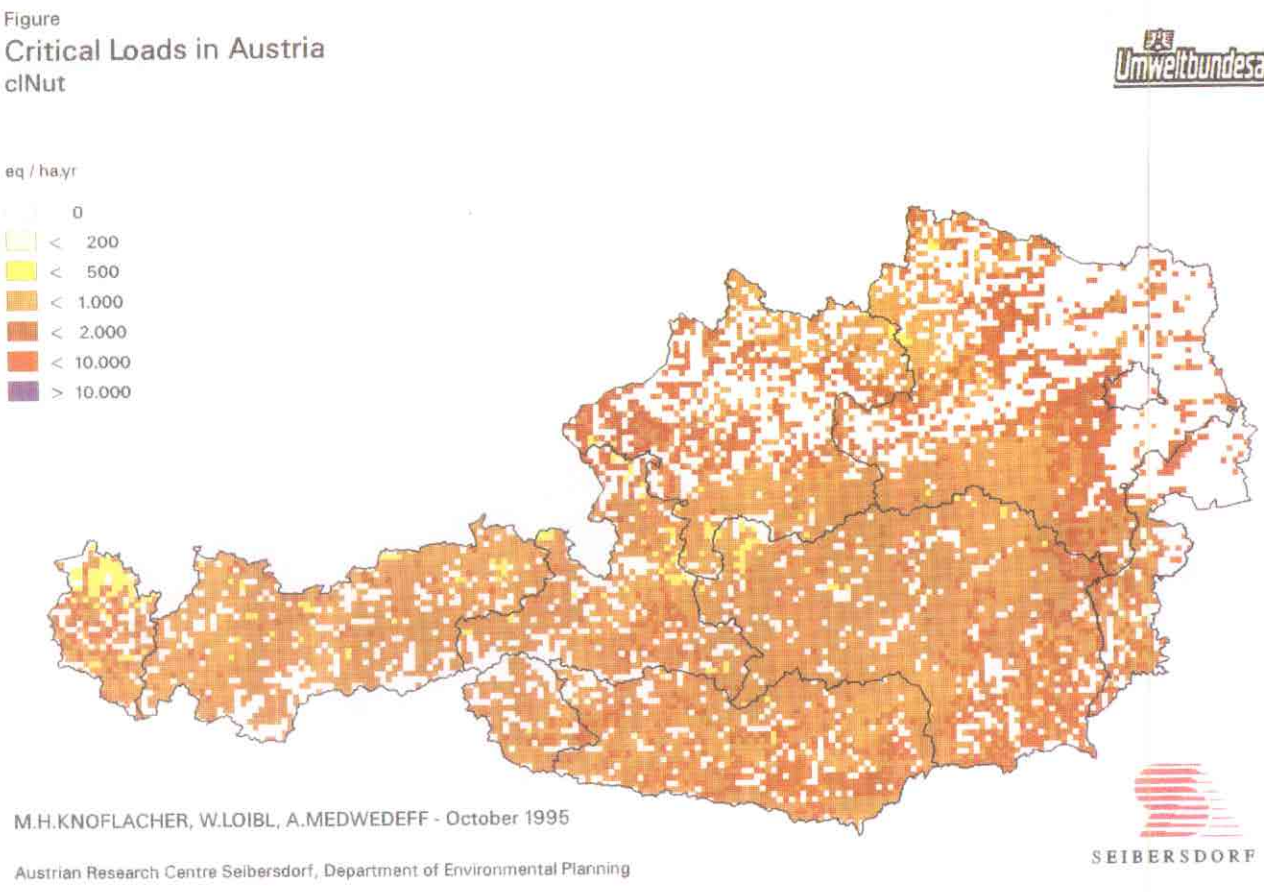


**Figure AT-1.** Critical loads of nutrient nitrogen.

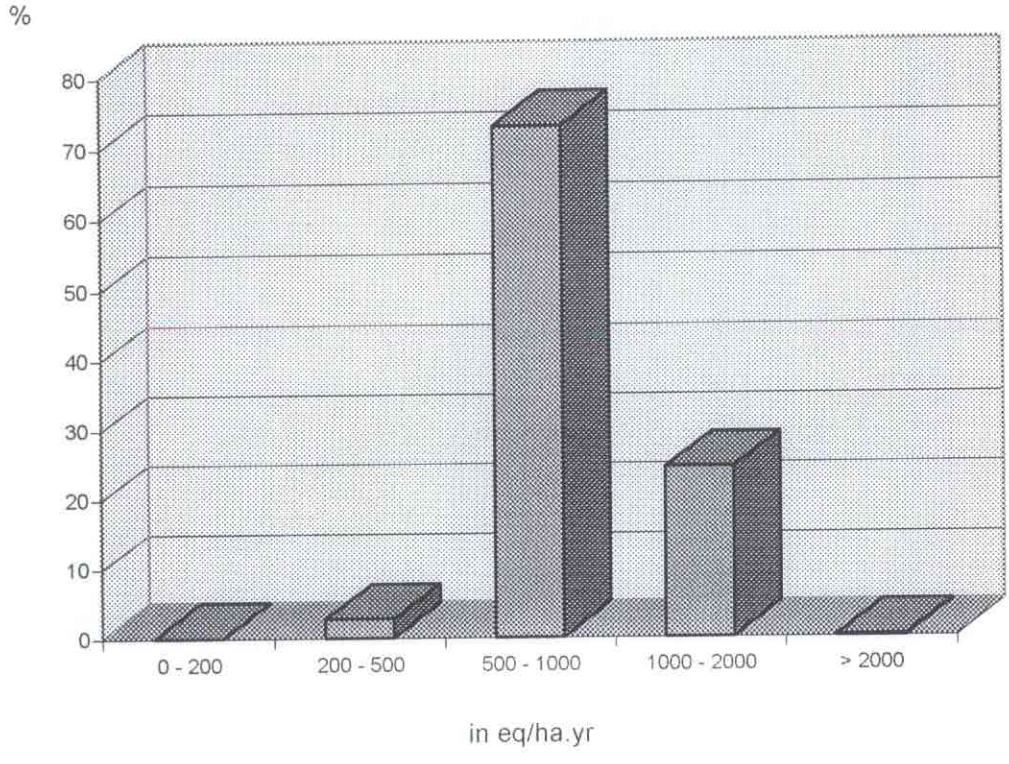


**Figure AT-2.** Distribution of classes of critical loads of nutrient nitrogen.

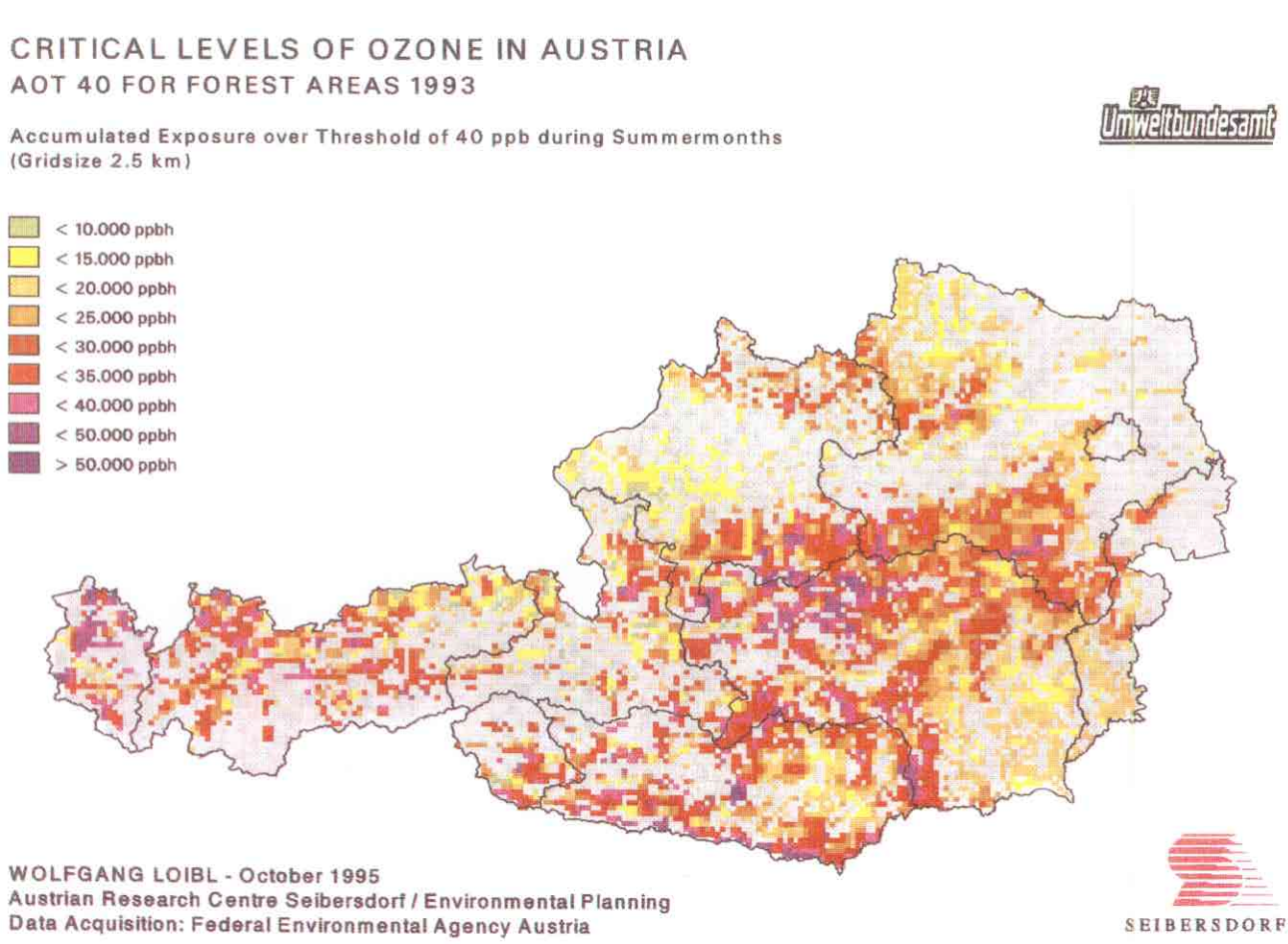


**Figure AT-3.** AOT40 for forest ecosystems (6-month growth period).

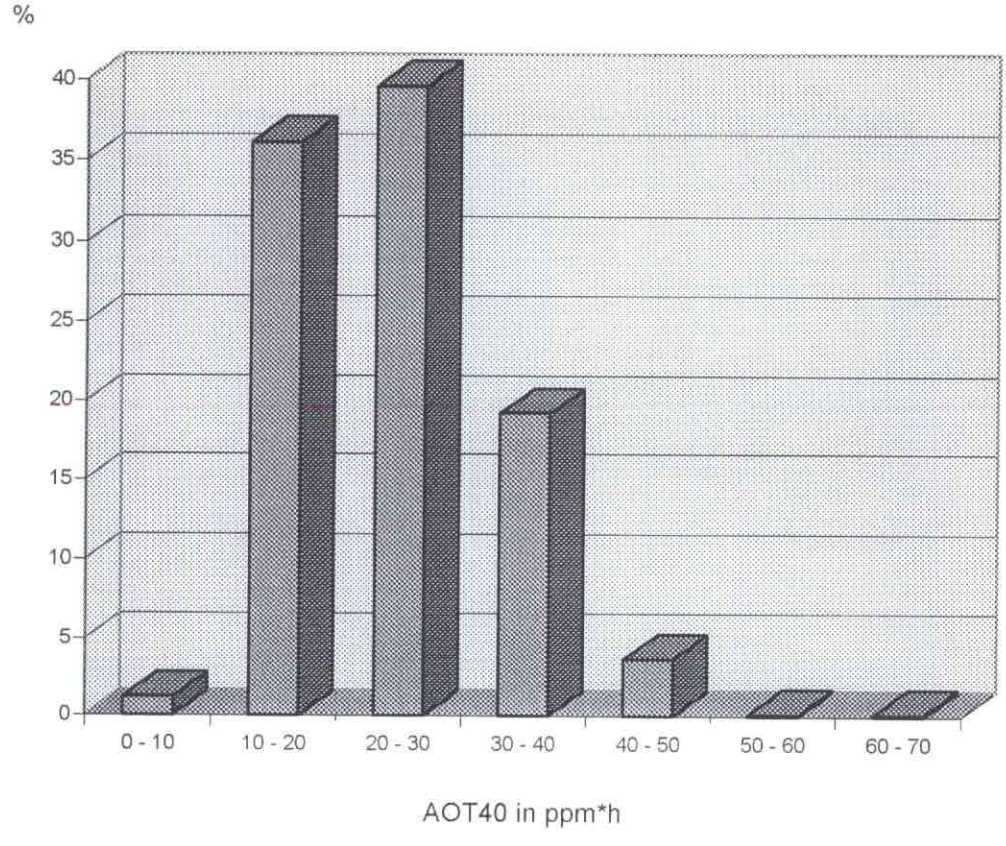


**Figure AT-4.** Frequency distribution of AOT40 for forest ecosystems in 1993.

# CZECH REPUBLIC

## National Focal Center/Contact:

Dr. Irena Skorepová & Šárka Roušarová
Czech Environmental Institute
Kaplanova 1931
148 00 Prague 4
tel: +42-2-7936585
fax: +42-2-7936648
email: skopera@ceu.ceu.cz

## Collaborating Institutions:

Dr. Tomáš Paces
Czech Geological Institute
Geologická 6
152 00 Praha 5

Pravoslav Pokorný
Forest Management Institute
Nábřežní 1326
250 02 Stará Boleslav

## List of national maps produced:

The mapping of critical loads of acidity, nitrogen and sulfur is based on 400 forest soil receptor points. The results are processed for a 37.5 x 37.5 km subgrid of the EMEP net. The evaluation of the critical loads in the ARC/INFO system involves these 5-percentile maps:

- critical loads of acidity
- critical loads of sulfur - minimum
- critical loads of sulfur - maximum
- critical loads of nitrogen - minimum
- critical loads of nitrogen - maximum
- critical loads of nutrient nitrogen

## Calculation method:

The simple mass balance method summarized in the CCE Status Report (1993) was used for the evaluation of the critical loads. The values of critical weathering rates were derived from Olsson & Melkerud relationship (1990). Calculations and results were reviewed by the CCE. The calculations include the following equations:

- $ANC_w = 3.68 \cdot 10^{-3} \cdot [(X_{ca} + X_{mg}) \cdot \Sigma (T>5°C)] - 0.37$
- $CL(A) = ANC_w + 0.09 \cdot Q + 0.2 \cdot Q$
- $CL_{nut}(N) = N_{u(crit)} + N_{i(crit)} + N_{l(crit)} / (1-f_{de})$
- $CL_{min}(N) = N_{u(crit)} + N_{i(crit)}$
- $CL_{max}(S) = CL(A) + BC_d - BC_{u(crit)}$
- $CL_{min}(S) = CL_{max}(S) - N_{l(crit)}$
- $BC_{u(crit)} = BC_d + ANC_w - Q \cdot [BC]_{crit}$
- $N_{l(crit)} = Q \cdot [N]_{crit}$

where:
$ANC_w$ = alkalinity produced by weathering at critical load
$X_{ca}$ and $X_{mg}$ = content of basic cations in the soil exchangeable pool
$\Sigma$ ($T$>5°C) = annual sum of daily temperatures above 5°C
$Q$ = runoff of water under root zone (groundwater runoff was used)
$N_{u(crit)}$ = uptake of nitrogen at critical load
$N_{i(crit)}$ = immobilization rate of nitrogen at critical load
$N_{l(crit)}$ = leaching of nitrogen at critical load
$f_{de}$ = denitrification fraction
$BC_d$ = atmospheric deposition of basic cations
$BC_{u(crit)}$ = uptake of basic cations at critical load
$[BC]_{crit}$ = concentration of basic cations in the soil solution at critical load
$[N]_{crit}$ = concentration of nitrogen in the soil solution at critical load
$CL(A)$ = critical load of acidity
$CL_{nut}(N)$ = critical load of nutrient nitrogen
$CL_{min}(N)$ = minimum critical load for nitrogen
$CL_{max}(N)$ = maximum critical load for nitrogen
$CL_{min}(S)$ = minimum critical load for sulfur
$CL_{max}(S)$ = maximum critical load for sulfur
$[H^+]_{crit}$ = critical concentration of protons

The list of constant values used in the calculations of critical loads:

| Constant | Value and unit |
|---|---|
| $[N]_{crit}$ | 0.0157 eq $m^{-3}$ |
| $[BC]_{crit}$ | 0.01 eq $m^{-3}$ |
| $[H^+]_{crit}$ | 0.09 eq $m^{-3}$ |
| $[Al^{3+}]_{crit}$ | 0.2 eq $m^{-3}$ |
| $N_{i(crit)}$ | 357 eq $ha^{-1}$ $yr^{-1}$ |
| $f_{de}$ | 0.64 |

## Data Sources:

The input data were obtained from different sources. The chemistry of forest soils and vegetation characteristics of forests were provided by the Forest Management Institute. These data belong to the national forest monitoring system

carried out from the early 1980's. Hydrological and meteorological data in the forest stands were derived from hydrogeological maps of the scale of 1:200,000 issued by the Czech Geological Institute (1981). The modeled data were used for the atmospheric input of sulfur and oxidized nitrogen (Charles University, Dept. of Meteorology and Environmental Protection). The atmospheric deposition of ammonium nitrogen was assessed on the basis of measurements in the small catchments carried out by the Czech Geological Institute. The data on basic cation deposition were provided by the CCE from the European background data base.

### *Maps:*

The evaluation of critical loads is summarized in six schematic maps. The values are processed for a 37.5 x 37.5 km subgrid of the EMEP net. The white squares in the maps represent areas not evaluated due to a lack of soil chemistry data.

### *Comments and conclusions:*

Using different methods in assessing critical weathering rates results in different values in critical loads of acidity and sulfur in the border areas of the Czech Republic, in comparison to the results in Germany and Poland. The assessment of critical weathering rates based on soil types and texture classes will be included in the evaluation of critical loads for the 50 x 50 km subgrid of the EMEP network.

### *References:*


Downing, R.J., J.-P. Hettelingh and P.A.M. de Smet (eds.), 1993. Calculation and mapping of critical loads in Europe: Status Report 1993. RIVM Rep. 259101003, Bilthoven, the Netherlands.

Hettelingh, J.-P., R.J. Downing, and P.A.M. de Smet (eds.), 1991. Mapping Critical Loads for Europe. Technical Report No. 1, RIVM Rep. 259101001, Bilthoven, the Netherlands.

Olsson, M. and P.A. Melkerud, 1990. Determination of weathering rates based on geochemical properties of the soil. Proc. Conf. Environ. Geochemistry in Northern Europe. Symposium 34, pp. 45-61. Geol. Survey of Finland.

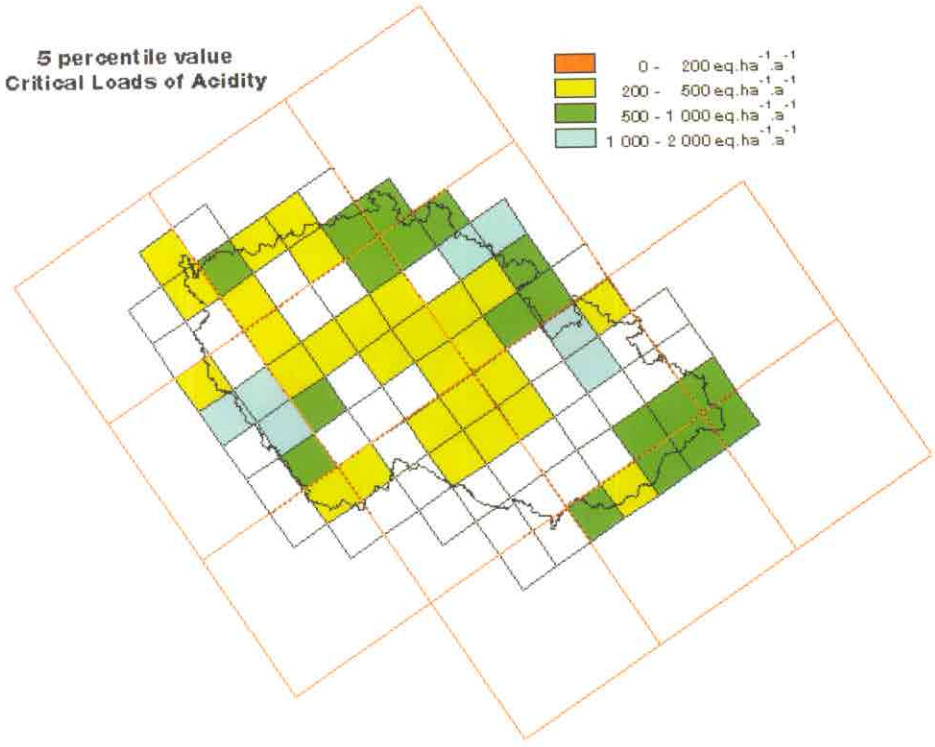


**Figure CZ-1.** Critical loads of acidity (5 percentile).

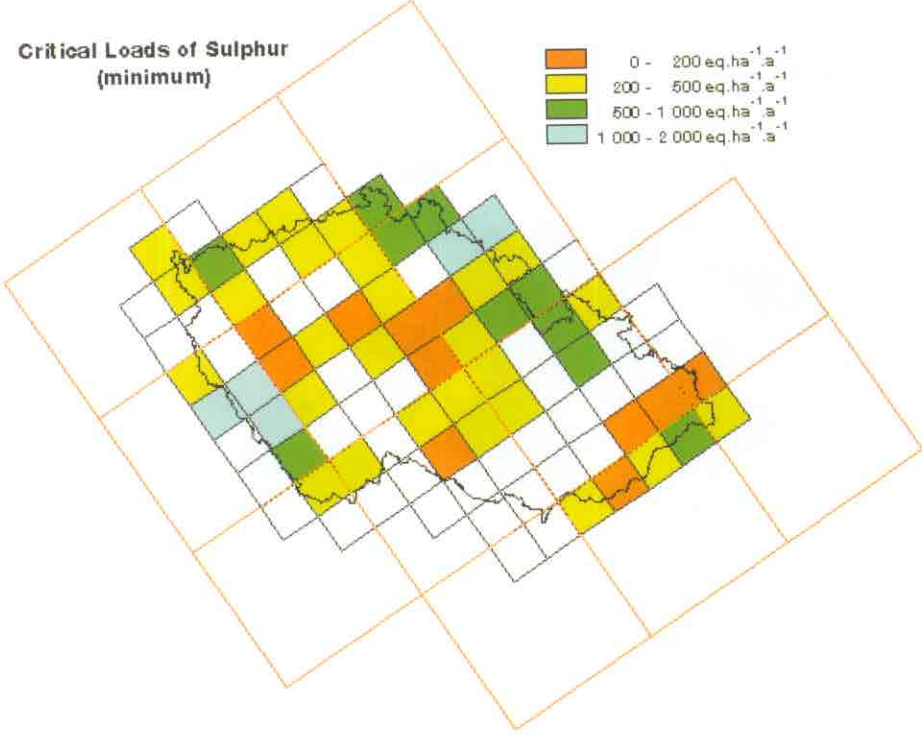


**Figure CZ-2.** Minimum critical loads of sulfur.

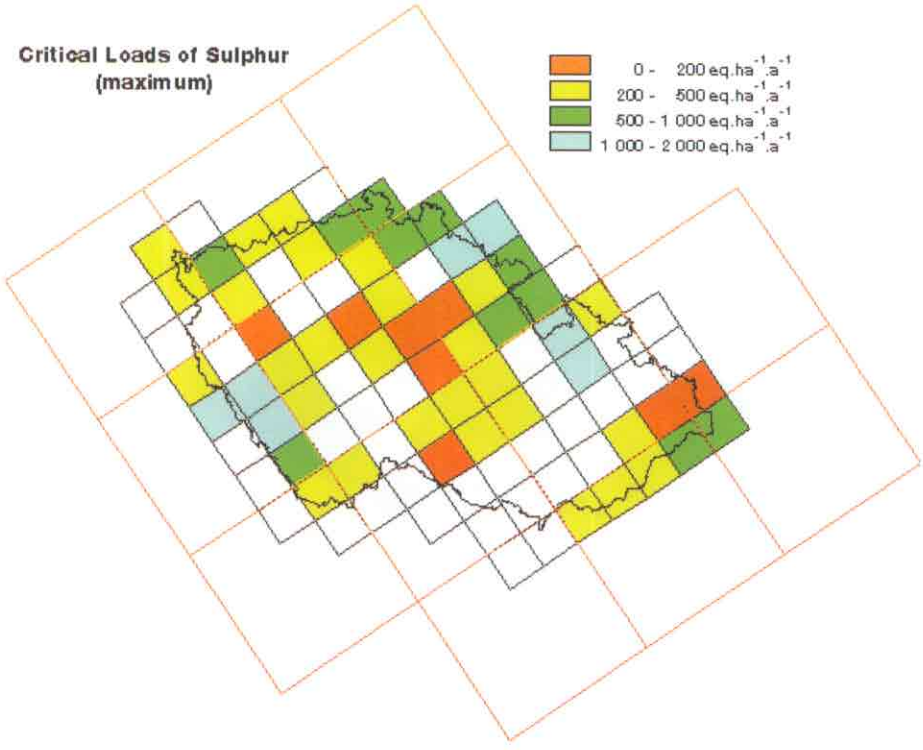


**Figure CZ-3.** Maximum critical loads of sulfur.

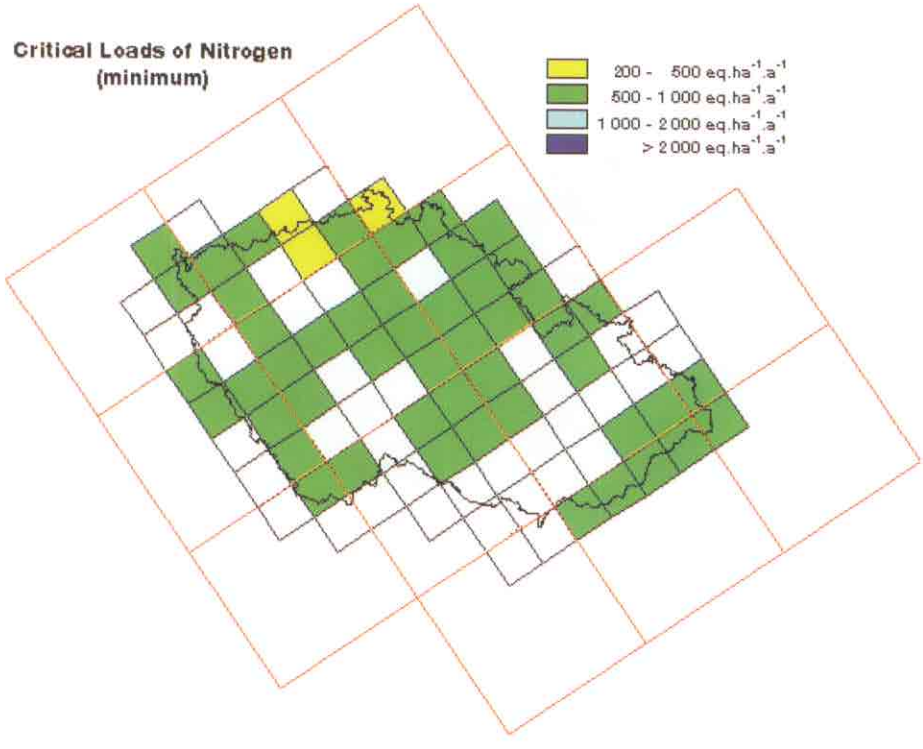


**Figure CZ-4.** Minimum critical loads of nitrogen.

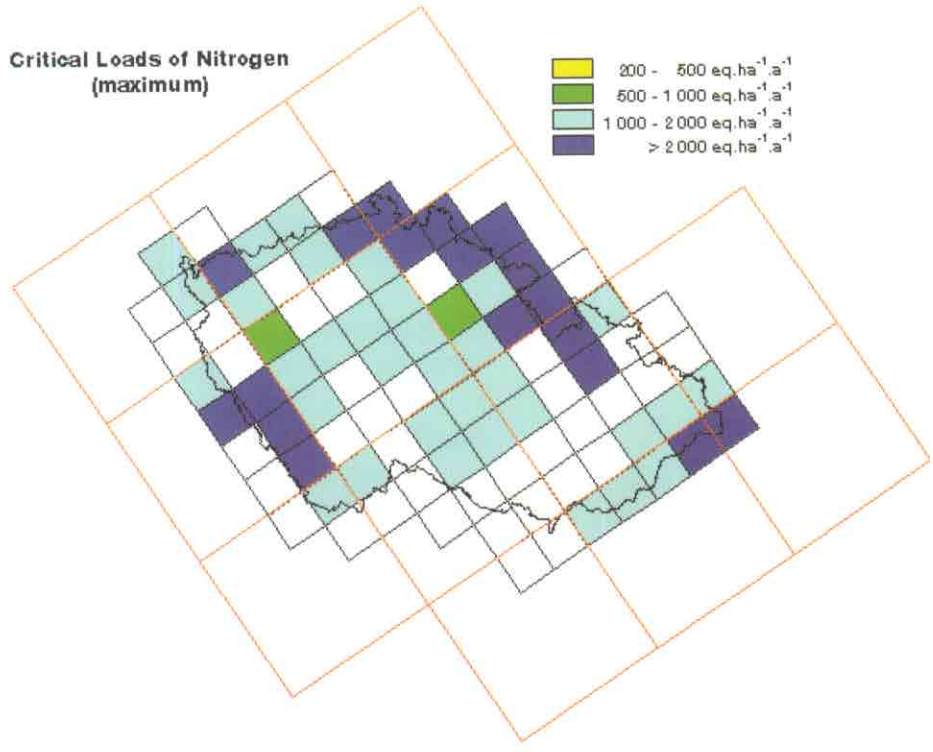


**Figure CZ-5.** Maximum critical loads of nitrogen.

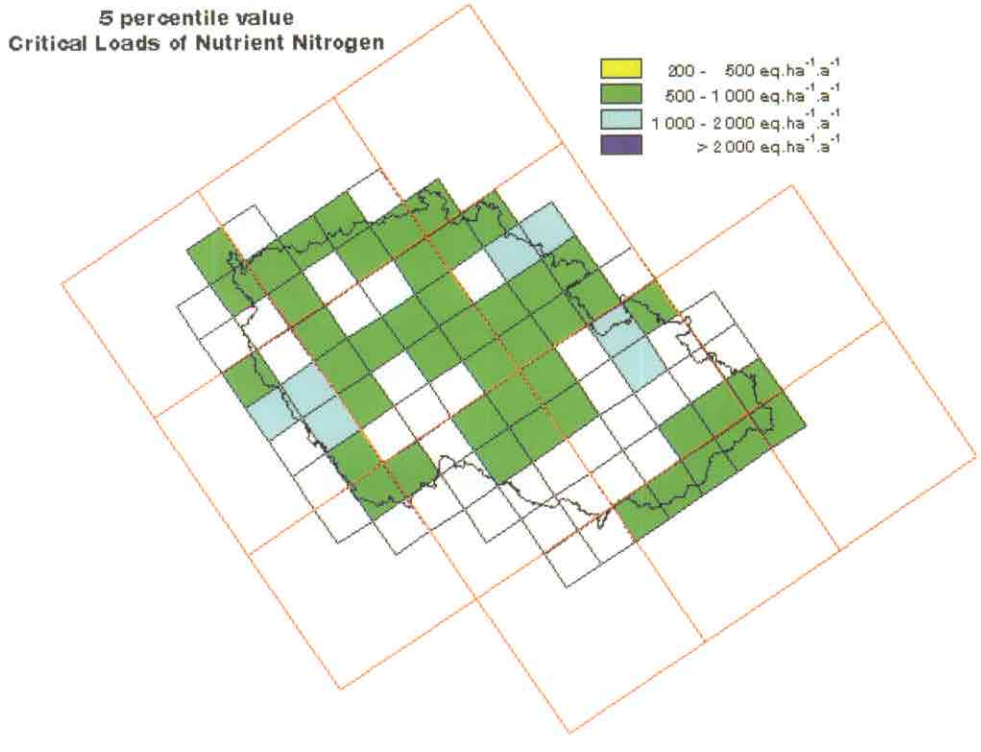


**Figure CZ-6.** Critical loads of nutrient nitrogen (5 percentile).

# DENMARK

## National Focal Center/Contact:

Jesper Bak, Hans Løkke
National Environmental Research Institute
Dept. of Terrestrial Ecology
25 Vejlsøvej
DK-8600 Silkeborg
tel: +45 89201400
fax: +45 89201414
email: tejb@wpgate.dmu.min.dk

## National maps produced:

- Critical deposition of acidity for forest soils and extensively managed grasslands calculated with PROFILE and, for grasslands, the SSMB model.
- Exceedances of the critical load of acidity.
- Critical load of nutrient nitrogen for production forest calculated with PROFILE.
- Exceedances of the critical load for nutrient nitrogen.

## Calculation method:

The PROFILE model has been used to calculate the critical load for acidity and nitrogen eutrophication and hence the values of $CL_{min}(S)$, $CL_{max}(S)$, $CL_{min}(N)$, $CL_{max}(N)$, and $CL_{nut}(N)$. In calculating the critical load of acidity for grasslands, the model has been used to calculate the weathering rate for eleven classes of mineralogy, while the critical load has been calculated with the SSMB equation (Downing *et al.* 1993):

$$CL(A) = ANC_w + \left( 1.5 \cdot \frac{0.8 \cdot ANC_w + BC_{dep} - BC_u - 0.015 \cdot Q}{200} \right)^{1/3} \cdot Q^{2/3} + 1.5 \cdot \left( 0.8 \cdot ANC_w + BC_{dep} - BC_u - 0.015 \cdot Q \right)$$

The PROFILE model evaluates the chemical criteria separately for stratified layers of the root zone, iteratively recalculating the weathering of primary minerals and the uptake of nitrogen and base cations. This is an important difference from applying the SSMB equation, where the chemical criterion is evaluated on the whole root zone. Also, the limiting nutrient approach is applied for the different soil layers, conferring uptake to the soil layer, where nutrients are available.

In calculating the critical load of nutrient nitrogen, the mass balance equation for nitrogen is solved by the model, which calculates weathering and nutrient uptake at critical load. The limiting nutrient approach is also applied for the different soil layers in this calculation.

The version of the mass balance equation (from the Mapping Manual) applied is:

$$CL_{nut}(N) = N_{l(crit)} + N_{i(crit)} + N_{u(crit)} + N_{de}$$

The applied stratification of the root zone is in general a 5-cm thick A/E horizon, a soil-dependent B and C horizon, and a maximum root depth dependent on the vegetation type (See Table DK-1).

All calculations are made for the vegetation types beech-, oak-, spruce- and pine-dominated forests. Critical loads of acidity are also calculated for permanent, extensively managed grasslands. The basic data have been collected on a 1x1 km national grid and calculations performed for ecosystems covering more than 25 ha within a grid cell. The total number of model calculations is included in Table DK-1.

**Table DK-1.** Values used in critical load calculations.

| | Root depth (cm) | BC uptake (keq km$^{-2}$) | N uptake (keq km$^{-2}$) | No. of calculations |
|---|---|---|---|---|
| Beech | 70 | 5.4 · PC | 10.4 · PC | 2825 |
| Oak | 90 | 6.8 · PC | 10.4 · PC | 448 |
| Spruce | 50 | 3.7 · PC | 3.9 · PC | 5480 |
| Pine | 50 | 1.8 · PC | 3.4 · PC | 1035 |
| Grass | 25 | 51 | 30 | 1000 |

PC: Production class, m$^3$ ha$^{-1}$ yr$^{-1}$

## Data Sources:

The main sources of data for this calculations have been the same as reported in the CCE 1993 Status Report. The sources and resolution of data are shown in Table DK-2.

**Table DK-2.** Sources and resolution of input data used in the Danish critical loads calculations.

| Parameter | Resolution | Sources |
|---|---|---|
| Soil mineralogy | 60 points | DLD, literature |
| Soil texture | 1 : 500,000 | DLD |
| Geological origin | 1 : 500,000 | DLD |
| Forest limits | 1 : 500,000 | DLD |
| Forest production, species | 1 : 500,000 | DLD, DSO |
| Ecosystem cover | 1 km grid | NERI |
| $SO_x$, $NH_x$, $NO_y$ deposition | 1/5 km grid | NERI, EMEP |
| Meteorological data | 1 : 1,000,000 | DLD, DMI |

DLD: Danish Institute of Plant and Soil Science, Dept. of Land Data
DSO: Danish Statistical Office
NERI: National Environmental Research Institute
NFNA: National Forest and Nature Agency

***Deposition:*** Deposition of $NO_y$ and $NH_x$ have been calculated an a national 5x5 km grid. For $NO_y$ wet deposition, the relationship to measured data was poor, and the average measured wet deposition of $NO_4$ was used instead. The $SO_x$ and base cation deposition have been calculated from EMEP and from Danish data on wet deposition and air concentrations, using an empirical relationship between air concentration and dry deposition derived from throughfall data from Danish monitoring sites.

***Vegetation:*** A total registration of tree species, forest age and production figures was performed in 1979-1982. These data are available in digital form and have been compared to more recent statistical information. There is no complete national registration available for permanent, unmanaged grassland, so this vegetation type has been distributed on arable land based on statistical information. The removal rate of nitrogen and base cations has been related to production figures for forest based on nitrogen content in stem and branches. For unmanaged grassland, a removal rate of 4 kg N $ha^{-1}$ $yr^{-1}$ has been assumed. (See Table DK-1.)

***Soil:*** Maps are of the texture and geological origin of the Danish topsoils. The content of primary minerals has, however, only been analyzed on 60 sites. A map of mineral content in the A/E, B and C horizons of the topsoil has been constructed by interpolating the point information within 11 classes of topsoil geology.

***Constants:*** For the calculations of the critical load of acidity, a criterion value of BC/Al = 1 $mol_c$ $mol_c^{-1}$ has been applied for all vegetation types. $ANC_w$ and $BC_u$ have been calculated with the PROFILE model. $Q$ has been calculated with a simple hydrological model and 30-year normal precipitation values.

For the calculation of the critical load for nutrient nitrogen, a critical leaching, $N_{le(crit)}$ of 2 kg $ha^{-1}$ $yr^{-1}$ and a immobilization, $N_{im(crit)}$ of 3 kg $ha^{-1}$ $yr^{-1}$ has been applied. $N_{u(crit)}$ has been calculated with the PROFILE model applying the limiting nutrient approach. $N_{de(crit)}$ has been calculated with PROFILE in accordance with Eq. 4.10 in the CCE 1993 Status Report.

## Comments and conclusions:

The main changes in methodology and in the underlying data from the Danish calculations of the critical load of acidity used in developing the 1994 sulfur protocol to the current calculations is:

- The PROFILE calculations are now performed with actual data for all mapped ecosystems which cover more than 25 ha on each square in a 1x1 km national grid.
- The BC/Al criterion is tested in all soil horizons in the root zone.
- The calculations now include the critical load of nutrient nitrogen, and the limiting nutrient approach has been applied in all calculations.

It is not foreseen that major changes in the calculations of the critical load of acidity will be made in the nearest future. For permanent grasslands where both the PROFILE model and the SSMB equation have been applied, the calculation methods have been compared on 1000 individual points. Results from the two methods are correlated with r=0.98. The change in methodology where the BC/Al criterion now is tested in all soil horizons has not led to major changes in the average of the calculated critical load values.

A project aimed at harmonizing the calculations of critical loads of nutrient nitrogen in the Nordic countries has been initiated and preliminary results discussed. A similar bilateral harmonizing exercise for the shared grids between Denmark and Germany is being considered.

The work plan for the Danish NFC now includes preparation of preliminary stock at risk and exceedance maps for ozone at the end of 1995. Work is undertaken to prepare national values for empirical critical loads for heathlands and raised bogs and to enhance the national calculations of exceedances of the critical load of nutrient nitrogen, including the effects of local sources of ammonia. Results will be available in 1996. Initial studies on the deposition and concentrations in soil of heavy metals have been initiated and will be concluded in 1995. The work plan now includes preparation of national maps of critical loads of heavy metals in 1999.

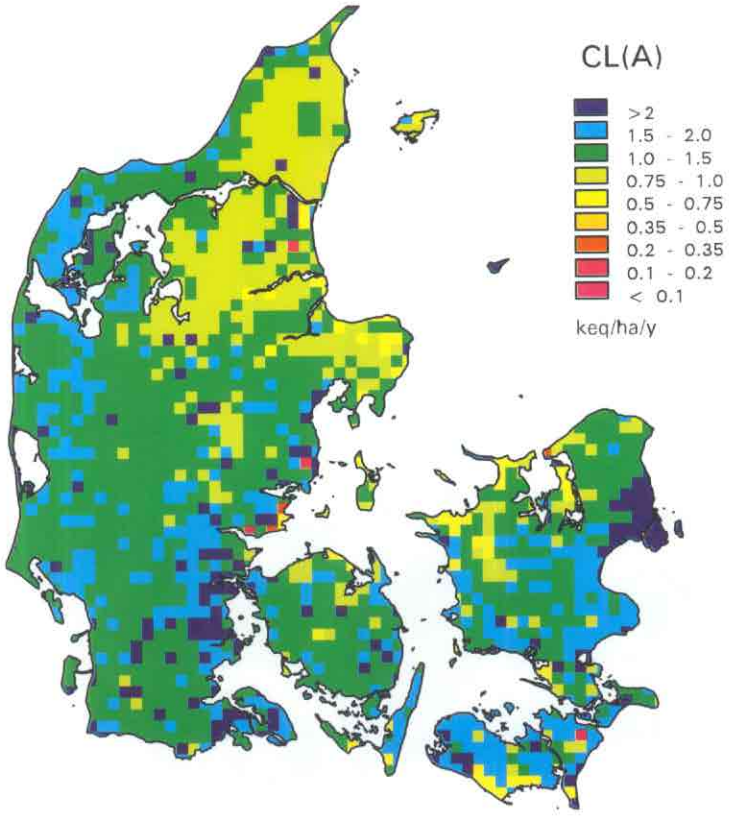


**Figure DK-1.** Critical loads of acidity.

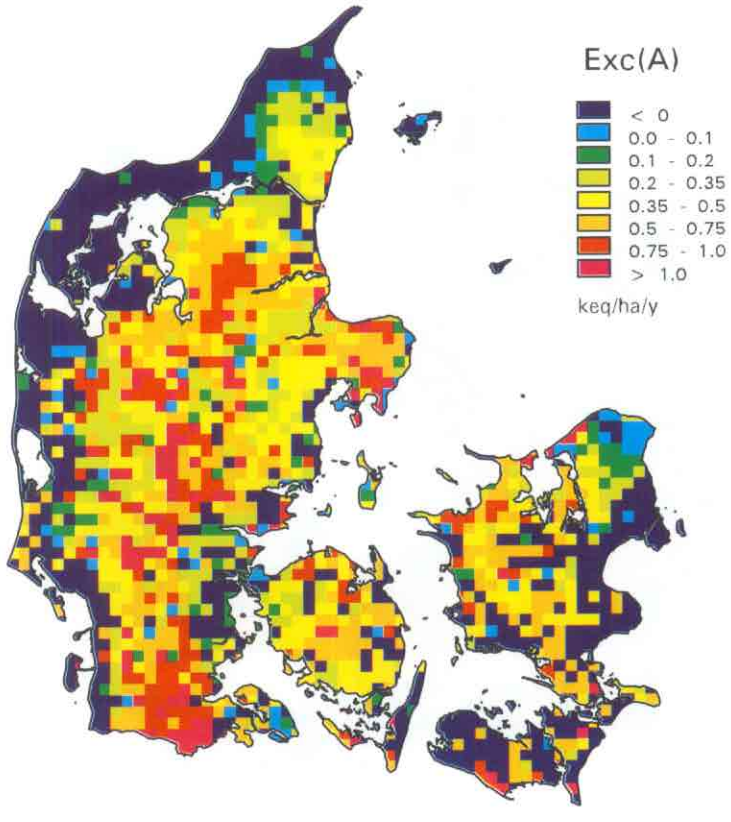


**Figure DK-2.** Exceedance of the critical loads of acidity.

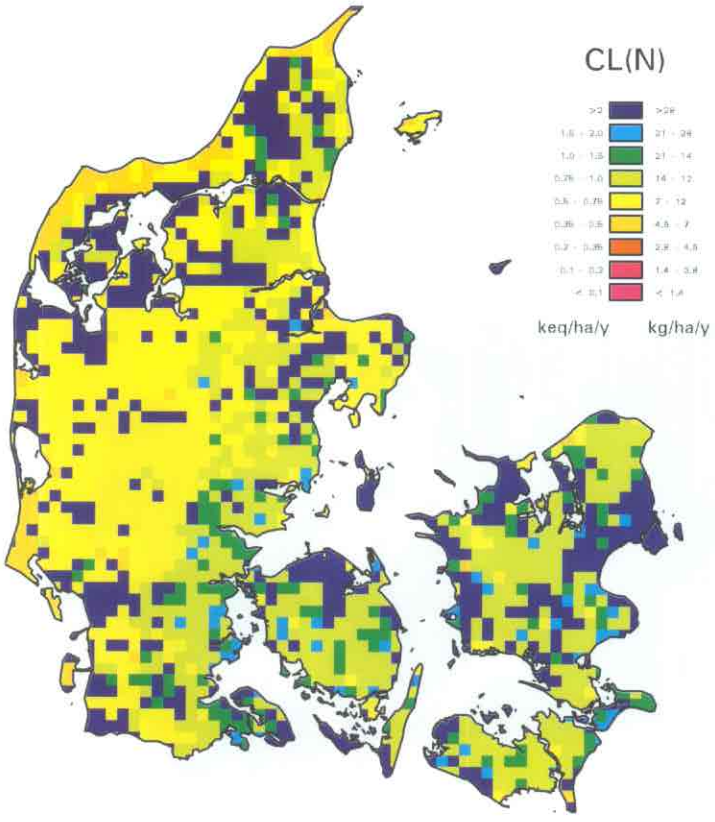


**Figure DK-3.** Critical loads of nitrogen.

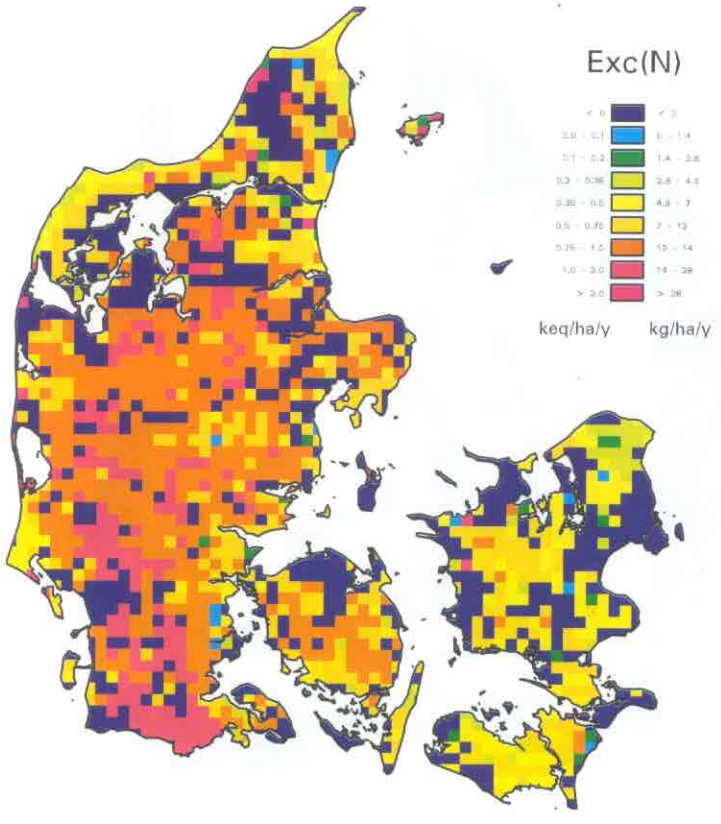


**Figure DK-4.** Exceedance of critical loads of nitrogen.

# ESTONIA


### National Focal Center/Contact:

Mr. Leo Saare
Estonian Environmental Information Center
Mustamäe tee 33
EE0006 Tallinn
Estonia
tel: 372.2.527654
fax: 372.6394071
email: eeic@sun.nlib.ee

### Collaborating Institutions/Contacts:

Dr. Tõnu Oja
Institute of Geography
University of Tartu
EE2400 Tartu
Estonia
tel: 372.7.430679
fax: 372.7.422084
email: oja@math.ut.ee


### List of national maps produced:

Critical loads for nitrogen (minimum, maximum and nutrient) and sulfur.

### Receptors mapped:

Forest soils. Additional receptors: plant communities, protected objects.

### Calculation method:

Steady-state mass balance method, empirical estimates for nutrient nitrogen affecting plant communities.

The equations used for calculation are taken from the CCE 1993 Status Report:

$$Cl_{max}(S) = CL(A) + BC_{dep} - BC_u$$

$$Cl_{nut}(N) = N_{u(crit)} + N_{i(crit)} + N_{l(crit)} / (1-f_{de})$$

$$Cl_{min}(N) = N_{u(crit)} + N_{i(crit)}$$

$$Cl_{max}(N) = N_{u(crit)} + N_{i(crit)} + CL_{max}(S) / (1-f_{de})$$

### Grid size:

A national basic grid of 0.25° x 0.125° (under completion), with preliminary calculations completed for the EMEP 150x150 km grid based on the distribution of ecosystems/soil types within the grid cell.

### Data sources:

- Soil map (1:200,000) of 1991, digitized at the Institute of Geography, University of Tartu.
- Vegetation map (1:600,000) 1960, digitized at the Institute of Geography, University of Tartu.
- Deposition loads: data from the Estonian National Monitoring system.

Forest types distinguished were Scots pine, Norway spruce and deciduous (mostly birch and alder). Soil types distinguished among podzolic (pseudo-podzolic), peatlands (raised bogs), wetlands (marshes) and very shallow soils on limestone bedrock (alvar).

### Comments and conclusions:

Mapping of critical loads in Estonia has been started and is going on. Mapping exceedances is limited because of the deposition measurment network being very rare and functioning only for a short time. However, the situation is improving. The situation in Estonia, in particular in the north-eastern part, with extremely high base cation deposition creates a need for additional analysis of the methods used: the simple mass balance method does not always behave reasonably under very high BC deposition. A question about the critical loads for base cation deposition has to be asked as in many naturally acidic environments (e.g. peat bogs) it causes unwanted changes in the plant community.

### Reference:


Posch, M., J.-P. Hettelingh, H.U. Sverdrup, K. Bull, and W. de Vries, 1993. Guidelines for the Computation and Mapping of Critical Loads and Exceedances of Sulphur and Nitrogen in Europe. In: Downing, R.J., J.P. Hettelingh, and P.A.M. Smet, (Eds.), 1993. Calculation and Mapping of Critical Loads in Europe: Status Report 1993.

**Table EE-1.** Calculated values of critical loads for different soil-vegetation types in the EMEP cells overlapping Estonia.

| cell x-y | Area % | Ecosystem type | $N_u$ | $N_i$ | $N_l$ | $N_{de}$ | $ANC_w$ | $ANC_l$ | $BC_{dep}$ | $BC_u$ | *CL min(N)* | *CL max(N)* | *CL nut(N)* | *CL max(S)* |
|---|---|---|---|---|---|---|---|---|---|---|---|---|---|---|
| 21-24 | 4 | pine-podzol | 224 | 214 | 100 | 40 | 750 | 0 | 1600 | 160 | 314 | 2740 | 425 | 2180 |
| | 0.4 | spr-alvar | 224 | 36 | 100 | 280 | 1250 | 0 | 1600 | 200 | 136 | 5436 | 336 | 2650 |
| | 0.4 | spr-podzol | 224 | 214 | 150 | 170 | 750 | 0 | 1600 | 200 | 364 | 5664 | 664 | 2650 |
| | 0.4 | pine-bog | 224 | 214 | 0 | 390 | 250 | 0 | 1600 | 160 | 214 | 8614 | 214 | 1680 |
| 22-24 | 1.3 | pine-podzol | 224 | 214 | 100 | 80 | 750 | 0 | 1000 | 160 | 314 | 1893 | 425 | 1580 |
| | 0.4 | spr-alvar | 224 | 36 | 100 | 450 | 1250 | 0 | 1000 | 200 | 136 | 4236 | 336 | 2050 |
| 21-25 | 1.8 | spr-alvar | 224 | 36 | 100 | 450 | 1250 | 0 | 1600 | 200 | 136 | 5436 | 336 | 2650 |
| | 1.8 | spr-podzol | 224 | 214 | 150 | 380 | 750 | 0 | 1600 | 200 | 364 | 6554 | 664 | 2650 |
| | 2.2 | dec-wet | 224 | 214 | 0 | 630 | 250 | 0 | 1600 | 270 | 214 | 8064 | 214 | 1570 |
| | 3.5 | pine-podzol | 224 | 214 | 100 | 70 | 750 | 0 | 1600 | 160 | 314 | 2736 | 425 | 2180 |
| | 1.8 | spr-alvar | 224 | 36 | 100 | 280 | 1250 | 0 | 2400 | 200 | 136 | 4036 | 336 | 3450 |
| | 1.3 | spr-podzol | 224 | 214 | 150 | 170 | 750 | 0 | 2400 | 200 | 364 | 7264 | 664 | 3450 |
| | 2.2 | dec-wet | 224 | 214 | 0 | 390 | 250 | 0 | 2400 | 200 | 214 | 12064 | 214 | 2370 |
| | 3.1 | pine-podzol | 224 | 214 | 100 | 40 | 750 | 0 | 2400 | 160 | 314 | 3591 | 425 | 2950 |
| 21-26 | 1.3 | spr-podzol | 224 | 214 | 150 | 380 | 750 | 0 | 3100 | 200 | 364 | 8664 | 664 | 4150 |
| | 1.3 | dec-podzol | 224 | 214 | 150 | 380 | 750 | 0 | 3100 | 270 | 364 | 7504 | 664 | 3570 |
| 22-26 | 0.4 | spr-podzol | 224 | 214 | 150 | 170 | 750 | 0 | 2400 | 200 | 364 | 7264 | 664 | 3450 |
| | 0.4 | bog | 224 | 214 | 0 | 390 | 250 | 0 | 2400 | 170 | 214 | 12564 | 214 | 2470 |
| | 0.4 | pine-bog | 224 | 214 | 0 | 390 | 250 | 0 | 2400 | 170 | 214 | 12564 | 214 | 2470 |
| | 0.4 | dec-wet | 224 | 214 | 0 | 390 | 250 | 0 | 2400 | 270 | 214 | 12064 | 214 | 2370 |
| | 0.4 | pine-podzol | 224 | 214 | 100 | 40 | 750 | 0 | 2400 | 170 | 314 | 3664 | 425 | 2970 |
| | 1.8 | spr-podzol | 224 | 214 | 150 | 320 | 750 | 0 | 3100 | 200 | 364 | 8664 | 664 | 4150 |
| | 1.8 | bog | 224 | 214 | 0 | 630 | 250 | 0 | 3100 | 170 | 214 | 16114 | 214 | 3180 |
| | 1.8 | pine-bog | 224 | 214 | 0 | 630 | 250 | 0 | 3100 | 170 | 214 | 16114 | 214 | 3180 |
| | 1.8 | dec-wet | 224 | 214 | 0 | 630 | 250 | 0 | 3100 | 270 | 214 | 15614 | 214 | 3080 |
| | 1.8 | pine-podzol | 224 | 214 | 100 | 70 | 750 | 0 | 3100 | 170 | 314 | 4302 | 425 | 3680 |
| 22-25 | 2.2 | spr-podzol | 224 | 214 | 150 | 170 | 750 | 0 | 1000 | 200 | 364 | 4464 | 664 | 2050 |
| | 4.4 | bog | 224 | 214 | 0 | 390 | 250 | 0 | 1000 | 170 | 214 | 5614 | 214 | 1080 |
| | 6.6 | pine-podzol | 224 | 214 | 100 | 40 | 750 | 0 | 1000 | 170 | 214 | 1969 | 425 | 1580 |
| | 4.4 | pine-bog | 224 | 214 | 0 | 390 | 250 | 0 | 1000 | 170 | 214 | 5614 | 214 | 1080 |
| | 2.2 | dec-podzol | 224 | 214 | 150 | 170 | 750 | 0 | 1000 | 270 | 364 | 3324 | 664 | 1480 |
| | 2.2 | spr-podzol | 224 | 214 | 150 | 170 | 750 | 0 | 1600 | 200 | 364 | 5664 | 664 | 2650 |
| | 4.4 | bog | 224 | 214 | 0 | 390 | 250 | 0 | 1600 | 170 | 214 | 8614 | 214 | 1680 |
| | 6.6 | pine-podzol | 224 | 214 | 100 | 40 | 750 | 0 | 1600 | 170 | 214 | 2636 | 425 | 2180 |
| | 4.4 | pine-bog | 224 | 214 | 0 | 390 | 250 | 0 | 1600 | 170 | 214 | 8614 | 214 | 1680 |
| | 2.2 | dec-podzol | 224 | 214 | 150 | 170 | 750 | 0 | 1600 | 270 | 364 | 4524 | 664 | 2080 |
| 23-25 | 3.1 | spr-podzol | 224 | 214 | 150 | 320 | 750 | 0 | 1000 | 200 | 364 | 4464 | 664 | 2050 |
| | 3.1 | pine-podzol | 224 | 214 | 100 | 70 | 750 | 0 | 1000 | 170 | 314 | 2069 | 425 | 1580 |
| | 2.7 | dec-podzol | 224 | 214 | 150 | 320 | 750 | 0 | 1000 | 270 | 364 | 3324 | 664 | 1480 |

5th percentile (eq/ha/yr)

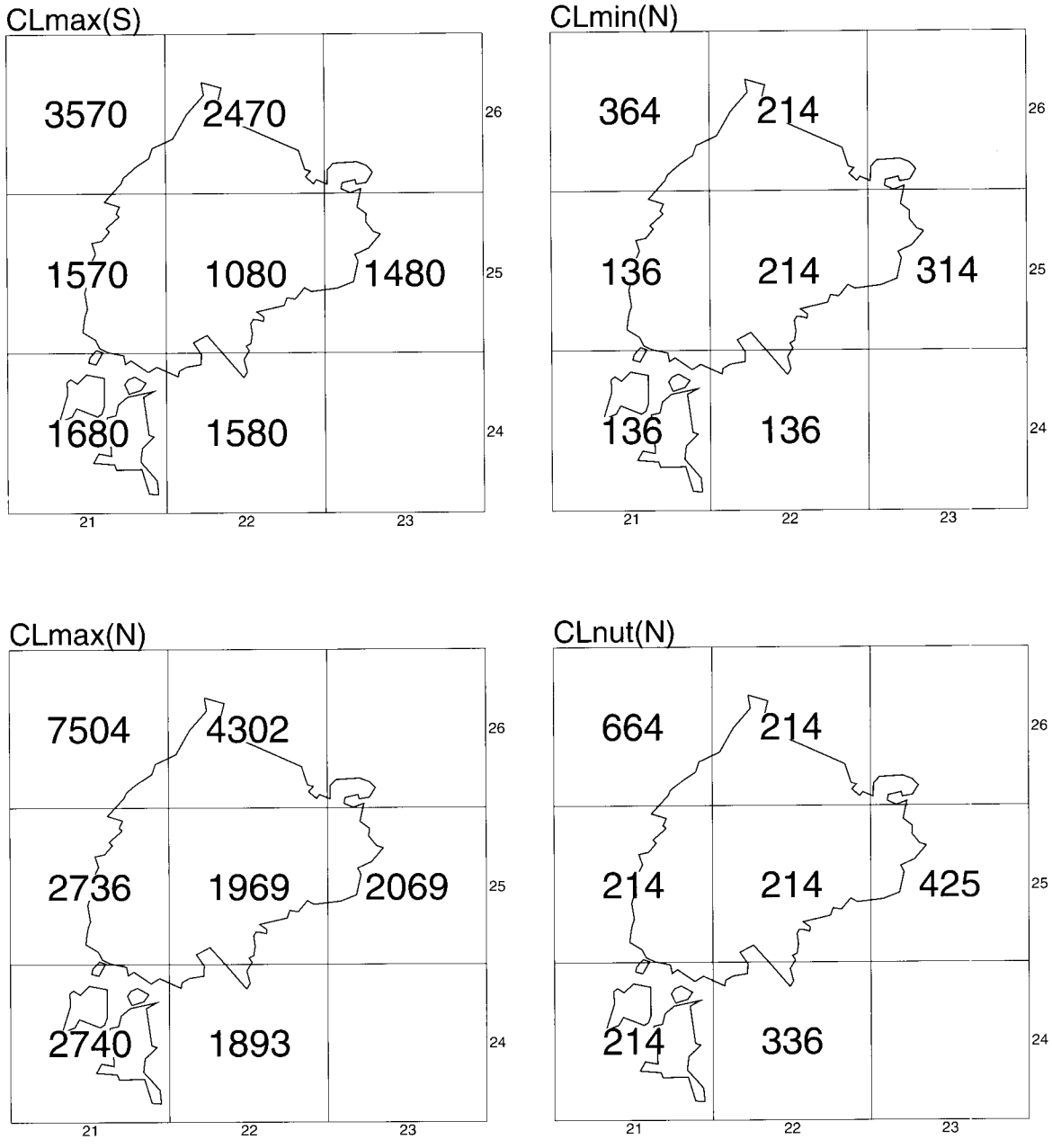


**Figure EE-1.** $CL_{max}(S)$, $CL_{min}(N)$, $CL_{max}(N)$, and $CL_{nut}(N)$ (5 percentile).

# FINLAND

## National Focal Center/Contact:

Matti Johansson, Head
Juha Kämäri
Martin Forsius
Sanna Syri
Finnish Environment Agency
P.O. Box 140
FIN-00251 Helsinki
tel: +358-0-403 000
fax: +358-0-403 00 390
email: matti.johansson@vyh.fi

## Collaborating Institutions/Contacts:

Tuomas Laurila
Virpi Lindfors
Finnish Meteorological Institute
Sahaajankatu 20 E
FIN-00810 Helsinki
tel: +358-0-75811
fax: +358-0-7581 396

Timo Tarvainen
Geological Survey of Finland
P.O. Box 169
FIN-02150 Espoo
tel: +358-0-46931
fax: +358-0-462205

## National maps produced:

The formulation of an exceedance function, i.e. the possibility of having the same exceedance for various combinations of S and N deposition, does not allow the specification of a unique reduction strategy. One way to display the required reductions of S and N is to define the position of the current or future deposition pair in relation to the ecosystem protection isoline. The S-N plane is divided into five areas: one where there is no exceedance at all and four with a combination of mandatory or exchangeable S and N reductions. To conserve as much information as possible on a national level in the map display but to keep it comprehensible, we have presented the ecosystem area in each EMEP grid cell falling into the predefined classes of 0 to 4 in the S-N plane in the year 1990 (see Figure FI-1).

Exceedances of critical levels for ozone have been mapped according to the recommendations from the UN-ECE workshop in Bern in 1993. In Figure FI-2 the yearly AOT40 (accumulated hourly exposure over threshold of 40 ppb displayed in ppm h) for agricultural crops (spring wheat) is displayed for the years 1991-94. A map for AOT values for agricultural crops and for forests in Scandinavia has recently been reported by a working group supported by the Nordic Council of Ministers (see report of NFC Sweden).

## Calculation methods:

For both receptors mapped, surface waters and forest soils, the possible pairs of critical load of acidity for N and S are derived from acidity balance considerations. For the sum of N and S deposition the following acidity balance is assumed (Kämäri *et al.* 1992, Henriksen *et al.* 1993):

$$N_{dep} + S_{dep} = fN_{upt} + (1-r)(N_{imm}+N_{de}) + rN_{ret} + rS_{ret} + BC_{le} - ANC_{le} \quad (1)$$

where the base cation (BC) leaching is given by

$$BC_{le} = BC_{dep} + (1-r)BC_{w} - fBC_{upt} \quad (2)$$

where $f$ is the fraction of forested land in the catchment area, $r$ is the lake:catchment area ratio, $N_{upt}$ and $BC_{upt}$ are the net growth uptake of N and BC, $N_{imm}$ is the immobilization of N in soils, $N_{de}$ is N denitrified in soils, $N_{ret}$ and $S_{ret}$ are the in-lake retention of N and S, $BC_{w}$ is the BC weathering, and $ANC_{le}$ is the alkalinity leaching. For lake catchments the term $(1-r)$ limits the influence of $N_{imm}$, $N_{de}$ and $BC_{w}$ to the terrestrial area, and $f$ limits the uptake to the forested area only. For forest soils one has to set $f$=1 and $r$=0.

Inserting the deposition-dependent expressions for soil denitrification and in-lake N and S retention into Eq. 1, one obtains:

$$a_N N_{dep} + a_S S_{dep} = b_1 N_{upt} + b_2 N_{imm} + BC_{le} - ANC_{le} \quad (3)$$

where the dimensionless constants $a_N$, $a_S$, $b_1$ and $b_2$ are all smaller than one and depend on ecosystem properties only: denitrification fraction ($f_{de}$), net mass transfer coefficients for S and N ($s_S$ and $s_N$), and runoff ($Q$). For soils, $BC_{le}$ at critical load is computed from Eq. 2. For lakes the net base cation

leaching at critical load is computed from water quality data (cf. Henriksen *et al.* 1992).

$$BC_{le(crit)} - ANC_{le(crit)} = Q([BC] - [ANC]_{limit}) \quad (4)$$

where $ANC_{le(crit)}$ is $ANC_{le}$ at critical load, $Q[BC]$ is the pre-acidification leaching of base cations from the catchment area, and $Q[ANC]_{limit}$ is the critical alkalinity leaching. By prescribing a maximum allowable leaching of N, the critical load of nutrient nitrogen can be computed for soils, using the mass balance

$$CL_{nut}(N) = N_{upt} + N_{imm} + N_{de} + N_{le(crit)} \quad (5)$$

The methods for the calculation of critical loads in Finland are in accordance with the guidelines (Posch *et al.* 1993).

## Input data:

For forest soils, information is needed for $BC_{dep}$, $BC_w$, $BC_{upt}$, $N_{upt}$, $N_{de}$, $N_{imm}$, and $ANC_{le(crit)}$. $BC_{dep}$ is interpolated from the data from the years 1991-93 of a nationwide network of stations measuring monthly bulk deposition (Järvinen and Vänni 1990). The long-term average $BC_w$ was estimated by applying the results of the field studies of Olsson and Melkerud (1993) and using the effective temperature sum (ETS) and the total element content of Ca and Mg in the C-horizon as input data. Total analysis data on the < 2.0 mm fraction of till required by the method were obtained for 1057 plots from the Geological Survey of Finland. $N_{upt}$ and $BC_{upt}$ refer to the net uptake of nutrients in the stem and bark biomass via harvesting. They are estimated from annual forest growth and the element contents in biomass. Average forest growth was calculated for each major tree species based on ETS, whereas element contents were taken from unpublished Swedish data (Rosén, pers. comm.). $N_{de}$ was assumed proportional to the net incoming N, and the denitrification fractions were related to the soil type by linearly interpolating between a low value of 0.1 for podzolic mineral soils and a value of 0.8 for peat soils, depending on the soil type fractions (De Vries *et al.* 1993). For $N_{imm}$, including $N_{fix}$, a value of 2.0 kgN $ha^{-1}$ $a^{-1}$ as a long-term average was used for Finnish forest soils (Downing *et al.* 1993). For $BC_{le(crit)}$ a limiting concentration, below which trees can no longer extract nutrients from soil solution, is set to 10 µeq $l^{-1}$. $ANC_{le(crit)}$ is calculated by adding the critical aluminum leaching, obtained from the molar Al/BC ratio of 1.0, the hydrogen leaching, calculated from a gibbsite equilibrium ($K_{gibb} = 10^{8.3}$). The nitrogen leaching is derived with runoff using the concentration criterion 0.3 mgN $l^{-1}$ (Downing *et al.* 1993). The runoff values needed for converting concentrations to fluxes were obtained from a digitized runoff map for 1961-1975 (Leppäjärvi 1987).

For lakes, additional information is needed for $f$, $r$, $S_{ret}$, $N_{ret}$, $[BC]$ and $[ANC]_{limit}$. The data for lakes were mostly obtained from a national statistically based lake survey of 970 lakes conducted in 1987. The spatial distribution of the lake data set reflects the actual lake density in different regions. Both lake and catchment areas, as well as the forest fraction, were measured from topographic maps. $S_{ret}$ and $N_{ret}$ were computed from kinetic equations (Kelly *et al.* 1987). The mass transfer coefficients $s_S$ and $s_N$ were taken from retention model calibrations in North America (Baker and Brezonik 1988, Dillon and Molot 1990). $[BC]$ was estimated using the so-called F-factor, which relates the change over time in the leaching of base cations to long-term changes in inputs of strong acid anions in a lake, estimated as a function of the present base cation concentration. $[SO^{-}]$ was estimated from the relationship between present sulfate and base cation concentrations from 251 lakes located in northern Fennoscandia receiving very low acidic deposition (Henriksen *et al.* 1993). An $[ANC]_{limit}$ value of 20 µeq $l^{-1}$ was selected as the chemical criterion based on results of a fish status survey conducted in Norway (Lien *et al.* 1992).

## Comments and conclusions:

The input data for forest soils calculation has been refined, especially the weathering rate estimate. As for lakes, a new lake survey is to be carried out this fall in Finland together with other Scandinavian countries using unified sampling and analysis methods.

Finland and Russia have conducted bilateral negotiations on an air pollution prevention protocol. The first part, concentrating on acidification caused by sulfur, is based on the critical load approach, including the harmonization of input data in the border area. Examples on emission reduction strategies to achieve non-exceedance for the ecosystems considered have been presented during the negotiations.

Ozone research is carried out in the Finnish Meteorological Institute (FMI). Ozone concentrations are measured in several stations, and estimates on crop yield losses have been made (Laurila and Lättilä 1994). Forest effect estimates are still rather uncertain in the northern conditions. A version of the Harwell trajectory model for ozone (Lindfors *et al.* 1995) has been adopted at FMI. Several case studies have been done on the regional reduction requirements for $NO_x$ and VOC emissions.

## *References:*


Baker, L.A. and P.L. Brezonik, 1988. Dynamic model of in-lake alkalinity generation. *Wat. Resour. Res.* **24**:65-74.

De Vries, W., M. Posch, G.J. Reinds and J. Kämäri, 1993. Critical loads and their exceedance on forest soils in Europe, Rep. 58 (revised version). DLO The Winand Staring Centre for Integrated Land, Soil and Water Research. Wageningen, The Netherlands. 77 pp.

Dillon, P.J., and L.A. Molot, 1990. The role of ammonium and nitrate in the acidification of lakes and forested catchments. *Biogeochem.* **11**:23-43.

Downing, R., J.-P. Hettelingh and P. de Smet (eds.) 1993. Calculation and mapping of critical loads in Europe: Status Report 1993. CCE/RIVM, Rep. 259101003, Bilthoven.

Henriksen, A., J. Kämäri, M. Posch and A. Wilander, 1992. Critical loads of acidity: Nordic surface waters. *Ambio* **21**:356-363.

Henriksen, A., M. Forsius, J. Kämäri, M. Posch, and A. Wilander, 1993. Exceedance of critical loads for lakes in Finland, Norway and Sweden: Reduction requirements for nitrogen and sulfur deposition. Acid Rain Research Rep. 32/1993, Norwegian Institute for Water Research. Oslo, Norway.

Järvinen, O. and T. Vänni, 1990. Bulk deposition chemistry in Finland. In: P. Kauppi, P. Anttila and K. Kenttämies (eds.), Acidification in Finland, Springer. Berlin, pp. 151-165.

Kämäri, J., D.S. Jeffries, D.O. Hessen, A. Henriksen, M. Posch and M. Forsius, 1992. Nitrogen critical loads and their exceedance for surface waters. In: P. Grennfelt and E. Thörnelöf (eds.), Critical loads for nitrogen. Rep. Nord 1992:41, Nordic Council of Ministers. Copenhagen, Denmark, pp. 161-200.

Kelly, C.A., J.W.M. Rudd, R.H. Hesslin, D.W. Schindler, P.J. Dillon, C.T. Driscoll, S.A. Gherini and R.H. Heskey, 1987. Prediction of biological acid neutralization in acid sensitive lakes. *Biogeochem.* **3**:129-140.

Laurila, T. and H. Lättilä, 1994. Surface ozone exposures measured in Finland. *Atmos. Env.* **28**(1)103-114.

Leppäjärvi, R. (ed.), 1987. Hydrological Yearbook 1981-1983. Publications of the Water Research Institute Finland 66, 238 pp.

Lien, L., G.G. Raddum and A. Fjellheim, 1992. Critical loads of acidity to freshwaters — fish and invertebrates. NIVA Rep. 0-89185, Norwegian Institute for Water Research. Oslo, Norway.

Lindfors, V., T. Laurila and H. Hakola, 1995. A model study of photochemical oxidant formation in the Finnish environmental conditions. In: P. Anttila, J. Kämäri and M. Tolvanen (eds.) Proceedings of the 10th World Clean Air Congress, Vol. 2 Atmospheric Pollution, The Finnish Air Pollution Prevention Society.

Olsson, M., K. Rosén and P.A. Melkerud, 1993. Regional modelling of base cation losses from Swedish forest soils due to whole-tree harvesting. *Appl. Geochemistry, Suppl. Iss.* **2**:189-194.

Posch, M., J.-P. Hettelingh, H. Sverdrup, K. Bull and W. de Vries, 1993. Guidelines for the computation and mapping of critical loads and exceedances of sulphur and nitrogen in Europe. In: R. Downing, J.-P. Hettelingh and P. de Smet (eds.) 1993. Calculation and mapping of critical loads in Europe: Status Report 1993. CCE/RIVM, Bilthoven.

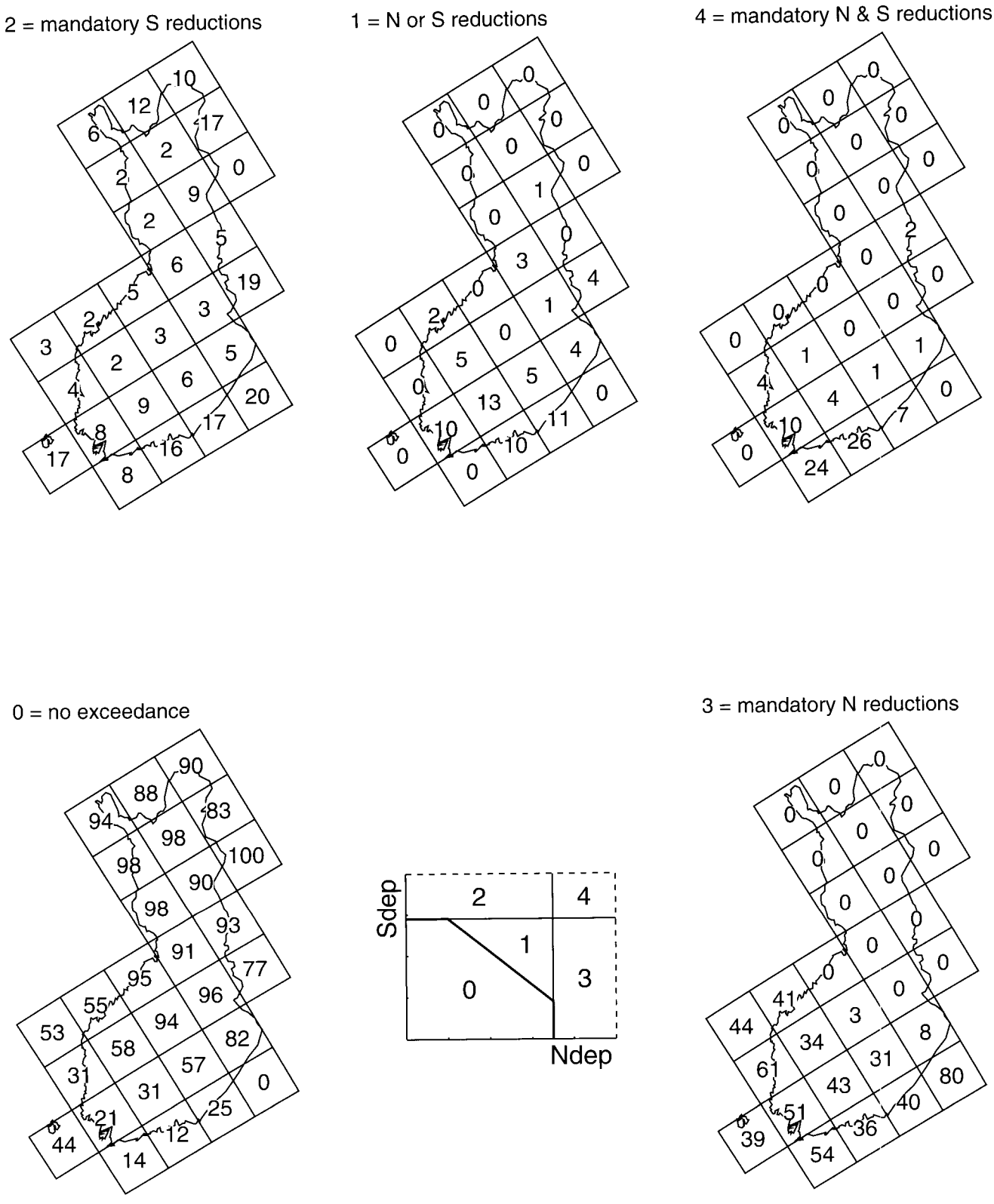


**Figure FI-1.** Total lake and forest soil area percentage in each predefined area in the S-N plane indicating mandatory or exchangeable sulfur and nitrogen reduction requirements in the year 1990.

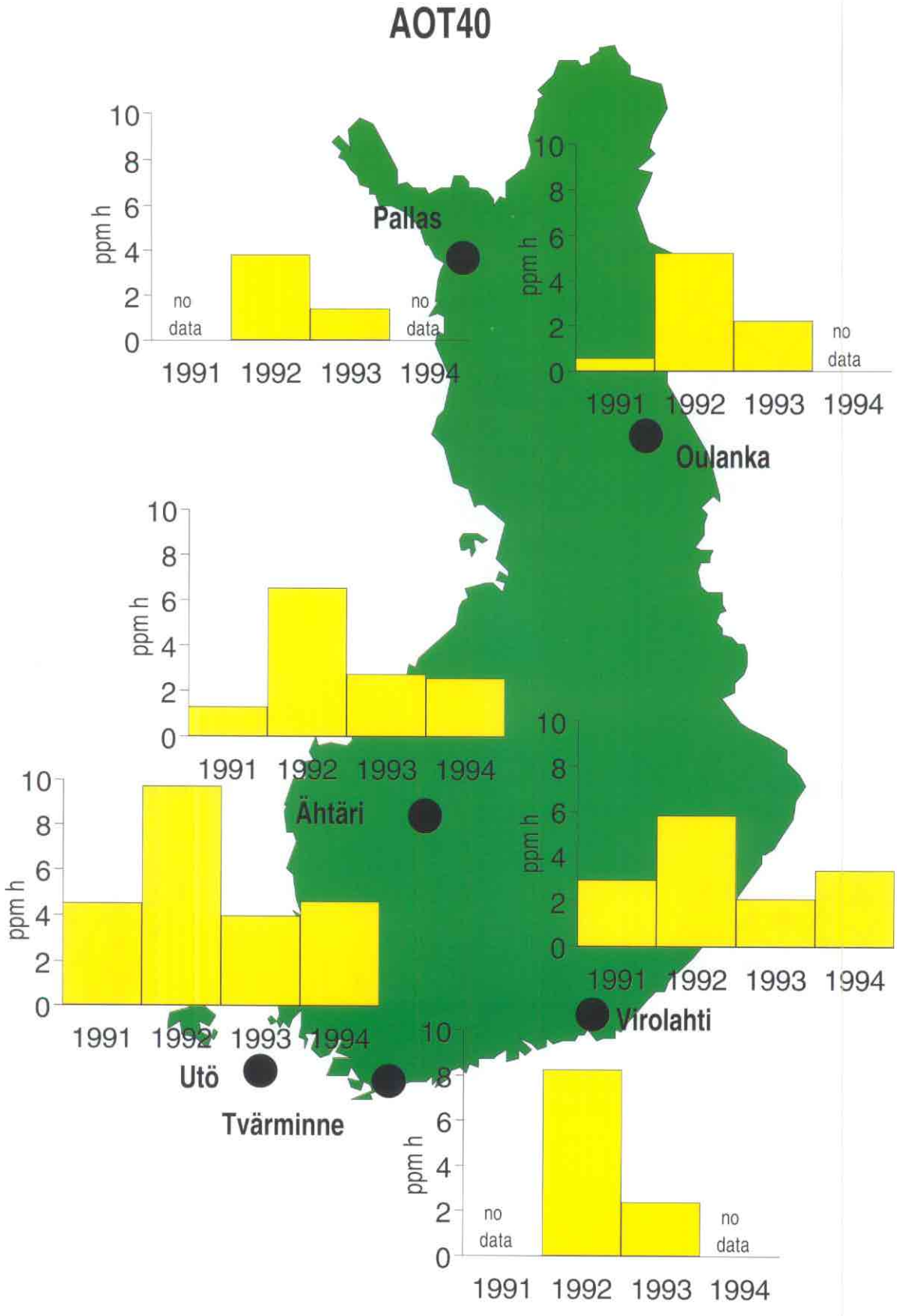


**Figure FI-2.** The measured yearly AOT40 (accumulated hourly exposure over threshold of 40 ppb) in ppm h for agricultural crops (spring wheat) for the years 1991-94.

# FRANCE

## National Focal Centers/Contacts:

Dr. Anne Probst
Mr. Jean-Paul Party
Centre de Géochimie de la Surface
CNRS
1, rue Blessig
F-67084 Strasbourg
tel: (33) 88 35 85 93 / (33) 88 31 32 36
fax: (33) 88 36 72 35 / (33) 88 31 32 36
email: aprobst@illite.u-strasbg.fr

Dr. Etienne Dambrine
Centre de Recherches Forestières
INRA / Champenoux
F-54280 Nancy
tel: (33) 83 39 40 71
fax: (33) 83 39 40 69
email: dambrine@nancy.inra.fr

## Collaborating Institutions/Contacts:

Dr. Dominique King
Ms. Anne-Laure Thomas
Service d'Etude des Sols-Carte pédologique de France
INRA / Ardon
F-45160 Orléans
tel: (33) 38 41 78 45
fax: (33) 38 41 78 69
email: dominique.king.@orleans.inra.fr

Dr. Jean-Marc Stussi
Centre de Recherches en Pétrographie et en Géologie
CNRS
15, rue Notre Dame des Pauvres
Vandœuvre
F-54500 Nancy
tel: (33) 83 59 42 48
fax: (33) 83 51 17 98

Ms. Pascale Ebner
Mr. Michel Robert
Ministère de l'Environnement
20, avenue de Ségur
F-75007 Paris
tel: (33) 1 42 19 17 29
fax: (33) 1 42 19 17 71

Mr. Denis Savanne
Mr. Christian Elichegaray
ADEME
Centre de Paris-Vanves
Service recherche impacts et milieux
27, rue Louis Vicat
F-75015 Paris
tel: (33) 1 47 65 22 25
fax: (33) 1 40 95 74 53

## Receptors mapped:

Surface waters, forest soils

The main steps of critical load mapping of acidity have been as follows:
1. The use of the data of reference catchments in the Vosges Massif to adapt the calculation methods. At present 3 catchments for soils and 38 concerning surface waters have been retained because of exhaustive data. For soils, the extrapolation of critical load mapping lays on a data base of granitoid bedrocks. For surface waters, the extrapolation has been done with pH and alkalinity data.
2. The definition of extrapolation laws for accurate critical load calculations with statistical and geographical test by GIS.
3. Finally, the mapping of critical load for the whole France has been based on the level 0 method and controlled by expert advices only for forest soils at present. This step is a necessary preliminary work to prepare the future calculations (Level 1 methods).

## Grid size:

In order to optimize the recent national data acquisitions, we used the grid system of the ICP Forests. All of Europe was divided into grids, each covering about 16 x 16 km. In France, the land area has been covered by about 2,200 grids (550 for forest soils).

## Data sources:

Regional monitoring data in the Vosges massif:
- 900 chemical analyses of silicate bedrocks,
- 800 pH and alkalinity analyses,

- 800 springwater analyses with 20/30-year record data, and
- a network of 11 measurement stations of atmospheric deposition.

National synthetic maps of:
- sensitive bedrocks and surface waters,
- sensitive superficial deposits,
- sensitive soils (desaturated, aluminum-enriched and hydromorphic), and
- sensitive land cover (forests and grasslands).

## Calculation method:

### A. Surface Waters:

We have calculated critical load values of acidity using RIVM model adapted for the Vosges. The steady-state water chemistry method (SSWC) has been applied to surface waters (Party *et al.* in press). Critical loads were calculated according to the following equations:

$$CL_1 = Q\,[BC]_0$$

where $[BC]_0$ is the original ante-pollution concentration of base cations ($mol_c\ ha^{-1}\ yr^{-1}$) in streamwaters.

$$[BC]_0 = [BC]_t - F\,([SO_4^{2-} + NO_3^-]_t - [SO_4^{2-} + NO_3]_0)$$

where F is the ratio between change in base cation concentration and change in strong acid anion concentration (Henriksen 1984). $[SO_4^{2-} + NO_3^-]_t$ is the present-day (sulfate + nitrate) concentration and $[SO_4^{2-} + NO_3^-]_0$ is the original (sulfate + nitrate) concentration specially calculated for the Vosges Massif conditions. $F = \sin(90 \cdot SBC^*/S)$ where $S$ = 300 meq liter $^{-1}$; $[SO_4^{2-} + NO_3^-]_0 = 0.15\ SBC^*$ (Probst *et al.* 1995, adapted from Henriksen *et al.* 1990).

### B. Forest soils:

The steady-state mass balance model (SSMB) was applied to soils (Party *et al.* 1994). Critical loads have been calculated according to the following equations:

$$CL(Ac_{act}) = BC_w + Q \cdot [H^+]_{crit} + R_{crit} \cdot (BC_d + BC_w - BC_u)$$

where $[H^+]_{crit}$ = critical hydrogen concentration in drainage water (= 40 meq liter$^{-1}$ which corresponds to pH = 4.4 adapted for the Vosges forest soils, Dambrine *et al.* 1993); $R_{crit}$ is the critical aluminum/calcium ratio (= 1.2 $mol_c\ mol_c^{-1}$ for the Vosges conditions, Dambrine *et al.* 1993).
$BC_w$ = weathering of base cations, $BC_d$ = base cation deposition, $BC_u$ = uptake of base cations ($mol_c\ ha^{-1}\ yr^{-1}$) and $Q$ = annual runoff ($m^3\ ha^{-1}\ yr^{-1}$).

## Results:

### A. Surface Waters:

In the Vosges massif, the chemical data from 38 catchments (70% with an alkalinity lower than 20 meq liter$^{-1}$) were used to calculate critical loads of acidity to surface waters. The values range between 0.2 and more than 2.0 Keq $ha^{-1}\ yr^{-1}$. For 70% of these streamwaters, critical load is below 1.2 Keq $ha^{-1}\ yr^{-1}$ and for about 50% below 0.5 Keq $ha^{-1}\ yr^{-1}$, whereas for 20% of these catchments, values are around 0.2 Keq $ha^{-1}\ yr^{-1}$ or less. According to these results, a first map has been drawn up for the Vosges massif (Figure FR-1, Party *et al.* in press).

### B. Forests soils:

In the Vosges massif, calculations have been applied to geopedological landscape units. The results are preliminary particularly because of the lack of precision on weathering and drainage data. Nevertheless, a second map has been tentatively drawn up (Figure FR-2). As shown in Figure FR-1, critical load values range between 0.2 and more than 2.0 Keq $ha^{-1}\ yr^{-1}$. The critical loads for soils present 5 classes:

1: < 0.5
2: 0.5-0.8
3: 0.8-1.2
4: 1.2-2.0
5: > 2.0 Keq $ha^{-1}\ yr^{-1}$.

For France, we have 3 potential pedogeochemical sensitivities (Figure FR-3) and 5 current sensitivities (Figure FR-4) mainly represented by the old mountains in the Eastern part of France and the Massif Central. This sensitivity scale to acidification successively combined in a grid-system:
- bedrock geochemistry and associated soils,
- surface water characteristics,
- glacial deposits and geomorphology
- vegetation influence.

## Discussion and perspectives:

### A. Surface waters:

In the Vosges massif, measured proton inputs to forests (taking into account atmospheric inputs and production by forest growth) vary from 1 Keq $ha^{-1}$ $yr^{-1}$ for the northwestern and eastern sides of the Vosges, 1.5 Keq $ha^{-1}$ $yr^{-1}$ in the southwestern part, and 2 Keq $ha^{-1}$ $yr^{-1}$ for the central part edge. Exceedance values show that catchments on sandstone covered by Scots pine in the north-western part of the Vosges have long ago certainly lost their buffering capacity.

Among the crucial environmental factors, the relationships between bedrock and surface water chemistry show that bedrock and soils characteristics alone cannot explain surface water chemistry. Superficial deposits have a significant effect, deposition like moraine or abrasion are essential parameters to be taken in account. Long-term data of springwater chemistry in the Vosges will be used to apply dynamic models.

For France, following investigations will be focused on evaluation of groundwater in relation to bedrock and superficial deposits, mineralogy and geochemistry followed by an exhaustive extrapolation.

### B. Forest soils:

Our work will now consider weathering data of about new small representative catchments (saprolite, weathered rock and soil layers) on sandstones and granitoids in the Vosges massif, Massif Central and on schists in the Ardennes mainly.

The French critical load program carried out by the ADEME gives preliminary values for the reference massif of the Vosges by the Level 1 method. For France, we are presently considering data of about 20 well-studied representative reference sites or catchments. Accurate regional values for soils and surface waters are necessary in order to calibrate the Level 1 method. Finally, we will apply dynamic models (Level 2 methods) already in use in Europe.

## Note:

Harmonized maps for critical loads of acidity and exceedance to surface waters and forest soils are in progress in France. New maps for nitrogen will also be computerized.

## References:


Dambrine E., A. Probst, and J.P. Party, 1993. Détermination et cartographie des charges critiques de polluants atmosphériques pour les écosystèmes naturels, en particulier forestiers. *Pollution atmosphérique*, N° spécial "Charges critiques", pp. 21-28.

Fevrier, C., 1995. Analyse temporelle de l'évolution de quelques paramètres chimiques des sources d'eau potable du Massif Vosgien. Application au département des Vosges. Mémoire de maitrise de Géologie. ULP Strasbourg, 25 pp.

Landmann G. and M. Bonneau, 1995. Forest decline and atmospheric deposition effects in the French mountains. In: G. Landmann and M. Bonneau (eds.), Springer Verlag, New York, 461 pp.

Massabuau, J.C., A. Probst, and F. Guerold, 1995. Critical loads of acidity to streamwaters in the Vosges mountains: biological criteria. In: Forest decline and atmospheric deposition effects in the French mountains. G. Landmann, M. Bonneau (eds.), Springer Verlag, New York, pp. 203-225.

Party, J.P. and A. Probst, 1995. Calcul et cartographie des charges critiques en France. Rapport ADEME d'avancement des travaux et prospective. Période 1992-1994, 16 pp.

Party, J.P., A. Probst, and E. Dambrine, 1993. Détermination et cartographie des charges critiques en polluants atmosphériques dans les Vosges. Rapport scientifique ADEME, année 1992, 66 pp. + annexes.

Party, J.P., A. Probst, E. Dambrine, and A. Thomas, 1994. Détermination et cartographie des charges critiques en polluants atmosphériques dans les Vosges. Rapport scientifique ADEME, année 1993, 51 pp.

Party, J.P., A. Probst, E. Dambrine, and A. Thomas, 1995. Critical loads of acidity to surface water in the Vosges massif (Northeast of France). *Water Air Soil Pollut.* (in press).

Pedro, G., and S. Sherer, 1974. Essai d'interprétation géochimique de la carte pédologique de France. Caractérisation et répartition des principaux types de milieux pédogéochimiques. *Ann. Agro.* 25(1):25-49.

Probst, A., F. Lelong D. Viville, P. Durand, B. Ambroise, and B. Fritz, 1995. Comparative hydrochemical behavior and element budgets of the Aubure (Vosges massif) and Mont Lozère (Massif Central) spruce forested catchments. In: Forest decline and atmospheric deposition effects in the French mountains. G. Landmann, M. Bonneau (eds), Springer Verlag, New York, pp. 203-225.

Probst, A., J.C. Massabuau, J.L. Probst, and B. Fritz, 1990. Acidification des eaux de surface sous l'influence des précipitations acides: rôle de la végétation et du substratum, conséquences pour les populations de truites. Le cas des ruisseaux des Vosges. *CR Acad. Sci. Paris*, 311(II)405-411.

Probst, A., J.L. Probst, J.C. Massabuau, and B. Fritz, 1995. Surface water acidification in the Vosges mountains: relation to bedrock and vegetation cover. In: Forest decline and atmospheric deposition effects in the French mountains. G. Landmann, M. Bonneau (eds.), Springer Verlag, New York, pp. 371-386.

SCEES-INRA, 1989. Grand Atlas de la France Rurale, Ed. De Monza, 510 pp.

Stussi, J.M., 1995. Cartographie de sensibilité à l'acidification des roches mères plutoniques des écosystèmes forestiers des Vosges. CRPG Nancy, 33 pp. + annexes.

Thomas, A.L., 1994. Analyse spatiale de la sensibilité des écosystèmes vosgiens à l'acidification. Pour une cartographie des "charges critiques" de polluants atmosphériques dans les

Vosges. DEA Univ. Paris I-Paris IV-Museum d'Histoire Naturelle-ENGREF Nancy, 40 pp.

Troadec, M., 1995. Analyse temporelle de l'évolution de quelques paramètres chimiques des sources d'eau potable du Massif Vosgien. Application aux départements de Moselle et de Meurthe et Moselle. Mémoire de maitrise de Géologie. ULP Strasbourg, 25 pp.

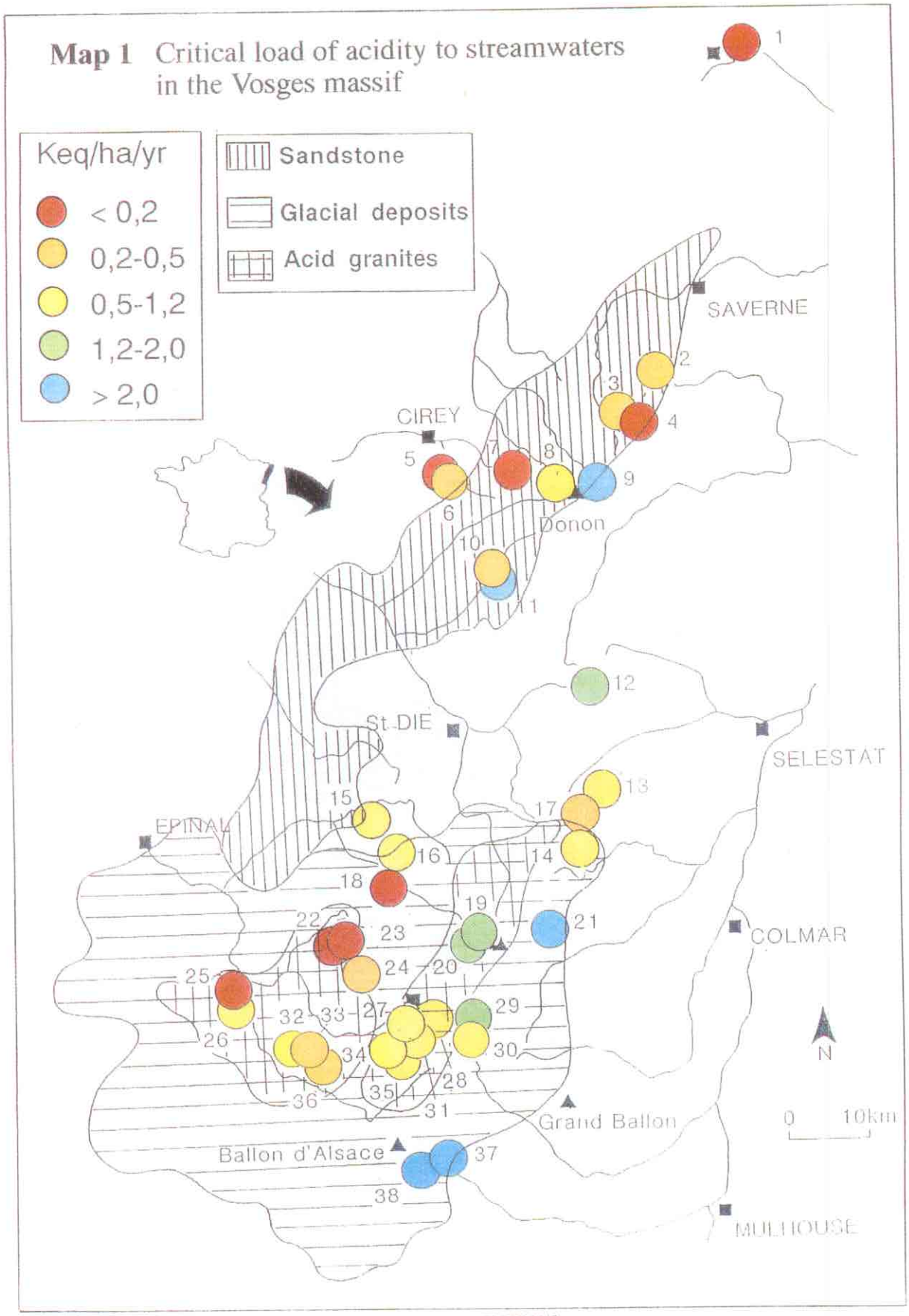


**Figure FR-1.** Critical load of acidity to streamwater and sensitive areas in the Vosges massif.

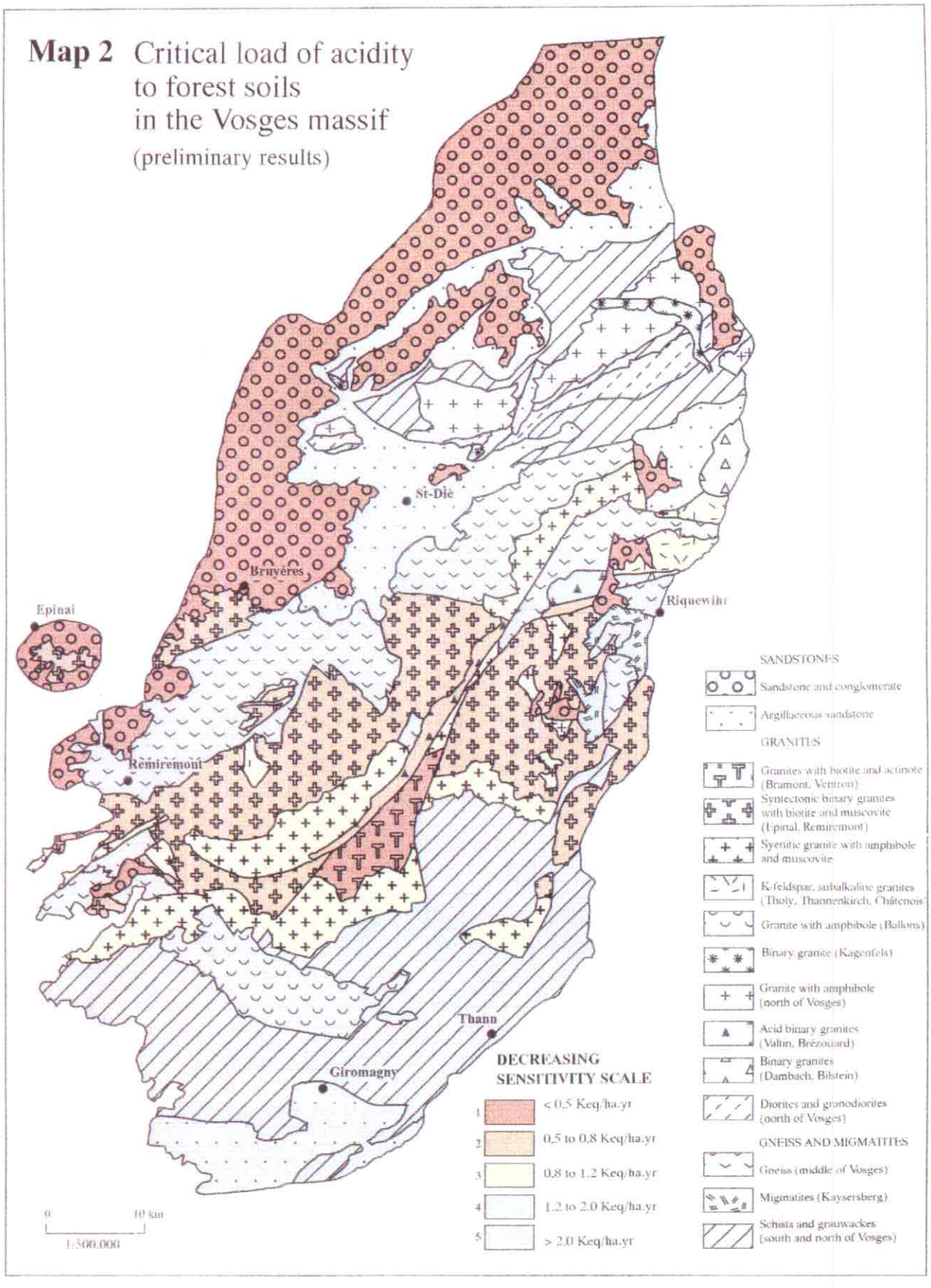


CNRS/CGS Strasbourg - INRA Nancy Cycles Biogéochimiques - INRA Orléans SES CPF, 1995

Financial support : Agence de l'Environnement et de la Maitrise de l'Energie ADEME - Ministère de l'Environnement

**Figure FR-2.** Critical load of acidity to forest soils in the Vosges massif (preliminary results).

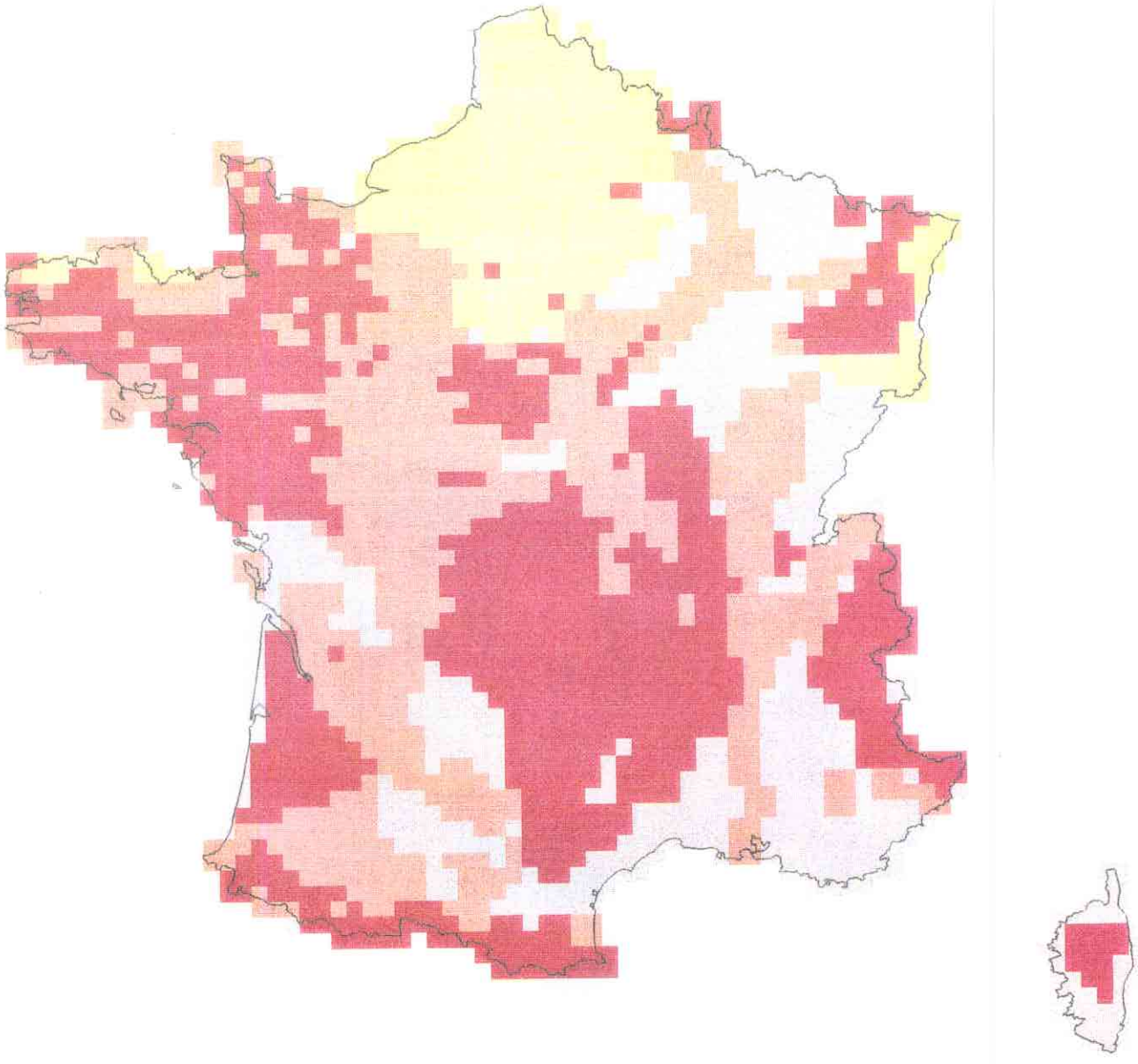


**Figure FR-3.** Potential sensitivity of the French regions to the acid atmospheric deposition.

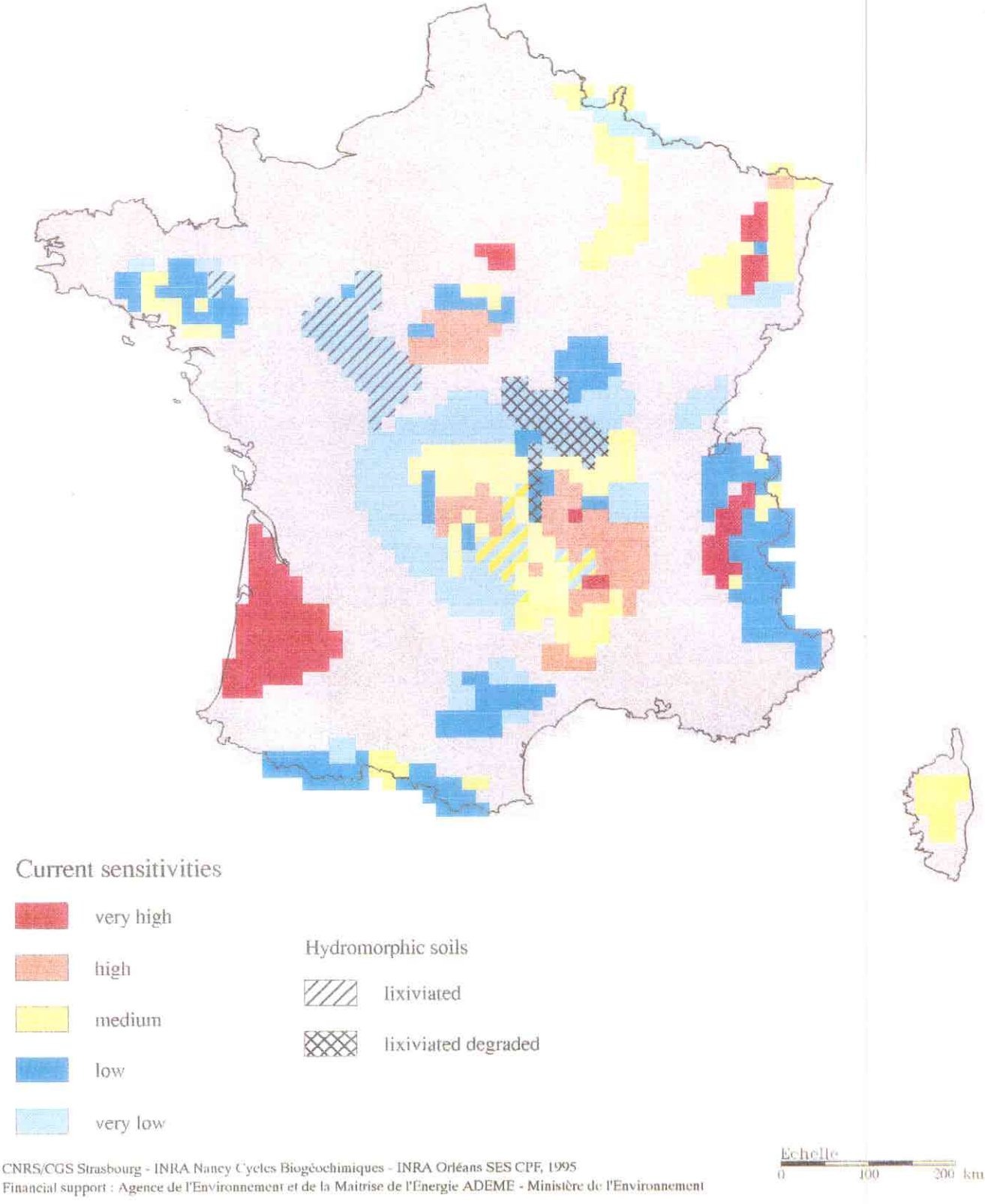


**Figure FR-4.** Current sensitivity of the French regions to the acid atmospheric deposition.

# GERMANY

## National Focal Center/Contact:

Dr. Heinz D. Gregor
Ms. Beate Werner
Federal Environmental Agency
P.O. Box 330022
Bismarckplatz 1
D-14191 Berlin
tel: 49-30- 231 45 846
fax: 49-30- 231 45 587

### Collaborating Institutions:

Dr. Hans-Dieter Nagel
ÖNU - Research Company for Ecology, Nature & Environmental Protection
Müncheberger Str. 1
D-15345 Prädikow
tel: 49-33436- 281
fax: 49-33436- 281

Dr. Gerhard Smiatek
Institute of Navigation
Stuttgart University
Keplerstr. 11
D-70174 Stuttgart
tel: 49-711- 121 3746
fax: 49-711- 121 3740

## List of national maps produced:

### Critical Loads of Nitrogen Maps:

Projection: Lambert Azimuthal
Grid size: 1 x 1 $km^2$
Grid origin: Forest Distribution Map (satellite image)

- Critical Net Uptake of Nitrogen ($N_u$), Figure DE-1 (left).
- Critical Immobilization of Nitrogen ($N_i$), Figure DE-1 (right).
- Critical Leaching of Nitrogen ($N_l$)
- Denitrification of Nitrogen ($N_{de}$)
- Critical Loads of Nutrient Nitrogen ($CL_N$), Figure DE-2.
- Exceedance of Critical Loads of Nutrient Nitrogen

### Critical Levels of Ozone Maps:

Projection: Lambert Azimuthal
Grid size: 0.25 degrees longitude by 0.125 degrees latitude

- Ozone AOT40 for Agricultural Crops, 1992 (based on Measurements at Rural Sites)
- Ozone AOT40 for Agricultural Crops, 1992 (based on Measurements at all Sites)
- Ozone AOT40 for Forests, 1992 (based on Measurements at Rural Sites)
- Ozone AOT40 for Forests, 1992 (based on Measurements at all Sites)
- Distribution of Critical Levels for Ozone in Germany
- Exceedance of Ozone AOT40 Thresholds for Forests and Crops, 1992 (based on Measurements at Rural Sites), Figure DE-3

### Deposition Maps:

Projection: Lambert Azimuthal
Grid size: 10 minutes longitude by 10 minutes latitude

- $SO_4$-, $NH_4$-, $NO_3$- and Base Cations Bulk Deposition 1986-90
- $SO_4$-, $NH_4$-, $NO_3$- and Base Cations Bulk Deposition 1989
- $SO_4$-, $NH_4$-, $NO_3$- and Base Cations Bulk Deposition 1990-92
- $SO_4$-, $NH_4$-, $NO_3$- and Base Cations Dry Deposition 1989 (RIVM-LLO)
- $SO_4$-, $NH_4$-, $NO_3$- and Base Cations Dry Deposition 1993 (RIVM-LLO)

## Calculation Methods:

### Nitrogen:

$N_u$: The critical nitrogen uptake was calculated using a matrix where the supply with base cations due to weathering ($BC_w$), the annual mean temperature ($T$) and the precipitation surplus ($PS$) are assigned to yield classes.

| $BC_w$ (eq $ha^{-1}$ $yr^{-1}$) | >500 | | | | | | 250-500 | | | | | | <250 | | | | | |
|---|---|---|---|---|---|---|---|---|---|---|---|---|---|---|---|---|---|---|
| T (°C) | >8 | 8 | 7 | 6 | 5 | <5 | >8 | 8 | 7 | 6 | 5 | <5 | >8 | 8 | 7 | 6 | 5 | <5 |
| PS (mm) | | | | | | | | | | | | | | | | | | |
| >=1000 | | | Ia | I | II | IV | | | I | II | III | IV | | | I | II | IV | V |
| 999-800 | | Ia | Ia | I | II | IV | | | I | II | III | IV | | | I | II | IV | V |
| 799-600 | Ia | Ia | I | I | II | IV | | I | I | II | III | IV | | I | II | II | IV | V |
| 599-400 | Ia | I | I | I | II | | | I | II | II | III | IV | | II | II | III | IV | |
| 399-200 | I | II | II | II | III | | II | II | III | III | III | | II | III | IV | IV | | |
| <200 | III | III | III | III | | | III | III | IV | IV | | | III | IV | V | V | | |

For coniferous and deciduous forests every yield class is represented by a nitrogen uptake value within the range from 2 to 10 kg N $ha^{-1}$ $yr^{-1}$ (coniferous)
or 3.5 to 15 kg N $ha^{-1}$ $yr^{-1}$ (deciduous).

| Nitrogen Uptake (kg N $ha^{-1}$ $yr^{-1}$) | | | | | |
|---|---|---|---|---|---|
| | deciduous | coniferous | | deciduous | coniferous |
| Ia | 15 | 10 | III | 8 | 5 |
| I | 13.5 | 8.5 | IV | 7 | 4 |
| II | 11.5 | 6.5 | V | 3,5 | 2 |

Using this method most of the forest areas of Germany (about 80%) have critical nitrogen uptake values between 4 and 10 kg N $ha^{-1}$ $yr^{-1}$. This can be accepted under long-term steady state conditions.

| Range (kg N $ha^{-1}$ $yr^{-1}$) | Forest area (%) |
|---|---|
| ≥ 2 to < 4 | 0.1 |
| ≥ 4 to < 6 | 25.9 |
| ≥ 6 to < 8 | 27.8 |
| ≥ 8 to < 10 | 23.7 |
| ≥ 10 to < 12 | 15.2 |
| ≥ 12 | 7.3 |
| | 100.0 |

$N_i$: The long-term natural immobilisation of nitrogen was estimated to be in the range of 1 kg to 5 kg N $ha^{-1}$ $yr^{-1}$. These values are assigned to the annual temperature at the forest sites.

| Temp. (oC) | Immobilization (kg N $ha^{-1}$ $yr^{-1}$) | Forest area (%) |
|---|---|---|
| < 5 | 5 | 1.1 |
| 5 | 4 | 5.0 |
| 6 | 3 | 15.3 |
| 7 | 2 | 32.8 |
| 8 | 1.5 | 40.5 |
| > 8 | 1 | 5.3 |
| | | 100.0 |

$N_i$: The critical leaching of nitrogen was computed in accordance to the CCE 1993 Status Report (Eq. 4.9) for all forest types (coniferous and deciduous) with $[N]_{crit}$ = 0.2 mg N/l (or 0.0143 eq/$m^3$). Nearly 80% of forest sites are calculated with a critical leaching below 1 kg N $ha^{-1}$ $yr^{-1}$.

| Nitrogen leaching (kg ha$^{-1}$ yr$^{-1}$) | Forest area (%) |
|---|---|
| 0 – 0.5 | 29.6 |
| 0.5 – 1 | 50.8 |
| 1 – 1.5 | 10.1 |
| 1.5 – 2 | 5.2 |
| 2 – 2.5 | 1.8 |
| 2.5 – 3 | 1.5 |
| 3 – 3.5 | 1.0 |
| | 100.0 |

$N_{de}$: Following the Equation 4.15 of the CCE 1993 Status Report, the constant denitrification fraction was used to estimate the denitrification of nitrogen which is below 1 kg N ha$^{-1}$ yr$^{-1}$ for most forest sites.

| Denitrification (kg ha$^{-1}$ yr$^{-1}$) | Forest area (%) |
|---|---|
| ≥ 0 to < 1 | 90.5 |
| ≥ 1 to < 2 | 6.1 |
| ≥ 2 to < 3 | 1.4 |
| ≥ 3 to < 4 | 0.7 |
| ≥ 4 to < 7 | 1.0 |
| ≥ 7 to < 10 | 0.2 |
| ≥ 10 | 0.1 |
| | 100.0 |

$CL_N$: Critical loads of nutrient nitrogen are results of the function:

$$CL(N) = N_{u(crit)} + N_{l(crit)} + \frac{N_{l(crit)}}{1 - f_{de}}$$

given as Equation 4.18 in the CCE 1993 Status Report. About 50% of the critical load values of forests are below 10 kg N ha$^{-1}$ yr$^{-1}$.

| Critical Loads of Nutrient Nitrogen (kg N ha$^{-1}$ yr$^{-1}$) | Forest area (%) |
|---|---|
| 0 – 5 | 0.0 |
| 5 – 10 | 52.1 |
| 10 – 15 | 36.4 |
| 15 – 20 | 11.2 |
| 20 – 30 | 0.3 |
| > 30 | 0.0 |
| | 100.0 |

***Ozone:***

AOT40 values were calculated as defined at the Critical Levels for Ozone UN-ECE workshop in Bern, 1993:

**Crops:** Accumulated sum over a threshold of 40 ppb (1 hour mean) during daylight hours with a radiation over 50 W/m$^2$ from May – July (Critical Level = 5300 ppb-h).

**Forests:** Accumulated sum over a threshold of 40 ppb (1 hour mean) from April – September for the whole days (Critical Level = 10000 ppb-h).

The first maps for AOT40 values for ozone have been produced for the year 1992. For this year, data from 191 stations were available.

The AOT40 value for a measurement site was calculated if less than 25% of the measurements were missing during the period of interest.

A constant time period (from 6 a.m. until 7 p.m.) for the calculation of AOT40 values for agricultural crops was used. Comparisons with calculations based on time periods with radiation values over 50 W/m$^2$ during the day showed that calculation errors due to this simplification can be neglected.

Measurements near the sources of precursors of ozone show limited spatial validity. The selection of the measurement sites included for the spatial interpolation was based on site descriptions (rural or urban). 51 monitoring stations have been described as not influenced by local emissions.

***Deposition:***

Deposition maps are based on interpolated bulk-measurement in open areas. Deposition in forest areas was calculated until recently as a multiple of the measurements in open areas. Starting in 1995 dry deposition will be calculated separately using RIVM-LLO's EDACS model and added to the interpolated wet deposition fields.

## Data Sources:

### Nitrogen:

| Main Variables | Equation of CCE Report or national approach | Calculated using additional variables |
|---|---|---|
| $N_u$ (kg N $ha^{-1}$ $yr^{-1}$) | national approach | $BC_W$, T, PS |
| $N_i$ (kg N $ha^{-1}$ $yr^{-1}$) | national approach | T |
| $N_l$ (kg N $ha^{-1}$ $yr^{-1}$) | 4.9 | PS, [N]crit = 0.2 mg N/l |
| $N_{de}$ (kg N $ha^{-1}$ $yr^{-1}$) | 4.15 | $f_{de}$ |

| Additional Variables | Source of Data |
|---|---|
| Precipitation Surplus, PS (mm) | Hydrological Atlas FRG<br>N-A-U Map GDR |
| Base Cations Weathering, $BC_W$ (eq $ha^{-1}$ $yr^{-1}$) | Soil Map of Germany unified from CORINE Soil Map and Atlas of GDR (Map 6) |
| Annual Mean Temperature, T (°C) | Hydrological Atlas FRG<br>Atlas GDR (Map 17) |
| Denitrification Factor, $f_{de}$ | Soil Map of Germany (FAO - Soil types), method: CCE 1993 Status Report |

### Ozone:

Ozone 1/2 hourly measurements and information on measurement site:

- Federal Environmental Agency
- States Environmental Agencies (Baden-Württemberg, Hesse and Thuringia)

Radiation:

- States Environmental Agencies (Baden-Württemberg, Hesse)

Deposition measurements and information on measurement sites:

- Federal Environmental Agency
- States Environmental Agencies
- Forest Research Centers

## Comments and conclusions:

The National Focal Centers of Germany, Poland and the Czech Republic have compared the methods, results and maps based on the national database and calculated for the European Critical Load Mapping program. The differences in the critical load values computed by different NFCs for grid cells covering common borders was discussed, and data and experiences were exchanged to harmonize the values.

In Germany the method for computing critical loads for acidity (modified simple mass balance) was slightly changed. For all soils with base saturation above 20% the critical load of acidity is determined by the base cation weathering only.

Further research concerning mapping of AOT40 values of ozone will concentrate on:

- improving the interpolation technique, i.e. by including information on topography

• selecting the monitoring stations not influenced by local emissions, i.e. by analysing the NO and $NO_2$ concentrations.

A second main issue in future work will be the improvement of national deposition load maps. In cooperation with RIVM the deposition of $SO_4$, $NH_4$, $NO_3$ and base cations in forest areas will be calculated by adding measurement-based wet deposition in open areas and estimated, land cover-dependent dry deposition. Dry deposition estimations are based on model calculations including concentration values and dry deposition velocity fields.

## *References:*


Köble, R., *et al.*, 1993. Kartierung der Critical Loads & Levels in der Bundesrepublik Deutschland. Abschlußbericht zum Forschungsvorhaben FE 108 02 080 "Erfassung immissionsempfindlicher Biotope in der Bundesrepublik Deutschland und anderen ECE-Ländern" im Auftrag des Umweltbundesamtes, 183 pp.

Nagel, H.-D., G. Smiatek and B. Werner, 1994. Das Konzept der kritischen Eintragsraten als Möglichkeit zur Bestimmung von Umweltbelastungs- und -qualitätskriterien - Critical Loads & Levels. Materialien zur Umweltforschung, herausgegeben vom Rat von Sachverständigen für Umweltfragen, Heft 20. Metzler-Poeschel Stuttgart. 75 pp.

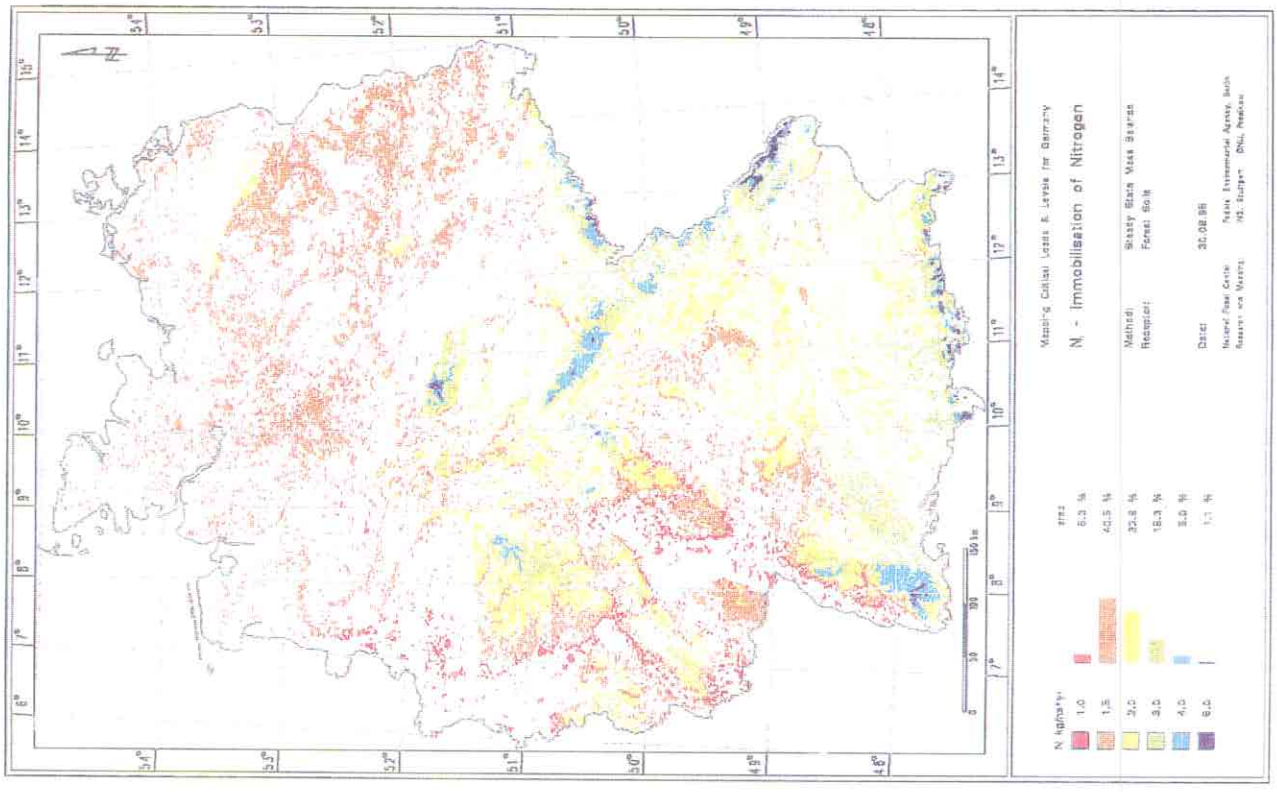


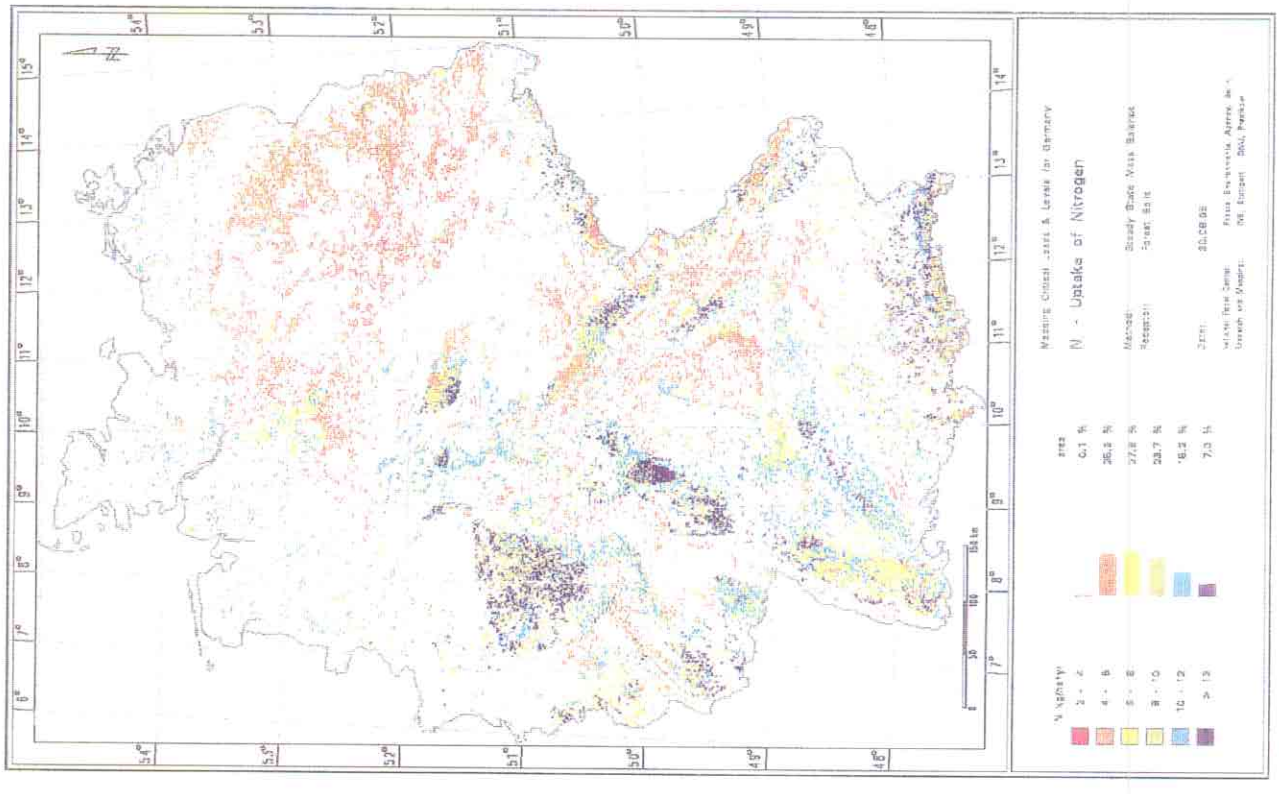


**Figure DE-1.** Critical nitrogen uptake (left) and critical immobilization (right) in forests (kg N $ha^{-1}$ $yr^{-1}$).

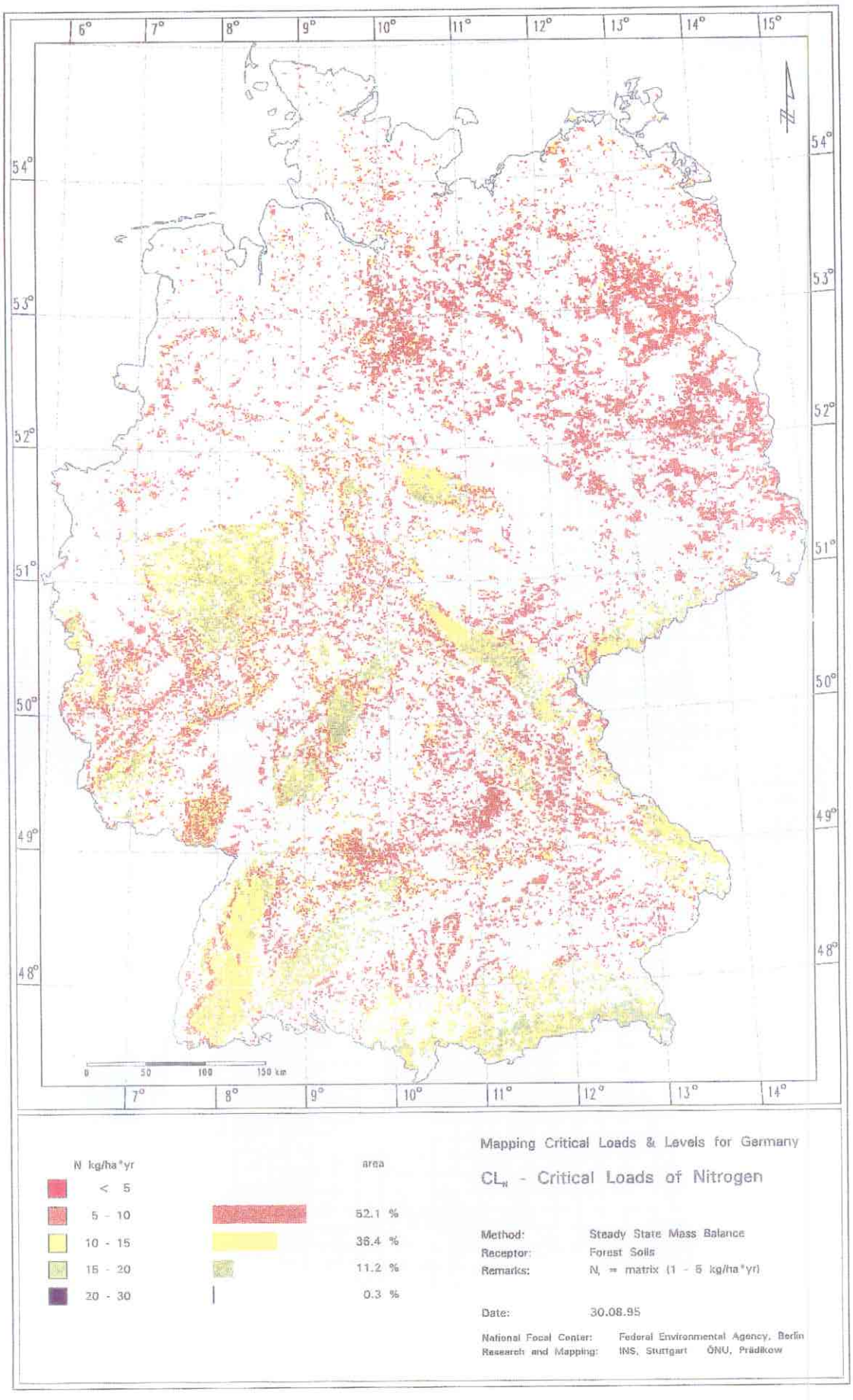


**Figure DE-2.** Critical loads of nutrient nitrogen for forest ecosystems (kg N $ha^{-1}$ $yr^{-1}$).

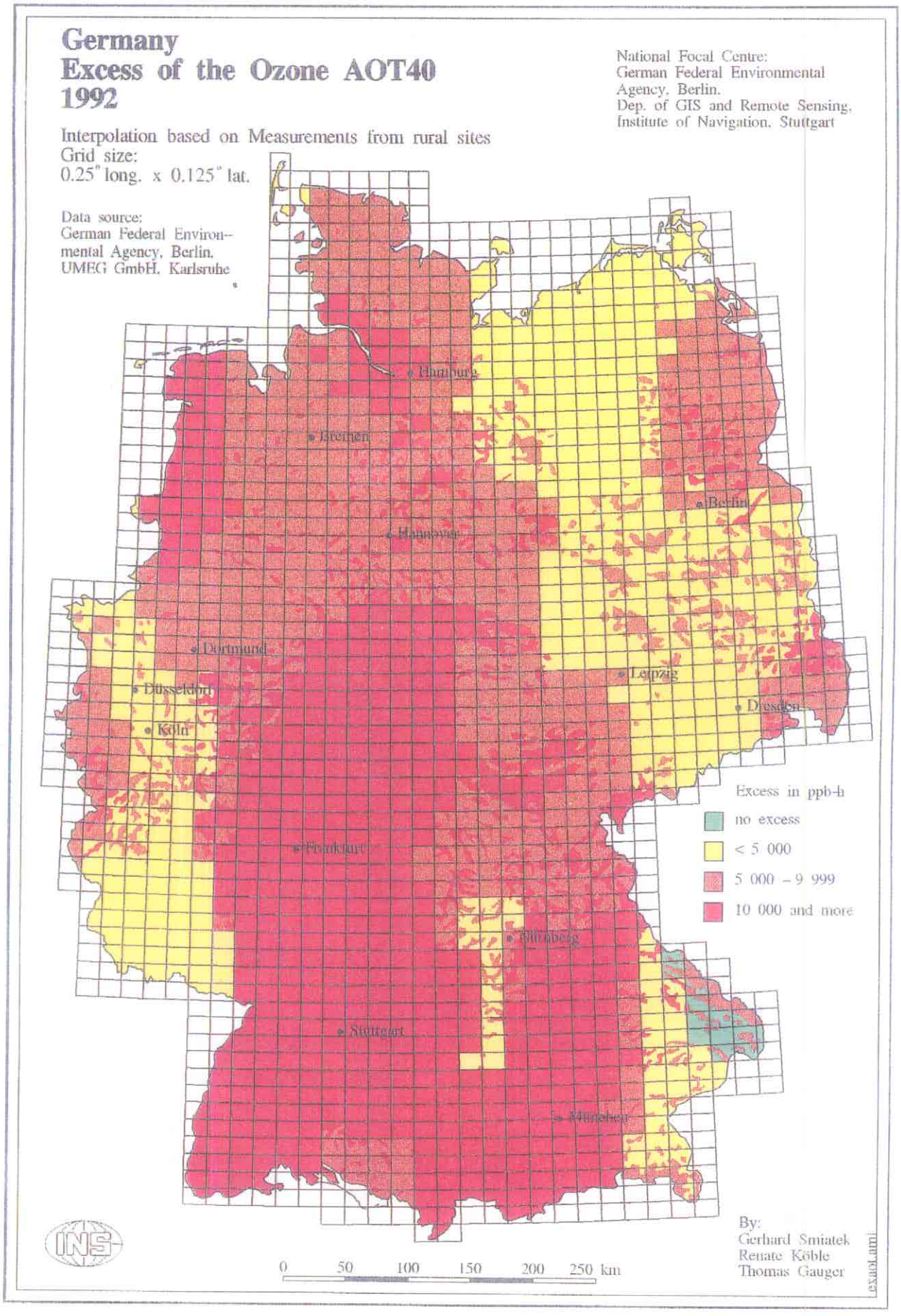


**Figure DE-3.** Exceedance of the ozone AOT40 values for forests and crops, 1992 (ppb-h).

# NETHERLANDS

## National Focal Center/Contact:

Ir. Bert Jan Hey
National Institute for Public Health and Environmental Protection (RIVM)
P.O Box 1
NL-3720 BA Bilthoven
tel: 31-30-2743832
fax: 31-30-2292897

## Collaborating Institutions/Contacts:

Dr. Wim de Vries
DLO Winand Staring Centre for Integrated Land, Soil and Water Research (SC-DLO)
P.O Box 125
NL- 6700 AC Wageningen
tel: 31-8370-74353
fax: 31-8370-24812
email: w.de.vries@sc.agro.nl

## National Maps Produced:

- Critical load of nutrient nitrogen for forest soils (SMB approach)
- Critical load of nitrogen for forest soils: minimum (SMB approach)
- Critical load of nitrogen for forest soils: maximum (SMB approach)
- Critical load of sulfur for forest soils: minimum (SMB approach)
- Critical load of sulfur for forest soils: maximum (SMB approach)

## Calculation Methods:

Critical loads for nitrogen as a nutrient, $CL_{nut}(N)$, and maximum and minimum values for the critical loads for N and S are calculated according to the CCE 1993 Status Report (cf. Posch *et al.* 1993, Eqs. 4.18, 4.35, 4.30, 4.29 and 4.38):

$$CL_{nut}(N) = N_{gu} + N_{im}(crit) + NO_{3,le}(crit) \,/\, (1\text{-}f_{de}) \quad (1)$$

$$CL_{max}(N) = N_{gu} + N_{im}(crit) + (BC^{*}_{td} + BC_{we} - BC_{gu} + Ac_{le(crit)}) \,/\, (1\text{-}f_{de}) \quad (2)$$

$$CL_{min}(N) = N_{gu} + N_{im}(crit) \quad (3)$$

$$CL_{max}(S) = BC^{*}_{td} + BC_{we} - BC_{gu} + Ac_{le(crit)} \quad (4)$$

$$CL_{min}(S) = BC^{*}_{td} + BC_{we} - BC_{gu} + Ac_{le(crit)} - NO_{3,le(crit)} \quad (5)$$

where:

| | | |
|---|---|---|
| $BC^{*}_{td}$ | = | the seasalt corrected total deposition flux of base cations |
| $BC_{we}$ | = | a base cation weathering flux |
| $BC_{gu}$, $N_{gu}$ | = | the growth uptake fluxes (net uptake needed for forest growth) of base cations and nitrogen respectively |
| $N_{im}(crit)$ | = | a critical long-term nitrogen immobilization flux |
| $Ac_{le}(crit)$ | = | a critical leaching flux of acidity |
| $NO_{3,le}(crit)$ | = | a critical $NO_3$ leaching flux |
| $fr_{de}$ | = | a denitrification fraction |

The critical acidity leaching flux, $Ac_{le}(crit)$, is calculated as the sum of Al leaching and H leaching. Three options are used for the calculation of the critical Al leaching flux, $Ac_{le(crit)}$, (De Vries, 1993):

1) a criterion for the Al concentration in the root zone:

$$Al_{le}(crit) = PS \cdot [Al](crit) \quad (6)$$

2) a criterion for the molar Al/Ca ratio in the root zone:

$$Al_{le}(crit) = RAlCa(crit) \cdot (Ca_{td} + Ca_{we} - Ca_{su}) \quad (7)$$

3) a negligible depletion of Al-hydroxides:

$$Al_{le}(crit) = 3 \cdot Ca_{we} + 0.6 \cdot Mg_{we} + 3 \cdot K_{we} + 3 \cdot Na_{we} \quad (8)$$

where $PS$ is the precipitation surplus leaving the rootzone ($m^3\ ha^{-1}\ yr^{-1}$), $[Al](crit)$ is a critical Al concentration (0.2 $mol_c\ m^{-3}$), $RAlCa(crit)$ is a critical equivalent Al/Ca ratio (1.5 $mol_c\ mol_c^{-1}$), $Ca_{we}$, $Mg_{we}$, $K_{we}$ and $Na_{we}$ are respectively the weathering rates of Ca, Mg, K and Na and the factors (3, 0.6, 3 and 3) refer to the stoichiometric equivalent ratio of Al to Ca, Mg, K and Na respectively. These stoichiometric ratios are based on Microcline (K), Albite (Na), Anorthite (Ca) and Chlorite (Mg).

The value of $Al_{le}(crit)$ used for the critical load calculation is the minimum value calculated by Eqs. 6, 7 and 8. The critical H leaching flux, $H_{le}(crit)$, is calculated as:

$$H_{le}(crit) = PS \cdot [H](crit) \quad (9)$$

where $[H](crit)$ is a critical H concentration, which is related to the critical Al concentration according to:

$$[H](crit) = ([Al](crit) / KAl_{ox})^{0.33} \quad (10)$$

where $KAl_{ox}$ is the Al hydroxide equilibrium constant ($10^8$ $mol^{-2}$ $l^2$). The value of the critical Al concentration is determined by the critical Al leaching flux divided by the water flux (precipitation surplus).

The critical nitrate leaching flux is calculated as:

$$NO_{3,le}(crit) = PS \cdot [NO_3](crit) \quad (11)$$

where $[NO_3](crit)$ is a critical $NO_3$ concentration (0.1 $mol_c$ $m^{-3}$)

## Data Sources:

Critical loads were calculated for all major combinations of tree species (12) and soil types (23) in gridcells of 10 km x 10 km because deposition estimates exist at this scale (Erisman). Tree species included were *Pinus sylvestris* (Scots pine, 38.2%); *Pinus nigra* (black pine, 5.9%); *Pseudotsuga menziesii* (douglas fir, 5.5%); *Picea abies* (Norway spruce, 5.1%); *Larix leptolepis* (Japanese larch, 5.7%); *Quercus robur* (oak, 17.4%); *Fagus sylvatica* (beech, 4.1%); *Populus spec* (poplar, 4.6%); *Salix spec* (willow, 2.4%); *Betula pendula* (birch, 7.4%); *Fraxinus excelsior* (ash, 1.9%) and *Alnus glutinosa* (black alder; 1.9%). Soil types were differentiated in 18 non-calcareous sandy soils, calcareous sandy soils, loess soils, non-calcareous clay soils, calcareous clay soils and peat soils on the basis of a recent 1:250,000 soil map of the Netherlands.

Information on the area (distribution) of each specific forest-soil combination in each gridcell containing forest was derived by overlaying the digitized 1:250,000 soil map, with a spatial resolution of 100 m x 100 m, and a data base with tree species information, with a spatial resolution of 500 x 500 m. The total number of forest soil combinations for all grids, ie, the total number of SMB calculations, equalled 17,102. The number of forest/soil combinations (calculations) in a grid varied between 1 and 125.

*Base cation deposition*: Bulk deposition data for base cations and Cl were derived from 22 monitoring stations for the period 1978-1985 using inverse distance interpolation to obtain values for each gridcell. Total deposition was calculated by multiplying the bulk (wet) deposition by a dry deposition factor.

*Weathering rates:* Base cation weathering rates are based on a correlation with total base cation contents. This correlation has been derived for nine non-calcareous sandy soils and six loess soils in the Netherlands. Weathering rates are based on information on base cation depletion rates in soil profiles, budget studies and on column and batch experiments, which have been conducted during five years on the most relevant non-calcareous sandy soils in the Netherlands. For clay and peat soils an indicative value has been derived from literature.

*Uptake:* The uptake of nitrogen, $N_{gu}$, and base cations, $BC_{gu}$, is calculated as the minimum of growth limited uptake and nutrient limited uptake. Growth limited uptake is calculated by multiplying the stem growth rate ($m^3$ $ha^{-1}$ $yr^{-1}$) with the stem density (kg $m^{-3}$) and the element contents in stems ($mol_c$ $kg^{-1}$). Nutrient limited (critical) base cation uptake is defined as that uptake which can be balanced by a long-term supply of base cations. This amount, which is referred to as the base cation uptake, $BC_u(crit)$, is calculated from mass balances for each base cation (Ca, Mg and K separately) by total deposition and weathering minus a minimum leaching of BC. We used a minimum leaching of 50 $mol_c$ $ha^{-1}$ $yr^{-1}$ for Ca and Mg and 0 $mol_c$ $ha^{-1}$ $yr^{-1}$ for K. From the critical base cation uptake, the corresponding critical N uptake ($N_u(crit)$) is calculated from the ratio between each cation and nitrogen in the biomass (cf Posch *et al.* 1993, Eqs. 4.7 and 4.8). The actual nitrogen uptake is now calculated as the minimum of growth-limited uptake and nutrient limited uptake. Forest growth estimates for all relevant combinations of forest and soil type and contents of the elements N, K, Ca and Mg in stems are based on a literature survey for all tree species included.

*Immobilization:* The critical N immobilization rate is calculated by accepting a change of 0.2% of nitrogen in organic matter in the upper soil layer (0–30 cm) during one rotation period (100 yr.). The pool of organic matter ($OM_{pool}$ in kg $ha^{-1}$) in this layer is calculated by multiplying the thickness of the soil layer (0.3 m), with the bulk density of the soil layer (kg $m^{-3}$) and the fraction of organic matter (-). Bulk density is calculated as a function of organic matter and clay content (cf. Van der Salm *et al.* 1993). Data for the contents of clay and organic matter are based on field surveys in 250 forest soils, i.e 150 sandy soils, 40 loess soils, 30 clay soils and 30 peat soils. N immobilization rates increased at higher organic matter contents and generally ranged between 100 and 350 $mol_c$ $ha^{-1}$ $yr^{-1}$. These values correspond well with a range between 2 and 5 kg $ha^{-1}$ $yr^{-1}$ mentioned by Posch *et al.* (1993).

*Denitrification fractions:* Denitrification fractions were derived for each soil type based on data in Breeuwsma *et al.* (1991) for agricultural soils. These data were corrected for the more acid circumstances in forest soils. Values thus derived varied between 0.1 for well-drained sandy soils to 0.8 for peat soils (cf. De Vries *et al.* 1994).

*Precipitation and evapotranspiration:* Precipitation estimates have been derived from 280 weather stations in The Netherlands, using interpolation techniques to obtain values for each grid. Interception fractions, relating interception to precipitation, have been derived from literature data for all tree species considered. Data for evaporation and transpiration have been calculated for all combinations of tree species and soil types with a separate hydrological model (cf. Van der Salm *et al.* 1993).

## Maps:

In Figures NL-1 through NL-3, maps are given of the 5 percentile, mean, median and 95 percentile of the following critical loads for forest soils in the Netherlands (for grid cells of 10 km x 10 km):

- nitrogen as a nutrient
- nitrogen as an acidifying pollutant (minimum value)
- sulfur as an acidifying pollutant (maximum value)

Maximum critical loads for nitrogen as an acidifying pollutant nearly always exceeded those for nitrogen as a nutrient, whereas minimum critical loads for sulfur are not really interesting. Therefore, both maps have not been presented.

Values vary as a function of soil type as shown in Table NL-1. Relatively low critical loads for both N as a nutrient and S were calculated for forests on non-calcareous sandy soils, which mainly occur in the central, eastern and southern parts of the country. Intermediate values for the critical loads for N and S were calculated for the loess soils in the southernmost part of the Netherlands and the clay soils in the western part of the country. High critical loads for N and low critical loads for S were calculated for the peat soils in the western part of the country (cf. Table NL-1). More information on the causes of the differences in given in De Vries *et al.* (1994).

**Table NL-1.** 5, 50 and 95 percentile values of critical loads ($mol_c$ $ha^{-1}$ $yr^{-1}$) for nitrogen and sulfur for Dutch forests on non-calcareous soils.

| | $CL_{nut}(N)$ | | | $CL_{min}(N)$ | | | $CL_{max}(S)$ | | |
|---|---|---|---|---|---|---|---|---|---|
| **Soil type** | **5%** | **50%** | **95%** | **5%** | **50%** | **95%** | **5%** | **50%** | **95%** |
| Sand | 594 | 841 | 1110 | 327 | 555 | 782 | 408 | 1109 | 1565 |
| Loess | 862 | 1113 | 1379 | 626 | 860 | 1146 | 556 | 1589 | 2438 |
| Clay | 767 | 1318 | 2060 | 318 | 689 | 1325 | 679 | 1528 | 2093 |
| Peat | 1251 | 1983 | 2709 | 626 | 911 | 1590 | 187 | 630 | 1171 |

## Comments and Conclusions:

Changes in the methods and data that were used to calculate critical loads of acidity and critical depositions of S in support of the second sulfur protocol are limited to the calculation of the uptake. Former calculations uptake of base cations were based on the growth-limited uptake approach only. BC uptake was thus calculated by multiplying the stem growth rate with the stem density and the contents of Ca, Mg and K in stems. In the present approach, the availability of these base cations by deposition and weathering is also accounted for (see above). The Netherlands also submitted critical loads for nitrogen for the former CCE report. Compared to these data, the present critical loads are changed due to:

- a different approach for the calculation of N uptake (see above).
- inclusion of N immobilization and denitrification as described in Eqs. 1, 2, and 3 and elaborated in the section on data sources. Both N fluxes were neglected in the former calculations.

Regarding the methodology used, it is important to note that the calculation may lead to negative values for the critical load of S (even the maximum value). This occurs when the uptake of Ca, Mg and K is higher than the total deposition and weathering of Ca, Mg, K and Na, corrected for seasalt input of chloride and sulfur, and the critical acidity leaching rate (cf Eq. 4). In the Netherlands, this occurred in 4 out of ca 17,000 calculations, i.e for poplar trees on peat soils. Note that the uptake calculation does not prevent this situation, since it only accounts for the availability of Ca, Mg and K, whereas Cl in the atmosphere may largely counteract the neutralizing impact of these substances in deposition.

Since the calculation of the critical loads presented in this report, various changes have been made to calculate critical loads for acidity and nitrogen for Dutch forests soils on a 1 km x 1 km scale. These changes include (cf. De Vries 1995):

- A critical Al concentration has no longer been used to calculate critical loads for accidity since laboratory experiments, correlative field research and model results do not unambiguously show a critical value in relation to root and/or shoot damage.
- A critical Al/Ca ratio has been changed into a critical Al/(Ca+Mg+K) ratio, since a recent review of results from laboratory experiments shows that this parameter gives the best correlation with root and/or shoot damage (Sverdrup and Warfvinge 1993). Based on this review, critical Al base cation ratios have no longer been applied uniformly, but are assigned as a function of tree species.
- A critical $NO_3$ concentration in leaching water related to the occurrence of vegetation changes has no longer been applied, since such changes may already occur at nearly natural low $NO_3$ leaching fluxes. Such a low flux has now been used instead in the calculation.
- The total deposition of base cations has been based on results of the DEADM model. In the present application, these values were based on bulk deposition of data for base cations from 14 monitoring stations during the period 1978–1985, multiplied by a so-called dry deposition factor.

Similar changes will be made in a next calculation of critical loads.

## References:


De Vries, W., 1993. Average critical loads for nitrogen and sulphur and its use in acidification abatement policy in the Netherlands. *Water Air Soil Pollut.* 68:399-434.

De Vries, W., J. Kros and J.C.H. Voogd, 1994. Assessment of critical loads and their exceedance on Dutch forests using a multi-layer steady state model. *Water Air Soil Pollut.* 76:407-448.

De Vries, W., 1995. Critical loads for acidity and nitrogen for Dutch forests on a 10 km x 10 km grid. DLO Winand Staring for Integrated Land Soil and Water Research, Rep.

Posch, M., J.P. Hettelingh, H.U. Sverdrup, K. Bull and W. de Vries, 1993. Guidelines for the computation and mapping of critical loads and exceedances of sulphur and nitrogen in Europe. In: R.J. Downing, J.P. Hettelingh, and P.A.M. de Smet (eds.), 1993. Calculation and mapping of critical loads in Europe. Coordination Center for Effects, Status Report 1993, Bilthoven, the Netherlands.

Salm, C. van der, J.C.H. Voogd and W. de Vries, 1993. SMB - a Simple Mass Balance model to calculate critical loads. Model description and user manual, DLO Winand Staring for Integrated Land Soil and Water Research, Techn. Doc. 11.

Sverdrup, H. and P. Warfvinge, 1993. The effects of soil acidification on the growth of trees, grass and herbs as expressed by the (Ca+Mg+K)/Al ratio. Lund University, Dept. Chemical Engineering II, Report 2:1993.

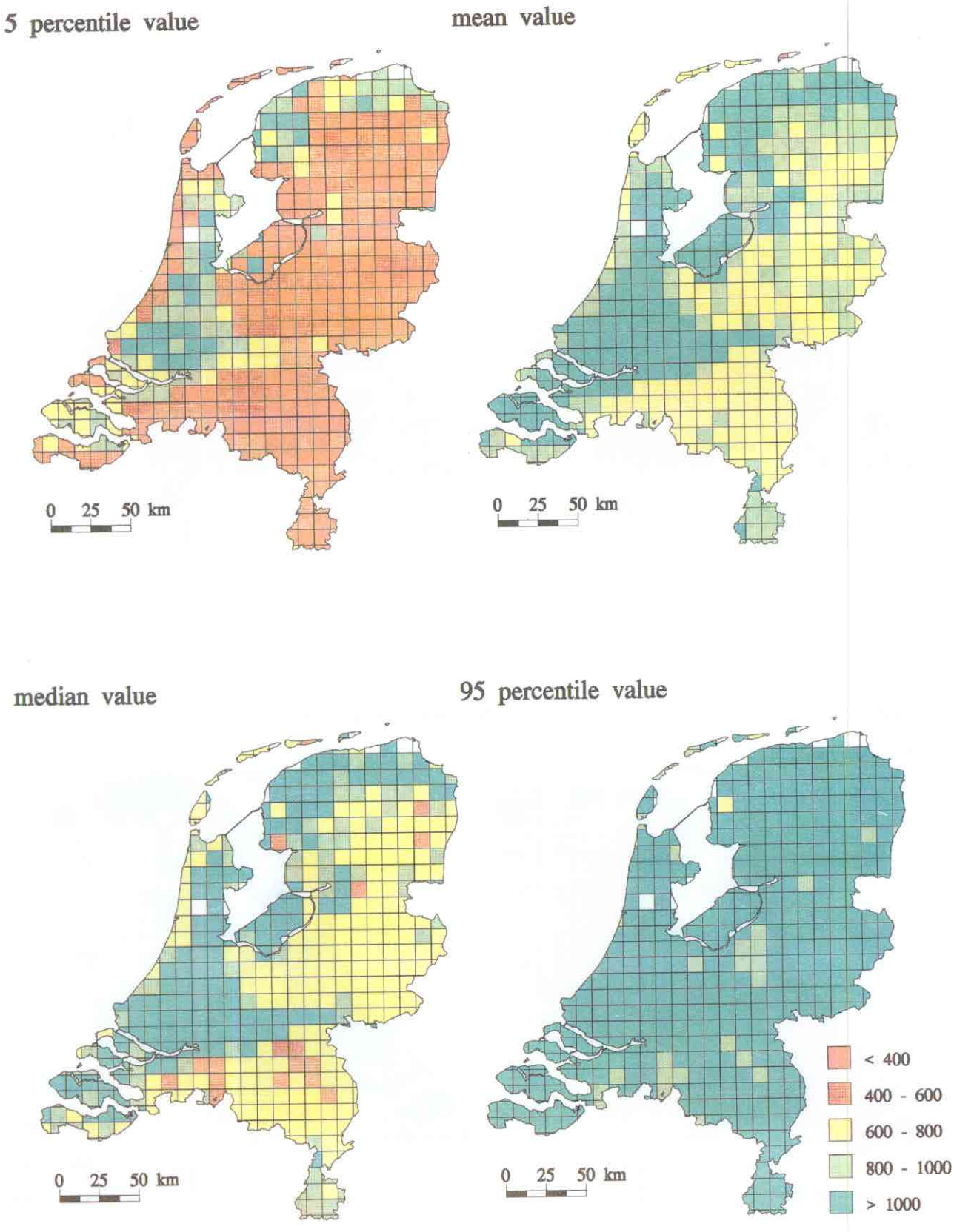


**Figure NL-1.** Critical load of nitrogen as a nutrient (5 percentile, mean, median and 95 percentile).

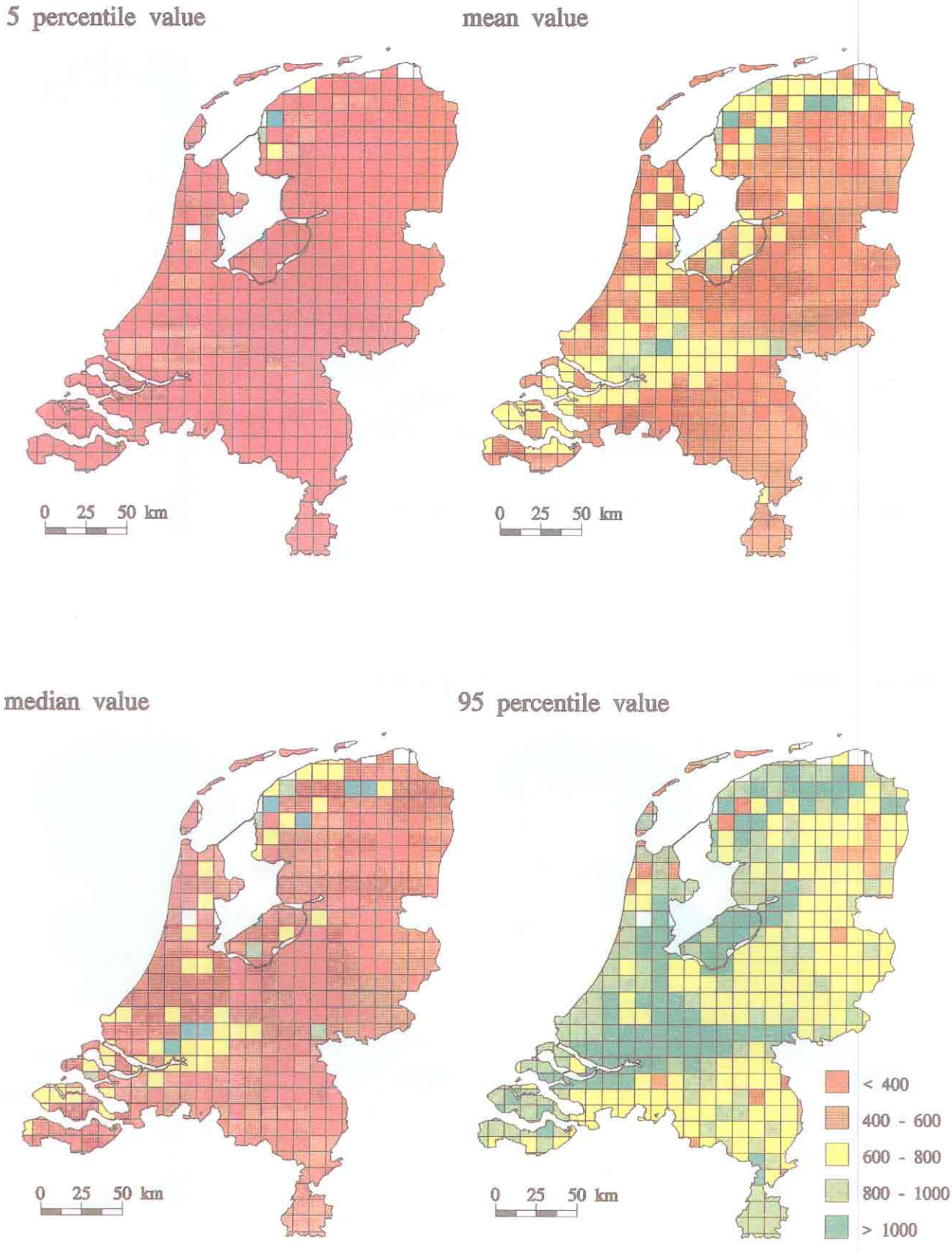


**Figure NL-2.** Critical load of nitrogen as an acidifying pollutant (minimum value) (5 percentile, mean, median and 95 percentile).

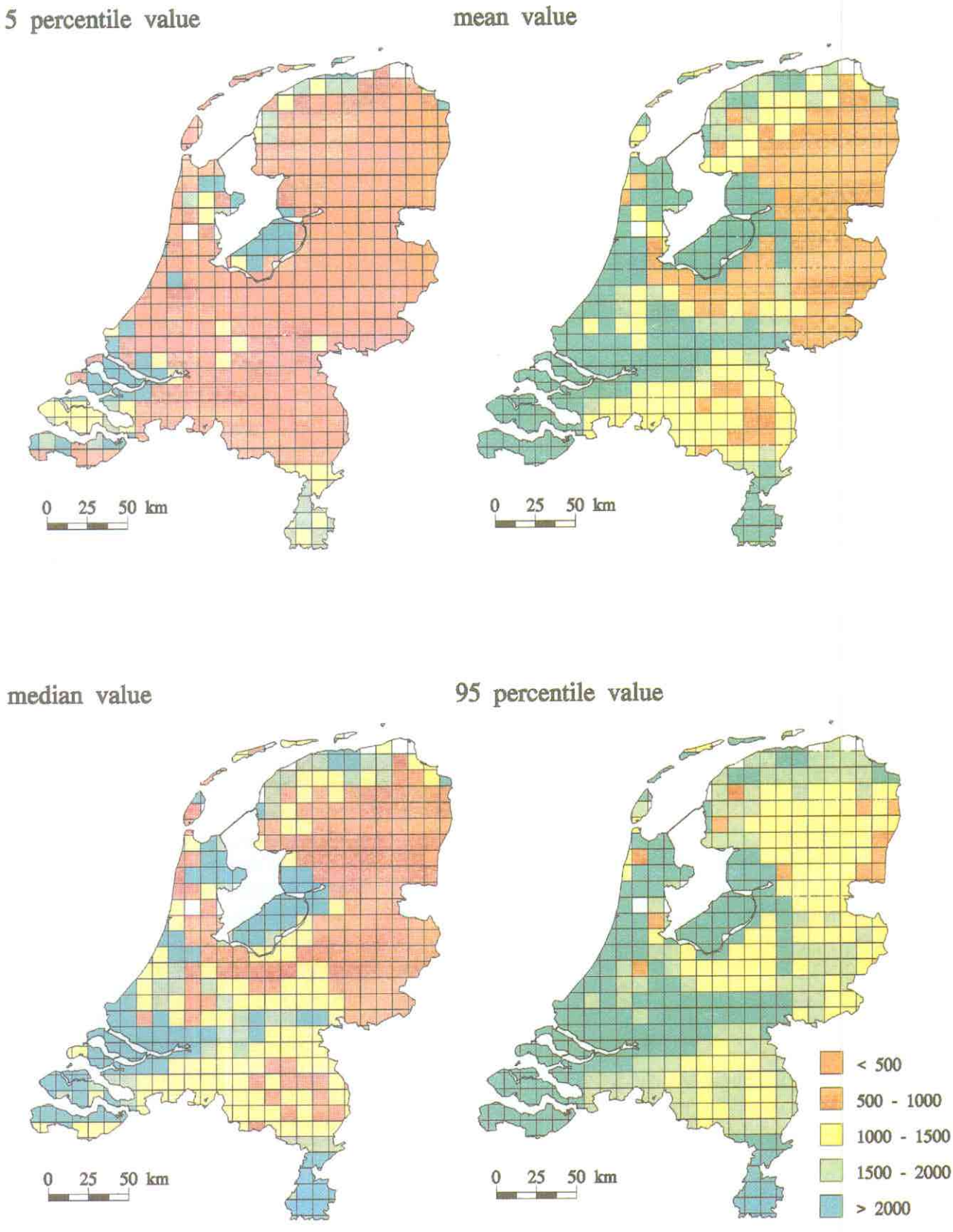


**Figure NL-3.** Critical load of sulfur as an acidifying pollutant (maximum value) (5 percentile, mean, median and 95 percentile).

# NORWAY

## National Focal Center/Contact:

Dr. Arne Henriksen
Norwegian Institute for Water Research
P.O. Box 173 Kjelsås
N-0411 Oslo
tel: +47 22 18 51 16
fax: +47 22 18 52 00
email: arne.henriksen@niva.no

## Collaborating Institutions/Contacts:

Mr. Kjetil Tørseth
Norwegian Institute for Air Research
P.O. Box 100
N-2007 Kjeller
tel: +47 63 898158
fax: +47 63 89 80 50
email: kjetil@nilu.no

Dr. Jan Mulder
Norwegian Forest Research Institute
Høgskolev. 12
N-1432 Ås
tel: +47 64 94 91 59
fax: +47 64 94 29 80
email: jan.mulder@nisk.nlh.no

Mr. Helge Styve
Norwegian Meteorological Institute
P.O. Box 43 Blindern
N-0313 Oslo
tel: +47 22 96 30 00
fax: +47 22 96 30 50
email: helge.styve@dnmi.no

## Receptors mapped:

Surface waters, forest soils, vegetation.

## A. Surface Waters

### Calculation Methods:

1. The Steady State Water Chemistry (SSWC) method was used to calculate critical loads of acidity and critical load exceedance for sulfur and for present exceedance for sulfur and nitrogen, using a variable ANClimit (Henriksen *et al.* 1995).

2. The critical load function (Posch *et al.* 1995) was used to calculate the required reduction requirements for S and N for each of the Norwegian grids (see below) at present deposition and according to current reduction plans (CRP) for sulfur in tyear 2010.

### Grid Size:

Each 1° longitude by 0.5° latitude grid was divided into 16 subgrids, each covering about 12 x 12 km in southern Norway, and with decreasing grid width at higher latitudes. The land area covered by each grid (2315) has been calculated.

### Data Sources:

National regional lake surveys and monitoring programs.

***Precipitation:*** A weighted average total deposition value for each NILU grid (a 3 by 3 subdivision of an EMEP grid) has been calculated from ambient air concentrations and wet deposition taking land use data (coverage of different receptors) into account (Tørseth and Semb, 1995). Weighted means for the period 1988-1992 were used. The deposition values for each of the surface water grids (see above) was estimated from the NILU-grid data base.

***Water:*** The chemistry of surface water within a subgrid was estimated by comparing available water chemistry data for lakes and rivers within each grid. The chemistry of the lake that was judged to be the most typical was chosen to represent the grid. If there were wide variations within a subgrid, the most sensitive area was selected, if it amounted to more than 25% of the grid's area. Sensitivity was evaluated on the basis of water chemistry, topography and bedrock geology. Geology was determined from the geological map of Norway (1:1,000,000) prepared by the Norwegian Geological Survey. Mean annual runoff data is from runoff maps prepared by the Norwegian Water and Energy Works. The database was revised in February 1995.

## B. Forest Soils

### Calculation Method:

The MAGIC (Model of Acidification of Groundwater in Catchments) dynamic model was used to produce maps for critical loads of acidity and exceedance for sulfur and nitrogen to forest soils (Cosby *et al.* 1985a, 1985b). The criterion is the Ca/Al molar ratio 1.0 in upper 60 cm soil solution.

### Grid Size:

The same grid system as for surface water was used. Of these, 706 grids are in productive forests both coniferous (spruce, pine) and deciduous (birch). The remaining grids cover unproductive forests and non-forested areas, for which critical loads for forest soils cannot be calculated.

### Data Sources:

National monitoring data.

### Precipitation:

The same data as for surface water was used.

### Soil:

The calculations are based on data from the NIJOS (Norwegian Institute of Land Inventory) forest monitoring plots on a 9 x 9 km grid and on the surface water data base referred to above. All input data are aggregated to the 12 x 12 km grid net. The NIJOS soils data are from areas in productive spruce and pine forests. A soil pit was objectively located within the representative vegetation type five meters from the plot center in the 9 x 9 km grid. The soil pit was dug to at least 50 cm where possible. Soil profile samples were taken and analyzed according to standard procedures.

## C. Critical Loads For Nutrient Nitrogen - Vegetation

Critical loads for nutrient nitrogen for vegetation has been estimated for Norway using empirically derived values for vegetation types. The vegetation types are taken from a 3 x 3 km network of forest sample plots as recorded by the National Forest Inventory. The same grid system as for water and soil (see above) was used. Only areas under the coniferous forest line are included. The most sensitive vegetation types are presumably ombrotrophic bogs and Calluna heath. A critical load value 5 kg N $ha^{-1}$ $yr^{-1}$ has been used for ombrotrophic bogs, a value of 15 kg N $ha^{-1}$ $yr^{-1}$ for Calluna heath and a value of 20 kg N $ha^{-1}$ $yr^{-1}$ for other forest types. The critical load map reflects the occurrence of Calluna heath on the west coast, whereas the bog areas occur throughout Norway. Alpine areas are not included in the data set and thus do not appear on the map (Tomter and Esser, 1995).

### Comments:

The SSWC method has been modified after the data used in developing the 1994 sulfur protocol. A variable ANClimit has been introduced instead of the fixed value of 20 μeq/l in the calculation formulae (Posch *et al.* 1995). Also, some of the data have been updated.

Exceedances of critical levels for Ozone has been mapped according to the recommendations from the UN-ECE workshop in Bern, 1993, by a working group supported by the Nordic Council of Ministers (NMR). Maps showing calculated AOT40 values for agricultural crops and for forests in Scandinavia are reported.

### References:


Cosby, B.J., G.M. Hornberger, J.N. Galloway, and R.F. Wright, 1985a. Modelling the effects of acid deposition: assessment of a lumped-parameter model of soil water and streamwater chemistry. *Water Resour. Res.* **21**:51-63.

Cosby, B.J., R.F. Wright, G.M. Hornberger, and J.N. Galloway, 1985b. Modelling the effects of acid deposition: estimation of long-term water quality responses in a small forested catchment. *Water Resour. Res.* **21**:1591-1601.

Henriksen, A., M. Posch, H. Hultberg, and L. Lien, 1995. Critical loads of acidity for surface waters - Can the $ANC_{limit}$ be considered variable? *Water Air Soil Pollut.* (in press).

Posch, M., J. Kämäri, A. Henriksen, M. Forsius and A. Wilander, 1995. Exceedance of critical loads for lakes in Finland, Norway and Sweden: Reduction requirements for acidifying nitrogen and sulfur deposition. Submitted to *Environ. Manage.*

Tomter, S.M. and J.M. Esser, 1995. Mapping critical loads for nitrogen, based on an empirical method. Naturens Tålegrenser, Rep. 70. (in Norwegian). National Forest Inventory (NIJOS), 1430 Ås, Norway.

Tørseth, K. and A. Semb, 1995. Sulphur and nitrogen deposition in Norway, status and trends. *Water Air Soil Pollut.* (in press).

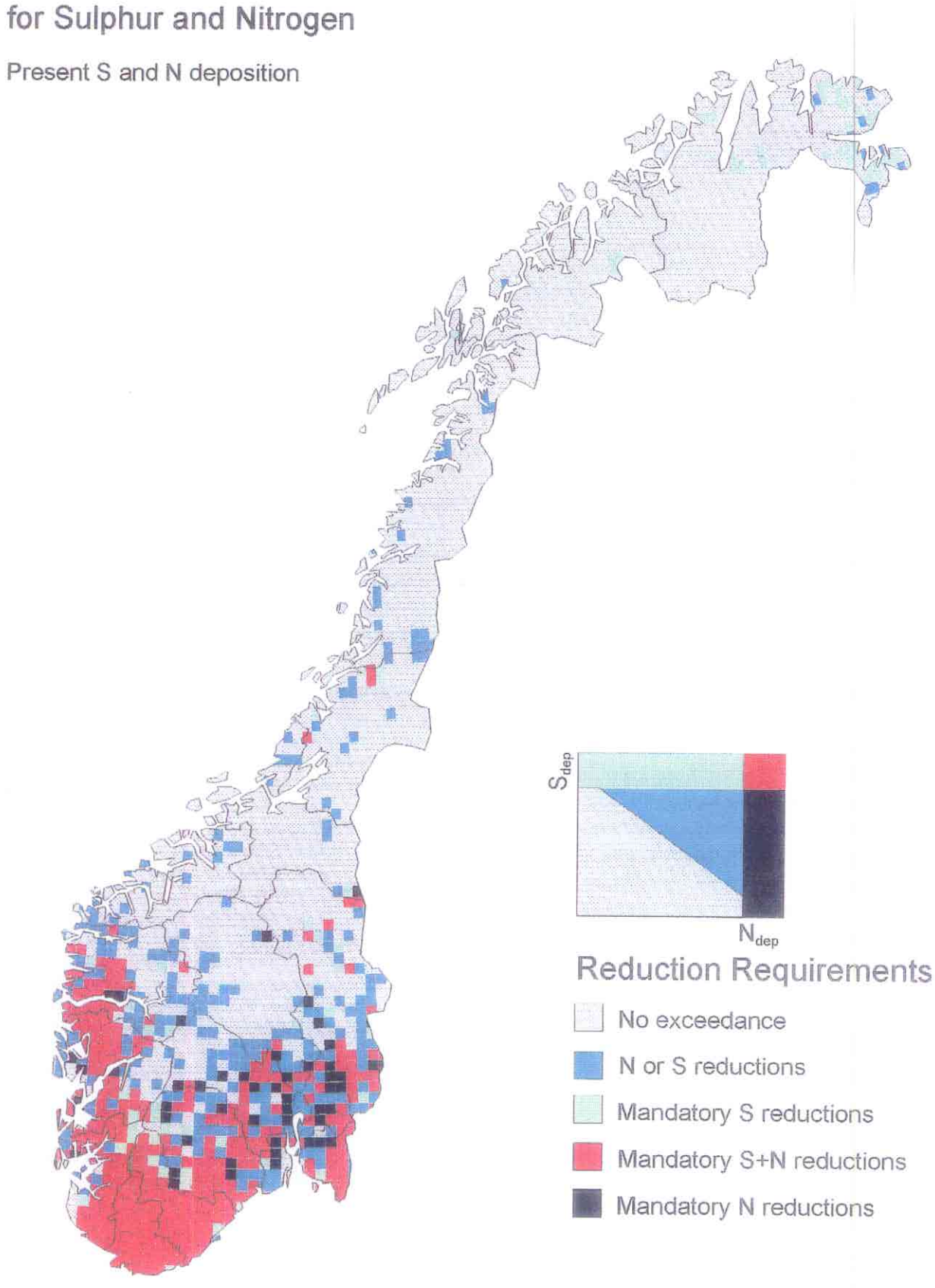


**Figure NO-1.** Critical load exceedance reduction requirements at present sulfur and nitrogen deposition using the critical load function.

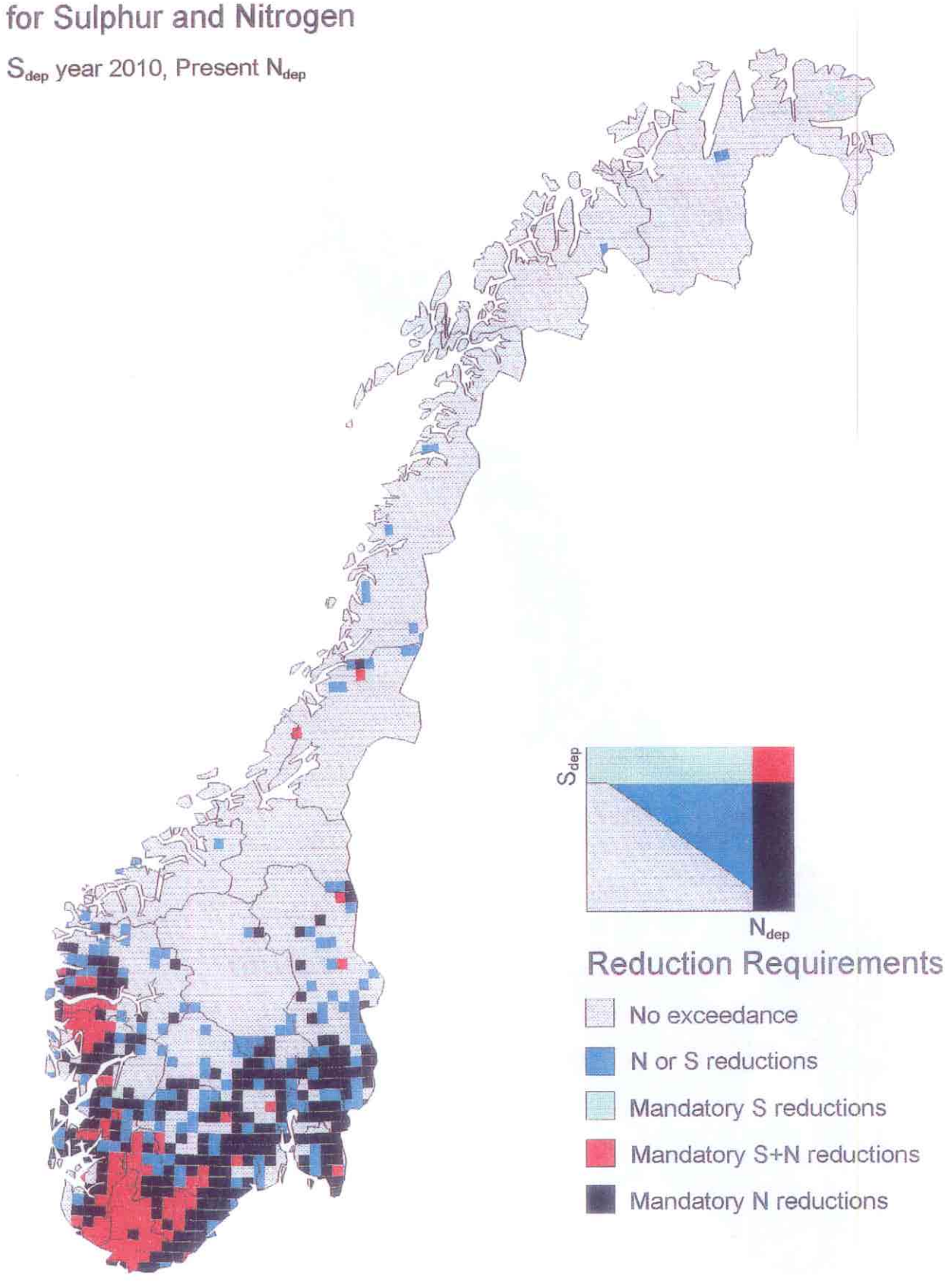


**Figure NO-2.** Critical load exceedance reduction requirements according to the Current Reduction Plans (CRP) emission scenario for 2010.

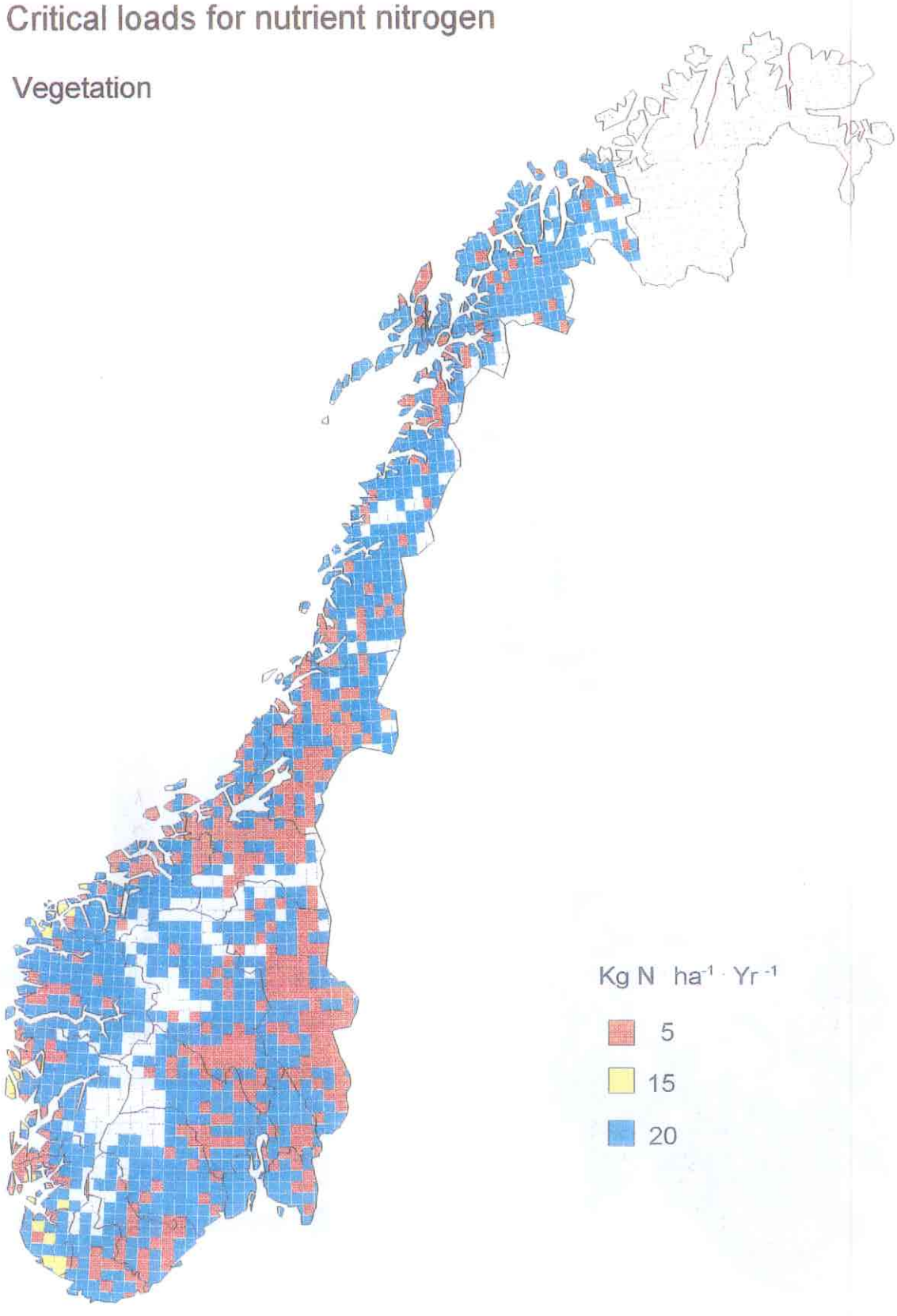


**Figure NO-3.** Critical loads for nutrient nitrogen, based on vegetation types.

# POLAND

## National Focal Center/Contact:

Dr. Wojciech Mill
Mr. Artur R. Wójcik
Ms. Dorota Rzychoń
Dr. Adam Worsztynowicz
Institute for Ecology of Industrial Areas
ul. Kossutha 6
40-832 Katowice
tel: +48-3-154.60.31
fax: +48-3-154.17.17
email: ietu@usctoux1.cto.us.edu.pl

## Collaborating Institutions/Contacts:

Forest Management and Geodesy Office
ul. Wawelska 52/54
Warsaw

Institute of Environmental Engineering
Warsaw University of Technology
ul. Nowowiejska 20
Warsaw

## List of National Maps Produced:

All maps have been produced for forest soils.

1. Poland. Critical loads of actual acidity
2. Poland. Critical loads of sulfur
3. Poland. Critical loads of acidifying nitrogen
4. Poland. Critical deposition of sulfur
5. Poland. Critical deposition of acidifying nitrogen
6. Poland. Exceedance of critical loads of actual acidity
7. Poland. Exceedance of critical loads of sulfur
8. Poland. Exceedance of critical loads of acidifying nitrogen
9. Poland. Critical loads of nutrient nitrogen
10. Poland. Exceedance of critical loads of nutrient nitrogen
11. Poland. Minimum critical load of sulfur
12. Poland. Minimum critical load of acidifying nitrogen
13. Poland. Maximum critical load of sulfur
14. Poland. Maximum critical load of acidifying nitrogen
15. Poland. Exceedance of critical deposition of sulfur
16. Poland. Exceedance of critical deposition of acidifying nitrogen

## Calculation Methods:

For calculation of all above listed parameters a Steady-State Mass Balance (SSMB) method, along with the procedure for calculation of critical loads for high-elevation areas, has been applied (Downing *et al.* 1993) (Sverdrup 1992). For calculation of nitrogen denitrification and critical loads of nutrient nitrogen the dynamic approach has been applied (Sverdrup and Ineson 1993).

### Grid Size:

Longitude/latitude 0.2° x 0.1° grids of nearly 10 x 10 km size; 930 receptor points covered by forests divided into coniferous and deciduous species.

## Data Sources:

Most of the input data used to determine the critical loads values were taken or generated from the national data sources as reported in Mill *et al.* (1992, 1993, 1994).

**Soil Data:** The dominating types of soil in particular grids were adopted on the basis of the data from the *Polish Soil Atlas 1:300,000* (1961). Forty types of predominant soils in Poland were applied for the calculations, and adequate values of base cation weathering were attributed to them.

**Meteorological Data:** The data concerning precipitation, runoff and average annual temperature were obtained from the *Hydrological Atlas of Poland* (1986) published by the Institute of Meteorology and Water Management for the years 1951-1975.

**Forest Data:** The data concerning the spatial location of forests, were based on the *Forest Map of Poland*, edited by the Forest Management and Geodesy Office. The data concerning resources, forest growth and age of trees were obtained from the data bank of the Forest Management Office. For calculation of critical loads, the chosen forestry areas those in which the percentage of forests in the grid surface was greater then twenty percent. Calculation has been made both for coniferous and deciduous forests.

**Uptake Data:** The updated (Madrzykowski *et al.* 1994) uptake data: $BC_u$, $N_u$, $N_i$, and $N_l$ were

determined on the basis of forest growth in particular grids and the contents of particular elements in steams and branches. On the basis of national data the rate of denitrification ($N_{de}$) and sulfur fraction ($S_f$) were calculated.

***Deposition Data:*** The data concerning sulfur and nitrogen deposition were taken from national data sources provided by Institute of Environmental Engineering of the Warsaw University of Technology (Abert *et al.* 1993). Deposition data for the years 1987 and 1990 as well as for the 5 year period (1987-1991) have been applied in calculations. The base cation deposition data were adopted from EMEP data provided by CCE-RIVM.

## Comments and Conclusions:

As a case study, in cooperation with the Norwegian Institute for Water Research (NIVA), Oslo, critical loads of acidity, sulfur and nitrogen for two selected lakes have been estimated (Rzychoń *et al.* 1994). The Steady-State Water Chemistry Method was applied. The study area, located in Tatra Mountains, is one of the most sensitive to acidification. However, because of being not representative to the rest of Polish water resources, critical loads for this small catchment were not the subject of mapping.

Due to some cross-border differences in critical loads between Poland, Czech Republic and Germany, on invitation of the German Federal Environmental Agency and the NFC, a trilateral workshop took place in Prädikow/Berlin, 7-11.05.1995 (Trilateral Workshop, 1995). In result of this workshop corrections to the nitrogen uptake rates data have been made by the Polish NFC, which significantly improved the correlation of the calculated critical loads in the cross-bordering grids.

For further national use of the critical loads concept, a new approach of mapping with a 1 x 1 km spatial resolution, based on the EMEP 50 x 50 km grid system, is under development.

## References:


Abert K., K. Budziński and K. Juda-Rezler, 1993. Regional scale air pollution models for Poland. (Paper accepted to publication in Ecological Engineering, The Journal of Ecotechnology).

Downing R.J., J.-P. Hettelingh and P.A.M. de Smet, 1993. Calculation and mapping of critical loads in Europe: Status Report 93, RIVM Rep. 259101003, Bilthoven, The Netherlands.

Hydrological Atlas of Poland, 1986. Instytut Meteorologii i Gospodarki Wodnej, Wydawnictwa Geologiczne, Warsaw.

Map of Polish Soils, 1961. Instytut Uprawy, Nawonia i Gleboznawstwa, Wydawnictwa Geologiczne. Warsaw.

Madrzykowski M., *et al.*, 1994. Catalog of the data on forest characteristics in Poland. Unpublished manuscript, Warsaw.

Mill W., D. Rzychoń, and A. Wójcik, 1992. Mapping critical loads for Poland: National Focal Center Report No.1, Institute for Ecology of Industrial Areas, Katowice, Poland.

Mill W., A. Wójcik A., and D. Rzychoń, 1993. Mapping critical loads for Poland: National Focal Center Report No.2, Institute for Ecology of Industrial Areas, Katowice, Poland.

Mill W., A. Wójcik, and D. Rzychoń, 1994. Mapping critical loads for Poland: National Focal Center Report No.3, Institute for Ecology of Industrial Areas, Katowice, Poland.

Rzychoń, D., A. Worsztynowicz A. and W. Mill, 1994. Evaluation of surface waters acidification resulting from acid deposition: National Focal Center Report No.3, Institute for Ecology of Industrial Areas, Katowice, Poland.

Sverdrup H. and P. Ineson P., 1993. Kinetics of denitrification in forest soils. Manuscript.

Sverdrup, H., 1992. Calculating critical loads in Alpine regions. Manuscript, Univ. Lund, Sweden.

Trilateral Workshop Report, OENU/UBA, Berlin, 1995.

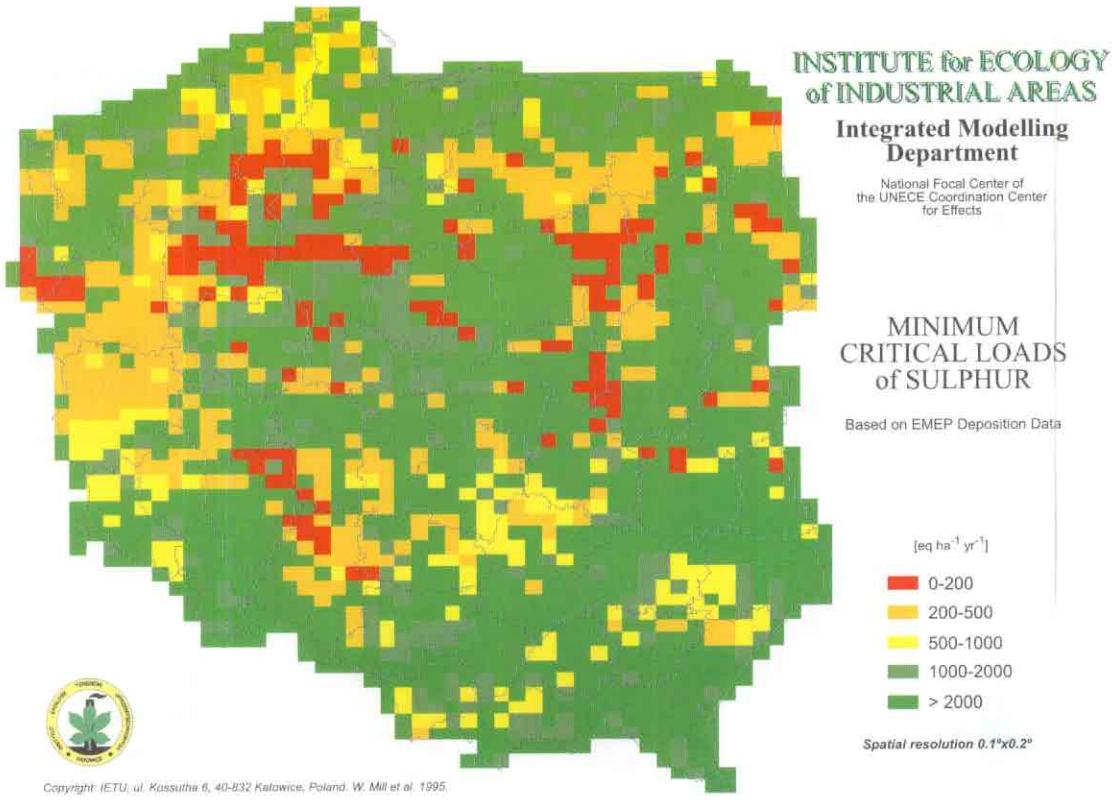


**Figure PL-1.** Minimum critical loads of sulfur.

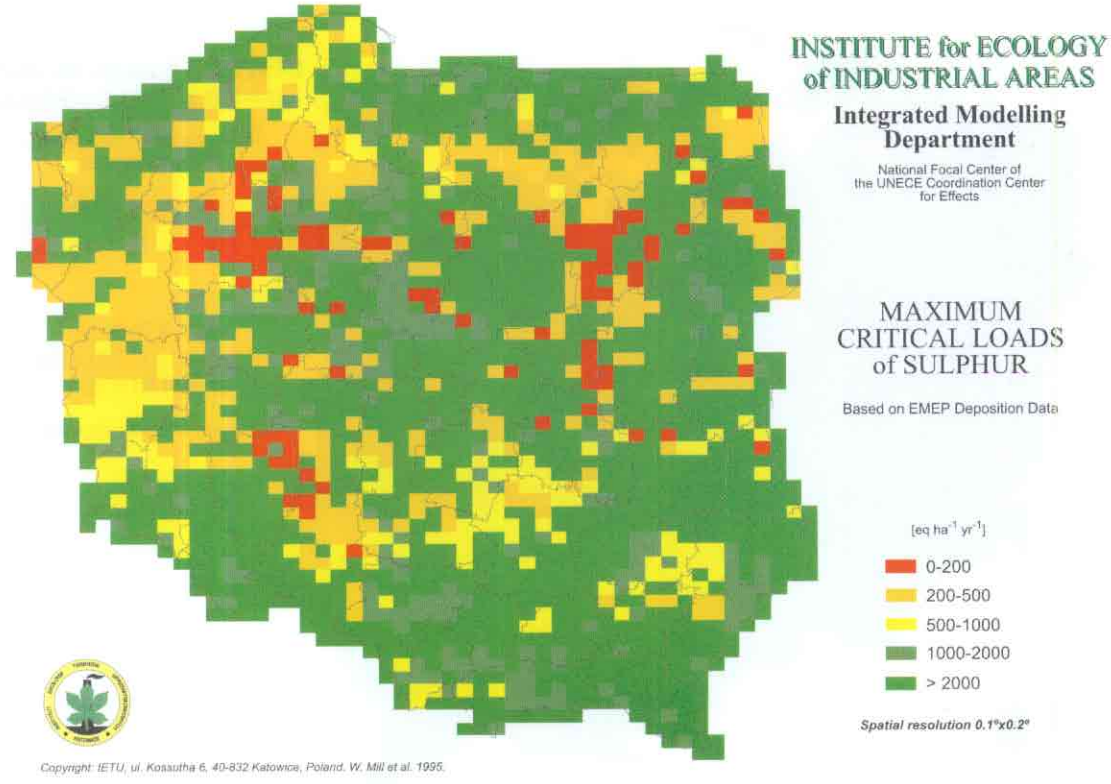


**Figure PL-2.** Maximum critical loads of sulfur.

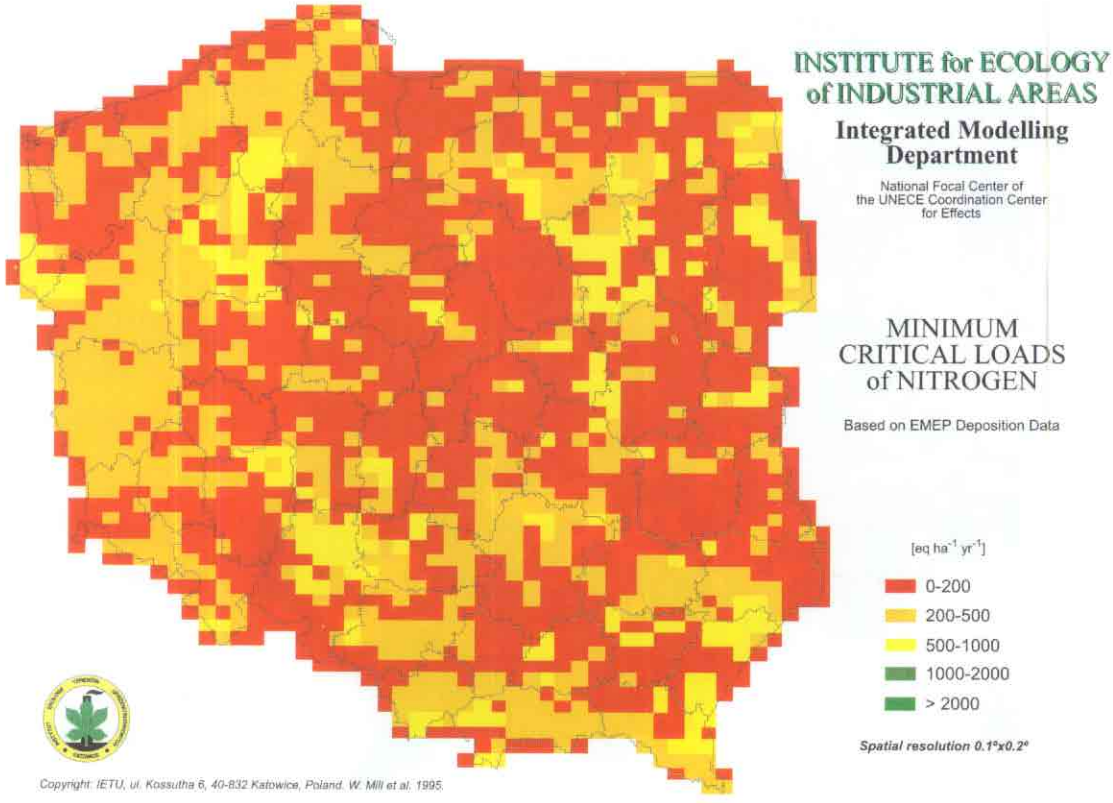


**Figure PL-3.** Minimum critical loads of nitrogen.

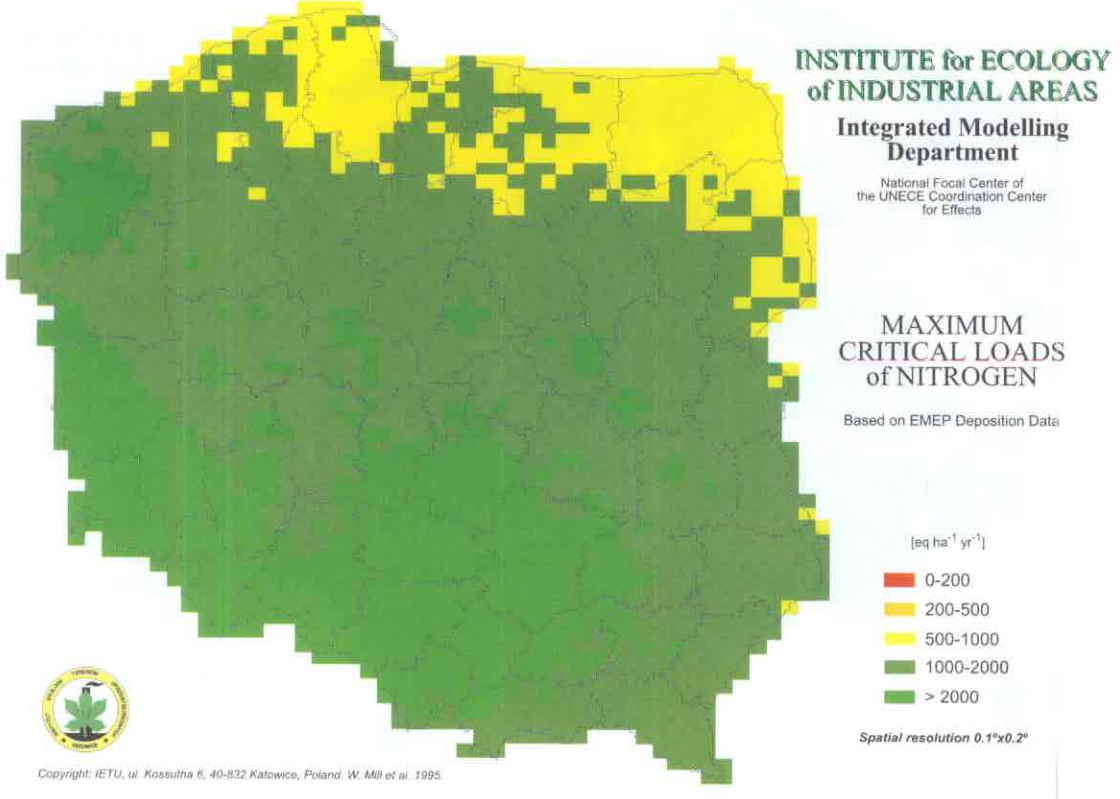


**Figure PL-4.** Maximum critical loads of nitrogen.

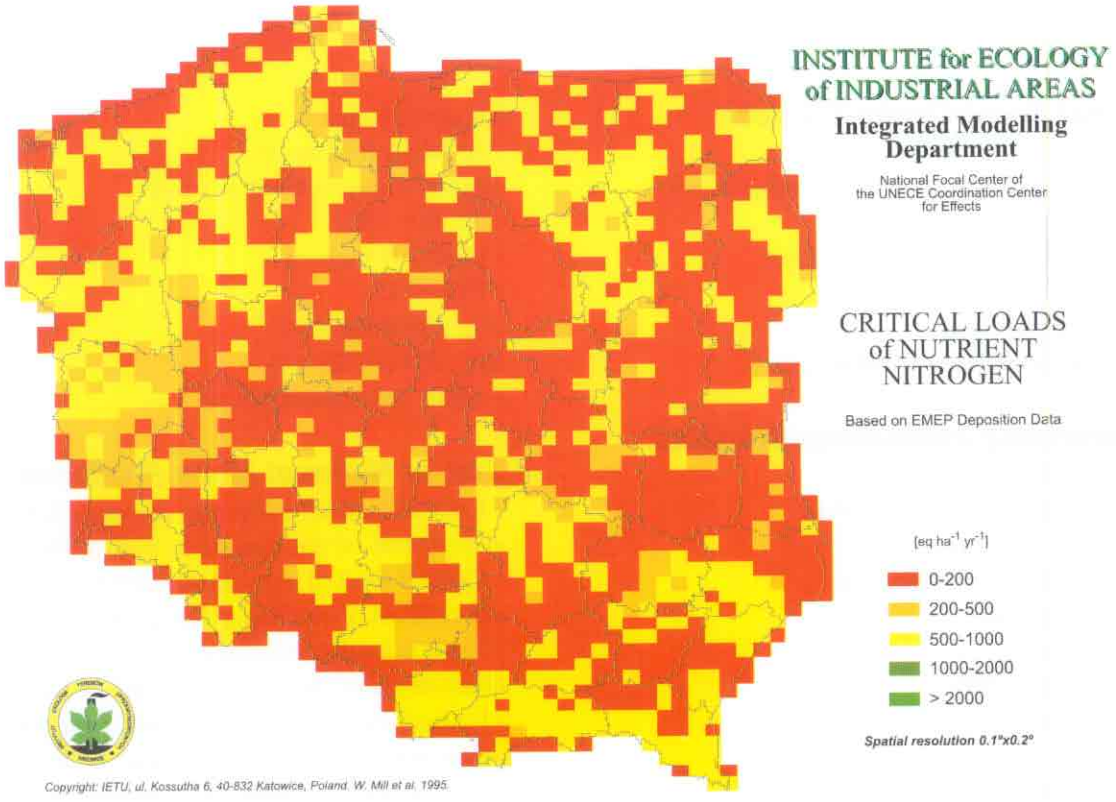


**Figure PL-5.** Critical loads of nutrient nitrogen.

# RUSSIAN FEDERATION

## *National Focal Center/Contact:*

Prof. Vladimir N. Bashkin
Institute of Soil Science and Photosynthesis
Russian Academy of Sciences,
Pushchino, Moscow region, 142292
tel: +(0967)-73-38-45
fax: +(095)-923-3602
email: bashkin@issp.serpukhov.su

## *Collaborating Institutions/Contacts:*

Dr. Andrei S. Peshkov
Head of Russian Federation NFC
Dr. Pavel P. Krechetov
Institute of Nature Protection
Sadki-Znamenskoe
113628 Moscow,
tel: +(095)-423-0233
fax: +(095)-423-0233

Dr.Michael Ya. Kozlov
Alex Yu. Abramychev
Irina V. Priputina
Oleg M. Golinets
Institute of Soil Science and Photosynthesis
Russian Academy of Sciences,
Pushchino, Moscow region, 142292
tel: +(0967)-73-38-45
fax: +(095)-923-3602
e-mail: bashkin@issp.serpukhov.su

Dr. Valentin G. Sokolovsky
Natalya A. Karpova
Ministry of Environmental Protection and
Natural Resources
Gruzinskya str. 4/6
123812 Moscow
tel: +(095)-254-60-74
fax: +(095)-254-8283

Sergei V. Dutchak
Dr. Leonid K. Erdman
Irina S. Dedkova
Meteorological Synthesizing Center-East
Kedrova str. 8a
Moscow
tel: +(095)-124-47-58
fax: +(095)-310-70-93

Dr. Juha Kämäri
Mr. Matti Johansson
Finnish Environment Agency
P.O. Box 250
FIN-00101 Helsinki
FINLAND
tel: 258-0-4028 347
fax: 358-0-4028 338
e-mail: johanssonm@vyh.fi

## *List of National Maps Produced:*

- Critical load of minimum nitrogen for terrestrial ecosystems of the European part of Russia
- Critical load of maximum nitrogen for terrestrial ecosystems of the European part of Russia
- Critical load of minimum nitrogen for terrestrial ecosystems of the European part of Russia
- Critical load of minimum sulfur for terrestrial ecosystems of the European part of Russia
- Critical load of maximum sulfur for terrestrial ecosystems of the European part of Russia

All maps were produced at 5 percentiles in accordance with the CCE 1993 Status Report (Downing *et al.* 1993).

## *Calculation Methods:*

On the basis of modified simple steady state mass-balance equations, the critical loads for nutrient and acidifying nitrogen as well as for sulfur and acidity have been calculated for various ecosystems of the European part of Russia. Due to the large dimensions of the area, all calculation and mapping procedures have been carried out using geographic information systems with elements of simplified expert modeling systems (Bashkin *et al.* 1993a). The initial information consisted of geological, geochemical, geobotanic, landscape, soil, hydrochemical, biogeochemical, hydrological etc. regionalization. For every elemental taxon the main links of biogeochemical cycles of N, S and base cations (BC) have been characterized quantitatively on a basis of available case studies. The grid cells were 1 degree x 0.5 degree.

The main differences with proposed method of critical loads calculations (Downing *et al.* 1993) have been related to the calculation of $N_u$, $N_i$, $N_{de}$ and $N_l$ for $CL_{nut}N$.

The algorithm for computer calculations included of critical load of nutrient nitrogen consist of the following equations:

$$CL_{nutr}(N) = {}^*N_u + {}^*N_i + {}^*N_{de} + {}^*N_{l(crit)} \quad (1)$$

where * means that each of the terms refers to the values at the actual total atmospheric precipitation at a site. $N_u$ and $N_i$ are permissible nitrogen uptake and soil immobilization, $N_{de}$ is permissible denitrification and $N_{l(crit)}$ is permissible critical nitrogen leaching.

Permissible atmospheric nitrogen uptake ($^*N_u$) was given as:

$$^*N_u = N_{upt} - N_u \quad (2)$$

where $N_{upt}$ is the annual accumulation of N in biomass and $N_u$ is the annual uptake of N from soil.

$N_{upt}$ was calculated accounting for the coefficients of annual biogeochemical turnover (Cb) the values of which values varied from < 0.1 up to >25. Annual Nu from soil was calculated on a basis of nitrogen mineralizing capacity (NMC) of soils which was determined experimentally or calculated using regression equations (Bashkin *et al.* 1993). Thus,

$$N_u = (NMC - N_i - N_{de})\ Ct \quad (3)$$

where:
$N_i$ = 0.15 NMC, if C:N < 10
$N_i$ = 0.25 NMC, if 10 < C:N < 14
$N_i$ = 0.30 NMC, if 14 < C:N < 20
$N_i$ = 0.35 NMC, if C:N > 20
$N_{de}$ = 0.145 NMC + 6.477, if NMC > 60 kg/ha/yr
$N_{de}$ = 0.145 NMC + 0.900, if NMC < 10 kg/ha/yr
$N_{de}$ = 0.145 NMC + 0.605, if 10 < NMC < 60 kg/ha/yr

The permissible immobilization of atmospheric N deposition ($^*N_i$) was found as:

$$^*N_i = [(0.2\ NH_4 + 0.1\ NO_3)\ /Cb]\ Ct \quad \text{if C:N} < 10 \quad (4a)$$

$$^*N_i = [(0.3\ NH_4 + 0.2\ NO_3)\ /Cb]\ Ct \quad \text{if } 10 < \text{C:N} < 14 \quad (4b)$$

$$^*N_i = [(0.35\ NH_4 + 0.25\ NO_3)/\ Cb]\ C_t \quad \text{if } 14 < \text{C:N} < 20 \quad (4c)$$

$$^*N_i = [(0.4\ NH_4 + 0.3\ NO_3)\ /Cb]\ C_t \quad \text{if C:N} > 20 \quad (4d)$$

where $C_t$ = hydrothermic coefficient given as a relative part of sum T > 5°C from the annual sum.

The permissible denitrification from atmospheric deposition ($^*N_{de}$) was found as:

$$^*N_{de} = (N_{de}\ /\ NMC)\ N_{td} \cdot C_t \quad (5)$$

where $N_{de}$ / $NMC$ = denitrification fraction, which depends on many features of soils and is calculated on the basis of experimental data, and $N_{td}$ = total N deposition. Finally, permissible critical leaching of atmospheric nitrogen [$^*N_{l(crit)}$] was given as:

$$^*N_{l(crit)} = Q \cdot C\ N_{crit} \quad (6)$$

where $Q$ = annual surplus of precipitation (runoff) and $C\ N_{crit}$ = the permissible nitrogen concentration in surface waters.

Critical loads for sulfur and acidity as well as exceedances for all studied parameters were calculated on the basis of the CCE 1993 Status Report.

The calculations of sulfur and nitrogen deposition were made by Meteorological Synthesizing Center-East (MSC-E) on the basis of meteorological data and emissions using the 150 x 150km EMEP grid (Dedkova 1992).

Uncertainty analysis was made using UNCSAM software (Janssen *et al.* 1992) and the results of which are published (Kozlov *et al.* 1995). The aim of this research was to present a comprehensive and quantitative estimate on the uncertainty of computed nitrogen and sulfur critical loads (CL) values for terrestrial ecosystems of European part of Russia. It has been shown that the uncertainties are related mainly to measurement inaccuracies and incorrect interpretations of computed results as well as the most influential sources are nitrogen uptake by vegetation and nitrogen leaching from terrestrial ecosystems.

## Data Sources:

***Geographical:*** The quantitative assessment and mapping of sulfur and nitrogen critical loads was carried out on the basis of number of regional parameters for a given ecosystem. For the European part of Russia the following data bases were identified:

- The inventory of soil types and subtypes (Liverovsky 1974).
- The inventory of values of surface runoff of nitrogen and phosphorus (Kondratjev and Koplan-Dix, 1988).
- Biogeochemical regionalization of terrestrial and freshwater ecosystems (Kovalsky 1974, Bashkin *et al.* 1993b).
- Annual biomass uptake (Bazilevich and Rodin 1971, Manakov 1972, Bashkin 1987, Bashkin *et al.* 1992).

## Comments and Conclusions:

This section of the NFC Report is devoted to the work that has been already carried out during 1993-1995 with the Finnish NFC in order to harmonize cross-border critical load values concerning differences in calculation methods and data sources.

The discussion on critical loads between Finland and Russia started during the meeting of the Working Group of Atmospheric Protection of the Russian-Finnish Commission for Environmental Protection, in March 1993. Since then the National Focal Centers of Finland and Russia have had four meetings, two of which were held together with Norwegian and Swedish experts. The meetings have had the following objectives:

1. In the meeting held in St. Petersburg on 21-23 April 1992, the methods for calculating critical sulfur loads were presented by both parties. The Russian participants expressed their concern about the fact that the Finnish critical loads were clearly lower than those on the Russian side.

2. In the meeting held in Helsinki on 19-21 May 1993, the critical sulfur depositions and the data used for calculating them were compared grid by grid and the reasons for the apparent discrepancies were noted. There were conceptual differences in the calculation methods as well as differences in the spatial resolution of data.

3. In the meeting held in Pushchino on 23-24 September 1993, the differences in the critical load estimates between the four countries, Russia, Finland, Sweden and Norway were discussed. In particular, attention was paid on the very low critical load values in Sweden and Norway which determined the reduction requirements of sulfur emissions in the European optimization runs.

4. In the meeting held in Helsinki on 9-11 February 1994, the methods for calculating critical loads were evaluated in detail, and the most significant discrepancies were identified in calculation methods of weathering rates and base cation deposition. These discrepancies could explain most differences in the critical load results.

5. On the basis of these negotiations it was agreed that the area considered should form the whole of Finland, and the nearby areas of the Russian Federation, ie, St.Petersburg, the Murmansk and Leningrad districts, and the Republic of Karelia. Emissions from those areas are significantly transported across the Finnish-Russian boundary. For all other areas emissions used for future scenarios are based on existing agreements (bilateral and multilateral protocols).

6. It was recommended that the target years for the scenario runs should correspond to those of the Oslo Protocol (ie 2000, 2005 and 2010). The reference years should be 1980 and 1990 since the best emission data exists for those years.

7. The experts from both parties provided some latest results concerning the sources of sulfur deposition to the areas considered, the harmonization critical loads and the exceedances of critical loads with respect to some emission scenarios.

8. Finally, during the Meetings in November 7-8 1994 (Helsinki, Finland) and February 3-6 1995 (Pushchino, Russia), based on the results on critical load harmonization, no obvious discrepancies were noted on the unified critical load map between the Finnish and Russian values, and therefore the critical load data is considered suitable to be used in identifying necessary reduction requirements for acidifying compounds. Further modifications to the data are made if errors are detected or if for some other reason alterations are found necessary by both parties.

## Work Plan for the Russian NFC:

At present the following maps are in progress:

*1995/1996:*

- maps of critical load of $CL_{min}N$, $CL_{max}N$, $CL_{nut}N$, $CL_{min}S$ and $CL_{max}S$ for northwestern part of Russia with EMEP grid size 25 x 25 km
- maps of ozone critical loads for the European part of Russia in EMEP grid size 150 x 150 km;
- maps of critical loads of sulfur and nitrogen for the Asian part of Russia

*1996/1997:*

- map of critical loads of heavy metals (Pb, Zn, Cu, Cd, Ni)
- map of critical loads of POPs (DDT, lindane).

## Acknowledgments:

The authors wish to thank the vice-minister of Ministry of Environmental Protection and Natural Resources of Russian Federation Prof. Alex F. Poryadin for financial support of scientific activity of National Focal Center for Effects.

## References:

Bashkin V.N., E.V. Efstafjeva, V.V.Snakin *et al.*, 1993a. Biogeochemical fundamentals of ecological standardization. Moscow, Nauka Publ.House, 312 pp.

Bashkin V.N., V.V. Snakin V.V., M.Ya. Kozlov *et al.*, 1993b. Russian Federation NFC Report. In: R.J.Downing *et al.* (eds.), 1993. Calculation and mapping of critical loads in Europe. CCE 1993 Status Report, RIVM Rep. 259101003, Bilthoven.

Bashkin, V.N., V.P. Uchvatov, A.Yu. Kudeyarova *et al.*, 1992. Ecological-agrogeochemical regionalization of Moscow region. Pushchino: ONTI, 170pp.

Bashkin, V.N., 1987. Nitrogen agrogeochemistry. Pushchino, 270pp.

Bazilevich, N. and L. Rodin, 1971. Productivity and element cycle in natural and cultural plant communities of the USSR. In: Bazilevich, N. (ed.), Biological Productivity and Chemical Element Cycle in Plant Communities. Leningrad: Nauka 5-32.

Downing R.J., J.-P. Hettelingh and P.A.M. de Smet (eds.), 1993. Calculation and mapping of critical loads in Europe. CCE 1993 Status Report, RIVM, Bilthoven.

Kondratjev, K.Ya. and I.S. Koplan-Dix, 1988. Evolution of phosphorus cycle and natural waters eutrophication. Leningrad: Nauka, 206p.

Kovalsky, V.V., 1974. Geochemical ecology. Moscow, Nauka.

Kozlov, M.Ya., V.N. Bashkin and O.M. Golinets, 1995. Uncertainty analysis of computed critical loads of sulphur and nitrogen for terrestrial ecosystems of European part of Russia. *Environmetrics*, in press.

Liverovsky, Yu.A., 1974. Soils of the USSR. Geographical characteristics. Moscow, Nauka.

Manakov, K.N., 1972. Productivity and biological turnover in tundra biogeocenoses. Leningrad, Nauka, 150 pp.

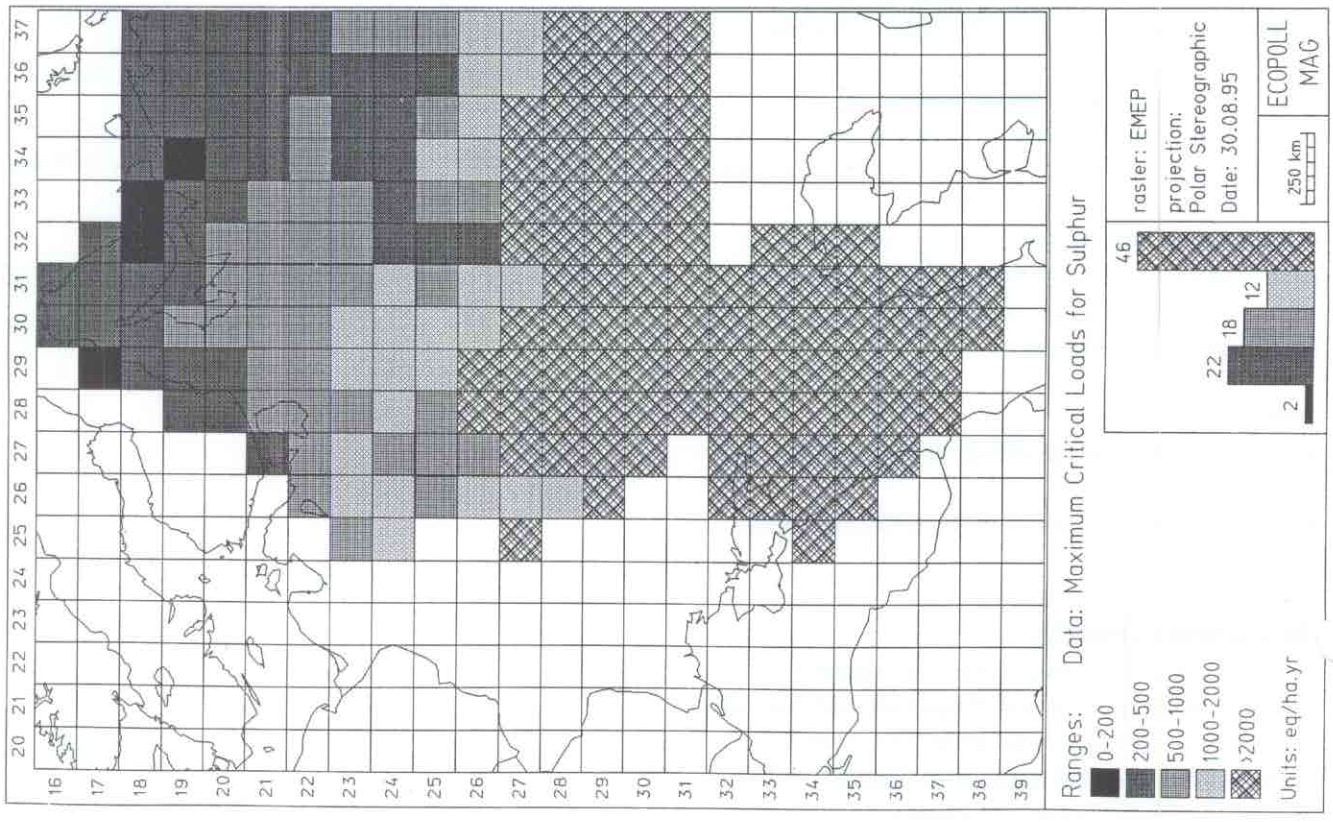


**Figure RU-1.** Maximum critical loads for sulfur.

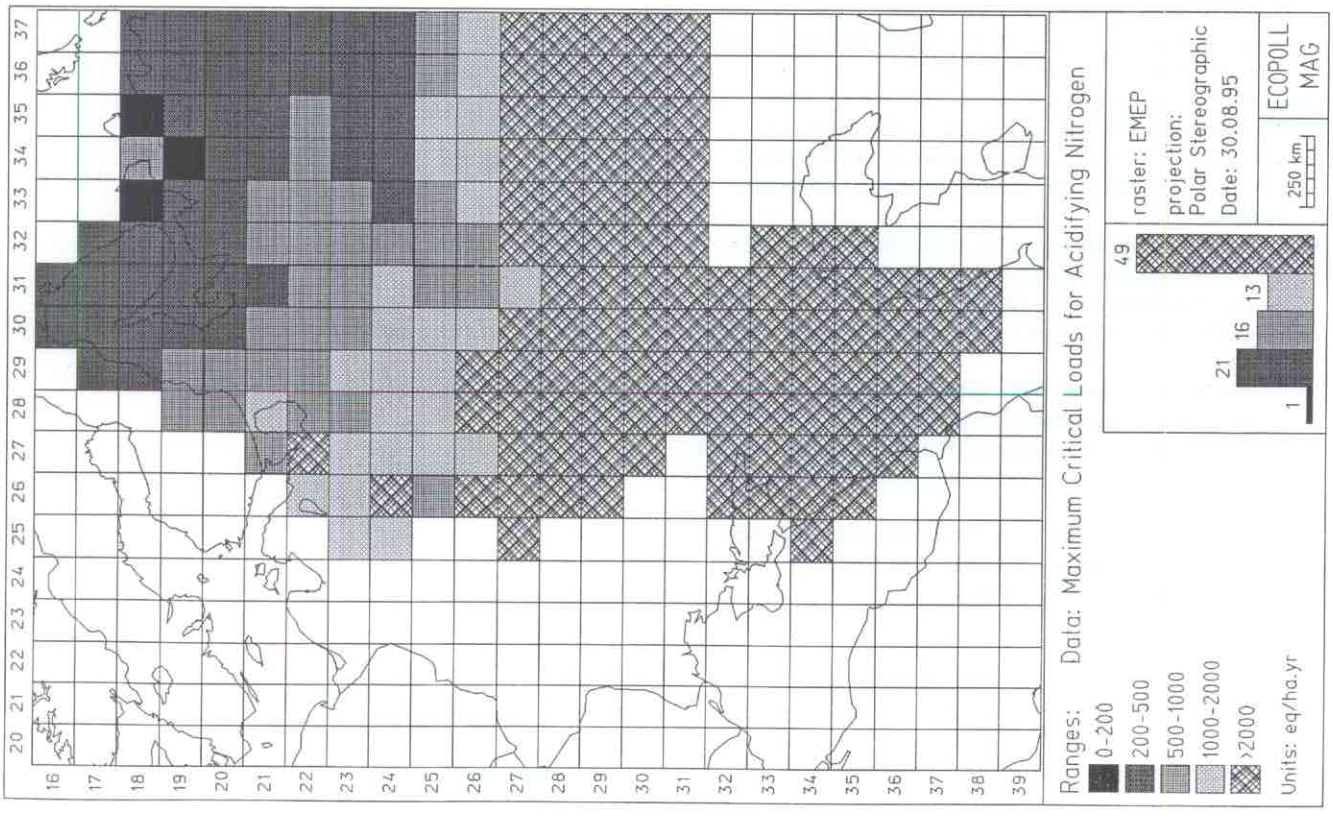


**Figure RU-2.** Maximum critical loads for acidifyin nitrogen.

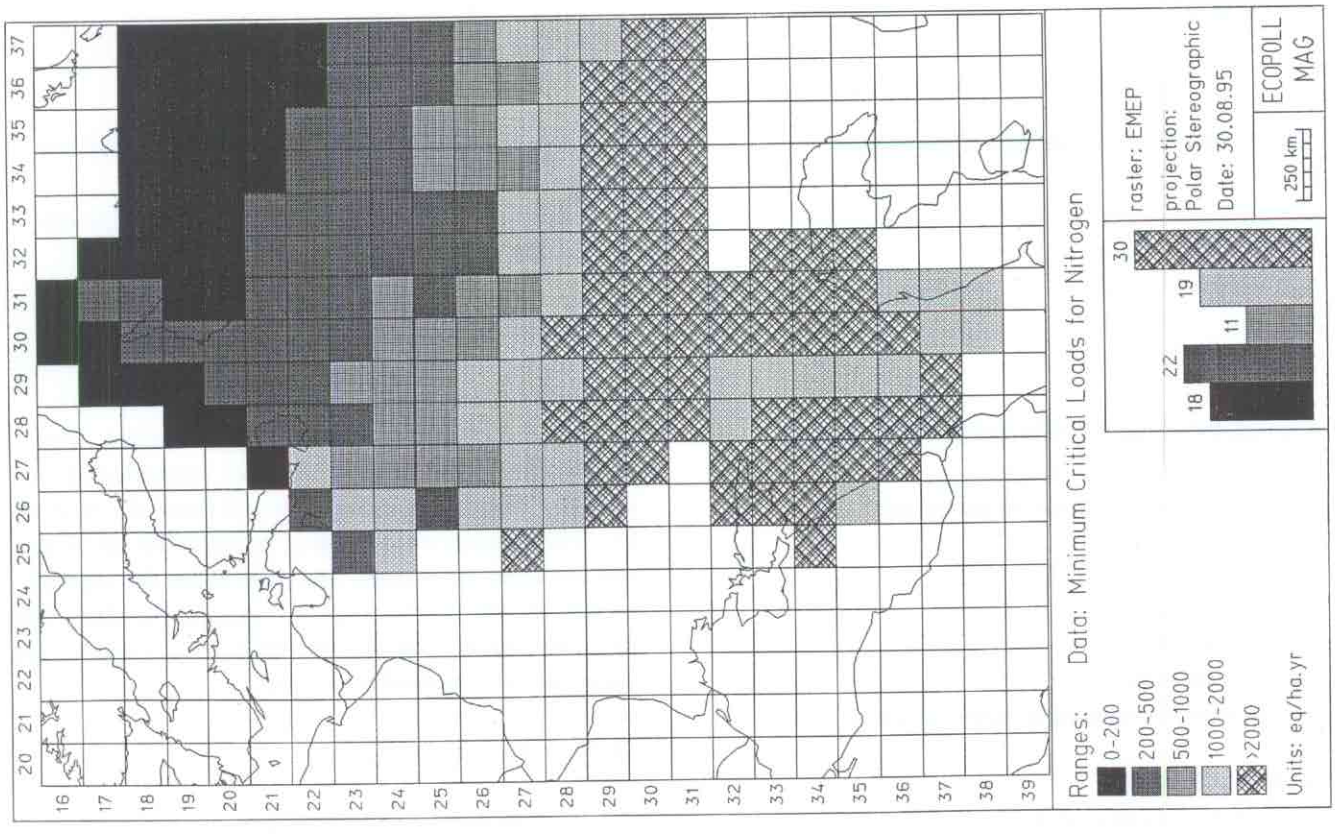


**Figure RU-3.** Minimum critical loads for nitrogen.

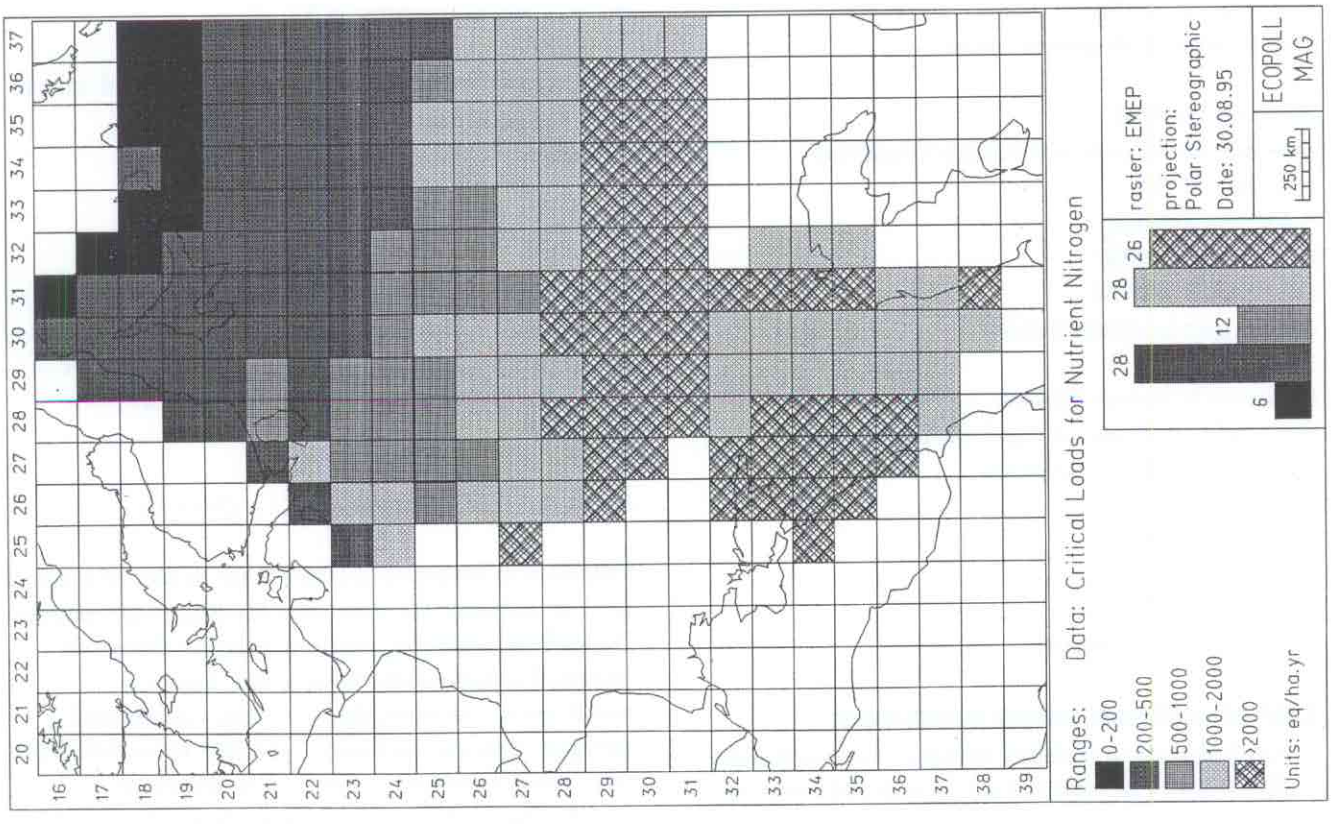


**Figure RU-4.** Critical loads for nutrient nitrogen.

# SWEDEN

## National Focal Center/Contact:

Dr. Håkan Staaf
Swedish Environmental Protection Agency
S-106 48 Stockholm
tel: +46 8 698 1442
fax: +46 8 698 1664
email: hks@environ.se

## Collaborating Institutions/Contacts:

Professor Harald Sverdrup
Department of Chemical Engineering
University of Lund
P.O. Box 124
S-221 01 Lund
tel: +46 46 108274
fax: +46 46 146030
email: harald.sverdrup@chemeng.lth.se

Dr. Kevin Bishop
Swedish University of Agricultural Sciences
Department of Forest Ecology
S-901 83 Umeå
tel: +46 90 166625
fax: +46 90 167750
email: kevin.bishop@sek.slu.se

Dr. Gun Lövblad
Swedish Environmental Research Institute
P.O. Box 47 086
S-402 58 Göteborg
tel: +46 31 460080
fax: +46 31 482180
email: gun.lovblad@ ivl.se

Professor S. Ingvar Nilsson
Swedish University of Agricultural Sciences
Department of Soil Sciences
P.O. Box 7014
S- 750 07 Uppsala
tel: +46 18 671276
fax: +46 18 672795
email: Ingvar.Nilsson@mv.slu.se

## List of national maps produced:

1. Critical load of nutrient nitrogen for forest soils.
2. Exceedance of critical load of nutrient nitrogen for forest soils.
3. Critical load of acidifying nitrogen for forest soils, with sulfur according to the Oslo protocol.
4. Exceedance of critical level of ozone (AOT 40) for agricultural crops.
5. Exceedance of critical level of ozone (AOT 40) for forests.

## Calculation methods:

Critical loads for forest ecosystems in Sweden were calculated using the steady state mass balance model, implemented in the PROFILE model. The soil profile is divided into 4 layers, using input data for the thickness of each soil layer (O, A/E, B, C). The criteria were applied in the 0–50 cm of the soil for coniferous trees, assumed to be the typical rooting depth for this type of forest in Sweden. To find the critical load of nutrient N; $N_{dep} = CL(N)$, the mass balance method was used:

$$CL(N) = N_u + N_{im} + N_{de} + N_l$$

$N_{dep}$ = atmospheric N deposition
$N_u$ = N uptake by forest
$N_{im}$ = N immobilization
$N_{de}$ = denitrification
$N_l$ = Critical leaching of N

The residual critical load of nitrogen related to acid was derived from a rearrangement of the exceedance expression:

$$EX(acid) = D(S) + D(N) - D(BC) - CL(acid)$$

where EX is exceedance, D is deposition and CL critical load. The expression can be rearranged to calculate the deposition of N that will cause EX=0, using the S deposition under the Oslo protocol. We have:

$$CL(N,Acid) = CL(acid) + D(BC) - D(S\text{-}Oslo)$$

PROFILE is based on a conceptual model of a forest soil. It contains the following chemical subsystems: Deposition, leaching, accumulation of dissolved chemical components, weathering kinetics, nitrification, denitrification, of base cations and nitrogen, canopy exchange, litterfall, immobilization and mineralization. Chemical feedback on weathering, uptake, nitrification, denitrification is included. Solution equilibrium reactions involving

the carbonate system, $CO_2$, speciation and complexing involving Al and organic acids.

In the PROFILE model, all soil processes communicate via the soil solution. The temperature dependence is considered for nitrification, denitrification, immobilization, weathering and solution equilibria. The implementation of the mass balance approach in PROFILE allows for iterative consideration of feedback between soil processes and soil chemistry. The PROFILE model has been set in an automated framework reading input data from a file containing the regional database.

Uptake in the model is based on input from the Swedish Forest Inventory. Uptake was calculated from growth as calculated with the HUGIN model. Average growth over one rotation period was calculated, and converted to uptake using present element composition in stemwood. This uptake is however calculated without any consideration to nutrient availability or soil chemistry feedback on plants.

***Critical nutrient uptake:***

The long-term uptake of N is defined as the N uptake that can be balanced by a long-term supply of base cations, in the effect of Liebig's law; "Growth is limited by the nutrient in least supply". This amount is referred to as the critical uptake $N_{crit}$. The calculations are thus not based on the present uptake rate, since the present growth may be enhanced by artificial or time-limited supply of nutrients, mobilized from exchange sites by acid deposition. The critical uptake is calculated from mass balances for the nutrient cations Mg, K and Ca separately. The production of different cations from weathering was calculated with the PROFILE model.

**Table SE-1.** Approximate deficiency nutrient ratios to be applied in the critical loads calculations in order to prevent long-term nutrient imbalances.

| Tree species | Ca/N | Mg/N | K/N | P/N | BC/N |
|---|---|---|---|---|---|
| Norway spruce | 0.4 | 0.13 | 0.17 | 0.1 | 0.8 |
| Scots pine | 0.5 | 0.17 | 0.12 | 0.1 | 0.8 |
| European beech | 0.4 | 0.2 | 0.2 | 0.1 | 0.8 |

Taking deposition and weathering as the sources of these nutrients, and uptake and leaching as the sinks the mass balance for a species becomes:

$$U(crit,BC) = D_{BC} + W_{BC} - Q \cdot [BC]_{lim}$$

where:
$U(crit, BC)$ = critical uptake
$D_{BC}$ = atmospheric deposition
$W_{BC}$ = weathering of base cations
$Q$ = water flux from the root zone
$[BC]_{lim}$ = limiting concentration for uptake

The limiting concentration is the level when the trees no longer can extract a nutrient from the solution. In the calculations, the limiting concentration for Ca and Mg has been set to 5 meq $m^{-3}$, and to 0 for K.

From the critical base cation uptake, maximum N uptake is calculated using the nutrient to N limiting ratio. The ratio determines the maximum N that can be taken up without inducing P or base cation deficiency:

$$N_{crit} = min\ \{U(crit,Ca)/Ca{:}N,\ U(crit,K)/K{:}N,\ U(crit,Mg)/Mg{:}N,\ U(crit,P)/P{:}N\}$$

where:
$N_{crit}$ = critical N uptake
$BC{:}N$ = nutrient stress limit

The critical ratios have been listed in Table SE-1. The critical uptake is limited by present deposition of N, no growth is allowed beyond that value even if more weathering is available.

***Immobilization:***

Long-term immobilization in forest ecosystems has been estimated using present content divided by soil age. Such estimates ignores the occasional purging of the system when forest fires occur, and also long-term effects of denitrification and fixation. Immobilization as estimated from soil age and stored amount has a value of 0.5–1.5 kg N $ha^{-1}$ $yr^{-1}$. This is very much lower than estimates for present immobilization. At present many forest ecosystems accumulate 7–15 kg $ha^{-1}$ $yr^{-1}$ in the forest floor. The assumptions made in this approach are that immobilization is caused by retarded decomposition and microbiological fixation. The rate is given by:

$$N_{im} = k_{im1} \cdot N_{litterfall} + k_{im2} \cdot [N]$$

The coefficients $k_{im1}$ and $k_{im2}$ depend on soil acidity, soil wetness and temperature in the model. The value of the coefficients have been estimated from field observations. The expressions has been calibrated in two ways for the calculation: (1) Immobilization in northern Sweden was assumed to be 0.5 kg $ha^{-1}$ $yr^{-1}$ at soil pH 5.5 and N deposition 2 kg $ha^{-1}$ $yr^{-1}$, and (2) immobilization was assumed to be 8 kg $ha^{-1}$ $yr^{-1}$ at present at soil pH 4.2 and the deposition 30 kg $ha^{-1}$ $yr^{-1}$. The immobilization estimate for present is based on a study on denitrification by Sverdrup and Ineson (1995-96). Retarded decomposition has as process priority over microbiotic fixation.

***Denitrification:***

The Sverdrup-Ineson expression for denitrification was used:

$$N_{de} = k_{de} \cdot [NO_3] / ( K_M + [NO_3] )$$

The coefficient $k_{de}$ depends on soil acidity, soil wetness and temperature. The general expression for modifying rate coefficients is:

$$k = k_0 \cdot f(pH) \cdot g(water) \cdot h(T)$$

All coefficients for denitrification, nitrification and immobilization ($k_{de}$, $k_{nit}$, $k_{im1}$, $k_{im2}$) are modified this way.

***Nitrogen leaching ($N_l$):***

At steady-state, and with a balanced nutrient supply, the N leaching should amount to the natural leaching from N-limited stands. In the calculations performed for Sweden, initially the basic assumption behind the critical uptake concept was $N_l = 0$. However, not all ecosystems are necessarily dominated by trees.

When nitrogen appear in significant amounts in the soil solution, herbs and plant species composition of the heath and ground vegetation may be changed. Lichen type of vegetation lose to lingonberry (*Vaccinium vitis-idaea/Caluna*) type of vegetation. These in turn lose ground to blueberry type vegetation (*Vaccinium myrtillus*), blueberry vegetation types lose ground to a grass type vegetation, grass vegetation lose to a type dominated by herbs. The maximum permitted leaching is given by the percolation from the bottom of the root zone (ie, runoff rate) and the critical N soil solution concentration.

$$N_l = Q \cdot [N]$$

In comparison with the nutrient limitation balance approach described above, the difference is that the leaching term no longer is 0, but linked to a critical concentration related to some type of sensitive plant species. Still it must be considered that long-term sustainable tree uptake at steady state cannot be set higher than what is given by the liming nutrient calculation.

**Table SE-2.** The limiting concentrations of nitrogen for inducing vegetation changes. The limits have been based on Swedish forest vegetation survey data as well as a review and partly reevaluation of studies by Tillman and Ellenberg.

| Ecological change | [N] in mg M $l^{-1}$ | $N_l$ in kg $ha^{-1}$ $yr^{-1}$ |
|---|---|---|
| Coniferous trees → Nutrient imbalances | 0 – 0.2 | 0 – 2 |
| Deciduous trees → Nutrient imbalances | 0.2 – 0.4 | 2 – 4 |
| Lichen type → Lingonberry type | 0.2 – 0.4 | 1 – 2 |
| Lingonberry type → Blueberry type | 0.4 – 0.6 | 2 – 4 |
| Blueberry type → Grass type | 1 – 2 | 5 – 10 |
| Grass type → Herb/meadow type | 3 – 5 | 15 – 25 |

### Data Sources:

All data in this work is based on data and soil samples collected in the Swedish Forest Inventory (Rikskogstaxeringen/Ståndortskarteringen) from 1983-1985. The inventory consists of a network of 27,000 and 2,200 stations, respectively, evenly spread over the complete forest area of Sweden (267,000 $km^2$). Soil samples down to the C-layer at approximately 60 cm soil depth were collected. The basic soil parameters for this study were analyzed on these samples.

Several other parameters such as $CO_2$ pressure, soil solution dissolved organic carbon, distribution of uptake and evapotranspiration and gibbsite coefficients have less influence and are entered as standard values taken from the literature and stay generally constant between runs and sites. Annual average air temperature, precipitation and runoff was taken from the official statistics of the Swedish Meteorological Institute (SMHI), for each NILU grid (50 x 50 km). Other input data were derived strictly in accordance with Sverdrup *et al.* (1990).

### Uptake:

Basic vegetation data has been measured the 2,200 sites of the "Ståndortskarteringen" within the Swedish Forest Inventory. Each tree species is considered separately, and the total uptake weighted together for each calculation point.

### Mineralogy:

Absolute soil mineralogy was derived for 140 sites by measurement by the Swedish Geological Survey (SGU) at Uppsala and at the Czech Geological Survey in Prague. Total elemental content of the soil after complete dissolution was determined for all 1804 sites. These were analyzed using generic wet chemistry methods for Ca, Mg, Na, K, Al, Si, Fe, Ti and trace metals.

The model UPPSALA is a back-calculation model for reconstructing the mineralogy from the total analysis in order to provide input to models like PROFILE from simple survey data. The minerals have been grouped into assemblies of minerals with similar composition and dissolution rate. The equations used in the UPPSALA model for calculation of the percentage weight content of the individual minerals are shown below.

The equations of the UPPSALA model used to reconstruct mineralogy from total analysis. Oxide contents are percent weight.

I K-Feldspar = Max {0 , 5.88· $K_2O$ – 0.588· $Na_2O$}
II Plagioclase = Max {0 , 11.1· $Na_2O$ – 0.22· K-Feldspar}
III Apatite = 2.24· $P_2O_5$
IV Hornblende = Max {0 , 6.67· CaO – 3.67· Apatite – 0.2· Plagioclase}
V Muscovite = Max {0 , 2.08· $K_2O$ – 0.208· $Na_2O$}
VI Chlorite = Max {0 , 3.85· MgO – 0.39· Hornblende – 0.39· Muscovite}
VII Epidote = Max {0 , 0.1· Hornblende + 0.03· Plagioclase – 0.3}
VIII Quartz = $SiO_2$ – 0.63· Plagioclase – 0.68· K-Feldspar – 0.38· Muscovite – 0.33· Chlorite – 0.45· Hornblende – 0.42· Epidote

In calcareous soils, Eqs. V-VII are omitted and Eq. IV is replaced by:

Calcite = Max {0, 1.79· CaO – 3.67· Apatite – 0.2· Plagioclase}

Residual Al is used to form clay minerals in a group called vermiculite if they can be matched by a small amount of residual base cations, other residual Al is considered inert. The calculation is checked by calculating the amount of quartz and adding all components. Only such sites which lie within the range 95–105% are accepted. If a negative content arises in the calculation, it implies that there are no more adequate ions available, and that mineral is set to zero. For 1804 out of 1913 sites calculated, the mineralogy was accepted, and of the rejected sites, approximately 30 were estimated to be calcareous soils.

### Texture:

Texture was measured by granulometry and BET/ adsorption analysis on the 124 mineralogy analysis samples, and correlated against field texture classification. The texture for all 1804 sites were read from the correlation using the field classification. The relation between the field classification of soil texture and laboratory measurements of exposed surface is:

$$A_{tot} = 0.093 \cdot e^{(0.51 \cdot TX)}$$

where $TX$ is the texture class, and $A_{tot}$ is the total surface in $10^6$ $m^2/m^3$ soil. The relation is based on

determinations of surface area and texture class on 100 soil samples.

***Deposition:***
Deposition data were prepared by the Institute of Water and Air Research (IVL) at Göteborg, from the Swedish deposition monitoring network and EMEP data, modified with filtering factors for different vegetation types. The total deposition is calculated for each calculation point using the filtering factors and the vegetation mixture for that point. The deposition used correspond to 1988 deposition level.

## *List of national maps produced:*

The list show all maps produced in the Swedish critical load mapping program. Any map or the PROFILE model can be requested from the National Calculation and Mapping Center in Lund or the National Focal Center in Stockholm.

1. Critical load for acidity, forest soils
2. Critical load for acidity, lakes
3. Critical load for acidity, groundwater
4. Exeedance of critical loads of acidity, forest soils, 4 different depositions
5. Exeedance of critical loads of acidity, lakes, 4 different depositions
6. Exeedance of critical loads of acidity, groundwater, 4 different depositions
7. Steady state chemistry, soils, pH, 4 different depositions
8. Steady state chemistry, soils, BC/Al, 4 different depositions
9. Steady state chemistry, soils, groundwater ANC, 4 different depositions
10. Steady state response, soils, growth potential, 4 different depositions
11. Critical loads of nutrient nitrogen, forest ecosystems
12. Critical loads of nutrient nitrogen, grass type biome
13. Critical loads of nutrient nitrogen, heather type biome
14. Exeedance of nutrient nitrogen critical loads, forest ecosystems
15. Exeedance of nutrient nitrogen critical loads, grass type biome
16. Exeedance of nutrient nitrogen critical loads, heather type biome
17. Critical loads of nutrient nitrogen, lakes, based on N/P ratio
18. Exeedance of nutrient nitrogen critical loads, lakes, based on N/P ratio
19. Weathering, forest soils, 0-50cm, total BC, Ca, Mg, K, P
20. Weathering, lakes and catchment
21. Weathering, groundwater, 2 soil depth
22. Immobilization, forest soils, PROFILE model
23. Denitrification, Sverdrup-Ineson model
24. Exceedance of critical level of ozone (AOT 40) for agricultural crops
25. Exceedance of critical level of ozone (AOT 40) for forests

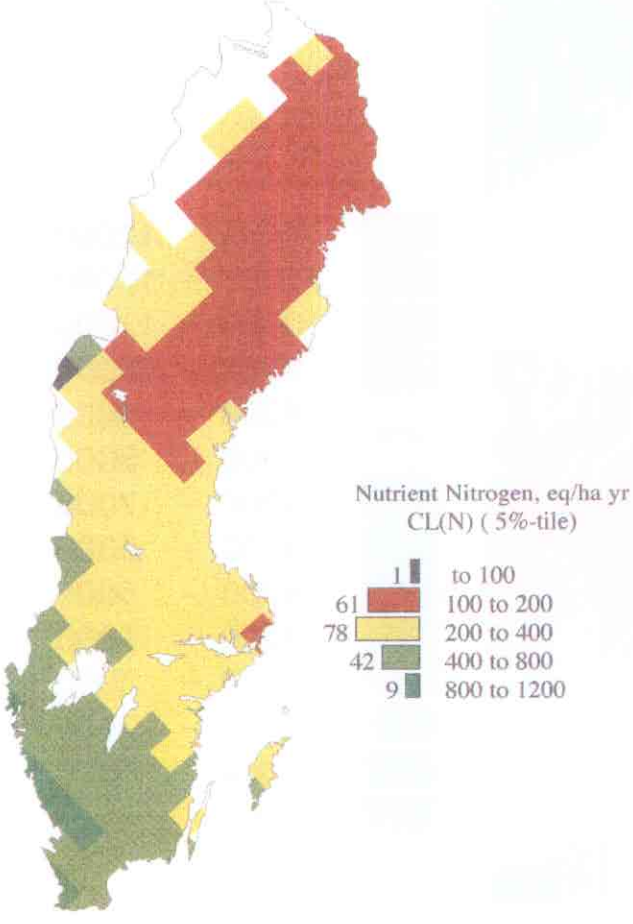


**Figure SE-1.** Critical loads of nutrient nitrogen, forest ecosystems.

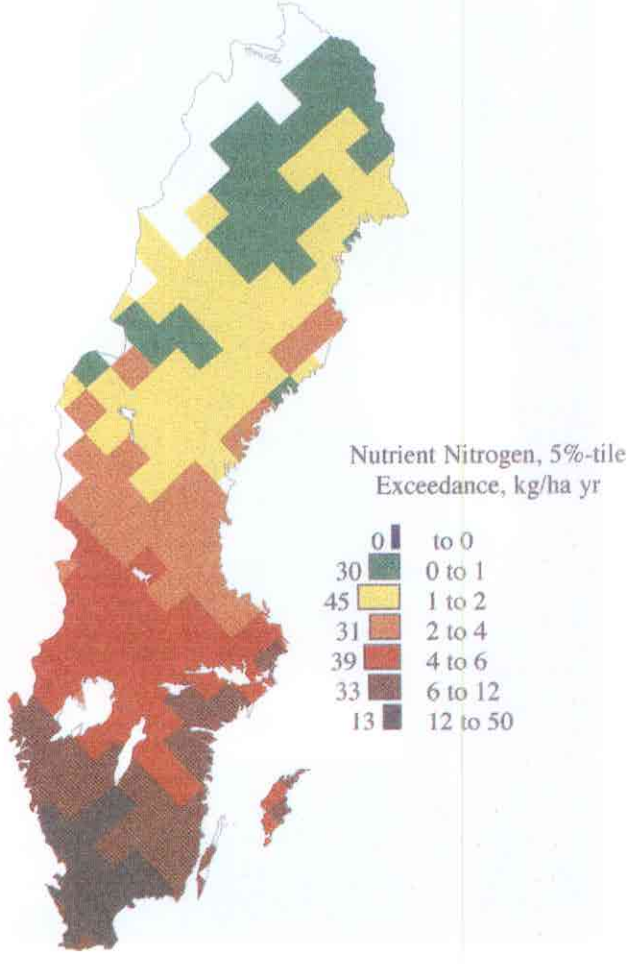


**Figure SE-2.** Exeedance of nutrient nitrogen critical loads, forest ecosystems.

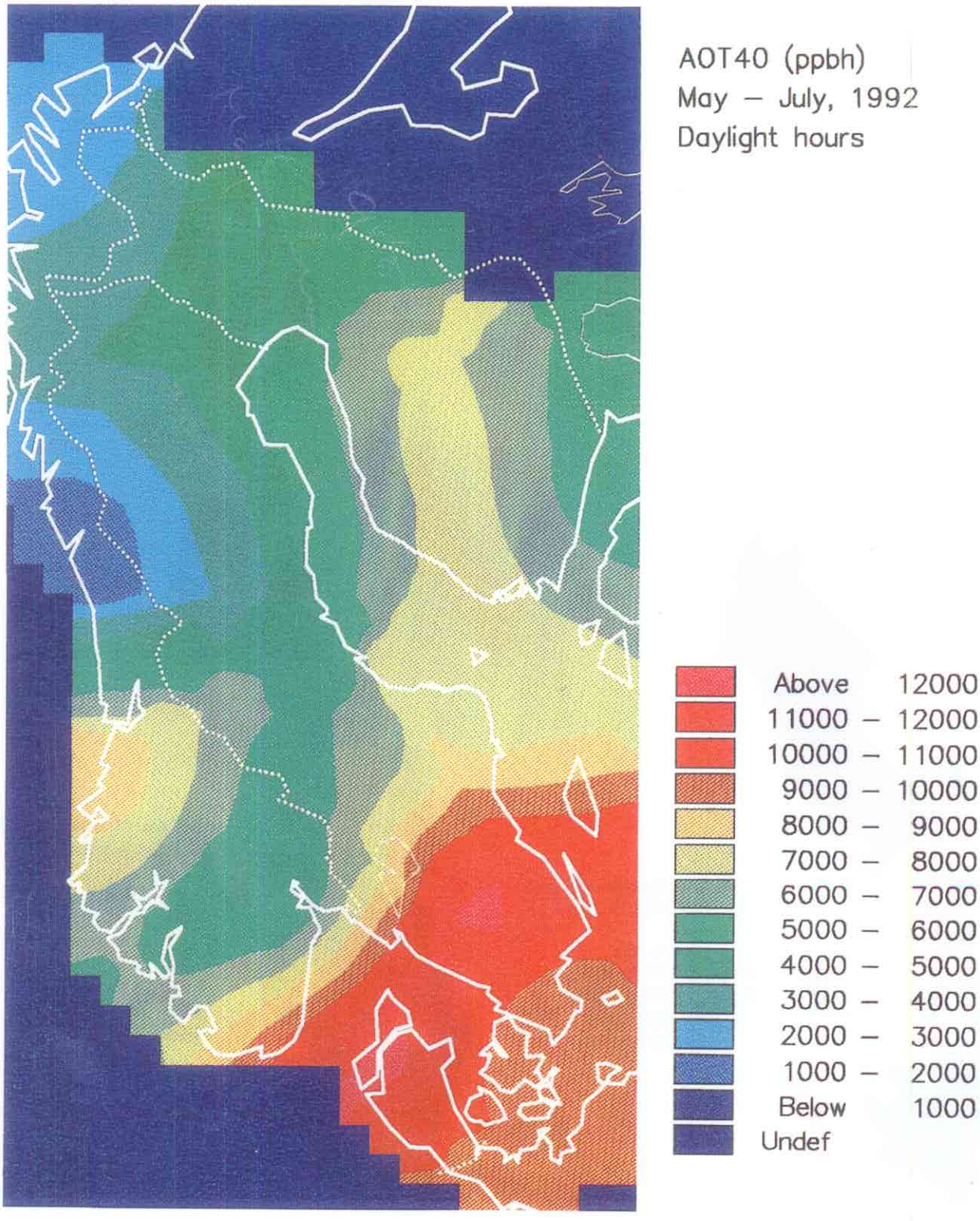


**Figure SE-3.** Exceedance of critical level of ozone (AOT 40) for agricultural crops.

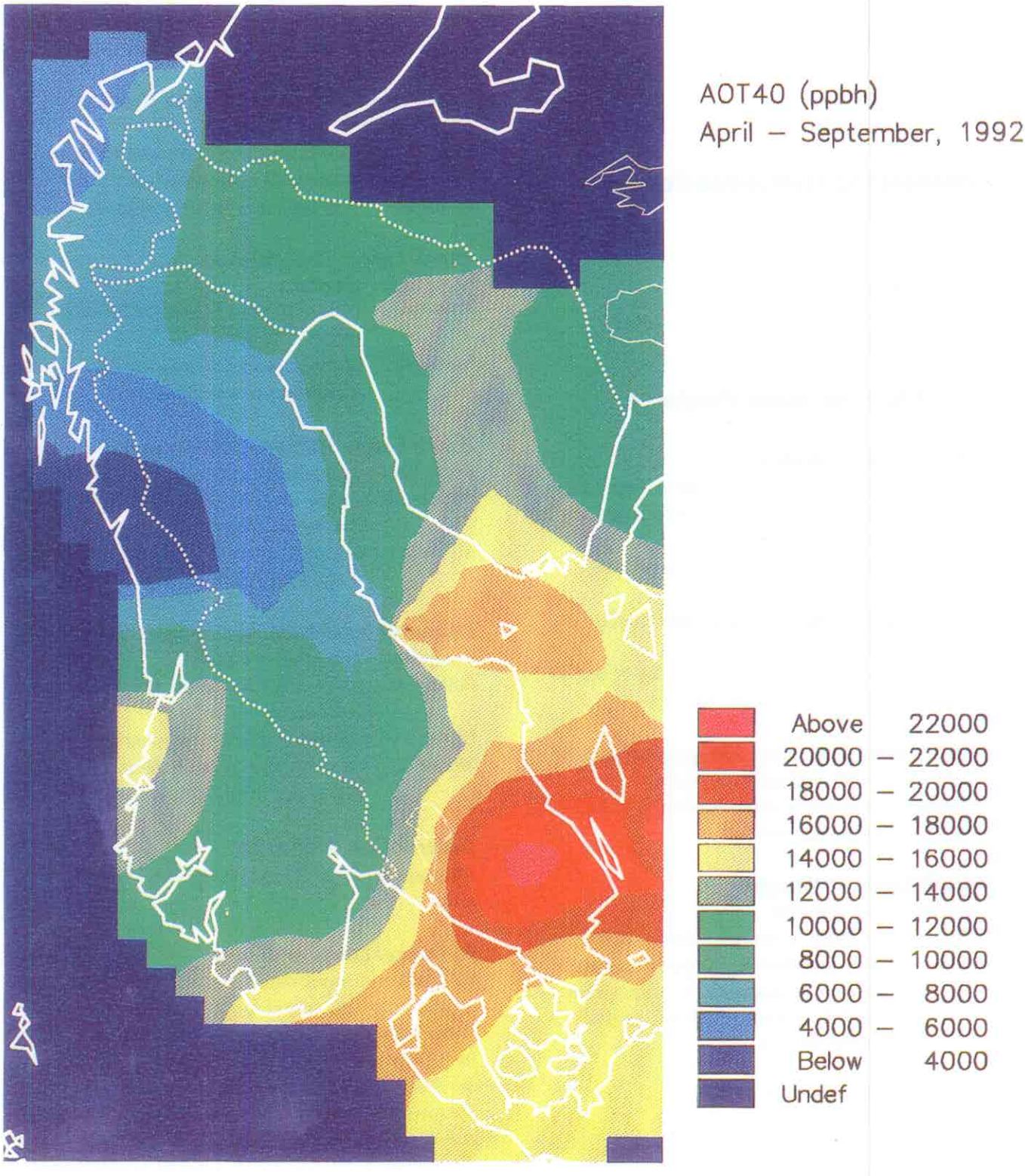


**Figure SE-4.** Exceedance of critical level of ozone (AOT 40) for forests.

# SWITZERLAND

## National Focal Center/Contact:

Mr. Beat Achermann
Federal Office of Environment, Forests and Landscape
Air Pollution Control Division
CH-3003 Bern
tel: 41-31-322.99.78
fax: 41-31-382.15.46

## Collaborating Institutions/Contacts:

Mr. Beat Rihm
METEOTEST
Fabrikstrasse 29
CH-3012 Bern
tel: 41-31-301.74.17
fax: 41-31-301.42.64

## List of National Maps Produced:

### Critical Loads of Acidity

Receptors: forest soils and sensitive alpine lakes
Pollutants: acidifying S and N compounds (eq $ha^{-1}$ $yr^{-1}$)
Method: steady state mass balance (SMB)

### Critical Loads of Nutrient Nitrogen (SMB)

Receptors: managed forests
Pollutants: nutrient N compounds (kg N $ha^{-1}$ $yr^{-1}$)
Method: steady state mass balance

### Critical Loads of Nutrient Nitrogen (empirical)

Receptors: (semi-)natural ecosystems
Pollutants: nutrient N compounds (kg N $ha^{-1}$ $yr^{-1}$)
Method: empirical method

### Present Loads of Nitrogen

Receptors: 1x1 km grid
Pollutants: nutrient N compounds (kg N $ha^{-1}$ $yr^{-1}$)
Method: concentration and deposition data, resistance analogue dry deposition models, statistic methods, spatial interpolations

### Present Loads of Sulfur

Receptors: 1x1 km grid
Pollutants: S compounds (eq $ha^{-1}$ $yr^{-1}$)
Method: concentration and deposition data, resistance analogue dry statistic methods, spatial interpolations

### Exceedance of Critical Loads of Acidity

Receptors: forest soils and sensitive alpine lakes
Pollutants: acidifying S and N compounds (eq $ha^{-1}$ $yr^{-1}$)
Method: present loads vs. critical loads

### Exceedance of Critical Loads of Nutrient Nitrogen

Receptors: forests and (semi-)natural ecosystems
Pollutants: nutrient N compounds (kg N $ha^{-1}$ $yr^{-1}$)
Method: present loads vs. critical loads

### Ozone Levels 1992 (forests)

Receptors: forests
Pollutants: ozone, AOT40 values (24 hours, 6 months, (ppm h)
Method: altitude functions and inverse-distance-weighting interpolations

### Ozone Levels 1992 and 1994 (crops)

Receptors: agricultural crops
Pollutants: ozone, AOT40 values (daylight hours, 3 months, (ppm h))
Method: altitude functions and inverse-distance-weighting interpolations

### Corrected Yield Reduction in heat, 1992 & 1994

Receptors: agricultural crops
Pollutants: ozone, AOT40 values (daylight hours, 3 months)
Units: relative reduction, percentage
Method: dose-response relationship, including soil water availability

## Calculation Methods:

All maps were produced on the basis of a 1x1 km grid.

### (1) Critical Loads of Acidity

Methods and input data for mapping critical loads of acidity are described in detail in FOEFL (1994). There have been no changes since the Status Report 1993. For forest soils, both the Al:BC criterion and the Al-depletion criterion were applied and then the lower of the two calculated critical load values was chosen on a grid cell by grid cell basis.
The equation for the critical load of acidity based on the Al:BC criterion is, according to UBA Vienna (1993):

$$CL(A) = BC_w + \left( 1.5 \cdot \frac{0.8 \cdot BC_w + BC_d - BC_u - 0.015 \cdot Q}{200} \right)^{1/3} \cdot Q^{2/3}$$
$$+ 1.5 \cdot (0.8 \cdot BC_w + BC_d - BC_u - 0.015 \cdot Q)$$

Applying the Al-depletion criterion, the limiting aluminum flux $Al^{3+}_{limit}$ is determined by the amount of aluminum produced by weathering, $Al_w$. Al leaching is not allowed to be in excess of $Al_w$. $Al_w$ is related to the weathering of base cations through the stoichiometric composition of the minerals of the particular soil. Typical $Al_w$:$BC_w$ ratios are in the range from 1.0 to 3.0. For the present calculation a value of 1.5 was taken:

$$CL(A) = 2.5 \cdot BC_w + \left( 1.5 \frac{BC_w}{K_{gibb}} \right)^{1/3} \cdot Q^{2/3}$$

For small lake catchments the SMB method was applied as follows. The ecological criterion for lakes is a critical alkalinity concentration of 0.02 eq $m^{-3}$:

$$CL(A) = BC_w(catch) - 0.02 \cdot Q$$

where:
$BC_w(catch)$ = weathering of base cations on the whole path (not only the root zone) which the runoff percolates (eq $ha^{-1}$ $yr^{-1}$).

### (2) Critical Loads of Nutrient Nitrogen (SMB):

The following SMB equation proposed in the mapping manual was applied for 10,393 sampling points of the Swiss National Forest Inventory. Only points representing managed forests are included:

$$CL_{nut}(N) = N_{u(crit)} + N_{i(crit)} + N_{l(crit)} / ( 1 - f_{de} )$$

### (3) Critical Loads of Nutrient Nitrogen (empirical):

Table CH-1 shows the ecosystems that are mapped in Switzerland, as well as the corresponding critical load of nitrogen values chosen within the proposed ranges. For the map the critical load value was computed on a grid cell by grid cell basis in the 1 x 1 $km^2$ grid by taking the lowest value from Table CH-1 that occurs in a specific grid cell.

### (4) Present Loads of Nitrogen:

The following compounds were considered for the calculation of present loads of nitrogen PL(N):

$$PL(N) = PL(NO_3^-, HNO_3^-, NO_2, NH_4^+, NH_3)$$

There are not many places where the deposition of those compounds was measured. Thus the present loads cannot directly be mapped on the basis of deposition measurements for the whole country with the required resolution of 1 x 1 $km^2$. Rather the various mechanisms of deposition are investigated and modeled separately. The deposition rates on the various deposition paths are quantified by straightforward analogy models, ie. the unknown spatial pattern of deposition is assessed by relating deposition parameters (eg. deposition velocity, pollutant concentrations) to geographical parameters that are known all over the country (eg. land use, topography). Models were developed for wet and dry deposition resulting in deposition maps for the period from 1986 to 1990. They are described in detail in FOEFL (1994).

### (5) Present Loads of Sulfur:

Similar models were applied as for present loads of nitrogen, including the compounds:

$$PL(S) = PL(SO_4^{2-}, SO_2)$$

### (6) Exceedance of Critical Loads of Acidity:

In accordance to the mapping guidelines the exceedance of critical loads of acidity was computed as:

$$Ex(A) = PL(S) + PL(N) - BC_{dep} - CL(A)$$

The high-resolution exceedance maps were produced for national purposes and for comparison with European exceedance maps, which are based on EMEP deposition data.

(7) Exceedance of Critical Loads of Nutrient Nitrogen
Present loads are used to compute exceedances of the critical load of nutrient nitrogen as follows:
$Ex_{nut}(N) = PL(N) - CL_{nut}(N)$

**Table CH-1.** The empirical method: selected ecosystems, corresponding critical loads of nitrogen for vegetation types in Switzerland (kg N $ha^{-1}$ $yr^{-1}$) and area of their occurrence ($km^2$).

| Ecosystem[1] | Critical load range[1] | Relevant vegetation types in Switzerland[2] | Critical load selected | Area ($km^2$) |
|---|---|---|---|---|
| Acidic (managed) coniferous forest | 10-20 | Molinio-Pinetum *(Pfeifengras-Föhrenwald)* | 17 | 333 |
| | | Ononido-Pinion *(Hauhechel-Föhrenwald)* | 12 | 361 |
| | | Cytiso-Pinion *(Geissklee-Föhrenwald)* | 12 | 17 |
| | | Calluno-Pinetum *(Heidekraut-Föhrenwald)* | 12 | 124 |
| Acidic (managed) deciduous forest | 15-20 | Quercion robori-petraeae *(Traubeneichenwald)* | 15 | 68 |
| Calcareous forests | 15-20 | Quercion pubescentis *(Flaumeichenwald)* | 15 | 633 |
| | | Fraxino orno-Ostryon *(Mannaeschen-Hopfenbuchwald)* | 15 | 28 |
| | | Erico-Pinion mugi (Ca) *(Erika-Bergföhrenwald auf Kalk)* | 15 | 592 |
| | | Erico-Pinion sylvestris *(Erika-Föhrenwald )* | 15 | 956 |
| Lowland dry heathland | 15-20 | none | | |
| Lowland wet heathland | 17-22 | none | | |
| Species-rich lowland heaths / acid grassland | 7-20 | so far not mapped | | |
| Arctic and alpine heaths | 5-15 | so far not mapped | | |
| Calcareous species-rich grassland | 14-25 | Mesobromion (erecti) *(Trespen-Halbtrockenrasen)* | 19 | 2686 |
| Neutral-acid species-rich grassland | 20-30 | Molinion (caeruleae) *(Pfeifengrasrieder)* | 25 | 612 |
| Montane-(sub)alpine grassland | 10-15 | Chrysopogonetum grylli *(Goldbart-Halbtrockenrasen)* | 15 | 6 |
| | | Seslerio-Bromion (Koelerio-Seslerion) *(Blaugras-Trespen-Halbtrockenrasen)* | 12 | 2198 |
| | | Festucetum paniculatae *(Goldschwingelrasen)* | 12 | 39 |
| | | Stipo-Poion molinerii *(Engadiner Steppenrasen)*, alpine | 10 | 523 |
| | | Elynion *(Nacktriedrasen)*, alpine | 10 | 836 |
| | | Seslerion (variae) *(Blaugrashalden)*, alpine | 10 | 5545 |
| | | Caricion ferrugineae *(Rostseggenhalden)*, alpine | 10 | 4046 |
| Shallow soft-water bodies | 5-10 | Littorellion *(Strandling-Gesellschaften)* | 8 | 49 |
| Mesotrophic fens | 20-35 | Scheuchzerietalia *(Scheuchzergras)* | 20 | 580 |
| | | Caricion fuscae *(Braunseggenried)* | 25 | 2240 |
| | | Caricion davallianae *(Davallsseggenried)* | 25 | 2986 |
| Ombrotrophic bogs | 5-10 | Sphagnion fusci *(Hochmoor)* | 8 | 902 |

[1]References: Grennfelt and Thörnelöf 1992, WHO/EURO 1995.
[2]References: Hegg *et al.* 1993, EDI 1991, WSL 1993.

### *(8) Ozone Levels 1992 (forests)*

A map showing AOT40 ozone levels for forests, as defined at the UN/ECE Workshop on Critical Levels for Ozone in Berne (Fuhrer and Achermann 1994), was produced for 1992. The map is based on the AOT40 levels calculated from measured hourly ozone values. Switzerland is divided into four regions, which have different ozone regimes: North, Alps, Valais and Ticino. Within each region the AOT40 values are spatially interpolated between the monitoring stations by using altitude functions, empirical relations to $NO_2$ concentrations and by applying an inverse-distance-weighting algorithm. Cities and agglomerations are calculated separately from rural areas. The maps are produced with a resolution of 0.5 x 0.5 km$^2$.

### *(9) Ozone Levels 1992 and 1994 (crops)*

Maps showing AOT40 ozone levels for crops, as defined at the UN/ECE Workshop on Critical Levels for Ozone in Berne, were produced for 1992 and 1994 in a similar way as for forests.

### *(10) Corrected Yield Reduction in Wheat 1992 and 1994*

The maps of potential yield reduction in wheat can be derived directly from the AOT40 maps by applying an empirical linear relationship between AOT40 and relative yield reduction (Fuhrer and Achermann 1994). In order to estimate realistic yield reductions in wheat the potential yield reduction is corrected by a factor derived for the soil water availability during the growth period (Fuhrer 1995). The correction factor is calculated as a function of the mean temperature, the mean solar radiation and the precipitation sum in June and July of the specified year.

## *Data Sources:*

### *(1) Critical Loads of Acidity*

Since 1993 there have been no changes in input data used for calculating critical loads of acidity. Therefore only a short summary is given here.

$BC_{si}$: Classification of soil types on the basis of a soil map 1:500,000 with 23 categories (L+T 1984). Corrections for calcareous soils utilizing pH measurements from the National Forest Inventory (EAFV 1988). The NFI is a 1 x 1 km$^2$ database containing various information on soils and forests for 11,863 sampling points.

$BC_{dep}$: EMEP data and dry deposition factors.

$BC_u$: Long-term wood harvesting rates for five different regions are multiplied by mean element contents in stems.

$Q$: calculated as precipitation minus evapotranspiration. Average precipitation values are available in a 1 x 1 km$^2$ grid from the Hydrological Atlas of Switzerland (National Hydrological and Geological Survey 1992). Evapotranspiration was calculated using altitude functions for three different climate zones. A digital elevation model is available in a 250 x 250 m$^2$ grid from the Federal Office for Statistics (GEOSTAT).

### *(2) Critical Loads of Nutrient Nitrogen (SMB)*

$N_{u(crit)}$: derived from the long-term wood harvesting rate; the range is from 0.7-7.0 kg N ha$^{-1}$ yr$^{-1}$.

$N_{i(crit)}$: set according to the mapping guidelines (where a range of 2-5 kg N ha$^{-1}$ yr$^{-1}$ is proposed) as follows: 3 kg N ha$^{-1}$ yr$^{-1}$ at low altitudes, increasing up to 5 at high altitudes (> 1500 m a.s.l.). In the 1993 version these values were in the range of 1-3 kg N ha$^{-1}$ yr$^{-1}$.

$N_{l(crit)}$: set according to the mapping guidelines: 4 kg N ha$^{-1}$ yr$^{-1}$ for coniferous forests, 5 kg N ha$^{-1}$ yr$^{-1}$ for deciduous forests. The forest classification was taken from the National Forest Inventory.

$f_{de}$: set to 0.3 for dry soils, 0.5 for moist soils, 0.7 for moderately wet soils and 0.8 for wet soils. The soil classification was taken from the National Forest Inventory.

### *(3) Critical Loads of Nutrient Nitrogen (empirical)*

In order to apply the empirical method in Switzerland the following data bases, which are available in digital form, have been used.

- Atlas of Vegetation Types Worthy of Protection (Hegg *et al.* 1993):

This atlas contains the spatial distribution of 97 vegetation types with a resolution of 1 x 1 km$^2$. 19 vegetation types sensitive to eutrophication were selected and assigned to one of the ecosystem types shown in Table CH-1.

Since the forest vegetation types addressed in Table CH-1 are in general poorly managed and contain an especially rich ground flora, the critical loads for these types were set near to the lower values of the proposed ranges.

For the ecosystem type "montane-subalpine grassland" alpine vegetation types were also selected. Their critical loads were set to 10 kg N ha$^{-1}$ yr$^{-1}$.

• Federal Inventory of Fenlands of National Importance:
This data set is available in vector format at the Swiss Federal Institute for Forest, Snow and Landscape Research (WSL 1993). It contains the geographic distribution of fenlands at a scale of 1:25,000. For this application only the mesotrophic fens are selected and rasterized into a 1 x 1 $km^2$ grid, as shown in Table CH-1. Eutrophic fens are omitted. Scheuchzerietalia was set to 20 kg N $ha^{-1}$ $yr^{-1}$ since it is nearer to an oligotrophic ecosystem.

• Federal Inventory of Raised and Transitional Bogs of National Importance (EDI 1991):
The geographic distribution of raised bogs was mapped at a scale of 1:25,000 and digitized in vector format. These maps are published by EDI 1991 as an annex to the corresponding Federal Ordinance on the Protection of Raised Bogs. The inventory contains only bogs with relevant occurrences of *sphagnion fusci*. For the application in the empirical method the outlines of all objects in the inventory were rasterized into a 1 x 1 $km^2$ grid.

### *(4), (5) Present Loads of Nitrogen and Sulfur*

Wet deposition is related to the precipitation amounts (Hydrological Atlas). On the basis of various wet deposition measurements (Förderer *et al.* 1991), the altitude dependencies of pollutant concentrations in precipitation are estimated. Dry depositions of aerosols, $SO_2$ and $NO_2$ are computed by combining land use dependent deposition velocities and pollutant concentration fields (annual means). The concentration fields are calculated as a function of (1) settlement density, (2) altitude, (3) distance to main roads/motorways and (4) traffic density on those roads. Settlement data were obtained from a land use database of the Federal Office of Statistics (GEOSTAT) with a resolution of 1 ha.

The dry depositions of $NH_3$ are related to the spatial distribution of agricultural livestock. These data are available per municipality (BFS 1986). They were rasterized to 1 x 1 $km^2$ utilizing the land use data for clipping non-agricultural areas.

### *(8), (9), (10) Ozone Maps*

For this mapping exercise the raw data of more than 80 stations of the national and cantonal monitoring networks (BUWAL 1993) have been compiled in order to calculate AOT40 values. Half of those stations represent rural sites.
The meteorological parameters needed to calculate the soil water availability are mapped on the basis of 64 Anetz monitoring stations of the Swiss Meteorological Institute (SMA 1994a,b). For the spatial interpolation specific methods are used, which were developed for Meteonorm (BEW 1995). They include altitude dependencies for different climatic regions as well as local temperature variations due to large lakes, exposition etc.

## *Comments and Conclusions:*

• Critical loads of nutrient nitrogen: For the Swiss input to the European map the results of the SMB and the empirical method were merged by choosing the lowest value on a (1 x 1 $km^2$) grid cell by grid cell basis. From the resulting data set the cumulative frequency distribution functions are formed for each EMEP grid cell.
• The values for critical loads of nutrient nitrogen (SMB) are somewhat higher compared with 1993, mainly due to increases of $N_i$ values after cross-border discussions with the NFCs of Germany and Austria.
• Critical loads of acidity have not changed since 1993.
• CLmin(N) for alpine lake catchments, which are mainly covered by grassland, has been set to 2 kg N $ha^{-1}$ $yr^{-1}$, instead of 0, in order to take into account $N_i$ and $N_u$.
• There are no longer national data submitted for the EMEP cells 2212 and 2414, as their Swiss portion is very small.
• Ozone critical levels and exceedance maps for crops and forests are ready to be submitted the CCE and to be compared with modeled data by EMEP.

## *References:*


BEW (ed.), 1995. METEONORM Ausgabe 1995 - Meteorologische Grundlagen für die Sonnenenergienutzung. Bundesamt für Energiewirtschaft, Berne.

BFS, 1986. Eidgenössische Betriebszählung 1985 - Nutztierbestände der Landwirtschaftsbetriebe 1985. Federal Office of Statistics (BFS), Berne.

BUWAL (ed.), 1993. Immissionsmesswerte 1992. Umwelt-Materialien Nr. 1. Bundesamt für Umwelt, Wald und Landschaft, Berne. 430 p.

EAFV, 1988. National Forest Inventory ("Schweizerisches Landesforstinventar, Ergebnisse der Erstaufnahme 1982-1986"). Eidgenössische Anstalt für das forstliche Versuchswesen (today WSL), Bericht Nr. 305, Birmensdorf.

EDI, 1991. Bundesinventar der Hoch- und Uebergangsmoore von nationaler Bedeutung. (Federal Inventory of Raised and Transitional Bogs of National Importance). Appendix to the

Federal Ordinance on the Protection of Raised Bogs. Eidgenössisches Departement des Innern (EDI), Berne.
FOEFL, 1994. Critical Loads of Acidity for Forest Soils and Alpine Lakes - Steady State Mass Balance Method. Environmental Series No. 234, Federal Office of Environment, Forests and Landscape, Berne, 68 p.
Förderer L. *et al.*, 1991. Depositionsdatensätze in der Schweiz. ökoscience. Interner Bericht des Bundesamtes für Umwelt, Wald und Landschaft (BUWAL), Berne.
Fuhrer J. and Achermann B. (eds.), 1994. Critical Levels for Ozone. A UN-ECE workshop report. Schriftenreihe FAC Nr. 16. Berne-Liebefeld. 328 pp.
Fuhrer J., 1995. Critical Levels for Ozone to Protect Agricultural Crops: Interaction with Water Availability. Acid Reign '95, 5th International Conference on Acidic Deposition, 26-30 June 1995, Göteborg, Sweden. *Water Air Soil Pollut.*, (in press).
Hegg O., Béguin C., Zoller H., 1993. Atlas schutzwürdiger Vegetationstypen der Schweiz (Atlas of Vegetation Types Worthy of Protection in Switzerland). Edited by Federal Office of Environment, Forests and Landscape, Berne.
Grennfelt P., Thörnelöf E. (eds.), 1992. Critical Loads for Nitrogen - Report from a workshop held at Lökeberg, Sweden 6-10 April 1992. NORD Miljörapport 1992:41, Nordic Council of Ministers, Copenhagen.
L+T, 1984. Atlas of Switzerland. 2nd edition 1984. Federal Office of Topography (L+T), Wabern-Berne.
National Hydrological and Geological Survey, 1992. Hydrological Atlas of Switzerland. Edited on behalf of the Swiss Federal Council, Bern.
SMA, 1994a. Annalen der Schweizerischen Meteorologischen Anstalt, 129. Jahrgang 1992. Zürich.
SMA, 1994b. Meteorologische Monatsberichte Jan-Dez 1994. Schweizerische Meteorologische Anstalt, Zürich.
UBA Vienna, 1993. Critical Loads of Acidity for High Precipitation Areas. Results from a Workshop held in Vienna, March 9-10, 1992. Umweltbundesamt Wien.
WSL, 1993. Federal Inventory of Fenlands of National Importance. Pers. commun. from A. Grünig and P. Schönenberger, Swiss Federal Institute for Forest, Snow and Landscape Research, Birmensdorf. Will be published as an Appendix to a Federal Ordinance 1995/96.

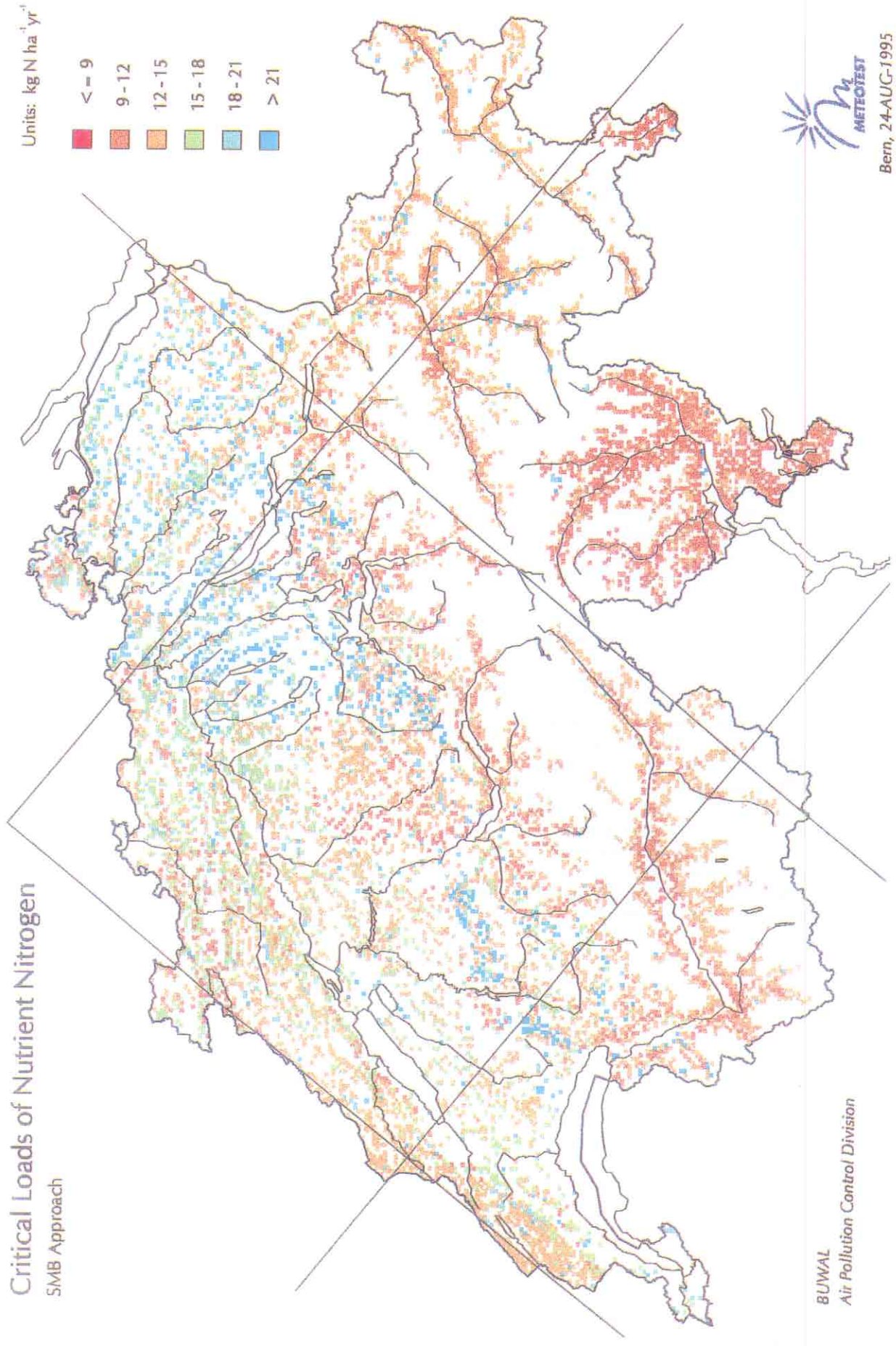


**Figure CH-1.** Critical Loads of Nutrient Nitrogen (SMB).

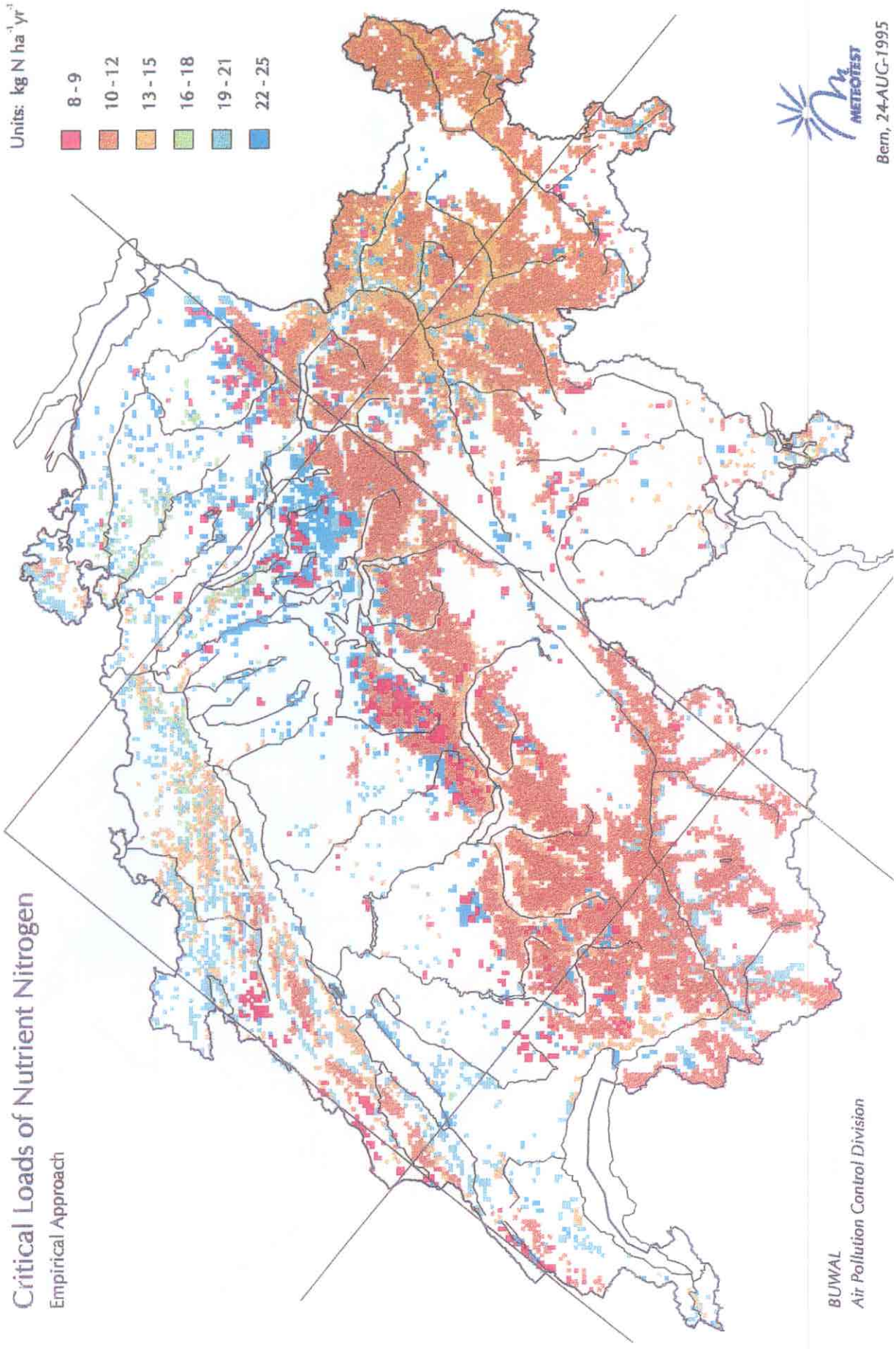


**Figure CH-2.** Critical Loads of Nutrient Nitrogen (empirical approach).

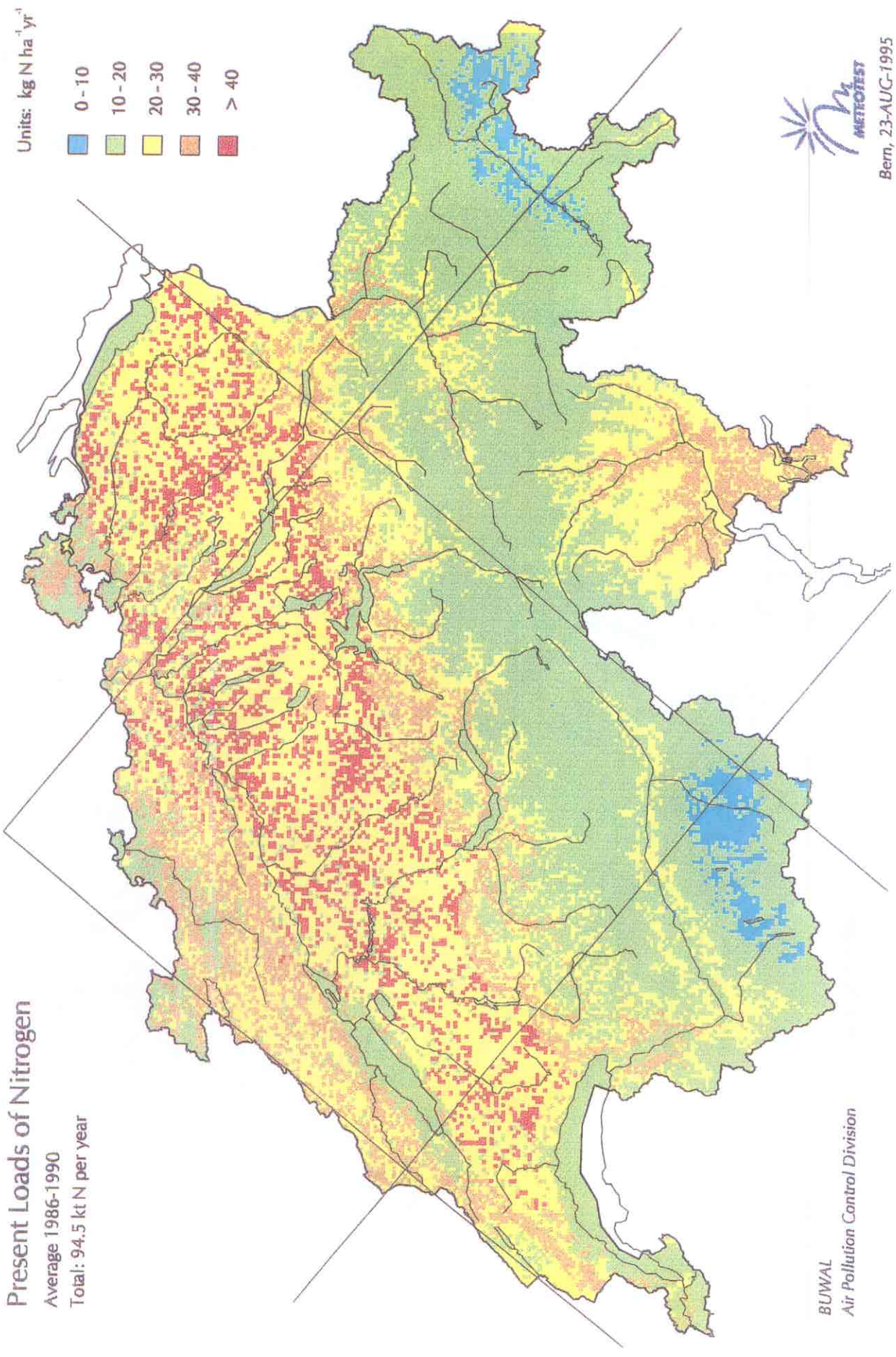


**Figure CH-3.** Present Loads of Nitrogen.

# UNITED KINGDOM

## *National Focal Center:*

Jane R. Hall (NFC primary contact)
Michael J. Brown, Helen Dyke, Jackie Ullyett
Environmental Information Centre
Institute of Terrestrial Ecology
Monks Wood
Abbots Ripton
Huntingdon PE17 2LS
tel: +44 1487 773381
fax: +44 1487 773467
email: J.Hall@ite.ac.uk

## *Collaborating Institutions/Contacts:*

Prof. Michael Hornung (Soils)
Institute of Terrestrial Ecology
Merlewood
Windermere Road
Grange-over-Sands
Cumbria LA11 6JU
tel: +44 15395 32264
fax: +44 15395 35226
email: M.Hornung@ite.ac.uk

Prof Rick Battarbee (Freshwaters)
Environmental Change Research Centre
Department of Geography
University College London
26 Bedford Way
London WC1H 0AP
tel: +44 171 380 7582
fax: +44 171 380 7565

Dr Michael Ashmore (Vegetation/Levels)
Centre of Environmental Technology
Imperial College London
48 Prince's Gardens
London SW7 2PE
tel: +44 171 594 9291
fax: +44 171 581 0245

Prof David Fowler (Deposition)
Institute of Terrestrial Ecology
Bush Estate
Penicuik
Midlothian EH26 0QB
tel: +44 131 445 4343
fax: +44 131 445 3943
email: D.Fowler@ite.ac.uk

Dr Sarah Metcalfe (HARM modelled deposition)
Department of Geography
University of Edinburgh
Drummond Street
Edinburgh EH8 9XP
tel: +44 131 650 8162
fax: +44 131 650 2524
email: SEM@geovax.ed.ac.uk

Dr Alan Jenkins (Dynamic modelling)
Institute of Hydrology
Maclean Building
Crowmarsh Gifford
Wallingford
Oxfordshire OX10 8BB
tel: +44 1491 838800
fax: +44 1491 692424
email: A.Jenkins@ioh.ac.uk

## *List of national maps produced:*

*Critical loads - acidity/sulfur*

(i) Critical loads and exceedances of acidity for soils (empirical).
(ii) Critical loads and exceedances of acidity for soils (simple mass balance) for 3 soil-vegetation systems (acid grassland, heathland, woodland).
(iii) Critical loads and exceedances of sulphur for freshwaters (Diatom model and Henriksen steady-state water chemistry model).
(iv) Critical loads and exceedances of acidity for freshwaters (Diatom model and Henriksen steady-state water chemistry model).
(v) Exceedance classes using the Critical Loads Function (CLF).
(vi) Critical loads of acidity for freshwaters (First-order Acidity Balance), in progress.

*Critical loads - nitrogen*

(i) Critical loads of nutrient nitrogen for 14 terrestrial ecosystems (empirical)
(ii) Critical loads of nutrient nitrogen for soils (mass balance) for 3 soil-vegetation systems (acid grassland, heathland, woodland)
(iii) Exceedances of the above critical loads by oxidised and reduced nitrogen deposition

*Critical Levels*

(i) Receptor vegetation maps showing the percentage areas of agriculture, arable, forestry, forestry and semi-natural vegetation, heathland, herbaceous semi-natural vegetation, all grasslands, semi-natural vegetation.

(ii) Receptor species maps showing the presence of green lichens, cyanobacterial lichens and the bryophyte *Pleurozium schreberi.*

(iii) Exceedances of the critical level of $SO_2$ for forestry and natural vegetation and for agricultural land.

(iv) Exceedances of the critical level of $NO_x$ for forestry and for natural vegetation.

(v) Exceedance of the critical level of ozone (5300 ppb.h) for arable crops, for herbaceous semi-natural vegetation and for wheat.

(vi) Exceedance of the critical level of ozone (10000 ppb-h) for forestry.

## Calculation methods:

### 1. Critical loads of acidity for soils (empirical)

This method has been described in detail by Hettelingh *et al.* (1991), Downing *et al.* (1993), and Hornung *et al.* (in press). The map has now been extended to incorporate 1km data for Northern Ireland. The map has been used to provide weathering rate ($ANC_W$) data for the simple mass balance calculations (see below).

### 2. Critical loads and exceedances of acidity for soils (simple mass balance equation)

The simple mass balance (SMB) model has been used to calculate critical loads of acidity for three soil-vegetation ecosystems ie acid grassland, heathland and woodland. In each case, values are calculated for each 1-km square of the UK assuming the ecosystem occurs in all squares. A land cover map derived from Landsat satellite imagery for Great Britain (Fuller *et al.* 1994), together with CORINE land cover data for Northern Ireland provides the information on ecosystem areas for the calculation of percentile critical loads. Further information on the simple mass balance model is described by Sverdrup *et al.* (1995). The form of the SMB equation used in the UK is as follows:

$$CL(A) = ANC_w + \frac{1.5 \cdot BC_{le}}{BC:Al} + \left( \frac{1.5 \cdot BC_{le}}{BC:Al \cdot K_{gibb}} \right)^{1/3} \cdot Q^{2/3}$$

$CL(A)$ = critical load of acidity
$ANC_w$ = acid neutralizing capacity
$BC_{le}$ = base cation leaching = $BC_a - BC_u$
$BC_a$ = base cation availability
$BC_a = max\ \{0.8 \cdot ANC_w + BC_{dep} - BC_{le(min)}), 0\}$
$BC_{dep}$ = non-marine base cation (Ca+Mg) deposition
$BC_{le(min)}$ = minimum base cation leaching
$BC_{le(min)} = Q * BC_l * 0.01$
$Q$ = runoff
$BC_l$ = limiting concentration for uptake of base cations
$BC_u$ = net uptake of base cations
$BC_u = min\ \{BC_u max, BC_a\}$
$BC_u max$ = maximum uptake of base cations
$BC_u max = (u \cdot yc) / 8$
$u$ = base cation uptake
$yc$ = yield class
$K_{gibb}$ = gibbsite coefficient
$BC:Al$ = base cation to aluminium ratio

**Table UK-1.** The specific values used in the UK for some of the parameters.

| Parameter | acid grassland | heathland | woodland |
|---|---|---|---|
| $BC_l$ | 2 μeq $l^{-1}$ | 2 μeq $l^{-1}$ | 2 μeq $l^{-1}$ |
| $Q$ | 1km data | 1km data | 1km data |
| $u$ | 0.0 | 0.0 | 0.278 |
| $yc$ | – | – | 10 |
| $K_{gibb}$ | 1 x $10^{8.5}$ | 1 x $10^{8.5}$ | 1 x $10^{8.5}$ |
| $BC:Al$ | 1.0 | 2.5 | 1.4 |
| $BC_{dep}$ | 20km low vegetation estimates | | 20km woodland estimates |
| $ANC_w$ | value from middle of Skokloster class range (ie 0.1, 0.35, 0.75, 1.5, 4.0 keq $H^+$ $ha^{-1}$ $year^{-1}$), except for squares dominated by peat, which are set to zero | | |

Exceedance maps have been calculated in the UK using national deposition data (20km resolution) comprising estimates for "low vegetation" and for woodland. The deposition values used are matched to the ecosystem type defining the critical load in each grid square ie low vegetation estimates for acid grassland and heathland soil-ecosystems, and woodland estimates for woodland soil-ecosystems.

### 3. Henriksen steady-state water chemistry model for freshwaters

The methods of freshwater sampling and calculation of critical loads for sulphur using the steady-state water chemistry (SSWC) model in the UK are described elsewhere (Battarbee *et al.* 1995, Downing *et al.* 1993). The maps of these data at 10km resolution for the UK have been completed and validated in the last year (Curtis, in press). The SSWC model has since been modified using the method developed by Kämäri *et al.* (1992) to determine critical loads for total acidity ie including the effects of nitrogen. This model has been applied using the water chemistry database of the freshwaters sampled for calculating sulphur critical loads (Harriman *et al.* 1995). Preliminary exceedance maps are similar to those for sulphur indicating that nitrogen impacted sites are generally in the same areas of the UK as those affected by sulphur. Although the distribution of exceeded squares remains relatively unchanged, the exceedance values tend to be greater (Harriman *et al.* 1995).

### 4. Diatom model for freshwaters:

The methods of freshwater sampling and calculation of critical loads for sulphur using the Diatom model in the UK are described elsewhere (Battarbee *et al.* 1995, Downing *et al.* 1993). The maps of these data at 10km resolution for the UK have been completed and validated in the last year (Curtis, in press). The Diatom model is currently being adapted to provide critical loads and exceedances for total acidity. The methods for deriving preliminary maps using the site data already collected are described by Allott *et al.* (1995) and Harriman *et al.* (1995). The increase in exceedance due to the inclusion of leached nitrogen deposition demonstrates that for large parts of the UK nitrogen deposition could account for significant exceedances (Allott *et al.* 1995).

### 5. First-order acidity balance (FAB) model for freshwaters

This model is based on an acidity mass balance and includes rate-limited processes for denitrification and in-lake retention which are assumed to increase with increasing nitrogen inputs. In the UK, the model has been applied to the 23 sites of the Acid Waters Monitoring Network and also to 527 of the 1573 waters sampled for the national freshwater critical loads survey. Data for the 527 sites have been submitted to the CCE. The work programme for the current year includes digitising catchment information for all 1573 sites, to provide catchment and forest areas and lake:catchment ratios, so that FAB may be applied to all sites. The equation for FAB is as follows:

$$N_{dep} + S_{dep} = fN_u + (1 - r)(N_i + N_{de}) + rN_{ret} + rS_{ret} + BC_l - ANC_l$$

where:
$N_{dep}$ = deposition of nitrogen
$S_{dep}$ = deposition of sulphur
$N_u$ = net growth uptake of nitrogen by vegetation
$N_i$ = immobilization of N in the catchment soils
$N_{de}$ = nitrogen denitrified in the catchment soils
$N_{ret}$ = in-lake retention of nitrogen
$S_{ret}$ = in-lake retention of sulphur
$BC_l$= base cations leaching from the catchment
$ANC_l$ = ANC leaching from the catchment
$f$ = fraction of forested area in the catchment
$r$ = lake:catchment area ratio

The variable $N_{de}$ is currently derived using a linear interpolation using the fraction of peat soils in the catchment. Default values are currently used for $N_u$ and $N_i$. In the future these variables will employ the same values used for calculating mass balance critical loads of nutrient nitrogen for soils. National data (20km) provide the values for sulphur and nitrogen deposition. Base cation leaching and ANC leaching values are derived using the Henriksen SSWC model. The fraction of forested area within the catchment and the lake:catchment area ratio are currently estimated, but will be derived using a geographic information system (GIS) once catchment boundaries are digitised. The remaining input variables can be estimated from additional information or set to fixed values. The model is described in more detail by Harriman *et al.* (1995), Kämäri *et al.* (1992), Posch *et al.* (1993b) and Henriksen *et al.* (1993).

### 6. Critical loads of nutrient nitrogen for 14 terrestrial ecosystems (empirical)

Work on mapping critical loads of nutrient nitrogen has continued in the UK using the empirical methods proposed at both the Lokeberg (Grennfelt and Thörnelöf, 1992) and Grange-over-Sands(Hornung *et al.* 1995) workshops. For each vegetation ecosystem a range of critical loads values have been defined and for some of these a single mapping value has also been suggested (Hornung *et al.* 1995). These values have been mapped for the UK by identifying the geographic distribution of the different ecosystems by combining the information from three data sets, the first two of which are held at ITE Monks Wood:

(i) the Land Cover Map of Great Britain, derived from Landsat satellite imagery (Fuller *et al.* 1994) shows the distribution of 25 land cover types, with statistics at 1km resolution;

(ii) the Biological Records Centre (BRC) maintains a database on the distribution of individual species in the UK, mapped at 10km resolution;

(iii) the National Vegetation Classification (NVC) identifies vegetation communities and their species compositions (Rodwell, 1991a, 1991b, 1992, 1994).

The methods used for mapping are also described by UKRGIAN (1994), Hall *et al.* (1995) and Bull *et al.* (in press). Critical loads of nutrient nitrogen for ecosystems found in soil-acid grassland and soil-heathland ecosystems using the empirical approach have been forwarded to the CCE. Data submitted for woodland ecosystems are based on the mass balance approach (see below).

### 7. Critical loads of nutrient nitrogen for soil-vegetation ecosystems (mass balance)

The mass balance approach to calculating critical loads of nutrient nitrogen has been used for three soil-vegetation ecosystems in the UK ie acid grassland, heathland and woodland (UKRGIAN, 1994, Bull *et al.* in press). In each case, values are calculated for each 1km square of the country assuming the ecosystem occurs in all squares. Using the same land cover data for Great Britain (derived from Landsat satellite imagery) as described above for acidity critical loads, ecosystem areas are defined enabling percentile nutrient nitrogen critical loads to be determined. The mass balance equation recommended at the Grange workshop is as follows:

$$CL_{nut}N = N_{l(crit)} + N_{i(crit)} + N_{u(crit)} + N_{de(crit)} - N_{fix(crit)} + N_{fire(crit)} + N_{erode(crit)} + N_{vol(crit)}$$

where:

$N_{l(crit)}$ = critical nitrogen leaching
$N_{i(crit)}$= critical nitrogen immobilization
$N_{u(crit)}$ = critical nitrogen uptake
$N_{de(crit)}$ = denitrification
$N_{fix(crit)}$ = nitrogen fixation
$N_{fire(crit)}$ = nitrogen losses in smoke from fires
$N_{erode(crit)}$ = nitrogen losses through erosion
$N_{vol(crit)}$ = nitrogen losses through volatilisation

Further details on the equation and methods for quantifying the variables are described by Hornung *et al.* (1995). The data for the UK currently held by the CCE are calculated from an earlier equation based on nitrogen leaching, nitrogen immobilization, nitrogen uptake and denitrification only and exclude Northern Ireland. The values used for these parameters are given in Table UK-2; some are fixed values for the whole country and others are values within the ranges shown.

The critical loads may be re-calculated following completion of a UN/ECE database on input variables for a range of ecosystems (Hornung *et al.* 1995). The UK has provided the CCE with mass balance calculated critical loads of nutrient nitrogen for soil-coniferous woodland ecosystems. For deciduous woodland ecosystems the lowest value of either the empirical value for deciduous woodland or the mass balance value for soil-woodland ecosystems has been applied.

### 8. The Critical Loads Function (CLF)

The CLF illustrates the relationship between depositions of sulphur and nitrogen and critical loads. Following the derivation of CL(A) (method 2 above), the following parameters used in the CLF can be determined:

$CL_{max}(S)$ = maximum critical load for sulphur
= $CL(A) + BC_{dep} - BC_u$
$BC_{dep}$ = non-marine base cation (Ca+Mg) deposition (20km)
$BC_u$ = base cation uptake, derived from SMB model

$CL_{min}(S)$ = minimum critical load for sulphur
= $CL_{max}(S) - N_{l(crit)}$
$N_{l(crit)}$ = critical nitrogen leaching, used in deriving $CL_{nut}N$

$CL_{max}(N)$ = maximum critical load for nitrogen
= $CL_{min}(N) + CL_{max}(S)$

**Table UK-2.** The specific values used in the UK for some of the parameters.

| Parameter | acid grassland | heathland | woodland |
|---|---|---|---|
| $N_{l(crit)}$ | 0.14 | 0.14 | 0.43 |
| $N_{i(crit)}$ | 0 to 0.14 | -0.07 to 0.14 | -0.14 to 0.0 |
| $N_{u(crit)}$ | 0.07 | 0.29 | 0.36 |
| $N_{de(crit)}$ | 0.03 to 2.90 | 0.03 to 2.90 | 0.08 to 3.12 |

$CL_{min}(N)$ = minimum critical load for nitrogen
= $N_{u(crit)} + N_{i(crit)}$
$N_{u(crit)}$ = critical nitrogen uptake value, used in deriving $CL_{nut}N$
$N_{i(crit)}$ = critical nitrogen immobilization value, used in deriving $CL_{nut}N$

The guidelines for using the CLF are described by Posch *et al.* (1993a). In the UK these parameters, together with the critical load for nutrient nitrogen ($CL_{nut}N$) have been calculated. From these data, seven classes of protection and exceedance for a CLF are identified (Bull *et al.* 1995):

(i) area of protection - critical loads are not exceeded
(ii) area of "options" - either sulphur or nitrogen reductions can offer protection
(iii) area where sulphur deposition should be reduced - reduction of nitrogen gives no benefits
(iv) area where nitrogen deposition should be reduced - reduction of sulphur gives no benefits
(v) area where sulphur is a major contributor to exceedance - sulphur must be reduced to provide the possibility of options
(vi) area where nitrogen is a major contributor to exceedance - nitrogen must be reduced to provide the possibility of options
(vii) area where sulphur and nitrogen are major contributors to exceedance - both must be reduced before there are options

Maps have been generated to show these seven regions for each soil-vegetation ecosystem using values of current nitrogen and sulphur deposition, and using current nitrogen deposition with modelled sulphur deposition scenarios (using the UK model HARM7.2) for 2005 and 2010. They illustrate the need to reduce emissions of nitrogen to prevent exceedance in some parts of the country, where further reductions of sulphur would give no additional benefits (Bull *et al.* 1995).

### *9. Critical levels - receptor maps and exceedances*

The ITE Land Cover Map (Fuller *et al.* 1994) and database have been used to identify the spatial distribution of a number of receptor vegetation types expressed as percentages of total land cover. The full resolution (25m) land cover data are aggregated to produce receptor maps of Great Britain for 1km, 5km or 20km squares. The scale of the mapping is determined by the scale of the pollutant data available. This method has been used to map the following receptors: arable land, forestry, grassland, natural vegetation, herbaceous semi-natural vegetation and heathlands The classification of receptors utilising the ITE land cover map was not suitable for all the vegetation types for which critical levels have been set. Consequently, additional data were employed in the mapping exercise. Maps showing the percentage areas of wheat and horticulture were derived from agricultural statistics and the ITE Land Classification database (Bunce and Heal, 1984, Barr, 1990). The latter is a 1km database where data are related to 32 land use classes into which the country is divided. The geographical distributions of bryophytes were determined from species presence/absence data on a 10km grid, held by the Biological Records Centre at ITE Monks Wood. Exceedances for the different receptors are illustrated by mapping the percentage area of receptor present within the regions where the critical level of the pollutant (eg $SO_2$, $NO_x$ or ozone) is exceeded. In this way, exceedances of the critical level of ozone for arable crops, for herbaceous semi-natural vegetation and for wheat (5300 ppb.h); and the critical level of ozone for forestry (10000 ppb.h); have been mapped.

## Data sources:

Some of the data sources and specific values used in equations are described above. Additional information on the sources of data are listed below.

***Critical loads of acidity for soils (empirical):*** 1km data assigned to critical loads classes according to the classification defined at the Skokloster workshop (Nilsson and Grennfelt, 1988). Data provided by the Soil Survey and Land Research Centre (England and Wales), the Macaulay Land Use Research Institute (Scotland) and the Department of Agriculture for Northern Ireland.

***Land use and land cover data:*** Four different sources of land use information are used:
(i) The ITE Land Cover Map of Great Britain is derived from Landsat satellite imagery (Fuller *et al.* 1994). The full resolution data (25m) covers Great Britain but excludes the Isle of Man. There are 25 classes of land cover types, which have been aggregated to 18 classes for the critical loads work. Summary statistics for each 1km square are also used.
(ii) CORINE land cover data for Northern Ireland on the Irish Grid at 1:1 million scale, provides the level 3 CORINE land classification. The 44 classes of land cover have been aggregated to match the 18 used for Great Britain to provide a UK dataset.
(iii) The ITE Land Classification divides the country into 32 classes based on climate, geology, physiography and other data (Bunce and Heal, 1984, Barr 1990). The data are for 1km squares of Great Britain. In addition, detailed field surveys of sample squares in each land class provide environmental information on a statistical basis.
(iv) Crop statistics for the counties of Great Britain from the Ministry of Agriculture, Fisheries and Food.

***Species data:*** Species distribution data for 10km grid squares of the UK are provided by the Biological Records Centre at ITE Monks Wood. For some aspects of the work these data have been used in conjunction with the National Vegetation Classification (NVC), which provides lists of species compositions used to define specific vegetation or habitat types.

***Measured deposition and concentration data:*** Data from the national monitoring network are provided by the National Environmental Technology Centre. Deposition data for the 20km squares of the UK are subsequently corrected at ITE Bush (Edinburgh) for altitude enhancements. These data are used in the calculation of exceedances. In addition, vegetation-specific estimates (for low vegetation and woodland) are provided for use with the simple mass balance calculations of critical loads and exceedances. Concentration data are provided for 20km squares of the UK for sulphur dioxide, nitrogen dioxide and $NO_x$, ammonia, precipitated sulphate and ozone. Some data (sulphur dioxide, nitrogen dioxide and $NO_x$) are also available at 5km resolution.

***Modelled deposition and concentration data:*** The Hull Acid Rain Model (HARM) provides both current and future predicted estimates of sulphur deposition and sulphur dioxide concentrations, by modelling dispersion from point and diffuse sources in the UK (Metcalfe *et al.* in press). The model includes estimates of European emissions and emissions from natural sources. The data are available for 20km squares of the UK.

***Runoff data:*** 1km data for the UK are provided by the Institute of Hydrology (Wallingford).

## Comments and conclusions:

The NFC is developing methods for the calculation and mapping of critical loads (acidity and nutrient nitrogen), critical levels (sulphur dioxide, nitrogen oxides and ozone) and exceedances in collaboration with members of the UK Critical Loads Advisory Group (CLAG), the CCE and the UNECE Task Force on Mapping.

Data have been submitted to the CCE for critical loads of acidity, nutrient nitrogen, maximum and minimum critical loads for sulphur and maximum and minimum critical loads for nitrogen. Northern Ireland is currently excluded (except for acidity), but will be included in the future as data become available for this area.

Future work by the NFC and collaborating institutions will focus on:
a) critical loads of nutrient nitrogen - to revise values if required following the findings from the Grange-over-Sands workshop and the availability of the database of default values for these calculations (Hornung *et al.* 1995);
b) the methods for defining vegetation types for both critical loads and levels;

c) the First-order Acidity Balance (FAB) model for freshwaters - this will be applied to all UK critical load freshwater sites, as digitised catchment information becomes available.


## Acknowledgements for maps and data:

Maps and data compiled by the UK National Focal Centre (ITE Monks Wood).

Critical loads data provided by the Critical Loads Advisory Group soils sub-group, vegetation sub-group, freshwaters sub-group.

Other data provided by the Institute of Terrestrial Ecology Monks Wood (ITE Land Cover, BRC species distributions), Institute of Terrestrial Ecology Merlewood (ITE Land Classification database), Institute of Terrestrial Ecology Bush Estate (deposition), Atomic Energy Authority - National Environmental Technology Centre (deposition), Hull University (HARM modelled deposition), Institute of Hydrology (runoff), Lancaster University (National Vegetation Classification), Ministry of Agriculture, Fisheries and Food (agricultural statistics), and CORINE (land cover for Northern Ireland).


## References:


Allott, T.E.H., R.W. Battarbee, C. Curtis, A.M. Kreiser, S. Juggins, and R. Harriman, 1995. An empirical model of critical acidity loads for surface waters based on Palaeolimnological data. In: Hornung, M., M.A. Sutton, and R.B. Wilson, (Eds.). Mapping and modelling of critical loads for nitrogen: a workshop report. Proceedings of the Grange-over-Sands workshop, 24-26 October 1994. 50-54.

Barr, C., 1990. Mapping the changing face of Britain. *Geographical Magazine* Oct. 1990.

Battarbee, R.W., T.E.H. Allott, K.R. Bull, A.E.G. Christie, C. Curtis, R.J. Flower, J.R. Hall, R. Harriman, A. Jenkins, S. Juggins, A. Kreiser, S.E. Metcalfe, S.J. Ormerod, and S.T. Patrick, 1995. Critical loads of acid deposition for UK freshwaters. Report of the Critical Loads Advisory Group, sub-group on Freshwaters, for the UK Department of the Environment. DOE London. In press.

Bull, K.R., H.M. Dyke, and J.R. Hall, 1995. Exceedances of acidity and nutrient nitrogen critical loads. In: Hornung, M., M.A. Sutton, and R.B. Wilson, (Eds.). Mapping and modelling of critical loads for nitrogen: a workshop report. Proceedings of the Grange-over-Sands workshop, 24-26 October 1994. 158-159.

Bull, K.R., M.J. Brown, H.M. Dyke, B.C. Eversham, R.M. Fuller, M. Hornung, D.C. Howard, and D.B. Roy, in press. Critical loads for nitrogen deposition for Great Britain. *Water Air Soil Pollut.*

Bunce, R.G.H. and O.W. Heal, 1984. Landscape evaluation and the impact of changing land use on the rural environment: the problem and an approach. In: Planning and Ecology, R.D. Roberts and T.M. Roberts (Eds.). Chapman & Hall, London, 164-188.

Curtis, C.J., in press. Validation of the UK critical loads for freshwaters. *Water Air Soil Pollut.*

Downing, R.J., J.-P. Hettelingh, and P.A.M. de Smet, (Eds.), 1993. Calculation and mapping of critical loads in Europe. CCE Status Report 1993. RIVM Rep. 259101003. National Institute of Public Health and Environmental Protection (RIVM), Bilthoven, the Netherlands.

Fuller, R.M., G.B. Groom, and A.R. Jones, 1994. The land cover map of Great Britain: an automated classification of Landsat thematic mapper data. *Photogrammetric Engineering & Remote Sensing* **60** (5):553-562.

Grennfelt, P. and E. Thörnelöf, E. (eds.), 1992. Critical loads for nitrogen: report from a workshop held at Lokeberg, Sweden 6-10 April 1992. Miljorapport 1992:41, Nordic Council of Ministers, Copenhagen.

Hall, J.R., H.M. Dyke, M.J. Brown, and K.R. Bull, 1995. Critical loads for nutrient nitrogen for soil-vegetation systems. In: Hornung, M., M.A. Sutton, and R.B. Wilson, (Eds.). Mapping and modelling of critical loads for nitrogen: a workshop report. Proceedings of the Grange-over-Sands workshop, 24-26 October 1994. 160-161.

Harriman, R., T.E.H. Allott, R.W. Battarbee, C. Curtis, A. Jenkins, and J.R. Hall, 1995. Critical loads of nitrogen and their exceedance in UK freshwaters. In: Hornung, M., M.A. Sutton, and R.B. Wilson, (Eds.). Mapping and modelling of critical loads for nitrogen: a workshop report. Proceedings of the Grange-over-Sands workshop, 24-26 October 1994. 39-49.

Henriksen, A., M. Forsius, J. Kämäri, M. Posch, and A. Wilander, 1993. Exceedance of critical loads for lakes in Finland, Norway and Sweden: reduction requirements for nitrogen and sulphur deposition. Report 32/1993 NIVA report for the Nordic Council of Ministers. 46pp.

Hettelingh, J-P., R.J. Downing, and P.A.M. de Smet, (Eds.), 1991. Mapping critical loads for Europe. CCE Technical Report No. 1, RIVM Rep. 259101001. National Institute of Public Health and Environmental Protection (RIVM), Bilthoven, the Netherlands.

Hornung, M., M.A. Sutton, and R.B. Wilson, (Eds.), 1995. Mapping and modelling of critical loads for nitrogen: a workshop report. Proceedings of the Grange-over-Sands workshop, 24-26 October 1994.

Hornung, M., K.R. Bull, M. Cresser, J.R. Hall, S.J. Langan, P. Loveland, and C. Smith, in press. An empirical map of critical loads of acidity for soils in Great Britain. *Environ. Pollut.*

Kämäri, J., D.S. Jeffries, D.O. Hessen, A. Henriksen, M. Posch, and M. Forsius, 1992. Nitrogen critical loads and their exceedance for surface waters. In: Grennfelt, P. and E. Thörnelöf, (Eds.). Critical loads for nitrogen: report from a workshop held at Lokeberg, Sweden 6-10 April 1992. Miljorapport 1992:41, Nordic Council of Ministers, Copenhagen. 161-200.

Metcalfe, S.E., J.D. Whyatt, and R.G. Derwent, in press. A comparison of model and observed network estimates of sulphur deposition across Great Britain in 1990 and its likely source attribution. *Quarterly Journal of the Royal Meterological Society* **121**.

Posch, M., J.-P. Hettelingh, H.U. Sverdrup, K.R. Bull, and W. de Vries, 1993a. Guidelines for the computation and mapping of critical loads and exceedances of sulphur and nitrogen in Europe. In: Downing, R.J., J.-P. Hettelingh, and P.A.M. de

Smet, (Eds.). Calculation and mapping of critical loads in Europe. CCE Status Report 1993. RIVM report no. 259101003. National Institute of Public Health and Environmental Protection (RIVM), Bilthoven, the Netherlands. 25-38.

Posch, M., M. Forsius, and J. Kämäri, 1993b. Critical loads of sulphur and nitrogen for lakes. I: Model description and estimation of uncertainty. *Water Air Soil Pollut.* **66:**173-192.

Rodwell, J.S. 1991a, 1991b, 1992, 1994. British plant communities: 1. Woodland and scrub. 2. Mires and heaths. 3. Grasslands and montane communities. 4. Aquatic communities, swamps and tall-herb fens. Cambridge: Cambridge University Press.

Sverdrup, H., W. de Vries, M. Hornung, M. Cresser, S. Langan, B. Reynolds, R. Skeffington, and W. Robertson, 1995. Modification of the simple mass balance equation for calculation of critical loads of acidity. In: Hornung, M., M.A. Sutton, and R.B. Wilson, (Eds.). Mapping and modelling of critical loads for nitrogen: a workshop report. Proceedings of the Grange-over-Sands workshop, 24-26 October 1994. 87-92.

UKRGIAN, 1994. Impacts of nitrogen deposition in terrestrial ecosystems (INDITE). Report of the United Kingdom Review Group on Impacts of Nitrogen Deposition on Terrestrial Ecosystems. Department of Environment, London.

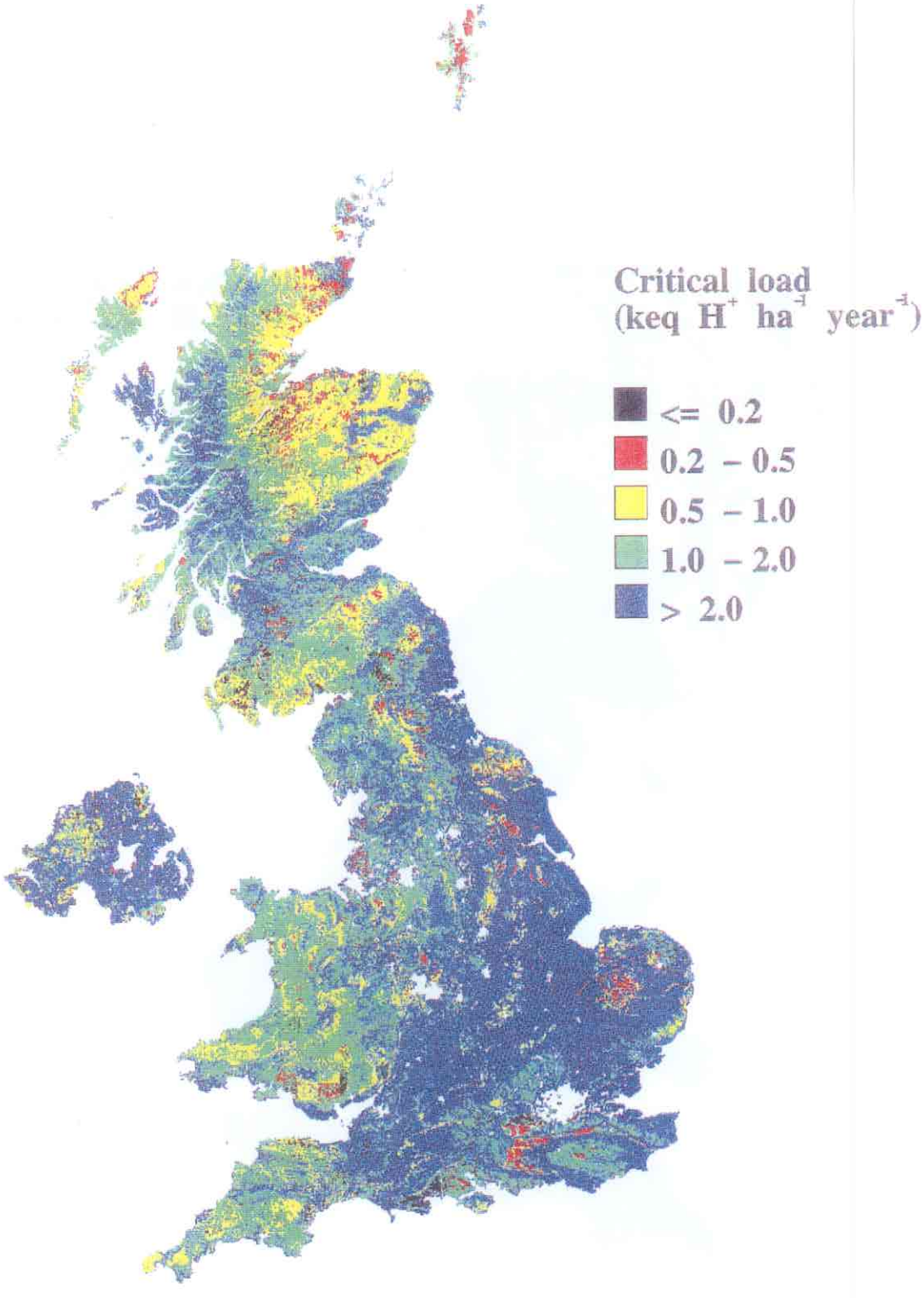


**Figure UK-1.** 5-percentile critical load of acidity. Critical load values are based on the simple mass balance (SMB) equation for three soil-vegetation ecosystems calculated for each 1km square of the country; and on the first-order acidity balance (FAB) model for 527 freshwaters. Ecosystem areas are defined from a UK map of land cover. NB: Great Britain and Irish data are mapped on their separate national grids, however, the location of Northern Ireland with respect to Great Britain is only approximate.

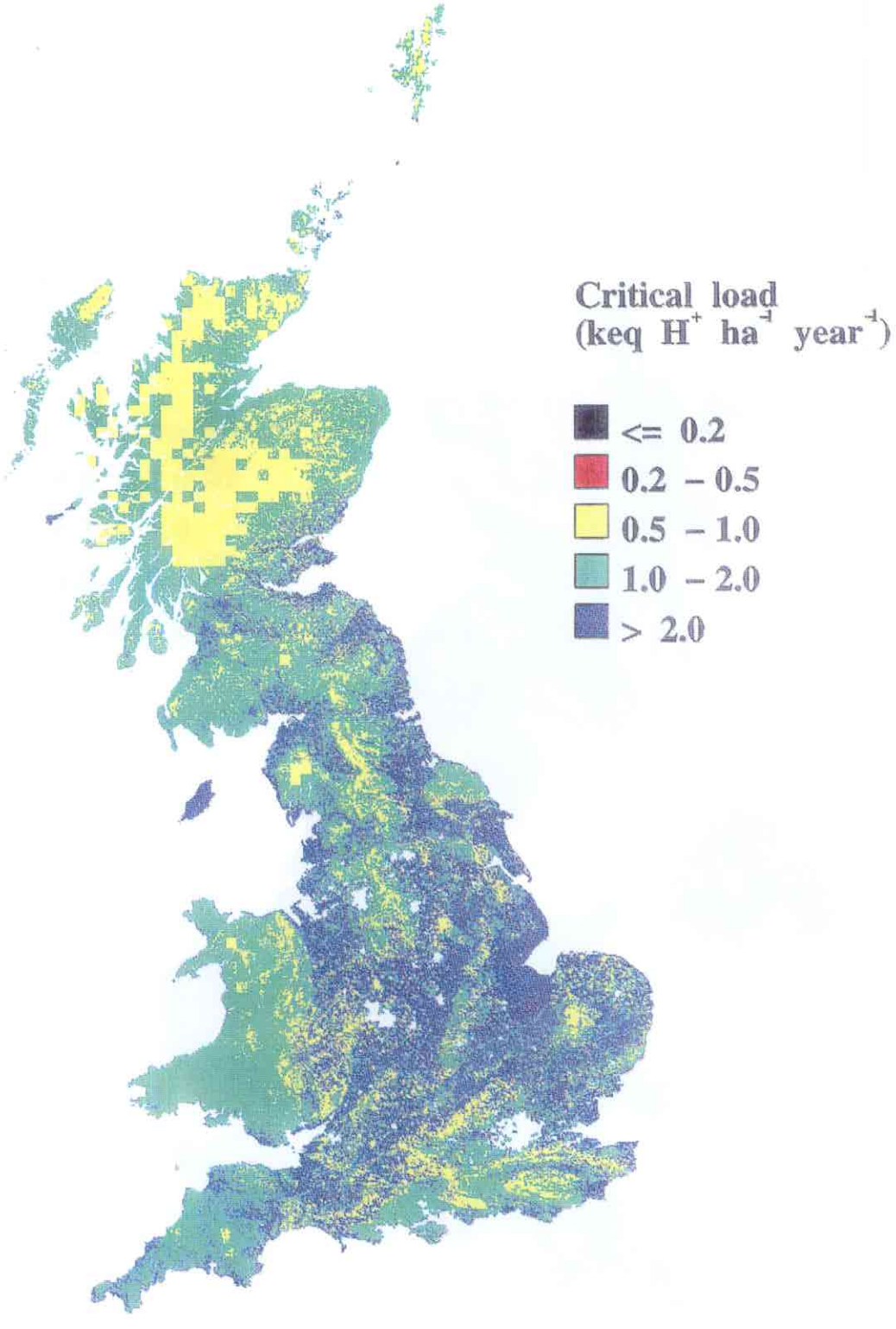


**Figure UK-2.** 5-percentile critical load of nutrient nitrogen. Critical load values are based on the empirical approach for soil-acid grassland and soil-heathland ecosystems; and on the mass balance approach for coniferous woodland soils. For deciduous woodland soils, the lowest value of either the empirical value for deciduous woodland or the mass balance value for coniferous woodland soils is applied.

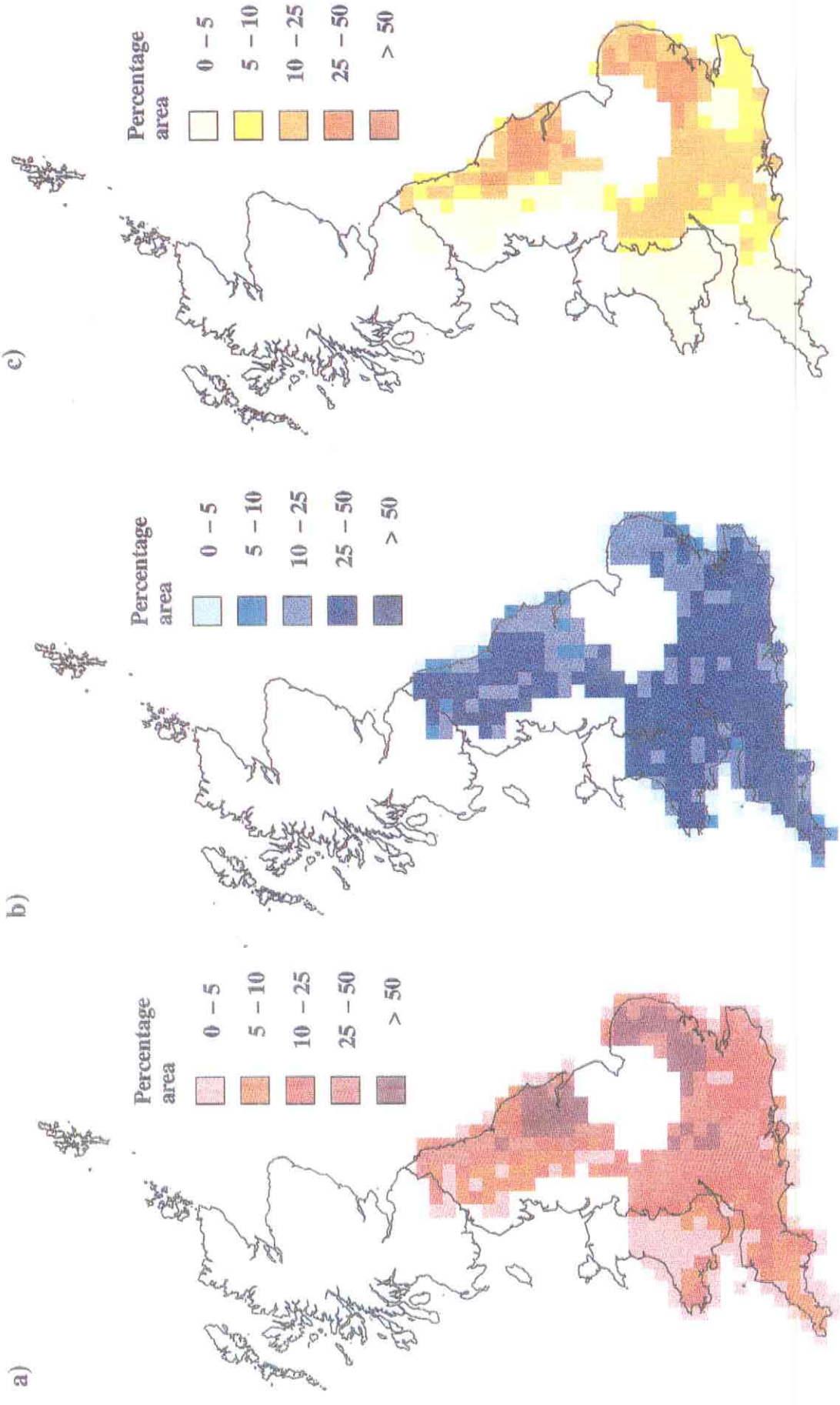


**Figure UK-3.** Exceedance of critical level of ozone (5300 ppb.h) in 1989 for a) arable crops, b) herbaceous semi-natural vegetation, and c) wheat. The maps show the percentage area of these land cover types in areas where the critical level is exceeded.

# APPENDIX A. The polar stereographic projection (EMEP grid)

To make critical load useful for pan-European negotiations on emission reductions one has to be able to compare them to deposition estimates. Deposition of sulfur and nitrogen compounds have up to now been reported by EMEP on a 150km×150km grid covering (most of) Europe, and in the future depositions will also be reported on a 50km×50km subgrid. These grid systems are based on the so-called polar stereographic projection which is described in this Appendix.

In the polar stereographic projection each point on the Earth's sphere is projected from the South Pole onto a plane perpendicular to the Earth's axis and intersecting the Earth at a fixed latitude $\phi_0$. Consequently, the coordinates $x$ and $y$ are obtained from the geographical longitude $\lambda$ and latitude $\phi$ (in radians) by the following equations:

$$x = x_p + M \tan\left(\frac{\pi}{4} - \frac{\phi}{2}\right)\sin(\lambda-\lambda_0) \tag{A.1}$$

and

$$y = y_p - M \tan\left(\frac{\pi}{4} - \frac{\phi}{2}\right)\cos(\lambda-\lambda_0) \tag{A.2}$$

where $(x_p,y_p)$ are the coordinates of the North Pole, $\lambda_0$ is a rotation angle, i.e. the longitude parallel to the $y$-axis; and $M$ is the scaling of the $x$-$y$ coordinates. In the above definition the $x$-values increase and the $y$-values decrease when moving towards the equator. For a given $M$, the unit length (grid size) $d$ in the $x$-$y$-plane is given by

$$d = \frac{R}{M}(1+\sin\phi_0) \tag{A.3}$$

where $R$ (=6370km) is the radius of the Earth. The inverse transformation, i.e. longitude and latitude as function of $x$ and $y$, is given by

$$\lambda = \lambda_0 + \arctan\left(\frac{x-x_p}{y_p-y}\right) \tag{A.4}$$

and

$$\phi = \frac{\pi}{2} - 2\arctan\left(\frac{\sqrt{(x-x_p)^2+(y-y_p)^2}}{M}\right) \tag{A.5}$$

The *arctan* in Eq.A.5 gives the correct longitude for quadrant 4 ($x>x_p$ and $y<y_p$) and quadrant 3 ($x<x_p$ and $y<y_p$); $\pi$ (=180°) has to be added for quadrant 1 ($x>x_p$ and $y>y_p$) and subtracted for quadrant 2 ($x<x_p$ and $y>y_p$). Note that quadrant 4 is the one covering (most of) Europe.

A **grid cell** $(i,j)$ is defined as a square in the $x$-$y$-plane with side length $d$ (see Eq.A.3) and its center point is given by the integral part of $x$ and $y$, i.e.

$$i = \text{nint}(x) \quad \text{and} \quad j = \text{nint}(y) \tag{A.6}$$

where 'nint' is the nearest integer (rounding function). Consequently, the corners of the grid cell have the coordinates $(i\pm½,j\pm½)$.

**The 150km×150km grid (EMEP150-grid):**

The coordinate system originally used by EMEP/MSC-W for the Lagrangian long-range transport model (and up to now by the CCE for mapping critical loads) is defined by the following parameters:

$$\phi_0 = \frac{\pi}{3} = 60°\text{N}, \quad \lambda_0 = -32°\,(\text{i.e.}\,32°\text{W}), \quad (x_p, y_p) = (3,37), \quad d = 150\text{km} \tag{A.7}$$

which yields $M$=79.2438...

**The 50km×50km grid (EMEP50-grid):**

In the future deposition fields will become also become available on a 50km×50km grid. This grid, which is also used by several other institutions (e.g. the Norwegian Institute for Air Research, NILU, and OECD) is a subdivision of the EMEP150-grid into 3×3=9 subgrids. Its parameters are given by

$$\phi_0 = \frac{\pi}{3} = 60°\text{N}, \quad \lambda_0 = -32°\,(\text{i.e.}\,32°\text{W}), \quad (x_p, y_p) = (8,110), \quad d = 50\text{km} \tag{A.8}$$

Consequently, calling these EMEP50-coordinates $p$ and $q$, they are obtained from the EMEP150-coordinates $x$ and $y$ via

$$p = 3x - 1 \quad \text{and} \quad q = 3y - 1 \tag{A.9}$$

And EMEP150-grid cell $(i,j)$ contains 9 EMEP50-grid cells $(m,n)$ with indices $m$=*3i-2,3i-1,3i* and $n$=*3j-2,3j-1,3j*. The two EMEP-grid systems are displayed in Figure A.

To convert a point *(xlon,ylat)*, given in degrees of longitude and latitude, into EMEP150-coordinates *(emepi,emepj)* the following Fortran subroutine can be used:

```
c
      subroutine  llemep  (xlon,ylat,emepi,emepj)
c
c     Computes for a point (xlon,ylat), where xlon
c     is the longitude and ylat is the latitude in degrees,
c     its EMEP150 coordinates (emepi,emepj).
c
c     pi180 = pi/180,  pi360 = pi/360
c     rd = (R/d)*(1+sin(pi/3)), R = 6370km, d = 150km
c
      data  pi180 /0.017453293/,  pi360 /0.008726646/
      data    rd  /79.24387880/
c
      tp = tan((90.-ylat)*pi360)
      rlamp = (xlon+32.)*pi180
      emepi = 3.+rd*tp*sin(rlamp)
      emepj = 37.-rd*tp*cos(rlamp)
                                      return
      end
```

The EMEP50-coordinates can then by obtained with the aid of Eq.A.9.

Conversely, given the EMEP150-coordinates of a point, its longitude and latitude can be computed with the following subroutine:

```
c
      subroutine  emepll  (emepi,emepj,xlon,ylat)
c
c     Computes for a point (emepi,emepj) given in the EMEP150
c     coordinate system its longitude xlon and latitude ylat in degrees.
c
c     pi180 = 180/pi,  pi360 = 360/pi
c     rd = (R/d)*(1+sin(pi/3)), R = 6370km, d = 150km
c
      data  pi180 /57.29577951/,  pi360 /114.591559/
      data   rd  /79.24387880/
c
      ex = emepi-3.
      ey = 37.-emepj
      r = sqrt(ex*ex+ey*ey)
      if (ex .eq. 0. .and. ey .eq. 0.) then ! North Pole
        xlon = -32. ! or whatever
      else
        xlon = -32.+pi180*atan2(ex,ey)
      endif
      ylat = 90.-pi360*atan(r/rd)
                                        return
      end
```

To convert the EMEP50-coordinates $(p,q)$ of a point to longitude and latitude, call the above subroutine with *emepi*=$(p+1)/3$ and *emepj*=$(q+1)/3$.

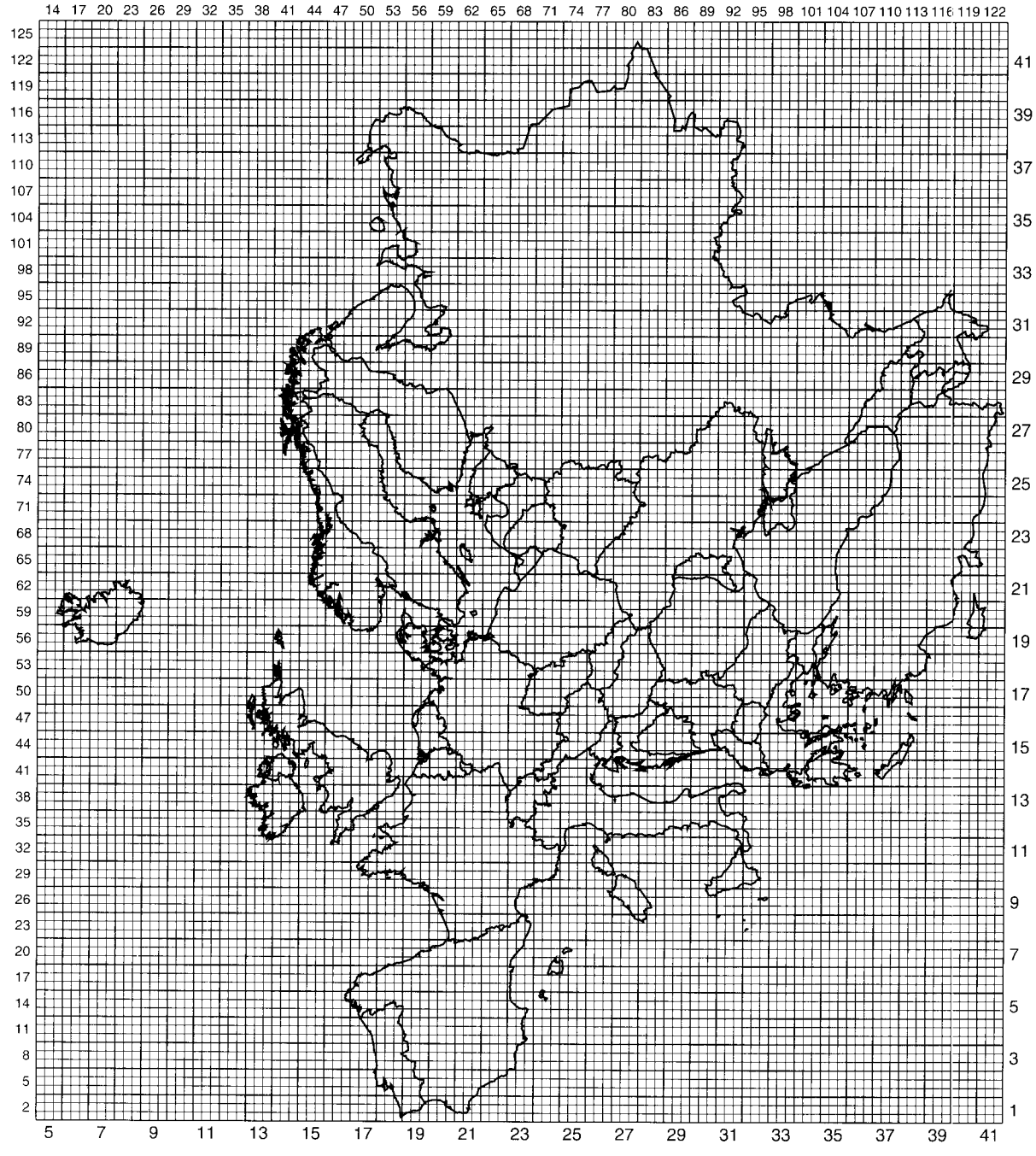


Figure A. The EMEP150-grid (thick lines) and the EMEP50-grid (thin lines). The labels at the bottom and right are the EMEP150-grid indices (every second), and the labels at the top and left are the EMEP50-grid indices (every third).

# APPENDIX B. Routines for computing percentiles and protection isolines

Here we provide Fortran subroutines which allow the computation of percentiles and can assist in the computation of protection isolines and protection percentages. The subroutines are provided on an as-is basis, and no guarantee is given for their correctness. The subroutines contain non-standard features of Fortran, but they work under Microsoft Fortran. It should not be a problem for the experienced user to convert these subroutines into another programming language.

*Computing quantiles (percentiles):*

A pre-requisite for computing quantiles is the sorting of the critical load values, not to forget the corresponding rearrangement of the weights. Routines to do that are easily available, for example the routine *sort2* in Press *et al.* (1992, p.326). In the following we assume that the vectors of critical loads are sorted in ascending order; however, the weights don't have to be normalized to one (e.g., they can be the original ecosystem areas).

A subroutine for computing an arbitrary quantile is then given by:

```
c
      subroutine  qantilcw  (q,num,vec,wei,xq)
c
c     Computes the q-quantile xq of the num values in vec()
c     - sorted in ascending order - with corresponding weights wei()
c     from the empirical distribution function.
c
      integer             num
      real                q, vec(*), wei(*), xq
c
      if (num .eq. 0) stop ' Quantile of nothing?!'
      if (q .lt. 0. .or. q .gt. 1.) stop ' q outside [0,1]!'
c
      wsum = wei(1)
      do k = 2,num
        wsum = wsum+wei(k)
      enddo
c
      qw = q*wsum
      sum = 0.
      do k = 1,num
        sum = sum+wei(k)
        if (qw .lt. sum) then
          xq = vec(k)
                                        return
        endif
      enddo
      xq = vec(num) ! if q=1
                                        return
      end
```

*Computing a protection isoline:*

For computing the points in the x-y plane defining a protection isoline the distance of the intersection of a ray with a given angle with a polygon (critical load function) is needed. This is accomplished by the following subroutine:

```
c
      subroutine  isectang  (xv,yv,npnt,ang,dist)
c
c     Computes the distance 'dist' from the origin of the intersection
c     point of a ray with angle 'ang' (in radian, measured from the x-axis)
c     with a polygon of 'npnt' points stored in xv() and yv().
c     Assumption: polygon monotonically decreasing in 1st quadrant:
c                 0=xv(1)<=...<=xv(npnt) and yv(1)>=...>=yv(npnt)=0
c
      integer            npnt
      real               xv(*), yv(*), ang, dist
c
      data  pihalf /1.5707/ ! = pi/2
c
      if (ang .le. 0.) then
        dist = xv(npnt)
                                        return
      endif
      if (ang .ge. pihalf) then
        dist = yv(1)
                                        return
      endif
      ta = tan(ang)
      tg = 1.e+30
      do n = 1,npnt
        if (xv(n) .gt. 0.) tg = yv(n)/xv(n)
        if (tg .le. ta) then
          xi = (yo*xv(n)-xo*yv(n))/(ta*(xv(n)-xo)-(yv(n)-yo))
          dist = sqrt(1.+ta*ta)*xi
                                        return
        endif
        xo = xv(n)
        yo = yv(n)
      enddo
      end
```

The distances to all critical load functions in a grid for a given angle are then stored in a vector, sorted in ascending order (together with their weights), and the desired percentile computed with the routine *qantilcw* given above. The projections of the percentiles onto the x- and y-axes yield the coordinates of the desired protection isoline (see Figure 4.5 in Part I).

In order to determine the percent of ecosystem area protected in a grid cell one has to be able to decide whether a given pair of deposition ($N_{dep}$,$S_{dep}$) lies inside or outside a given protection isoline. In other words, one needs a routine that determines if a point is inside a polygon or not.

Let $\boldsymbol{x}_1,...,\boldsymbol{x}_n$ with $\boldsymbol{x}_i=(x_i,y_i)$ ($i$=1,..,$n$) be $n$ points defining a closed polygon $P_n$, i.e. the polygon is obtained by connecting $\boldsymbol{x}_1$ with $\boldsymbol{x}_2$, ..., $\boldsymbol{x}_{n-1}$ with $\boldsymbol{x}_n$ and $\boldsymbol{x}_n$ with $\boldsymbol{x}_1$. For an arbitrary point $\boldsymbol{x}_0=(x_0,y_0)$ (inside or outside $P_n$) we define the angle $\phi_i$ by

$$\phi_i = \arccos\frac{(\boldsymbol{x}_i-\boldsymbol{x}_0)\cdot(\boldsymbol{x}_{i+1}-\boldsymbol{x}_0)}{|\boldsymbol{x}_i-\boldsymbol{x}_0|\cdot|\boldsymbol{x}_{i+1}-\boldsymbol{x}_0|}, \quad i=1,...,n \quad (\boldsymbol{x}_{n+1}\equiv\boldsymbol{x}_1) \tag{B.1}$$

In order to determine the *orientation* of the angle $\phi_i$ we multiply it by the sign of the external product of the defining vectors, i.e. by the sign of the expression $(x_i-x_0)(y_{i+1}-y_0)-(y_i-y_0)(x_{i+1}-x_0)$. The sum of the $n$ oriented angles determines then, whether the point $\boldsymbol{x}_0$ lies outside, on, or inside $P_n$:

$$\left|\sum_{i-1}^{n}\phi_i\right| = \begin{cases} 0 & \text{if } x_0 \text{ outside } P_n \\ \pi & \text{if } x_0 \text{ on } P_n \\ 2\pi & \text{if } x_0 \text{ inside } P_n \end{cases} \tag{B.2}$$

and the following subroutine *inside* does exactly this:

```
c
      subroutine  inside  (x,y,xv,yv,nbeg,nend,angle)
c
c     Computes the cumulative 'angle' (in radian) of a point (x,y)
c     with the nodes of the (closed) polygon (xv(n),yv(n),n=nbeg,nend).
c     If |angle|=2*pi, (x,y) is inside the polygon, if angle=0, outside.
c     [if |angle|=pi, then the point is ON the polygon]
c     Note: angle is <0 or >0, depending on the Umlaufsinn!
c
      integer             nbeg,nend
      real                x, y, xv(*), yv(*), angle
c
      data  pi /3.14159265/ ! = pi
c
      x2 = xv(nend)-x
      y2 = yv(nend)-y
      b = x2*x2+y2*y2
      if (b .eq. 0.) then
        angle = pi
                                        return
      endif
      angle = 0.
      do m = nbeg,nend
        x1 = x2
        y1 = y2
        x2 = xv(m)-x
        y2 = yv(m)-y
        a = b
        b = x2*x2+y2*y2
        if (b .eq. 0.) then
          angle = pi
                                        return
        endif
        arg = (x1*x2+y1*y2)/sqrt(a*b)
        if (arg .gt. 1.) arg = 1.
        if (arg .lt. -1.) arg = -1.
        sgn = sign(1.,x1*y2-x2*y1)
        angle = angle+sgn*acos(arg)
      enddo
                                        return
      end
```

This subroutine, together with the routine *isectang* given above, can be used to compute the percent of ecosystems protected in a grid cell for a given pair of deposition *(depn,deps)*; and the following program fragment does exactly that:

```
      .....
      do m = 1,miso
        read (1,*) npnt,(xv(n),yv(n),n=1,npnt)
        xv(npnt+1) = 0.    ! close polygon by
        yv(npnt+1) = 0.    ! adding origin (0,0)
        call  inside  (depn,deps,xv,yv,1,npnt+1,angle)
        if (abs(angle) .gt. 5.) then ! inside
          if (m .eq. 1) then ! 100% protection
            protper = 100.
          else ! interpolate
            z = sqrt(deps*deps+depn*depn)
            ang = atan2(deps,depn)
            call  isectang  (xv,yv,npnt,ang,dist)
            call  isectang  (xold,yold,npnto,ang,disto)
            per = vy(m)-(vy(m)-vy(m-1))*(dist-z)/(dist-disto)
            protper = amax1(100.-per,0.)
          endif
                                        goto 99 ! done for that grid
        else ! store isoline
          npnto = npnt
          do n = 1,npnt
            xold(n) = xv(n)
            yold(n) = yv(n)
          enddo
        endif
      enddo ! go and read next isoline
      protper = 0. ! outside all percentile isolines
99    continue
      .....
```

The do-loop runs over *miso* percentile functions read from a file. The corresponding percentages are stored in the vector *vy*: *vy(1)=0,..., vy(miso)=100.* As soon as 2 consecutive pre-computed percentile functions are found so that the given point lies inside one and outside the other, the protection percentage is estimated by linearly interpolating between the two *vy*-values using the distances (computed with *isectang*) to the two percentile functions. The program fragment has to be embedded into loops which run over the desired grid cells and do the necessary writing to an output file.

**Reference:**

Press, W.H., S.A. Teukolsky, W.T. Vetterling and B.P. Flannery, 1992. Numerical Recipes in Fortran - The Art of Scientific Computing. Second Edition, Cambridge University Press, 963 pp.

# APPENDIX C. The anonymous FTP server of the CCE

The CCE has an extended network of contacts throughout Europe, North America and Asia. Intensive communication related to the activities and responsibilities of the CCE and its collaborators takes place. In view of present and future activities, even more intensive communication is required and an extension of the network of collaborators is indispensable. To support this development the CCE has set up an *anonymous FTP server* with the name **deimos.rivm.nl**.

**What is an anonymous FTP server?**

Everybody from both inside and outside RIVM has unlimited access to the server. Therefore, it is called *anonymous*. The protocol on the server is the international standard for file transfer, 'File Transfer Protocol' (FTP). Therefore, this type of server is called an *anonymous FTP Server*. The user interface available for FTP on a site depends on the management of the computer system on that site.

**Why an anonymous FTP server?**

1) The internal RIVM computer network is not freely accessible via Internet. There is a so called 'fire wall' around the RIVM network that prevents persons from outside the RIVM to access it. To overcome this limitation the CCE has installed an FTP server outside this fire wall. The server is called deimos.rivm.nl (Deimos is one of the two moons of planet Mars; Phobos is the other one).
2) Most of the CCE contacts have access to Internet and have FTP software available. Besides, everybody from all over the world can access with FTP this server via Internet.
3) Until a year ago, national data contributions were mainly sent on diskettes by 'snail-mail' and occasionally by e-mail on Internet. One problem is the ever growing size of the databases: they have become so large that using diskettes or e-mail is not the most appropriate way of transfer. Reliable file transfer by FTP to a server at CCE with enough hard disk space is the alternative.

**Setup of the anonymous FTP server deimos.rivm.nl at the CCE**

*Confidential information:*
For the CCE and most of its contacts an additional complication arises when using an anonymous FTP server. Part of the information made available from and to the CCE via this server is *confidential*. To avoid access by non-authorized users a directory structure has been set up with specific limited read and write permissions for every directory (see Figure D.1). These limitations allow the CCE to apply restricted access authorization to selected groups of users. For example,
the CCE receives from National Focal Centers (NFCs) regular updates related to the critical loads activities. These data are submitted to the CCE by transferring them to a specific country directory under */pub/cce/incoming* with restricted read and write permissions. As file manager of the directories under */pub/cce* the CCE can read all directories. The CCE makes its results derived from national contributions available for reviewing to the NFC on a specific country directory under */pub/cce/outgoing*, again with restricted read and write permissions. Authorized users are informed about the 'key' to be able to transfer the file from deimos.rivm.nl to their site.

*Public information:*
The server contains one directory (*/pub/cce/world*) to which every user has unlimited read and write access. This directory is meant to serve as a 'bulletin board'. Public announcements, publications, databases, requests, etc. can be put on it by both the CCE and other users, as far as they concern the activities and responsibilities of the CCE and its contacts. For example, recently the RIVM has produced a second version of a Land Use Map of Europe. The CCE has contributed in this project and prepared a special database which is available on the freely accessible directory */pub/cce/world*. Everybody is invited to give comments on the quality of this database. No read or write permissions apply on this directory (see Figure D.1).

### The directory Structure of deimos.rivm.nl

Figure D.1 shows the directory structure under */pub/cce* on deimos.rivm.nl, available for external users. Permission settings for every subdirectory are indicated as well.

```
/                              = Home- and root directory.
|                                  Active: 'ls'.  Not active: 'put', 'get', etc.
|_pub                          = General top directory for RIVM public purposes.
    |                            Active: 'ls'.  Not active: 'put', 'get', etc.
    |_cce                      = Top directory of CCE-tree.
      |                          Active: -.  Not active: 'put', 'get', 'ls', etc.
      |_world                  = Public directory that serves as a 'bulletin board'.
          |                      Active: 'put', 'get', 'ls', etc.  Not active: -
          |_incoming           = Has one subdirectory per nation for incoming NFC files.
          | |                    Active: -.  Not active: 'put', 'get', 'ls', etc.
          | |_at   Austria     = National subdirectory were NFC can put confidential national
          | |_by   Belarus       submissions, available for the CCE only.
          | |_cz   Czech Rep.    For each country exists one directory.
          | |_hr   Croatia       Active:  '(m)put' <file name>.  Not active: 'get', 'ls', etc.
          | |_cz   Czech Rep.
          | |    etc.
          |
          |_outgoing           = Has one subdirectory per nation for outgoing CCE files for
              |                  a specific NFC (name refers to nations 2 character code).
              |                    ACTIVE: -.  NOT ACTIVE: 'get', 'put', 'ls', etc.
              |_at               = National subdirectories for NFCs for getting confidential
              |_hr                     data from the CCE.
              |_by                     ACTIVE:  'get' <file name>.  NOT ACTIVE:  'put', 'ls', etc.
              |_cz
              |      etc.
```

Figure D.1. Directory structure on the anonymous FTP server deimos.rivm.nl.

### How to access the FTP server deimos.rivm.nl

This section explains how external users can access the anonymous FTP server deimos.rivm.nl. The style conventions used are the following:
- User commands (UNIX) are between single quotes: '.....'
- Optional parts of commands are between square brackets: [.....]
- File related naming in commands is between angular brackets: <.....>
- Response from the server is between double quotes: "....."

*Connecting to deimos.rivm.nl*
On your system you need to have available FTP software and an Internet connection.

• To connect to the server you have to type:
'ftp deimos.rivm.nl' (it starts a ftp session and connects with deimos.rivm.nl),
or
'ftp' (it starts a ftp session on your system)
and 'open deimos.rivm.nl' (establishes a connection with deimos.rivm.nl).

If a connection is established, you get a message reading something like:
"Connected to deimos.rivm.nl.
220 deimos FTP server (Version wu-2.4(4) ..... ) ready."

• To log in you will be asked for a name and a password:

"Name:" type 'ftp' or 'anonymous'
"331 Guest login ok, send your complete e-mail address as password."
"Password:" type your complete e-mail address, e.g., 'Dick.Hertz@nowhere.nl'

Now you are will be logged to the root directory ("/") of deimos.rivm.nl with the prompt "ftp>".

• Go to the subdirectory of the CCE by typing:

'cd pub/cce' (cd= change directory)

With the command 'pwd' (= present working directory) you can always check the current directory of the FTP server you are in.
With 'ls' you get a file list of the current directory displayed on your screen, but only when a read permission is granted for this directory.
(To go one step up in the directory tree you can use 'cd ..', for example from */pub/cce* to */pub*.)

*File Transfer **to** deimos.rivm.nl*

To send (confidential) files to the server deimos.rivm.nl you select the relevant subdirectory under */incoming*, e.g. for Finland:

'cd incoming/fi'

Now, the Finnish user can send files with the command 'put' to subdirectory */pub/cce/incoming/fi*:

'put <file name> [<file name at deimos.rivm.nl>] '

(public information, like announcements for everybody, should be copied in the same way to */pub/cce/world*)

The server will inform you about the status and success of the file transfer, e.g. "Transfer complete" and the number of bytes that were transferred. No 'ls' and no transfer **from** the subdirectories under */incoming* is possible.
If a 'put' command was not executed successfully (e.g. when the file name already exists, due to sending a file with the same name earlier) a new attempt should be made with other file naming then used before. No overwriting of a file is possible!

*File Transfer **from** deimos.rivm.nl*

To retrieve confidential CCE files from deimos.rivm.nl you have to select the subdirectory under */outgoing* with your country two-letter country code, e.g. for Finland:

'cd pub/cce/outgoing/fi'

No 'ls', 'mget' or 'mput' is enabled for the subdirectories under */outgoing*. To transfer files to your site you have to use the 'get' command. E.g., a Finnish organization can retrieve confidential files from the subdirectory */pub/cce/incoming/fi*. An e-mail message from the CCE will inform the authorized user about the exact names of the files. In this way the file name serves as the 'key' necessary to retrieve the file from the server to your site with the command:

'get <file name at deimos.rivm.nl> [<file name>]'

It is advised to always use binary mode when transferring files from and to deimos.rivm.nl. A file of any format will then be transferred without the risk of corruption. Binary mode can be set in your FTP session by the command:

'binary' (back to ASCII mode with: 'ascii')

(When binary files are transferred in ASCII mode, corruption easily occurs)

*Terminating the connection with deimos.rivm.nl*

- To terminate a connection with the server deimos.rivm.nl type:

'close' (disconnects from server deimos.rivm.nl)

- To terminate the FTP session on your system use:

'bye' (terminates ftp session)
or
'quit' (same as 'bye')

(Shortcut: If you were still connected to the server and type 'bye' or 'quit', then both the connection to deimos.rivm.nl and the ftp session will be terminated.)

**Experience after one year of operation**

Since one year the CCE runs the anonymous FTP server deimos.rivm.nl. It has improved the communication between CCE and its contacts, and between contacts themselves. It has shown to increase the speed, frequency and convenience of this communication. The size of national databases (tens of Megabytes) has proven not to be a problem. However, it the connection between the remote users and deimos.rivm.nl was not always as stable as it should be. This can cause corruption of files which are transferred. An analysis of the behavior of the server and the RIVM network concluded that the instabilities are located elsewhere on the Internet.

Except for one country, all national data contributions received by the CCE and relevant for UN/ECE affiliated bodies, were submitted via the FTP server. Also, many contributions to this report were submitted in this way.

**List of commands with short definitions**

Extended descriptions of these and more sophisticated commands can be found in UNIX operating system manuals, FTP user manuals, network manuals, etc. Consult your system manager and operating system manuals for more details. The descriptions below are derived from a Sun PC-NFS Command Reference.

ftp Interactive program that enables you to transfer files to and from a remote file system. It prompts you for a command, acts on it, and prompts again for another command.

open Establish a connection to the specified host ftp server (i.e. remote server or remote file system). A login procedure to the remote server will start.

put Store a file of your file system on the remote file system.

mput Like 'put', but for multiple files. Wildcards can be used.

get Retrieve a file of the remote system and store it on your file system.

mget Like 'get', but for multiple files. Wildcards can be used.

pwd Display the name of the current working directory on the remote file system.

ls Display list of files in the current working directory on the remote file system.

cd Change directory on remote file system from current working directory to given directory, or with 'cd ..' it changes to one directory level higher in hierarchy (if possible).

binary Sets transfer control command to binary representation type, (which specifies the manner in which 'ftp' transfers files between your file system and the remote server).

ascii Sets transfer control command to ASCII representation type, (which specifies the manner in which 'ftp' transfers files between your file system and the remote server).

close Disconnects from the remote server and returns to ftp's command interpreter for another command. This allows you to start another session with another host.

quit Terminate the ftp session with the remote server by disconnecting from it (like the 'close' command), and exit 'ftp'.

bye Same as 'quit' command.

# APPENDIX D. List of mathematical notation and acronyms[1]

## Variables:

$Al$ = aluminum
$Alk$ = alkalinity
$Bc = Ca + Mg + K$
$BC = Ca + Mg + K + Na$
$Ca$ = calcium
$CD(N)$ = critical nitrogen deposition
$CD(S)$ = critical sulphur deposition
$Cl$ = chloride
$CL(A)$ = critical load of acidity
$CL(Ac_{act})$ = critical load of actual acidity
$CL(Ac_{pot})$ = critical load of potential acidity
$CL(N)$ = critical load of nitrogen
$CL(N \mid S_{dep})$ = critical load of nitrogen for a given sulfur deposition
$CL(S)$ = critical load of sulphur
$CL(S+N)$ = critical load of sulphur and nitrogen
$CL(S \mid N_{dep})$ = critical load of sulfur for a given nitrogen deposition
$CL_{max}(N)$ = maximum critical load of nitrogen
$CL_{max}(S)$ = maximum critical load of sulphur
$CL_{min}(N)$ = minimum critical load of nitrogen
$CL_{min}(S)$ = minimum critical load of sulphur
$CL_{nut}(N)$ = critical load of nutrient nitrogen
$Ex(N)$ = exceedance of the critical load of nitrogen
$Ex(S)$ = exceedance of the critical load of sulphur
$Ex(S+N)$ = exceedance of the critical load of sulphur and nitrogen
$f_{de}$ = denitrification fraction
$HCO_3$ = bicarbonate
$k$ = denitrification rate coefficient
$K$ = saturation coefficient (2900 eq $ha^{-1}$ $yr^{-1}$)
$K$ = potassium
$k_0$ = kinetic rate constant (1810 eq $ha^{-1}$ $yr^{-1}$)
$K_{gibb}$ = gibbsite coefficient ($m^6$ $eq^{-2}$)
$Mg$ = magnesium
$N$ = nitrogen
$Na$ = sodium
$NH_4$ = ammonium
$NO_3$ = nitrate
$P$ = phosphorus
$pH$ = soil solution pH
$Q$ = water flux from the bottom of the rooting zone ($m^3$ $ha^{-1}$ $yr^{-1}$)
$RCOO$ = organic anions
$r$ = stoichiometric ratio of aluminum to base cation weathering
$S$ = sulfur
$T$ = temperature (°C)
$w$ = relative soil moisture saturation ($\Theta/\Theta_s$)
$X$ = (element)
$x_{CaMgK}$ = fraction of Ca+Mg+K weathering of total weathering
$x_{X:N}$ = ratio of element $X$ to nitrogen during uptake (eq $eq^{-1}$)

[1]Mathematical notation and acronyms which appear *only* in NFC reports are not included here.

## Subscripts:

*ad* = adsorption
*crit* = critical
*de* = denitrification
*dep* = total deposition
*eros* = erosion
*fire* = fire
*fix* = fixation
*i* = net immobilization
*le* = leaching
*le(crit)* = critical leaching
*max* = maximum
*min* = minimum
*pr* = precipitation
*re* = reduction
*u* = net growth uptake
*vol* = volatilization
*w* = weathering

## Acronyms:

AOT40 = accumulated dose over threshold of 40 ppbh
CCE = Coordination Center for Effects
CDF = cumulative distribution function
CRP = Current Reduction Plans
EEA = European Environment Agency
EMEP = Cooperative Program for Monitoring and Evaluation of the Long-range Transmission of Air Pollutants in Europe
LRTAP = (Convention on) Long-Range Transboundary Air Pollution
NFC = National Focal Center
ppb = parts per billion
ppbh = parts per billion hour
ppm = parts per million
SMB = Simple Mass Balance model
SSMB = Steady-State Mass Balance model
TFIAM = (UN/ECE) Task Force on Integrated Assessment Modelling
TFM = (UN/ECE) Task Force on Mapping
UN/ECE = United Nations Economic Commission for Europe
USA = United States of America
WGE = (UN/ECE) Working Group on Effects
WGS = (UN/ECE) Working Group on Strategies

A publication of:

RIVM, NATIONAL INSTITUTE OF PUBLIC HEALTH AND THE ENVIRONMENT
P.O. Box 1, 3720 BA Bilthoven, The Netherlands

1995